Investigating the role of Oxr1 in mitochondria

Thesis submitted for the degree of Doctor of Philosophy

Hilary Term 2016

Yixing Wu

Hertford College

Department of Physiology, Anatomy
and Genetics

University of Oxford

Abstract

Investigating the role of Oxr1 in mitochondria

Yixing Wu

Hertford College, University of Oxford

Thesis submitted for the degree of Doctor of Philosophy

Hilary Term 2016

Oxidative stress (OS) and mitochondrial dysfunction are common features of neurodegenerative disease, suggesting that antioxidant defence systems are critical for cell survival in the central nervous system (CNS). Oxidation resistance 1 (OXR1) has emerged as an essential antioxidant protein that controls the susceptibility of neurons to OS; however, the function of this novel protein is unknown. The overall goal of this thesis was to investigate the potential role of Oxr1 in mitochondria and to understand more regarding the function of the gene in the oxidative stress response *in vitro* and *in vivo*.

It was demonstrated that different isoforms of Oxr1 are expressed in specific sub-cellular compartments and certain mitochondrial Oxr1 isoforms are associated with mitochondrial membrane. In addition, it was shown that over-expression of the shortest isoform of Oxr1 in the cytoplasm is protective; both against oxidative stress-induced apoptosis and against mitochondrial morphological changes caused by disease-associated TDP-43 mutations. Analysis of mitochondrial metabolism and fusion and fission proteins in *Oxr1* knockout (*bella*) tissue indicated that that *Oxr1* deletion alone does not trigger overt mitochondrial dysfunction but it may influence aspects of mitochondrial morphology.

To ascertain whether loss of *Oxr1* in specific neuronal populations would render them more susceptible to cell death, the conditional deletion of *Oxr1* in mouse dopaminergic neurons was studied. Preliminary data showed that aged mice displayed no motor or pathological abnormalities in the midbrain, suggesting that this particular conditional deletion does not lead to significant neurodegeneration. Finally, ENU mutagenesis screening of Oxr1 identified a point mutation in the highly-conserved TLDc domain of Oxr1 (Y644H). *In vitro* analysis suggested that this mutant rendered cells more vulnerable to oxidative stress, demonstrating that this region of the protein is functionally important.

Taken together, these studies deepen the understanding of Oxr1 as a novel antioxidant protein and offer new and important insights into its role in the OS-response and its potential use in future antioxidant therapies.

Declaration

The work presented in this thesis was performed in the Medical Research Council (MRC) Functional Genomics Unit, Department of Physiology, Anatomy and Genetics, University of Oxford, from 2012-2016. Unless otherwise stated, all work presented was conducted by the author (Yixing Wu) and has not been submitted for any other degree in this or any other university or institute of learning.

I dedicate this thesis to the memory of my beloved grandfather, Prof. Xixin Qu (曲喜新)

(1923-2009)

Acknowledgements

First and foremost, I would like to thank Prof. Dame Kay E. Davies for giving me this great opportunity to study in her lab at the MRC Functional Genomics Unit. I would like to say a very big thank you to her and my co-supervisor, Prof. Peter L. Oliver for their endless support and guidance throughout my four-year DPhil study. Under their dedicated supervision, I have grown up from a master's student with very limited knowledge and research experience to a DPhil student who can conduct independent research and make original contributions to the field of my DPhil research. Things that I have learnt from them will always be beneficial for my career in science.

Second, I want to thank Dr. Mattéa Finelli and Dr. Kevin Liu for their encouragement, help and valuable suggestions at some important moments of my research project. I also wish to thank Dr. Tamara Sirey, Dr. Michelle Potter, Dr. Karl Morten, Dr. Luis Sanchez-Pulido, Dr. Annemieke Kokm, Dr. Duncan Howie, Dr. Errin Johnson, Dr. Anna Pielach and Prof. Helen Christian for their helpful suggestions and technical assistance with mitochondrial functional assays and electron microscopy.

Next, I would also like to thank ALL the past and present members of Kay's group and the MRC Functional Genomics Unit. I had a truly unforgettable time with all of you! My special thanks goes to: Benjamin Edwards, Dr. Esther Becker, Dr. Rebecca Fairclough, Dr. Emmanuelle Bitoun, Dr. Leigh Paton, Helen Johnson, Arran Babbs, Sarah Squire, Nandini Shah, William Pembroke, Dr. Gauri Ang, Friederike Winter, Matthew Williamson, Daria Svistunova, Dr. Achilleas Livieratos, Dr. Huijia Chen, Dr. Amy Reddington, Dr. Simon Guiraud, Dr. Anna Dulneva, Dr David Burns, Dr. Katie Richardson, Dave Powell, Allyson Potter, Prof. Ji-Long Liu, Yong Huang, Dr. Omur Tastan, Dr. Sanjay Ghosh, Jing Zhang, Qingji Shen, Dr. Gerson Keppeke, Stephanie Hoekstra, Norbert Lidzba and Liam Argent.

Finally, I would like to thank my family members for their support. In particular, I owe a great debt of gratitude to my grandfather, Prof. Xixin Qu for his wholehearted support, guidance and unconditional love. Prof. Qu was a well-respected expert in electronic material and component, who had devoted himself to research, teaching and academic writing at University of Electronic Science and Technology of China (UESTC) for more than forty years. When I was a child, he took care of me and supported me in every possible way. His attitudes towards life and study had deeply influenced me, and will always inspire and encourage me throughout my life.

Table of Contents

List of figures and tables

Figures

Tables

Abbreviations

Aβ- Amyloid beta

ABAD- Amyloid β-binding alcohol dehydrogenase

AD-Alzheimer's disease

ALS- amyotrophic lateral sclerosis

ANOVA-Analysis of Variance

ARE- antioxidant response element

ATP- adenosine triphosphate

Bax- Bcl-2 associated X protein

Bcl-2- B-cell lymphoma 2

Cat- catalase

CI- Complex I

CII- Complex II

CIII- Complex III

CIV- Complex IV

CNS- central nervous system

CRISPR- Clustered regularly interspaced short palindromic repeats

CV- Complex V

DCPIP- 2, 6-dichloroindophenol

DJ-1- Protein deglycase DJ-1

DNAJC19- DnaJ (Hsp40) homolog, subfamily C, member 19

Drp1- dynamin-related protein 1

EM- electron microscope

ENU- N-ethyl-N-nitrosourea

ERα- estrogen receptor α

ERαbd- Estrogen Receptor α binding domain

ETC- electron transport chain

FTLD- frontotemporal lobar degeneration

FCCP- carbonilcyanide p-triflouromethoxyphenylhydrazone

FIME- Familial Infantile Epilepsy

Fis1- Fission, mitochondrial 1

GC- granule cell

GCL- granule cell layer

GPx- glutathione peroxidase

GRAM- Glucosyltransferases, Rab-like GTPase activators and Myotubularins

GRX2- glutaredoxin 2

GTPase- guanosine triphosphatases

HD- Huntington's disease

HSP- heat shock protein

htt- huntingtin

IFI44- interferon-induced protein 44

IM- inner membrane

IMS- intermembrane space

JNK- c-Jun N-terminal kinase

LRRK2- Leucine-rich repeat kinase 2

MAO- monoamine oxidase

Mfn- mitofusin

MIA- Mitochondrial Intermembrane space import and Assembly

MND- motor neuron disease

MOMP- mitochondrial outer membrane permiabilisation

MPP- Mitochondrial processing peptidase

MPTP- 1-methyl 4-phenyl-1,2,3,6-tetrahydropyridine

MS- multiple sclerosis

MSC- mesenchymal stem cell

MX-matrix

NCOA7- nuclear receptor coactivator 7

OM- outer membrane

OPA1- Optic atrophy 1

OS- oxidative stress

Oxr1- oxidative resistance 1

PAM- Protospacer adjacent motif

PD- Parkinson's disease

PFA- paraformaldehyde

PINK- PTEN-induced kinase

PME- Progressive Myoclonic Epilepsy

PPARγ- peroxisome proliferator-activated receptor γ

PUFA- polyunsaturated fatty acid

PVDF- polyvinylidene fluoride

ROS- reactive oxygen species

SAM- Sorting and Assembly Machinery

SEM- standard error of the mean

SLC25- Solute Carrier Family 25

SN-substantia nigra

SOD- superoxide dismutase

TBC1D24-TBC1 domain family, member 24

TBST- Tris-buffered saline and Tween 20

TDP- TAR DNA-binding protein

TEM- Transmission electron microscopy

TH- tyrosine hydroxylase

TIA-1- T cell-induced antigen 1

TIM- Translocase of the Inner Membrane

TLDc- Tre-2/Bub2/Cdc16 (TBC), Lysin motif (LysM), Domain catalytic

TOM- Translocase of the Outer Membrane

VDAC- voltage-dependent anion channel

VPS13C- vacuolar protein sorting 13C

VTA- ventral tegmental area

Chapter 1: Introduction

1.1 Oxidative stress and neurodegenerative diseases

Neurodegenerative diseases, which are disorders characterised by selective loss of neuronal structure and function, are an increasingly important clinical problem (Saxena and Caroni, 2011). Up to now, most, if not all the neurodegenerative diseases are incurable and the aetiology of these diseases remains unclear. Identifying common pathways of neurodegeneration may shed light on potential treatment. Oxidative stress (OS) has been found as a common feature of all the major neurodegenerative diseases (Barnham et al., 2004).

Reactive oxygen species (ROS), including oxide ions and peroxides, are produced as a by-product of aerobic metabolism. Although ROS can be detrimental to cells, under normal conditions, damage caused by ROS is limited by antioxidant defensive mechanisms in cells. For example, antioxidant enzymes such as catalase (Cat) and superoxide dismutase (SOD) are efficient in counteracting and neutralising cytotoxic effects caused by ROS. Oxidative stress occurs in consequence of the imbalance between ROS production and antioxidant response (**Figure1.1.**).

An excessive amount of ROS causes damage to critical cellular components such as DNA, RNA, lipid and proteins (Rowe et al., 2008). For example, upon oxidative stress, DNA base modification, single and double strand breaks as well as lesions such as 8-oxoguanine can be induced (Bohr, 2002). Accumulation of these modifications may ultimately lead to deleterious effects such as neurodegeneration. Amino acids residues can be oxidised and trigger subsequent protein damage (Berlett and Stadtman, 1997). Lipids, especially polyunsaturated fatty acid (PUFAs) residues are vulnerable to

oxidative stress and can be degraded through peroxidation (Halliwell and Chirico, 1993). Products of lipid peroxidation such as reactive aldehydes, including 4-hydroxynonenal further damage DNA and proteins (Esterbauer et al., 1991).

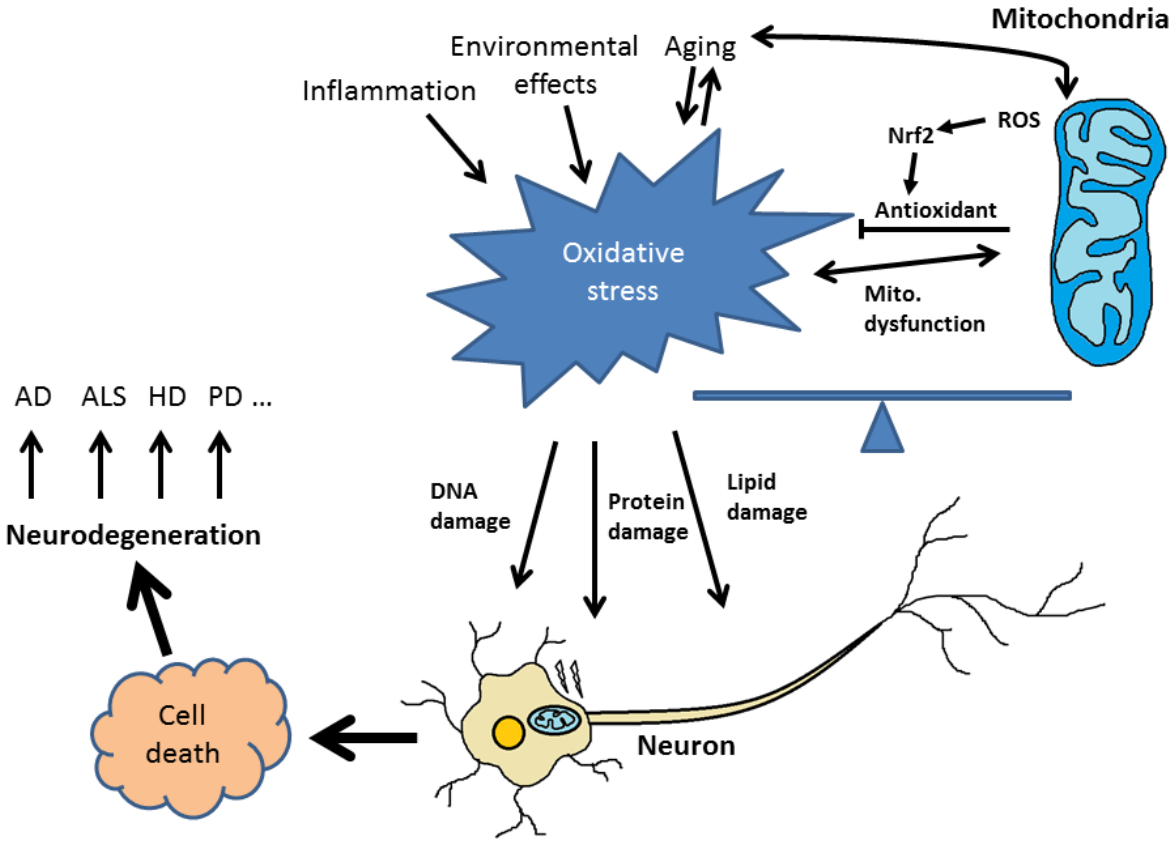

Figure 1.1. Oxidative stress and neurodegeneration

Oxidative stress is generated as the result of an imbalance between ROS production in mitochondria, which is a key physiological ROS producing site and antioxidant response. Aging, inflammation and environmental effects such as pollution are contributing factors of OS. OS causes damage to essential compositions of cells such as protein, DNA and lipids. It subsequently triggers cell apoptosis or necrosis that leads to various diseases including neurodegeneration.

Neurons are believed to be particularly vulnerable to oxidative stress due to their more active metabolism and lower cellular regeneration capacity in comparison with other cell types (Barber and Shaw, 2010). Gradual accumulation of oxidative damage in neurons can ultimately trigger cell apoptosis or necrosis through various intracellular signalling pathways (Xiao et al., 2011, Fernandez-Checa, 2010). On the basis of studies from patients suffering from a number of neurodegenerative diseases including Parkinson's disease (PD), amyotrophic lateral sclerosis (ALS), Alzheimer's disease (AD), and Huntington's disease (HD), detrimental effects associated with oxidative stress are repeatedly found in regions where programmed neuronal cell death occurs (Uttara et al., 2009). For example, both post-mortem and *in vitro* investigations revealed that neurodegeneration in AD might be partially attributed to peroxidation induced by amyloid beta peptide (Aβ) (Allan Butterfield et al., 2002). In the substantia nigra region of PD patients, the level of polyunsaturated free fatty acids was found to be reduced; whereas increasing levels of lipid peroxidation and oxidative stress indicators (malondialdehyde (MDA) and 4-hydroxynonenal (HNE)) were detected, suggesting lipoxidative damage (Dalfó et al., 2005). In HD patient brains, protein carbonylation, which is one of the indicators of oxidative stress was found to be increased compared to the controls (Sorolla et al., 2008), suggesting the involvement of OS in disease progression of HD.

Despite the fact that oxidative damage has been observed as a common feature of neurodegenerative disorders, whether this is the primary cause or, merely one of the effects of neurodegeneration, still remains unclear (Gandhi and Abramov, 2012). Interestingly, in the central nervous system (CNS), damage caused by oxidative stress increase with age (Radak et al., 2011), while the capability of antioxidant defence also changes with age (O'Donnell and Lynch, 1998). This is consistent with the fact that

neurodegenerative diseases are more prevalent in aged population. Apart from oxidative stress, protein aggregation, which is another common pathological feature of neurodegenerative diseases is also thought to be progressive with age (David et al., 2010). Discoveries have shed light on the relationship between oxidative stress and protein aggregation. For instance, incubating the PD-related protein α-synuclein with oxidative stress-inducing reagent H_2O_2 in combination with ferric ion induces aggregation (Hashimoto et al., 1999), while exposure of human embryonic kidney (HEK) 293 cells expressing wild-type and mutant α-synuclein to nitric oxide- and superoxide-generating compounds also triggers aggregation (Paxinou et al., 2001), suggesting an important contributing role of oxidative stress in protein aggregation. An AD-related protein amyloid beta (Aβ), which is the building block of the hallmark of AD - cortical amyloid plaques (Lansbury, 1996), is capable of generating hydrogen peroxide in rat primary cortical cultures (Behl et al., 1994) through a mechanism that requires metal ion reduction (Huang et al., 1999). This evidence indicates that Aβ is a source that causes the oxidative stress-related cytotoxicity and may contribute to the pathogenesis of AD (Butterfield et al., 2013, Huang et al., 1999). Moreover, other potential contributors for neurodegenerative diseases such as impairment in various kinase signalling pathways and synaptic transmission as well as perturbation of cellular calcium homeostasis, are also linked with oxidative stress (Gandhi and Abramov, 2012).

In summary, there is substantial evidence to support the idea that oxidative stress plays an essential role in neurodegeneration. Therefore, it is important to study more detailed mechanisms of oxidative stress and investigate anti-oxidative pathways in order to improve the treatment to neurodegeneration.

1.2 Mitochondrial dysfunction and neurodegeneration

Mitochondria are multifunctional eukaryotic organelles enclosed by an outer membrane (OM) and an inner membrane (IM). The unique double membrane structure creates two distinct chambers: an intermembrane space (IMS) and matrix (MX) (Alberts et al., 2008).

Mitochondrial dysfunction in aging and a wide variety of diseases has been intensively studied. In recent years, robust experimental evidence has demonstrated the relationship between mitochondria dysfunction and neurodegenerative diseases (Hroudová et al., 2014).

1.2.1 Mitochondrial bioenergetics

Mitochondria are considered as a cellular "power plant", because they generate adenosine triphosphate (ATP) as an energy source through a process named oxidative phosphorylation (Saraste, 1999). The site of oxidative phosphorylation is named the electron transport chain (ETC) (**Figure 1.2.**), which contains five main enzyme complexes embedded in the inner membrane: NADH dehydrogenase (complex I), Succinate-Q oxidoreductase (complex II), Q-cytochrome c oxidoreductase (complex III), Cytochrome c oxidase (complex IV) and ATP synthase (complex V). A series of redox reactions drive electrons along the ETC, which generate a proton gradient that powers the synthesis of ATP (Alberts et al., 2008).

Mitochondria contribute the most to intracellular ROS production. Neuron-damaging ROS is produced as a by-product of oxidative phosphorylation. Superoxide anion radical (O_2.-), for example, is mainly produced at the MX side of IM by complex I of the ETC (Turrens and Boveris, 1980, St-Pierre et al., 2002); while complex III generates O_2.- at both sides of IM (Muller et al., 2004). Apart from ETC complexes, several enzymes

located in other parts are also responsible for ROS production. For instance, localised at the outer membrane, monoamine oxidase (MAO) produces H_2O_2 which leads to an increased level of ROS in mitochondrial MX (Tipton, 1968, Orrenius et al., 2007).

Deficiencies in mitochondrial ETC complexes are associated with neurodegeneration. For example, reduced complex I activity or, to a lesser extent, complex III activity reduction, have been found in substantia nigra and platelet mitochondria of PD patients (Schapira et al., 1989, Parker et al., 1989); in the striatum of HD patients, reduced expression levels of two complex II subunits have been detected (Benchoua et al., 2006).

1.2.2 Mitochondrial anti-oxidative proteins

Mitochondria also have a sophisticated antioxidant defense system that contains both enzymatic and non-enzymatic anti-oxidants to neutralise reactive oxygen species produced by oxidative phosphorylation (Lin and Beal, 2006). For instance, Catalase (Cat), superoxide dismutase (SOD) and glutaredoxin2 (GRX2), are well studied anti-oxidative enzymes (Weisiger and Fridovich, 1973, Arita et al., 2006, Beer et al., 2004); while coenzyme Q10 (Q), cytochrome *c* (cyt *c*) and glutathione (GSH) are important non-catalytic mitochondrial regulators of anti-oxidative pathways (Ernster and Dallner, 1995, Korshunov et al., 1999, Pereverzev et al., 2003, Hayes and McLellan, 1999). Anti-oxidants work coordinately to detoxify mitochondrial ROS. For example, superoxide anion $O_2{\cdot}^-$, which is the primary ROS generated by the ETC, is converted to H_2O_2 by SOD (Turrens, 2003). H_2O_2 is further reduced to H_2O by Cat (Turrens, 2003).

Overexpression of antioxidants such as Cat has been found to have protective effects both *in vitro* and *in vivo*. For example, over-expressing Cat by adenoviral transfection in cortical neuronal cultures establishes neuroprotection against hydrogen peroxide induced cell death (Gáspár et al., 2009); while a transgenic mouse over-expressing mitochondrial

targeted human Cat has an extended lifespan and reduced oxidative damage (Schriner et al., 2005). Mutations in genes encoding several mitochondria related anti-oxidative enzymes are associated with various neurodegenerative diseases. Localised in both cytoplasm and mitochondria (Okado-Matsumoto and Fridovich, 2001, Sturtz et al., 2001), Cu-Zn SOD mutations are one of the causes of familiar ALS (Rosen et al., 1993). Partially localised in mitochondria, protein deglycase DJ-1, which is also known as Parkinson disease protein 7 (PARK7) also has anti-oxidative stress functions (Zhang et al., 2005, Taira et al., 2004a, Billia et al., 2013). Mutations in *DJ-1* contribute to autosomal recessive early onset form of PD (Bonifati et al., 2003a, Bonifati et al., 2003b).

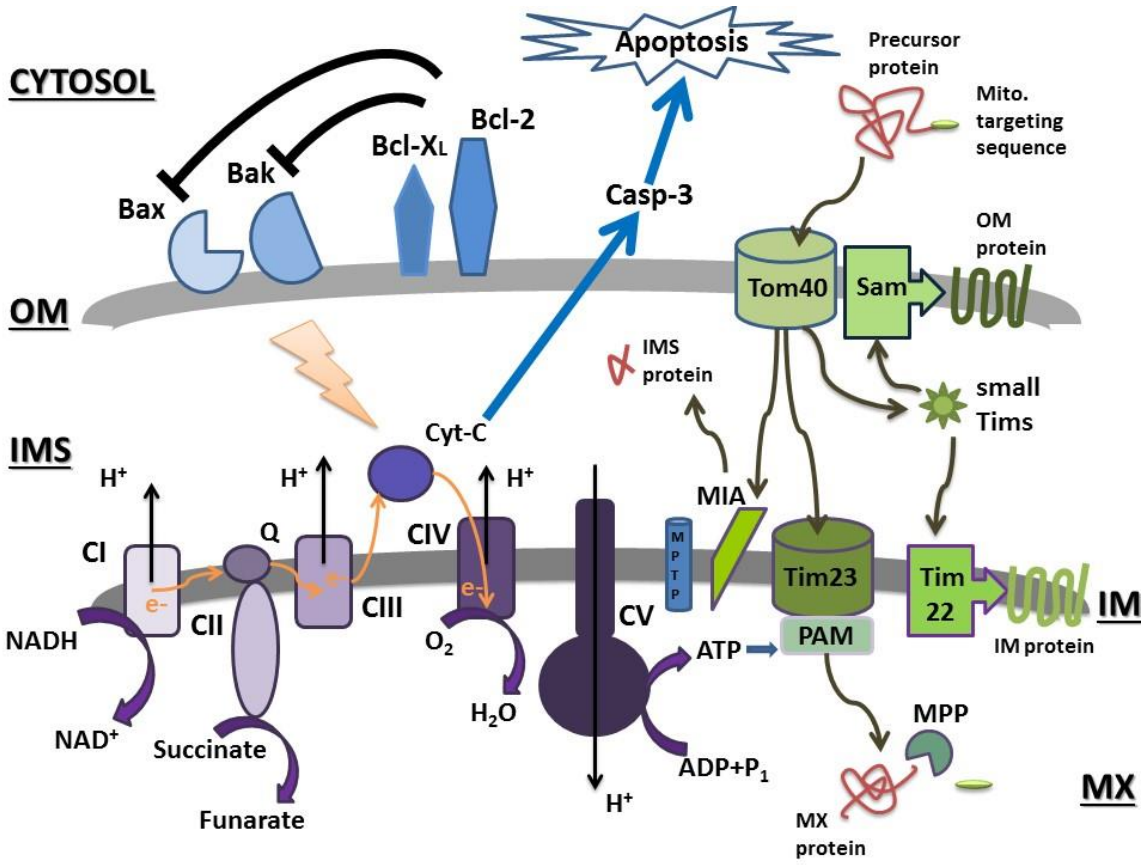

Figure 1.2. Schematic illustration of mitochondrial energy production, protein transport and apoptotic mechanisms and pathways

Mitochondrial energy production related proteins (in purple): Complex I (CI) receives electrons from NADH, an electron carrier of critic acid cycle and pumps out a proton from MX to IMS. Complex II (CII) also accepts electrons through succinate oxidation. Then electrons from both complexes move to coenzyme Q (Q). Q then passes electrons to complex III (CIII), which also pumps out a proton to MX. Electrons then move to CIV via Cyt-C. CIV reduces O_2 to H_2O using H^+ and electrons received from Cyt-C. The proton motive force generated by the three proton pumps then flow back to MX via complex V (CV), an ATP synthase, hereby synthesising ATP. Mitochondrial protein import-related proteins (in green): located at the OM, Translocase of the Outer Membrane (TOM) complex recognises precursor proteins synthesised in cytosol that contains a mitochondrial targeting sequence and then facilitates the entry of proteins across OM. Then, the proteins are diverted to their final destinations: IMS proteins are further guided by Mitochondrial Intermembrane space import and Assembly (MIA) machinery to appropriate locations; MX proteins are translocated across the IM via the Translocase of the Inner Membrane (TIM) complex and presequence translocase-associated motor (PAM). Once in MX, the mitochondrial targeting sequence is removed by mitochondrial processing peptidase (MPP); transmembrane proteins are first guided by small Tim chaperon proteins to Sorting and Assembly Machinery (SAM) located at

the OM, or TIM22 complex located at the IM, hereby facilitating the integration processes. Mitochondrial apoptotic pathway related pro-apoptotic proteins (in blue): The pro-apoptotic B-cell lymphoma 2 (Bcl-2) proteins such as Bcl-2 associated X protein (Bax) translocate to mitochondria upon receiving apoptotic signals, hereby trigger mitochondrial outer membrane permeabilisation (MOMP) that subsequently leads to the release of pro-apoptotic intermediates such as cytochrome C from IMS to cytosol. Cytochrome C release in turn activates subsequent apoptotic factors such as caspase cascades. In contrast, localised in mitochondrial OM, Bcl-2 and Bcl-xL establish anti-apoptotic function by preventing the release of cytochrome C. Additionally, mitochondrial permeability transition pore (MPTP) located in IM is also believed to play a regulatory role in apoptosis by facilitating the translocation of Bax.

1.2.3 Mitochondrial DNA

Mitochondria carry a unique and autonomous double stranded circular mitochondrial DNA (mtDNA) that is located in an irregularly shaped region called nucleoids. Human mtDNA contains 37 genes (**Figure 1.3**), 22 of which are transfer RNAs (tRNAs), 2 are mammalian ribosomal RNAs and 13 of which encode proteins that are requisite for oxidative phosphorylation, including 7 subunits of complex I, 3 subunits of complex IV, 2 subunits of complex V and cytochrome b, which is a subunit of complex III (Anderson et al., 1981, Holt et al., 2007, Garrido et al., 2003, Alexeyev et al., 2013). Proteins involved in mitochondrial DNA replication, transcription and maintenance, for example, the DNA helicase Twinkle, mitochondrial polymerase-γ (POLG), mitochondrial transcription factor A (TFAM), and mitochondrial single-stranded DNA-binding protein are localised in nucleoid (Garrido et al., 2003). Recently, it has been suggested that mitochondrial gene expression is organised and regulated via mitochondrial ribosome containing complexes (Kehrein et al., 2015). However, the mechanism of regulation remains unknown.

Despite the existence of mtDNA damage-repair mechanisms such as base excision repair (BER) and homologous recombination (Alexeyev et al., 2013), and numerous antioxidant proteins are localised in mitochondria (Lin and Beal, 2006), mtDNA is more susceptible to oxidative stress in comparison to nuclear DNA due to its close proximity to the ETC and a lack of protective histones (de Souza-Pinto et al., 2009). 8-oxoguanine is the most common lesion caused by ROS in mitochondria and can subsequently trigger transversion mutations from G:C to T:A (Maki, 2002). Multiple lines of evidence have demonstrated that mtDNA damage occurs more frequently during aging, in parallel with decreasing mitochondrial respiration efficiency (Kraytsberg et al., 2006, Khaidakov et al., 2003, Fayet et al., 2002). While most mtDNA mutations are non-pathogenic, more than

250 mutations have been identified to be deleterious (Tuppen et al., 2010); mitochondrial DNA damage is associated with a variety of neurodegenerative disorders such as the severe, early onset and incurable Leigh syndrome (Finsterer, 2008, Tatuch et al., 1992).

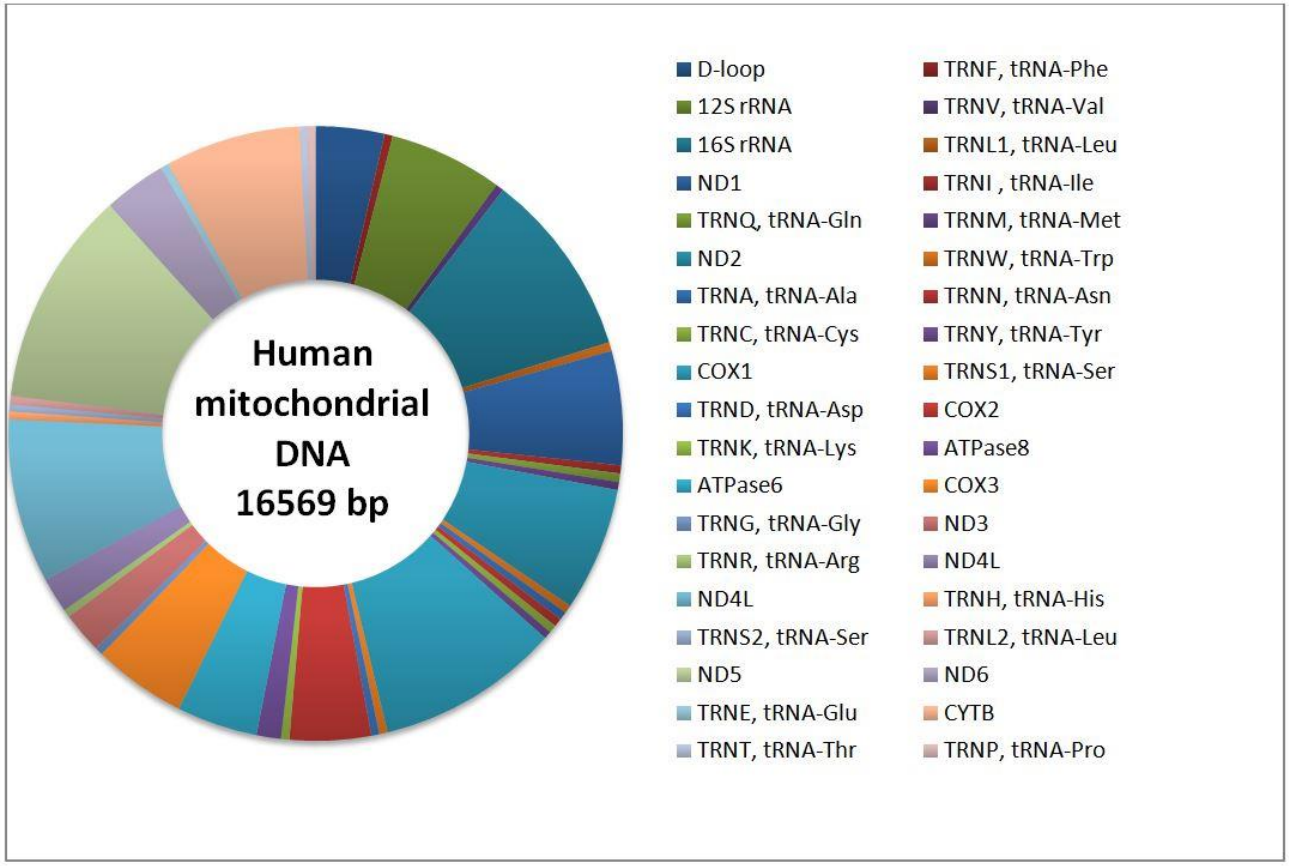

Figure 1.3. Schematic illustration of human mitochondrial DNA
16.6kb double stranded circular mitochondrial DNA contains 37 genes. 13 of them encode proteins that are requisite for oxidative phosphorylation: 7 subunits of complex I (ND1, ND2, ND3, ND4, ND4L, ND5 and ND6), 3 subunits of complex IV (COX1, COX2 and COX3), 2 subunits of complex V (ATPase 6 & 8) and cytochrome b (CYTB), which is a subunit of complex III; 2 ribosomal RNAs (12S and 16S rRNA) and 22 transfer RNAs (tRNAs).

1.2.4 Mitochondrial protein import system

The vast majority of proteins within mitochondria are encoded by nuclear DNA and are synthesised outside mitochondria in their precursor forms (Dolezal et al., 2006, Becker et al., 2011). A mitochondrial protein import system composed of cooperated protein translocases is employed to transport proteins into mitochondria (**Figure 1.2.**). Briefly, located at the outer membrane, Translocase of the Outer Membrane (TOM) complex recognises precursor proteins synthesised in cytosol and then facilitates the entry of proteins across OM. Then, the proteins are diverted to their final destinations: IMS proteins are further guided by Mitochondrial Intermembrane space import and Assembly (MIA) machinery to appropriate locations; MX proteins are translocated across the IM via the Translocase of the Inner Membrane (TIM) complex; transmembrane proteins are first guided by small Tim chaperon proteins to Sorting and Assembly Machinery (SAM) located at the OM, or TIM22 complex located at the IM, hereby facilitating the integration processes (Dudek et al., 2013).

Defects in mitochondrial protein import are associated with several neurodegenerative diseases. In HD, mutant huntingtin (Htt) directly and specifically associates with the TIM23 complex and consequently inhibits mitochondrial protein import (Yano et al., 2014b); mutation in translocase gene *TIMM8* affects the TIM22 pathway and causes deafness-dystonia-optic neuronopathy (DDON) (also referred to as Mohr-Tranebjaerg syndrome (MTS)) (Bauer and Neupert, 2001).

1.2.5 Mitochondria and apoptosis

Mitochondria also act as crucial regulators of programmed cell death. Cells undergo apoptosis mainly through either an extrinsic pathway, which is induced by the binding of

extracellular ligands to cell-surface death receptors; or an intrinsic pathway, which is triggered by the release of internal cell death signals from mitochondria (Green and Llambi, 2015). Essentially involved in the intrinsic pathway (**Figure 1.2.**), mitochondria have interactions with both pro- and anti-apoptotic B-cell lymphoma 2 (Bcl-2) family of proteins. The pro-apoptotic Bcl-2 proteins such as Bcl-2 associated X protein (Bax) translocate to mitochondria upon receiving apoptotic signals, thereby trigger mitochondrial outer membrane permeabilisation (MOMP) that subsequently leads to the release of pro-apoptotic intermediates such as cytochrome C from IMS to cytosol (Wolter et al., 1997, Chipuk and Green, 2008). Cytochrome C release in turn activates subsequent apoptotic factors such as caspase cascades (Zou et al., 1999). In contrast, localised in mitochondrial OM, Bcl-2 and Bcl-xL establish anti-apoptotic function by preventing the release of cytochrome C (Yang et al., 1997). Additionally, mitochondrial permeability transition pore (MPTP) located in the IM is also believed to play a regulatory role in apoptosis by facilitating translocation of Bax (De Giorgi et al., 2002).

Neuronal apoptosis is a hallmark of neurodegeneration (Okouchi et al., 2007). Mitochondria dependent-apoptosis is likely to play an important role in Parkinson's disease (Venderova and Park, 2012). For example, Bax activation was detected in the brain of PD patients (Hartmann et al., 2001). Striatal neuron apoptosis may contribute to HD (Portera-Cailliau et al., 1995); while upon stress, mitochondria-dependent apoptosis was detected in a human cytoplasmic hybrid of HD derived from fusing patient platelets with a mitochondrial DNA-depleted NTERA-2 cell line (Ferreira et al., 2010).

1.2.6 Mitochondrial dynamics

Mitochondria are dynamic and mobile structures that constantly modify their morphology through fusion and fission to meet the needs of cell proliferation, differentiation and stress mitigation (**Figure 1.4**.). Chiefly mediated by dynamin related guanosine triphosphatases (GTPases) (Hoppins et al., 2007), mitochondria form either a tubular network or isolated fragments (Bereiter-Hahn and Voth, 1994). A tubular mitochondrial network formed through fusion improves the efficiency of energy production by combining and redistributing mitochondrial enzymes and metabolites; whereas fragmented mitochondria as a result of fission is suitable for resting cells and the fission process is required to sequester damaged mitochondria (Westermann, 2012).

Mitochondria have a unique double membrane structure. In mammals, fusion of the OM requires cooperation of Mitofusins 1 & 2 (Mfn1 & 2) (Chen et al., 2003), while fusion of the IM is believed to be mediated by OPA1 (Cipolat et al., 2004, Meeusen et al., 2006). Several variants of OPA1 exist due to alternative splicing and processing carried out by IM localised presenilin-associated rhomboid-like (PARL) protein and mitochondrial MX localised protease paraplegin (Ishihara et al., 2006, Cipolat et al., 2006). Mitochondrial fission is facilitated by dynamin-related protein 1 (Drp1) through interacting with mitochondrial fission 1 protein (Fis1) (Smirnova et al., 2001), which is responsible for recruiting Drp1 to appropriate mitochondrial locations (Zhang and Chan, 2007, Yoon et al., 2003). In addition, the movement and distribution of mitochondria are facilitated by cytoskeletal structures such as microtubules (Mishra and Chan, 2014).

Mutations in dynamin related GTPases are the cause or contributing factor of several neurodegenerative disorders. For instance, mutations in Mfn2 causes Charcot-Marie-Tooth disease (Zuchner et al., 2004). Mutations in OPA1 are linked with autosomal dominant optic atrophy (Alexander et al., 2000, Delettre et al., 2000). Induction of

mitochondrial fission and fragmentation has also been observed in drug-stimulated PD models (Barsoum et al., 2006), suggesting that breaking the sophisticated balance between fusion and fission has significant impact in neurodegeneration.

1.2.7 Mitochondrial quality control

Mitochondria employ a form of selective autophagy called mitophagy to eliminate severely damaged mitochondria and prevent cells from apoptosis or necrosis (**Figure 1.4.**) (Lemasters, 2005).

Regulation of mitophagy is largely dependent on the tensin homologue (PTEN)-induced kinase 1 (PINK)/Parkin pathway (Narendra et al., 2008, Narendra et al., 2010). Upon mitochondrial damage, the serine/threonine-protein kinase PINK1 accumulates at depolarised mitochondria by interacting with the Translocase Of Outer Mitochondrial Membrane 7 (TOMM7) of the TOM complex (Hasson et al., 2013). It then phosphorylates ubiquitin at Serine 65 and subsequently activates the E3 ubiquitin ligase Parkin (Shimura et al., 2000, Kane et al., 2014, Koyano et al., 2014a), mediating Parkin translocation to mitochondria thereby activating the downstream pathway of mitophagy. It has been suggested that the activated Parkin then facilitates the formation of mitochondria-targeted poly-ubiquitin chains (Geisler et al., 2010), and these chains are linked via Lysine 27 and Lysine 63 (Geisler et al., 2010). Parkin then mediates the recruitment of autophagy adaptor protein P62/sequestosome-1 (SQSTM1) to mitochondria hereby promoting the final degradation of mitochondria (Geisler et al., 2010). Recently, a Parkin independent mitophagy pathway has been identified, in which PINK1 recruits two autophagy receptors: nuclear dot protein 52kDa (NDP52) and optineurin (OPTN) to mitochondria and directly activates mitophagy without the facilitation of Parkin (Lazarou et al., 2015).

Defects in mitophagy have been shown to be associated with neurodegenerative diseases. For example, mutations of PINK1 or Parkin are believed to be an important contributing factor for the autosomal recessive form of PD (Valente et al., 2004, Kitada et al., 1998). Interestingly, it has recently been discovered that over-expressing PINK1 in a *Drosophila* model of HD is neuroprotective against the neuronal damage caused by HD and can restore mitochondrial morphological abnormalities (Khalil et al., 2015). Moreover, this protective effect is shown to be Parkin dependent, since over-expressing PINK1 in heterozygous Parkin loss-of-function HD flies fails to establish the protective effects, suggesting PINK/Parkin-mediated mitophagy exerts a neuroprotective role in HD (Khalil et al., 2015).

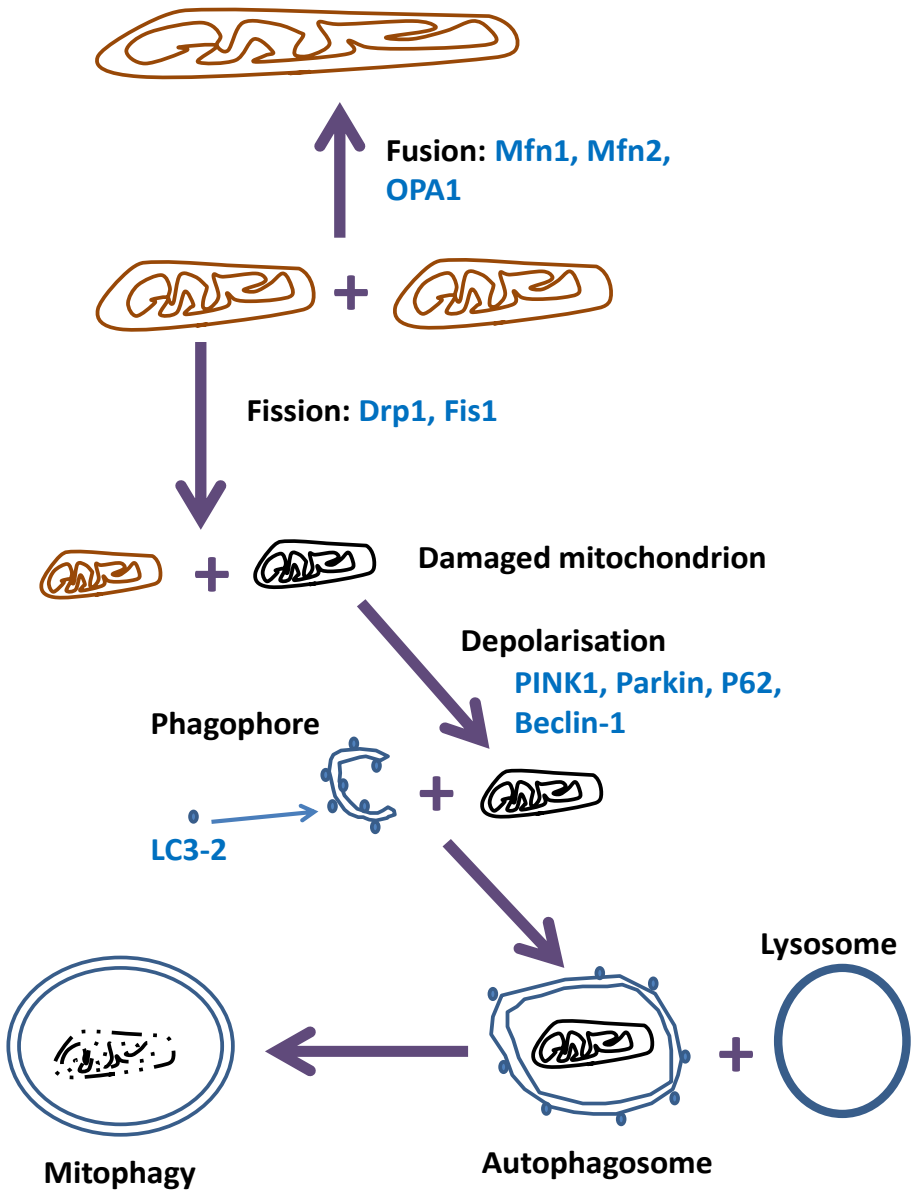

Figure 1.4. Schematic illustration of mitochondrial quality control mechanisms

Fusion is carried out by mitochondrial outer membrane mediators Mfn1 and Mfn2 as well as inner membrane mediator OPA1 to more efficiently produce energy; while fission is regulated by mitochondrial inner membrane mediators Drp1 and Fis1 to reduce energy production and sequester damaged mitochondria. Irreversibly damaged mitochondria are bound by regulators such as PINK, Parkin, P62 and beclin-1, which subsequently recruit LC-3 and forms autophagosome. The autophagosome in turn fuses with lysosome and degrades the damaged mitochondria in the processed called mitophagy.

1.2.8 Mitochondria as therapeutic targets

Due to multiple roles that mitochondrion plays in neurodegenerative diseases, it is considered to be a potential drug target for neurodegenerative disease treatment (Armstrong, 2007). Nowadays, three major classes of mitochondria related drug therapies have been proposed: metabolic antioxidants (general), mitochondrial-directed antioxidants and Szeto-Schiller (SS) peptides (Moreira et al., 2010).

Participating in energy production pathways, metabolic antioxidants such as α-lipoic acid, creatine, N-acetyl-camitine and coenzyme Q (CoQ) assist a number of metabolic enzymes as cofactors. CoQ10, the most predominant form of CoQ in humans and one of the critical cofactors of ETC, *in vitro* pre-treatment in neuronal cells such as human teratocarcinoma NT2N cell-lines stabilises mitochondrial membrane potential upon OS and reduces ROS levels (Somayajulu et al., 2005). Administration of CoQ *in vivo* also shows protective effects in several mouse models of neurodegeneration as well as patients with neurodegenerative disorders. For example, oral CoQ10 supplementation significantly extends the lifespan of a transgenic mouse model of ALS (G93A) (Matthews et al., 1998). For patients with mitochondrial phosphorylation disorders, CoQ10 treatment increases the efficiency of ATP synthesis in lymphocytes (Marriage et al., 2004). In a chronic neurotoxin precursor 1-methyl 4-phenyl-1,2,3,6-tetrahydropyridine (MPTP) mouse model for Parkinsonism, CoQ10 administration alleviates toxic effects in the substantia nigra pars compacta region (SNpc) (Cleren et al., 2008).

Delivering antioxidants directly to mitochondria is thought to increase their efficiency. Mitochondrial directed antioxidant treatment has emerged in some trials. For instance, MitoQ, which is a CoQ conjugated with a lipophilic triphenylphosphonium cation (TPP+), is targeted to mitochondria and interacts with mitochondrial complex II

(James et al., 2007). *In vitro* data have shown protective effects of MitoQ during OS and neurodegeneration. For example, in glutathione depleted human leukemic cells and ρ^0 cells derived from the leukemic cells which lack mtDNA, MitoQ down-regulates ROS production and prevents mitochondrial dysfunction (Lu et al., 2007); while in cultured Friedreich ataxia fibroblasts, MitoQ confers considerably greater protection against OS in comparison with untargeted antioxidants such as its anti-oxidative drug analogue idebenone (Jauslin et al., 2003).

However, most of antioxidant treatments targeting mitochondria are conducted in the onset stage of diseases. The potential prophylactic role of these treatments needs to be explored. Interestingly, it has been shown that targeting antioxidant plastoquinonyl-decyl-triphenylphosphonium (SkQ1) to mitochondria from an early age partially improves age-dependent physiological changes and toxic protein accumulation in an Alzheimer's disease-like senescence-accelerated rat (Stefanova et al., 2014), suggesting a possible prophylactic role of antioxidants in preventing the development of neurodegenerative diseases.

One type of positively charged, aromatic-cationic motif containing tetrapeptide named Szeto-Schiller (SS) peptide is a highly potent compound that targets mitochondria (Zhao et al., 2004, Jin et al., 2014). Particularly, SS-31 targets mitochondrial IM, which is the site of ROS production, hereby maintaining mitochondrial integrity and functions (Zhao et al., 2004). Interestingly, it has been shown that SS-31 prevents both mouse and human neuronal cell-lines, Neuro-2a (N2a), and SH-SY5Y, respectively, from mitochondrial depolarization and apoptosis during oxidative insult triggered by an organic peroxide called tert-butyl-hydroperoxide (tBuOOH) (Zhao et al., 2005). In N2a cells incubated with amyloid beta (Aβ), the major component of amyloid plaque found in AD, SS-31 treatment prevented mitochondrial fragmentation caused by Aβ toxicity

(Manczak et al., 2010); while in primary neurons from a transgenic mouse model of AD, SS-31 treatment increases neurite outgrowth (Manczak et al., 2010). This evidence suggests that SS peptide is a potential drug candidate against neurodegenerative diseases.

To date, a number of proteins with mitochondrial localisation or are functionally linked to mitochondria have been shown to be associated with various neurodegenerative diseases (**Table 1.1.**). These proteins are also potential candidates of novel approaches in treating mitochondrial related neurodegenerative disorders.

Table 1.1.

Mitochondrial related proteins in major neurodegenerative diseases (AD, HD, PD and ALS)

Disease	Protein	Mitochondria related features/functions
AD	APP	---accumulation found in mitochondrial import channels of human AD brains and forms complexes with TOM40 and TIM23 (Devi et al., 2006) ---over-expression of WT and mutant APP shows modifications in mitochondrial morphology and distribution (Wang et al., 2008a)
	Aβ	---establishes mitochondrial accumulation (Caspersen et al., 2005) ---imported into mitochondria via TOM complex and localised to cristae of mitochondrial IM (Hansson Petersen et al., 2008) ---involved in establishing mitochondrial toxicity via Aβ-binding alcohol dehydrogenase (ABAD) (Lustbader et al., 2004)
	PS1 & PS 2	---interact with mitochondrial membrane protein FKBP38 to regulate apoptosis (Wang et al., 2005)
	Tau	---accumulation of tau leads to deficiency in mitochondrial distribution (Kopeikina et al., 2011) ---over-expression of tau leads to mitochondrial elongation by preventing association of fission regulator Drp1 with mitochondria (DuBoff et al., 2012)
ALS	SOD1	---localised in multiple sub-cellular compartments including mitochondria. Mitochondrial fraction is mainly in the IMS (Sturtz et al., 2001) ---loss of SOD1 is more likely to induce oxidative stress in mitochondria than cytosol (Fischer et al., 2011) ---mutant SOD1 introduces abnormalities to both mitochondrial transport and morphology (Magrané et al., 2014)

		---mitochondrial ETC dysfunction detected in transgenic mice expressing mutant SOD1 (Jung et al., 2002)
	TDP-43	---ALS disease-linked TDP-43 mutations impair both mitochondrial dynamics and function (Wang et al., 2013) ---targeting mitochondrial localisation of TDP-43 protects neurons from TDP-43-related toxicity (Wang et al., 2016)
HD	htt	---localised on the cytosolic side of mitochondrial OM (Choo et al., 2004) ---mutant htt causes impairment of mitochondrial protein import (Yano et al., 2014a) ---mutant htt binds mitochondrial fission protein Drp1 and enhances mitochondrial fragmentation (Song et al., 2011)
PD	α-Synulcein	---mitochondrial localisations identified in mouse and human brain (Devi et al., 2008, Li et al., 2007) ---accumulation of α-Synulcein in mitochondria increases ROS level and causes impairment of mitochondrial complex I activity (Devi et al., 2008) ---over-expressing α-Synulcein results in mitochondrial morphological abnormalities (Hsu et al., 2000) ---over-expressing WT and mutant α-Synulcein in mitochondria leads to oxidative stress (Parihar et al., 2008)
	DJ-1	---mainly cytosolic in basal conditions, recruited to mitochondria under oxidative stress (Junn et al., 2009) ---mitochondrial localisations has been found in IMS and MX (Zhang et al., 2005) ---over-expressing mitochondrial DJ-1 results in enhanced neuroprotection against oxidative stress (Junn et al., 2009)
	LRRK2	---localised on the mitochondrial OM (Biskup et al., 2006) ---over-expression of WT and mutant LRRK2 leads

		to mitochondrial fragmentation and slow mitochondrial fusion (Wang et al., 2012b)
	PINK1	---a serine/threonine kinase that establishes mitochondrial localisation (Valente et al., 2004) ---genetically linked to mitochondrial fusion and fission proteins, e.g. Drp1, Mfn2 and Opa1(Deng et al., 2008) ---accumulated on OM of depolarised mitochondria (Matsuda et al., 2010) ---activating the downstream interactor Parkin through phosphorylation of ubiquitin (Koyano et al., 2014b, Kane et al., 2014) --- recruits two autophagy receptors: NDP52 and OPTN to mitochondria and directly activates mitophagy without the facilitation of Parkin (Lazarou et al., 2015)
	Parkin	---mainly cytosolic in basal conditions, recruited to mitochondria by PINK1 under stress (Matsuda et al., 2010) ---functions downstream of PINK1 as an E3 ubiquitin ligase participated in mitophagy (Imai et al., 2000, Narendra et al., 2008) ---the E3 ubiquitin ligase activity is activated through phosphorylation of ubiquitin by PINK1 (Koyano et al., 2014b, Kane et al., 2014)

1.3 Oxr1, an important neuroprotective factor against oxidative stress

1.3.1 The role of Oxr1 as an anti-oxidative protein

Oxidation Resistance 1 (OXR1) was firstly identified in a screen for genes preventing DNA damage in oxidative repair-deficient *E. coli* (Volkert et al., 2000). Oxr1 induction occurs in consequence of stress such as oxidative stress and heat (Elliott and Volkert, 2004).

The anti-oxidative role of Oxr1 orthologues has also been shown in several organisms. For instance, in *Saccharomyces cerevisiae*, deletion of the open reading frame (ORF) of scOXR1 increases sensitivity to H_2O_2 damage (Volkert et al., 2000). LMD-3, which is homologous to human Oxr1, is found not to have enzymatic activities against oxidative stress (Sanada et al., 2014). However, *Caenorhabditis elegans* (*C. elegans*), which carries a LMD-3 mutation has a considerably increased sensitivity to OS and a shorter lifespan than the wild type; whereas deleting mitochondrial SOD genes *sod-2* and *sod-3* improves the lifespan of *lmd-3* mutant, suggesting a potential cooperation of the three proteins (Sanada et al., 2014). Moreover, over-expression of Oxr1 from silkworm (*Bombyx mori*) in fruit fly (*Drosophila melanogaster*) significantly extents the life-span of fruit flies regardless of H_2O_2 insult (Kobayashi et al., 2014). Interestingly, a study in mosquitoes (*Anopheles gambiae*) showed that injection of H_2O_2 into female mosquitoes induces expression of several anti-oxidative enzymes including Cat, Glutathione peroxidase (Gpx), c-Jun N-terminal kinase (JNK) and all mosquito Oxr1 (AgOxr1) isoforms (Jaramillo-Gutierrez et al., 2010). Knocking down the mRNA level of Oxr1 in mosquitoes (approximately 75% reduction) reduces endogenous mRNA levels of both Cat and Gpx, but the level of JNK is not affected (Jaramillo-Gutierrez et al., 2010).

Knocking down JNK (50% reduction) not only reduces the mRNA levels of Cat and Gpx, but also decreases the mRNA level of Oxr1 (Jaramillo-Gutierrez et al., 2010). These results suggested that both Oxr1 and JNK are in an anti-oxidative pathway upstream of Cat and Gpx, and Oxr1 functions downstream of JNK (Jaramillo-Gutierrez et al., 2010). Furthermore, a resistance to *Vibrio cholera* infection in *Drosophila* has been detected when increasing the expression level of a *Drosophila* protein homologous to Oxr1 named mustard (mtd) (Wang et al., 2012c). A gain-of-function mutation in this protein is also sufficient to induce the resistance to *Vibrio cholera* infection in *Drosophila* (Wang et al., 2012c). This resistance is likely to be via the innate immune pathway of *Drosophila* (Wang et al., 2012c). Finally, protective effects have been seen when specifically targeting OXR1 to mouse kidney by mesenchymal stem cell (MSC) injection to treat experimentally-induced renal injury and inflammation (Li et al., 2014). Taken together, these discoveries indicate an evolutionarily conserved role of Oxr1 in stress defence mechanisms, but its function still remains unclear.

1.3.2 Oxr1 has an evolutionally conserved TLDc domain

Oxr1 has several orthologues present in all eukaryotic organisms ranging from yeast to humans (Elliott and Volkert, 2004). They all share a well conserved C-terminal Tre-2/Bub2/Cdc16 (TBC), Lysin motif (LysM), Domain catalytic (TLDc) domain, which consists of approximately 200 amino acids (Durand et al., 2007, Doerks et al., 2002). It was initially hypothesised that the TLDc might have an enzymatic activity (Doerks et al., 2002). However, biochemical experiments later demonstrated that although Oxr1 is found to have direct interaction with H_2O_2 through a conserved C-terminal cysteine residue (Cys753) (Oliver et al., 2011), the rate of this reaction was not in the catalytic range (Oliver et al., 2011).

According to the crystal structure of the TLDc domain of oxidation resistance protein 2 (Oxr2) from zebrafish (Blaise et al., 2012), it shows a combination of anti-parallel β-sheets and α-helices in a conformation distinct from any other known structures.

To date, multiple Oxr1 isoforms have been determined in human and mouse (Oliver et al., 2011, Stowers et al., 1999). The full length (Oxr1-FL) isoform has 3 known domains: a Lysin Motif (LysM), a Glucosyltransferases, Rab-like GTPase activators and Myotubularins (GRAM) and the TLDc domain; whereas the shortest Oxr1 (Oxr1-C) isoform mainly contains the TLDc domain (Fischer et al., 2001, Shkolnik et al., 2008, Volkert et al., 2000). Interestingly, *in vitro* peroxide sensitivity assays demonstrated that the full length and shortest isoforms of Oxr1 were able to protect cells against oxidative damage (Oliver et al., 2011). This suggests that the TLDc domain may have a role in anti-oxidative stress. Recently, a mouse model with an insertion that disrupts the TLDc domain has been generated by mutating the TLDc domain-coding exons (Finelli et al., 2016b). Mice homozygous for this insertion have the same phenotype as the recessive *oxr1* deletion *bella* mouse, thereby further confirms the functional importance of the TLDc domain in Oxr1 (Finelli et al., 2016b).

1.3.3 Oxr1 belongs to a TLDc domain containing protein family

Oxr1 is one member of a TLDc domain containing protein family, which also includes nuclear receptor coactivator 7 (NCOA7), TBC1 domain family, member 24 (TBC1D24), chromosome 20 open reading frame 118 (C20ORF118), KIAA1609 and interferon-induced protein 44 (IFI44) (Falace et al., 2010, Durand et al., 2007, Shkolnik et al., 2008).

According to the alignment of the TLDc containing proteins, the closest member to Oxr1 in this family is NCOA7 (Shkolnik et al., 2008). NCOA7 was first identified as a

nuclear receptor binding protein that regulates the transcriptional activities of oestrogen receptor α (ERα) and peroxisome proliferator-activated receptor γ (PPARγ) (Shao et al., 2002). Similar to Oxr1, NCOA7 also has a smaller isoform called NCOA7B, which mainly contains the TLDc domain (Shkolnik et al., 2008) (**Figure 1.5.A**). Both NCOA7 and NCOA7B have been found to have anti-oxidative roles (Durand et al., 2007, Finelli et al., 2016b). For example, over-expressing either NCOA7 or NCOA7B prevented oxidative stress induced cell death after arsenite treatment (Finelli et al., 2015b). However, the protein level of NCOA7 remains unchanged after oxidative stress insult, despite an increase in the mRNA level (Finelli et al., 2015b, Durand et al., 2007). Additionally, mRNA quantification revealed that similar to Oxr1, the full length NCOA7 is highly expressed in CNS (**Figure 1.5.B and C**); whereas both NCOA7 and NCOA7B have a higher expression level in peripheral organs such as lung, kidney and liver (Finelli et al., 2016b) (**Figure 1.5.B**). However, the function of NCOA7 and NCOA7B still remains largely unknown.

TBC1D24 contains a TBC domain at its N-terminus and a TLDc domain at its C-terminus (Corbett et al., 2010) and is widely expressed in the developing and adult CNS (Falace et al., 2010, Guven and Tolun, 2013) (**Figure 1.5.C**). Importantly, TBC1D24 mutations have been found in a range of disorders (Mucha et al., 2015), including Familial Infantile Epilepsy (FIME) and Progressive Myoclonic Epilepsy (PME) (Muona et al., 2015, Falace et al., 2010). The exact function of TBC1D24 in the nervous

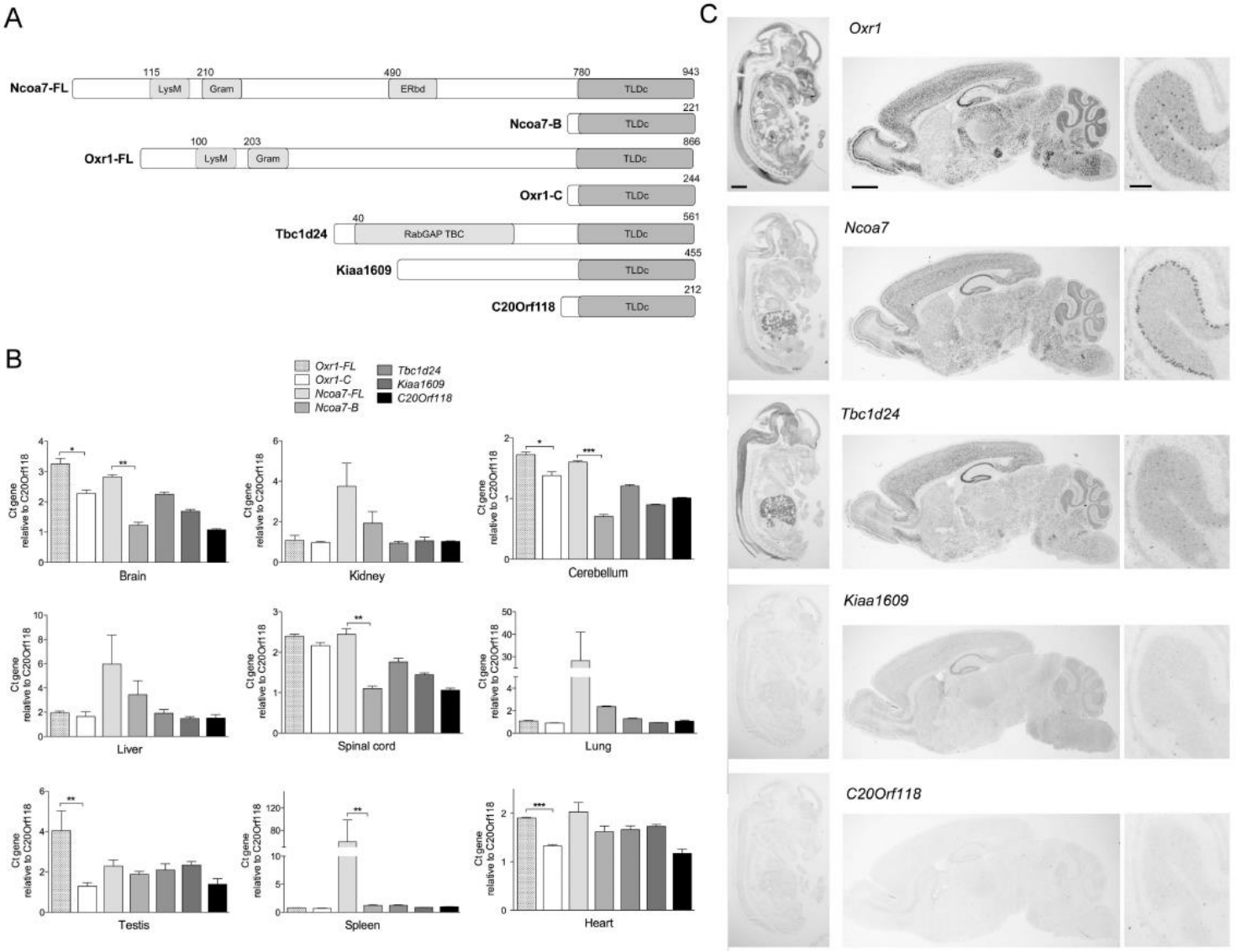
A
Ncoa7-FL
115
210
490
780
943
LysM
Gram
ERbd
TLDc
Ncoa7-B
221
Oxr1-FL
100
203
866
Oxr1-C
244
Tbc1d24
40
561
RabGAP TBC
Kiaa1609
455
C20Orf118
212
B
Oxr1-FL
Oxr1-C
Ncoa7-FL
Ncoa7-B
Tbc1d24
Kiaa1609
C20Orf118
Ct gene relative to C20Orf118
Brain
Kidney
Cerebellum
Liver
Spinal cord
Lung
Testis
Spleen
Heart
C
Oxr1
Ncoa7
Tbc1d24
Kiaa1609
C20Orf118

Figure 1.5. Schematic illustration and expression of TLDc domain containing proteins in mouse embryonic and adult organs

(A) A schematic illustration of the TLDc domain containing proteins: Ncoa7-FL, Ncoa7-B, Oxr1-FL, Oxr1-C, Tbc1d24, Kiaa1609 and C20Orf118. Both Ncoa7-FL and Oxr1-FL have a LysM, lysin motif and a GRAM domain; Ncoa7 has an ERbd, oestrogen receptor binding domain. **(B)** Expression levels of TLDc domain containing proteins in various organs of male mice were quantified by qRT-PCR. Data are shown relative to the expression level of *C20Orf118* and are means ± SEM, analysed by Student's t-test. (*p<0.05; **p<0.01; ***p<0.001). **(C)** TLDc domain-containing genes in the embryo (E14.5, left panel), adult brain (middle panel) or adult cerebellum (right panel) from wild-type male mice revealed by in situ hybridization. Scale bar=1 mm (left and middle panel) and 200μM (right panel). Taken from: Finelli, M. J., L. Sanchez-Pulido, K. X. Liu, K. E. Davies and P. L. Oliver (2016). "The evolutionarily conserved Tre2/Bub2/Cdc16 (TBC), Lysin motif (LysM), Domain catalytic (TLDc) domain is neuroprotective against oxidative stress." Journal of Biological Chemistry, 291: 2751-2763.

system still remains unclear. However, it is known to interact with ADP-ribosylation factor 6 (ARF6) (Falace et al., 2010), which is a Ras superfamily small GTPase involved in dendrite development, branching and formation of dendritic spine (Jaworski, 2007). Of note, over-expression of TBC1D24 in mouse primary cortical neurons significantly elongates the neurons and increases neurite branching, whereas over-expressing a FIME related mutation (A509V) located in the TLDc domain eliminates such effects, but does not affect the interaction between TBC1D24 and ARF6 (Falace et al., 2010). In addition, over-expressing another FIME-related mutation (D147H) located in the TBC domain only partially reduces the neurite morphological features comparing to over-expressing the wild-type TBC1D24, but severely disrupts the interaction with ARF6, suggesting that apart from the TBC domain, the TLDc domain is also functionally relevant to the role of TBC1D24 (Falace et al., 2010). Intriguingly, the structural model of TLDc proposed by Blaise, Alsarraf et al. showed that A590 is in the vicinity of an oxidation reactive C530 residue. The A590V mutation can potentially trigger steric hindrance hereby modifying the structure of TLDc and disrupting its functions (Blaise et al., 2012).

In summary, accumulating evidence has suggested a potential anti-oxidative role of the TLDc family proteins. Mutations in some of these proteins such as the TBC1D24 are associated with several neurological diseases such as FIME and PME (Muona et al., 2015, Falace et al., 2010). However, the function of these proteins remains unclear and worthy of further study.

1.3.4 The role of Oxr1 in the central nervous system

Through studying the recessive *Oxr1* deletion mutant mouse called *bella (bel)*, it was revealed that Oxr1 was important for neurodegeneration. Homozygous *bella* mice have apparently normal growth and development in the first 18 days postnatally (P18),

followed by growth retardation and a severe ataxic gait then develops progressively and leads to death by P26. Apoptosis in cerebellar granule cell layer (GCL) is the only detectable pathological feature in the brain at end-stage (Oliver et al., 2011) (**Figure 1.6. A and B**). Positional cloning revealed that a 190 kb region containing Oxr1 and muscle activator of Rho signalling (STARS) was deleted in *bel* mice (Oliver et al., 2011). Expression studies on wild-type mice detected a high level of *Oxr1* expression, in the cerebellum and the rest of the brain, but expression of STARS was not found in these regions (Oliver et al., 2011) (**Figure 1.6. C**). This suggested that lack of Oxr1 is associated with the establishment of neuropathological features. Furthermore, *bella* mutants showed normal growth patterns after a genetic rescue of *Oxr1* expression in the brain, thereby confirming that the lack of Oxr1 leads to the *bel* phenotype (Oliver et al., 2011). In addition to *in vivo* observations, primary cerebellar granule cells (GCs) from *bella* mice have a significantly higher apoptosis level in comparison with the WT after hydrogen peroxide (H_2O_2) treatment (Oliver et al., 2011). Similar effects were observed when knocking-down Oxr1 in WT GCs using shRNA and over-expressing Oxr1 rescues these phenotypes. Taken together, this evidence further suggests a potential role of Oxr1 in protecting neurons against OS (Oliver et al., 2011).

In addition, Oxr1 has been found to be up-regulated in a pre-symptomatic mouse model of Huntington disease (Liu, K. X., Unpublished data), and spinal cord of both ALS patients' biopsy samples and a pre-symptomatic $SOD1^{G93A}$ mouse model of ALS (Oliver et al., 2011) (**Figure 1.6.D**). These findings indicate a potential role of Oxr1 as an early marker in oxidative-stress linked neurodegenerative diseases.

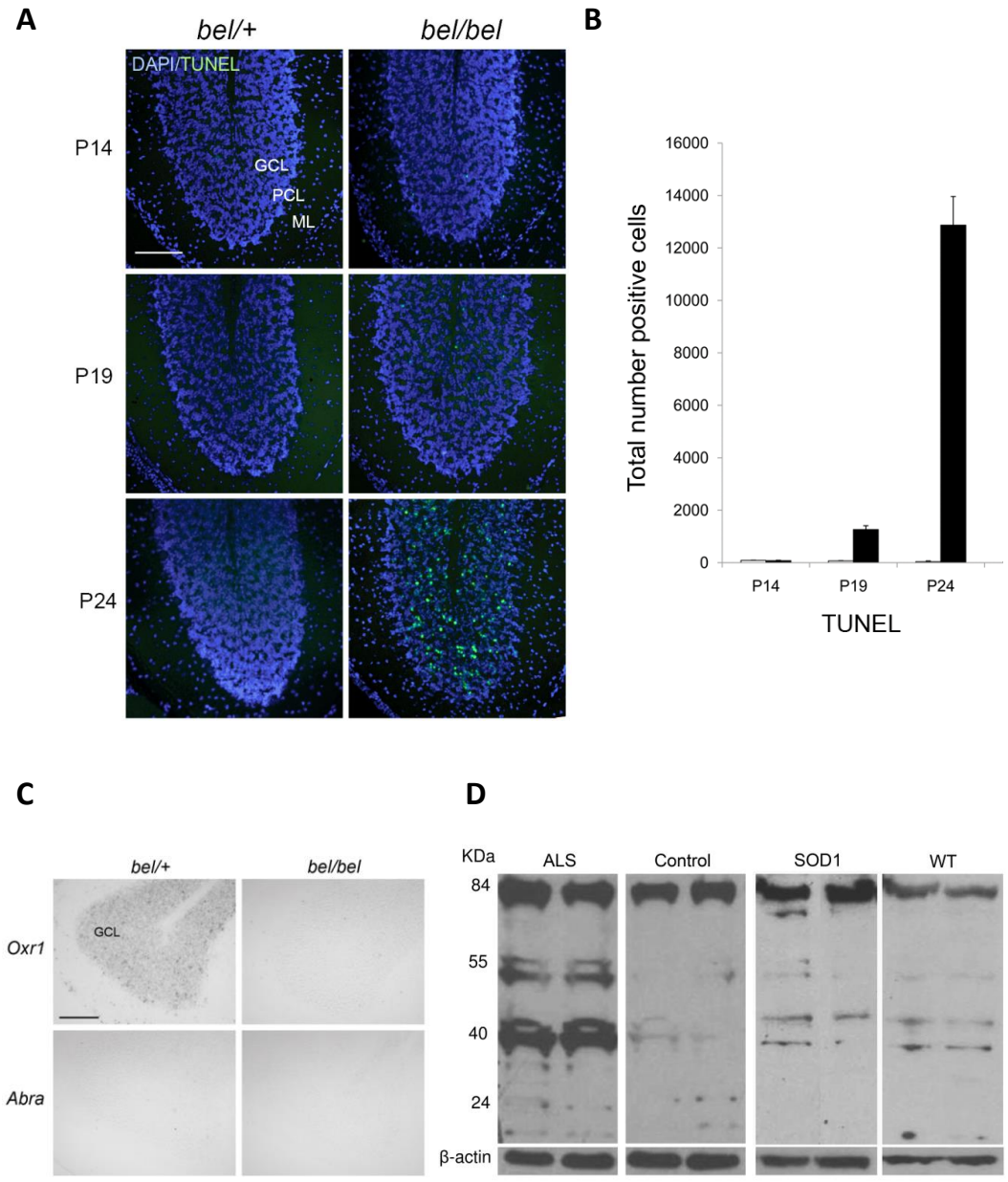

Figure 1.6. Potential role of Oxr1 in the CNS

(A) Cell apoptosis were observed in cerebellar GCL of bel mice. GC apoptosis becomes detectable after P19 by TUNEL staining. **(B)** Quantification of GC cell death: total number of TUNEL staining positive cells is 6 times higher at P24 in comparison with P19. **(C)** The presence of *Oxr1* but not *Abra* in the GCL of the cerebellum in heterozygous (*bel/+*) mice (P24) revealed by *in situ* hybridization. Both *Oxr1* and *Abra* are absent in homozygous (*bel/bel*) mice. **(D)** In comparison with age-matched controls, increasing level of OXR1 is found by western blot in spinal cord biopsy samples from ALS patients. The expression of Oxr1 from the spinal cord tissue of pre-symptomatic

SOD1 G93A low-copy transgenic mice versus the WT. Adapted from: Oliver, P. L., M. J. Finelli, et al. (2011). "Oxr1 Is Essential for Protection against Oxidative Stress-Induced Neurodegeneration." PLoS Genet 7(10): e1002338.

1.4 Aims of thesis

Considerable evidence has shown that Oxr1 plays an important protective role against oxidative stress in different organisms. However, its function is still unknown. So far, some preliminary data on the localisation of Oxr1 within different cell types have been generated. Immunofluorescence suggests mitochondrial localisation of Oxr1 in yeast, HeLa cells and granule neurons (Elliott and Volkert, 2004, Oliver et al., 2011). It has also been suggested that up-regulation of Oxr1 occurs in mitochondria during oxidative stress (Elliott and Volkert, 2004). However, the significance of this is not known.

Since mitochondria are critically involved in ROS generation, anti-oxidative defence mechanisms and neurodegeneration, and Oxr1 is known to play a protective role against OS-induced neurodegeneration, we hypothesise that Oxr1 may have a potentially important regulatory role in mitochondria.

The significance of the localisation of Oxr1 and potential structural or functional alterations in mitochondria lacking Oxr1 need to be studied, and may provide clues as to the function of the protein.

Therefore, the first two aims of this project were to:

1. Investigate the cellular and mitochondrial localisation of different Oxr1 isoforms within the CNS and neuronal cell lines as well as mitochondria-related Oxr1 functions against oxidative stress
2. Determine whether loss of Oxr1 *in vivo* causes mitochondrial disruption/dysfunction

OXR1 has been shown to be down-regulated in the posterior cingulated cortex of PD patients (Stamper et al., 2008), indicating a potential link to PD. Mitochondrial dysfunction is a common feature of PD (Ryan et al., 2015), and dopaminergic neurons in the substantia nigra (SNc) are the neuronal population vulnerable to PD (Double, 2012). Since cerebella granule neurons are the only neuronal population affected in the end-

stage of the *Oxr1* deleted *bella* mouse (Oliver et al., 2011), it is unknown whether loss of Oxr1 can influence other neuronal populations outside of the cerebellum, for example, dopaminergic neurons. Due to the short lifespan of *bella*, it is not a good model for examining much later onset and more slowly progressive neurodegenerative disorders such as PD. Given the potentially important role of OS in PD, it was decided that conditional deletion of *Oxr1* in dopaminergic neurons would be a new and valuable model for assessing selective vulnerability in the midbrain.

Therefore, the third aim of this project was to:

3. Examine whether specific loss of *Oxr1* in dopaminergic neurons causes neurodegeneration *in vivo*

A protein's function is critically dependent on its structure (Studer et al., 2013). Mutations in the amino acid sequence of the protein can have a significant impact on its structure and function (Studer et al., 2013). The crystal structure of the TLDc domain of Oxr2 in zebrafish has been determined (Blaise et al., 2012). Studying potential mutations in the conserved structural region of this doamin may provide clues to its function. Moreover, the Oxr1 deletion mouse model (*bella*) has shown a complete loss-of-function phenotye (Oliver et al., 2011). A less servere intermediate phenotype also needs to be studied. A mutant mouse generated after ENU-induced mutagenesis screening can be a potentially suitable candidate.

Therefore, the fourth aim of this project was to:

4. Identify and characterise ENU-induced mutations in Oxr1 as well as predicting the phenotype of the mouse.

Chapter 2: Material and Methods

2.1 Ethics statement

All procedures relating to animal use have been carried out according to UK Home Office regulations and have been approved by the University of Oxford Ethical Review Panel.

2.2 Mouse Strains

The *bella* (*bel*) mutant contains a genetic deletion of 190 kb spanning the entre Oxr1 gene as previously described (Oliver et al., 2011). The generation of the homozygous *bel*/*bel* mice was carried out by intercrossing heterozygous *bel*/+ mice derived from backcrossing for over 10 generations to the original C3H/HeH female background. Genotyping of the *bella* mutant was carried out as previously described (Oliver et al., 2011), using *bella* specific primers combined with a wild-type control primer or using a polymorphic microsatellite marker: DNA Segment, Chr 15, Massachusetts Institute of Technology 229 (D15Mit229) that is localised in the vicinity of the *bel* deletion. Genotying of the mice was carried out using a polymorphic microsatellite marker D15Mit229.

Oxr1$^{tm1a(EUCOMM)Wtsi}$ knockout-first conditional allele mice with LoxP sites flanking (flox) *Oxr1* exon 15 and 16 generated by the Wellcome Trust Sanger Institute, transgenic mice with β-actin driving FLPe variant recombinase (B6.SJL-Tg(ACTFLPe)9205Dym/J) (Jackson Laboratory) and Rosa26 locus lacZ reporter mice (B6;129S4-Gt(*ROSA*)26*Sor*^{tm1Sor}/J) (Jackson Laboratory) used to confirm the expression of *cre* transgene were all maintained on a C57BL/6 background. DAT-Cre transgenic mice, in which Cre recombinase is specifically expressed in dopaminergic neurons regulated by

bacterial artificial chromosome (BAC) with the endogenous DAT-promoter, was also maintained on a C57BL/6 background.

Mice were housed on a 12-hour light: 12-hour dark cycle and supplied with food and water *ad libitum***.**

2.3 Mitochondria isolation

The purification of mitochondria from tissues and eukaryotic cells was performed using Qproteome mitochondria isolation kit (Qiagen) as per the manufacturer's protocol with minor modifications: freshly excised tissue (whole brain, cerebellum or spinal cord) was washed with 0.9% (w/v) NaCl solution. Then, 500 µl Lysis Buffer containing 1X Protease Inhibitor Solution was added to each sample. The sample was then homogenized using an electric homogenizer (Radleys) at the lowest speed for approximately 10 seconds. Then, 1.5ml Lysis Buffer was added and the homogenate was incubated on a rotator for 10 minutes at 4°C followed by centrifugation at 1000 x g for 10 minutes at 4°C. Cell pellet was then re-suspended in pre-chilled Disruption Buffer containing 1X Protease Inhibitor Solution and the suspension was then subjected to complete cell disruption by a 2 ml syringe with a blunt-ended needle (0.6×25 mm) for at least 10 repeated ejections. Then, the lysate was centrifuged at 1000 x *g* for 10 minutes at 4°C. The supernatant was collected and centrifuged at 6000 x *g* for 10 minutes at 4°C. The pellet was then re-suspended in 1 ml Mitochondrial Storage Buffer and centrifuged at 6000 x *g* for 20 minutes at 4°C. The purified mitochondria were kept in -20 to -80°C prior to experiments.

2.4 Western blotting

Protein samples were separated by 12% or 16% SDS polyacrylamide (SDS-PAGE) gel electrophoresis followed by transferring to PVDF membranes (GE Healthcare). Membranes were incubated in blocking solution containing 5% skimmed milk in TBST (10 mM Tris-HCl pH 7.6, 150 mM NaCl and 0.1% Tween 20) for 1 hour prior to incubation with primary antibodies (**Table 2.1.**) for either 1 hour at room temperature or overnight at 4°C. After washing with TBST three times, membranes were incubated with appropriate HRP-conjugated secondary antibodies (1: 5,000, GE Healthcare). Blots were then developed with the ECL kit (GE Healthcare).

Table 2.1 List of primary antibodies

Purpose	Name and Animal of Origin	Dilution and Company
Sub-cellular and sub-mitochondrial fractionation (western blot)	Anti-COX IV, rabbit	1:2000, Abcam
	Anti- Cyt-C, rabbit	1:1000, Cell Signaling
	Anti-GAPDH, rabbit	1:5000, Sigma-Aldrich; or 1:1000, Cambridge Bioscience
	Anti-TOM20, rabbit	1:200, Santa Cruz
	Anti-VDAC, rabbit	1:1000, Cell Signaling
	Anti-HSP60	1:1000, Cell Signaling
Electron transport chain	MitoProfile total OXPHOS rodent WB antibody cocktail, mouse	1:250, Abcam
	Anti-OxPhos Complex Kit,	1:250, Invitrogen

proteins (western blot)	mouse	
Mitochondrial fusion and fission (western blot)	Anti-Mfn1, mouse	1:250, Abcam
	Anti-Mfn2, mouse	1:250, Abcam
	Anti-OPA1, goat	1:500, Santa Cruz
	Anti-Drp1, rabbit	1:1000, Cell Signaling
	Anti-Fis1, rabbit	1:500, Santa Cruz
	Anti-phospho-Drp1 (Ser616), rabbit	1:1000, Cell Signaling
	Anti-phospho-Drp1 (Ser637), rabbit	1:1000, Cell Signaling
Others (western blot)	Anti-Myc, mouse	1:5000, Sigma-Aldrich
	Anti-HA, mouse	1:1000, Abcam
	Anti-Oxr1, rabbit	1:500, (Oliver et al., 2011)
Immunotstaining	Anti-cleaved Casp3, rabbit	1:200, 400 or 1400, Cell Signaling
	Anti-COX IV, rabbit	1:200, 500 or 1000, Abcam
	Anti-Myc, mouse	1:100, Sigma-Aldrich
	Anti-HA, mouse	1:100 or 1:1000, Abcam
	Anti-HA, rat	1:100, Sigma-Aldrich

	Anti-Flag, mouse	1:100, Sigma-Aldrich
	Anti-TIA-1, goat	1:100, Santa Cruz
	Anti-MAP2, mouse	1:500, Abcam
	Anti-tau, chicken	1:1000, Abcam
	Anti-GABA (A) receptor alpha 6 subunit, rabbit	1:100, Merck Millipore
	Anti-Ubiquitin, rabbit	1:250, Abcam
Immunohistochemistry	Anti-TH, rabbit	1:750, Abcam

2.5 Mitochondria subfractionation

Mitochondria were sub-fractionated by following a swelling-shrinking procedure originally described by Hovius *et al* (Hovius et al., 1990), with minor modifications. Isolated mitochondria from tissues were suspended in buffer A (10 μM KH_2PO_4, pH 7.4) and placed on ice for 20 minutes, then 1 volume of buffer B (32% sucrose, 30% glycerol, and 10 mM $MgCl_2$, pH 7.4) was added. The mixture was sonicated 6 times for 5 seconds using a Soniprep 150 sonicator (Jencons-PLS) then centrifuged at 10 000 g at 4°C for 10 minutes. The pellet was re-suspended in buffer A (10 μM KH_2PO_4, pH 7.4) and incubated on ice for 20 minutes. Then, 1 volume of buffer B (32% sucrose, 30% glycerol, and 10 mM $MgCl_2$, pH 7.4) was added followed by further sonication as above. The re-suspended pellet was centrifuged at 150 000 g at 4°C for 1 hour using a Ti70 rotor (Beckman Coulter). Four fractions were obtained corresponding to the outer membrane (OM), the intermembrane space (IMS), the inner membrane (IM) and the matrix (MX). The IMS and MX supernatants were concentrated using Ultracel-10K filters (Millipore).

The identity of the fractions was confirmed by western blotting using markers specific mitochondrial compartments (**Table 2.1.**).

2.6 Trypsin susceptibility assay

The trypsin susceptibility assay was carried out as described by Choo *et al.* (Choo et al., 2004) with minor modifications. Briefly, increasing concentrations of trypsin (0, 10, 100 and 500 µg/ml) was used to treat isolated mitochondria (150 µg) on ice for 30 minutes. The mitochondria were then centrifuged at 6 000 g at 4°C for 10 minutes for separation from the trypsin solution. Samples were then subjected to western blotting with the Oxr1 antibody and mitochondrial markers as indicted in **Table 2.1**.

2.7 Plasmids

The full-length (NM_130885) or the short mouse Oxr1 isoform (based on NM_001130164 with an additional 28 amino-acid second exon that is shared with Oxr1-FL) was cloned into pCMV/myc/cyto (Invitrogen) to generate the myc-tagged cytoplasmic Oxr1 constructs Oxr1-FL-cyto and Oxr1-C-Cyto, respectively. Oxr1-C was targeted to the mitochondria by cloning into pCMV/myc/mito containing an N-terminal mitochondrial targeting signal (MSVLTPLLLRGLTGSARRLPVPRAKIHSL) (Invitrogen) (Rizzuto et al., 1992) to generate Oxr1-C-Mito. Upon translocation into the mitochondria, the targeting sequence is removed apart from at least four additional amino acids (IHSL) left at the N-terminus of Oxr1.

Site-directed mutagenesis was conducted by using QuikChange II XL Site-Directed Mutagenesis Kit as per the manufacturer's protocol (Agilent Technologies) with minor changes. Primer sequences for mutagenesis PCR (Oxr1 Y644H F and R) were indicated in the List of Primers (**Table 2.2**). PCR was carried out using PfuTurbo DNA polymerase

(Agilent Technologies) with the following reaction conditions: 95°C for 30 seconds (initial denaturation), 55°C for 30 seconds (annealing) and 68°C for 10 minutes (elongation), 13 cycles.

Table 2.2. List of primers

mOxr1 FL SalI F mOxr1 S SalI F mOxr1 NotI R	5'-GAGAGTCGACTCTTTTCAGAAGCCTAAAGGAACC-3' 5'-GAGAGTCGACTCCCGTGTGTGGTATGGGAAAAAAGG-3' 5'-GAGAGCGGCCGCTTCAAAAGCCCAGATTTCAATG-3'
10 kb mitochondria fragment	5'-GCCAGCCTGACCCATAGCCATAATAT-3' 5'-GAGAGATTTTATGGGTGTAATGCG G-3'
117 bp mitochondria fragment	5'-CCCAGCTACTACCATCATTCAAGT-3' 5'-GATGGTTTGGGAGATTGGTTGATGT-3'
mOxr1-FL Kpn F mOxr1-S Kpn F mOxr1 Xba HA R	5'GAGAGGTACCATGGCCTCTTTTCAGAAGC CTAAAGGAAC-3' 5'-GAGAGGTACCATGGCCTCCCGTCTCTG GTATGGGAAAAAAGG-3' 5'-GAGATCTAGATCAAGCGTAATCTGGAACATC GTATGGGTATTCAAAAGCCCAGATTTCAATG-3'
Oxr1 Y644H F Oxr1 Y644H R	5'-CCATGGACGCTTGTGC[1]ACGGTACTGGGAAGCAT-3' 5'-ATGCTTCCCAGTACCGTGCACAAGCGTCCATGG-3' [1] T>C mutation

2.8 Cell cultures

Mouse Neuro-2a (N2a) cells, human negroid cervix epithelioid carcinoma (HeLa) cells and mouse motor neuron cell line (NSC-34) were grown routinely in 75 cm^2 or 175 cm^2 Falcon flasks containing DMEM (Life Technologies) supplemented for 10% Fetal bovine serum (FBS) and 1% Penicillin/Streptomycin (Life Technologies) in a humidified incubator at 37°C in 5% CO_2. Cell passaging was conducted by following the mammalian cell tissue culture techniques protocol (Abcam) when cells reach 90%-100% confluency. The range of passage numbers was between 1 and 20.

Culturing mouse primary cerebellar granule cells (GCs) was conducted as previously described (Bilimoria and Bonni, 2008) with minor modifications: cerebella were dissected from cervical dislocated and decapitated mouse pups (P7). After removing large blood vessels and meninges, cerebella were washed at least 3 times with HHGN dissection solution (1X HBSS (Life Technologies), 2.5mM HEPES (pH7.4), 35mM glucose, 4mM $NaHCO_3$). After washing, the cerebella were immersed in Trypsin-DNase solution (10mg/ml trypsin and 0.1mg/ml DNase in HHGN dissection solution) for 10 minutes at room temperature. Then, the cerebella were washed with HHGN dissection solution 3 times and triturated in DNase solution (0.1mg/ml DNase in BME medium (Life Technologies)). After dissociation, the cells were subject to centrifugation at 200 x *g* for 5 minutes at room temperature followed by resuspension in culture medium for granule neurons (25 mM KCl, 10 bovine growth serum (Hyclone), 1X penicillin-streptomycin-glutamine). Live cell numbers were examined by staining with trypan blue solution and approximately $2*10^5$ cells and $6*10^4$ -$8*10^5$ cells were plated per well of a 96 well plate and per coverslip in a 24 well plate pre-coated with poly-L-ornithine, respectively. 24 hours after plating, cytosine-1-β-D-arabinofuranoside (AraC) was added to give a final concentration of 10μM and a final concentration of glucose (25mM) was

added on day *in vitro* 3 (DIV3). The primary cell culture was maintained by routinely adding glucose (25mM) and culture medium for granule neurons approximately every 48 hours until conducting experiments.

2.9 Transfection

FuGENE 6 method: Transfection of HeLa cells was carried out as per the manufacturer's protocol (Promega). HeLa cells were plated approximately 20 hours prior to the transfection. On the day of transfection, cells were 50%-80% confluence. To conduct transfection, FuGENE 6 reagent (Promega) and DNA were mixed in a ratio of 3:1 (v/w) (e.g. 0.6 µl of FuGENE 6 reagent and 0.2 µg DNA per well of a 24 well plate, or 0.15 µl of FuGENE 6 reagent and 0.05 µg DNA per well of a 96 well plate) in serum free media followed by incubating the mixture for 15 to 45 minutes. Then, the mixture was added to cells and incubated for approximately 1 day at 37°C in 5% CO_2 prior to further experiments.

Magnetofection method: Transfection of NSC-34 cells was carried out as per the manufacturer's instructions (OZ Biosciences). First, NeuroMag reagent (OZ Biosciences) was mixed with DNA diluted in serum free media in a ratio of 3.5:1 (v/w) (e.g. 3.5 µl of NeuroMag reagent and 1 µg DNA per well of a 24 well plate, or 1.75 µl of NeuroMag reagent and 0.5 µg DNA per well of a 96 well plate). The mixture was then incubated at room temperature for 15 to 20 minutes, followed by adding the mixture to cells. After this, the cell culture plate was placed on a magnetic plate for 15 minutes. After removing the magnetic plate, cells were incubated for 18 hours at 37°C in 5% CO_2 prior to further experiments.

2.10 Immunostaining

Cells (HeLa, N2a and GC) on cover slips were washed with PBS followed by incubation in 4% PFA at room temperature for 20-30 minutes. Then, cover slips were washed 3 times in PBS and permeabilised with 0.1% Trition X-100 prior to incubation in blocking solution containing 5% bovine serum albumin (Sigma-Aldrich) and 5% goat serum for 1 hour at room temperature. After this, cover slips were incubated with appropriate primary antibodies (**Table 2.1**) for either 1 hour at room temperature or overnight at 4°C. The cover slips were then washed 3 times in PBS and incubated with Alexa Fluor goat polyclonal secondary antibodies (IgG H&L) (Life Technologies). After the incubation, the cover slips were washed 3 times in PBS and mounted in mounting medium with 4', 6-diamidino-2-phenylindole (DAPI).

2.11 Cell Death Assay

HeLa cells expressing Oxr1-myc with cytoplasmic (Oxr1-C-Cyto) and mitochondrial (Oxr1-C-Mito) signals were exposed to 250 μm H_2O_2 for 4 hours. Cell apoptosis was observed by labelling cells with an anti-cleaved Caspase-3 (Asp175) antibody (1:1400, Cell Signalling). For quantification, five 20× microscopic fields were randomly selected for each coverslip.

2.12 Mitochondria quantification

To quantify COX IV-stained mitochondria in cultured primary GCs, confocal images (1024×1024 pixels) were acquired using by a Leica TCS SP5II confocal microscope (×63 oil objective; scan speed: 200Hz) with LAS AF software. Images were then exported and processed with NIH ImageJ FIJI software; the entire range of grey values (0-255) was

covered by contrast optimization, then, binary images of mitochondria were generated. The number of mitochondria per cell and the average area of a mitochondrion were subsequently evaluated using the particle analysing tool (size in pixel units: 10-infinity; circularity: 0.00-1.00).

2.13 Luxcel Mitoexpress oxygen consumption assay

Luxcel Mitoexpress oxygen consumption assay was carried out by following the manufacturer's protocol (Luxcel Biosciences, Ireland) with minor changes. In brief, NSC-34 cells were plated approximately $3.3x10^5$ cells/cm^2 in DMEM and BME growth media (Life Technologies), respectively in 96-well Falcon plates. The cells were incubated at 37°C, 5% CO_2. On the day of assay, the FLUOstar Omega microplate reader (BMG Labtech) was warmed to 37°C. Then, the Mitoexpress probe was reconstituted in 1 ml of Millipore water and warmed to 37°C before adding to each well at a dilution factor of 1:10. Then, 100 µl of pre-warmed high sensitivity oil was quickly added to each well immediately before the measurement. The plate was then inserted into the pre-warmed instrument and oxygen probe signals were measured with a time-resolved mode using excitation and emission wavelengths of 380 nm and 650 nm, respectively.

2.14 Mitochondrial damage test

Mitochondrial damage assay was conducted based on the amplification of long mitochondrial DNA fragments (Jendrach et al., 2005). Total DNA was isolated from cerebella of WT and *bella* mice. Both a long (10.1 kb) and short (117 bp) mitochondrial fragments were amplified (**Table 2.2.**). PCR for the long mitochondrial fragment was carried out using La-Taq DNA polymerase (Takara) with the following PCR conditions: Initial denaturation at 94°C for 1 minute, followed by 24 cycles of 94°C for 30 seconds,

60°C for 30 seconds and 72°C for 20 minutes. PCR for the short mitochondrial fragment was carried out using Taq DNA polymerase (Sigma-Aldrich) with the following PCR conditions: Initial denaturation at 94°C for 2 minutes, followed by 35 cycles of 94°C for 30 seconds, 56°C for 30 seconds and 72°C for 1 minute. The amount of DNA before and after the PCR reactions was quantified fluorometrically using the PicoGreen dsDNA quantitation reagent (Life Technologies). The fluorescent signal was measured at excitation and emission wavelengths of 485 nm and 528 nm, respectively, using a FLUOstar Omega microplate reader (BMG Labtech).

2.15 Mitochondrial membrane potential assay

TMRE mitochondrial membrane potential was measured in a 96 well black wall microtiter plates (BD Bioscience) by following the manufacturers' protocol (Abcam and ImmunoChemistry Technologies), with minor modifications. GCs were plated at $2*10^5$ cells/well in culture medium for granule neurons (25 mM KCl, 10% bovine growth serum (Hyclone), 1× penicillin-streptomycin-glutamine). Approximately 10 minutes before the assay, 20 μM of FCCP was added to each sample in media. Then, tetramethylrhodamine methyl ester (TMRM) or tetramethylrhodamine ethyl ester (TMRE) was warmed up to room temperature and added to each sample to final concentration of 500 μM. After this, the plate was incubated for 20 minutes at 37°C. After staining, cells were washed with 0.2% BSA in PBS for once. Then TMRE staining was measured with a florescence intensity mode using excitation and emission wavelengths of 549nm and 575nm, respectively.

2.16 Transmission Electron Microscopy (TEM)

Mouse perfusion fixation was performed by Prof. Peter Oliver using the fixative for ultra-structural analysis (2.5% glutaraldehyde, 4% paraformaldehyde and 4.35% sucrose in 0.1M sodium cacodylate buffer, pH=7.2). Fixed brain tissue was prepared according to standard TEM protocols with assistance from Prof. Helen Christian, Department of Physiology, Anatomy and Genetics and Dr. Anna Pielach, Sir William Dunn School of Pathology. Blocks were sectioned using a UC7 ultramicrotome (Leica) and a Diatome diamond knife. Sections (90 nm) were post-stained with lead citrate and imaged on a Tecnai 12 TEM (FEI) operated at 120 kV. Digital images were acquired using a US1000 CCD camera (Gatan) and OneView (Gatan) with assistance from Dr. Errin Johnson, Sir William Dunn School of Pathology.

2.17 BN-PAGE analysis

Blue Native-PAGE analysis was performed using the NovexH Bis-Tris Gel system (Life Technologies) as per the manufacturer's protocol: isolated mitochondrial samples were lysed in sample buffer containing 2.5% n-dodecyl-b-Dmaltoside (DTT) made using the Native PAGE Sample Prep Kit (Invitrogen). The samples were subjected to centrifugation at 17 000 g at 4°C for 30 minutes and loaded (50 µg) onto a native polyacrylamide Novex 3–12% Bis-Tris Gel (Life Technologies). Electrophoresis (PAGE) was then carried out at 4°C. After electrophoresis, proteins were transferred to a PVDF membrane (GE Healthcare) and fixed with 8% acetic acid and blocked with 5% skimmed milk in TBST for 1 hour. Mitochondrial complexes were probed with appropriate antibodies (**Table 2.1.**).

2.18 Mitochondrial complex activity assay

2.18.1 Complex I activity assay

Complex I activity assay was conducted by two methods: The first method was modified from (Ragan et al., 1987), using a spectrophotometric measurement of NADH oxidation at 340 nm in intact mitochondria fractions. Firstly, 1ml of Complex I assay buffer (0.025M potassium phosphate buffer, pH=7.2, 5mM $MgCl_2$, 13mM NADH, 65 µM coenzyme Q (Sigma-Aldrich), 0.25% fatty acid free albumin, 3.6 µM Antimycin A (Sigma-Aldrich)) was added to a cuvette and warmed to 30°C. Secondly, 100 µg of mitochondria were added and mixed with the Complex I assay buffer followed by immediate measurement in a **s**pectrophotometer (Shimadzu) at 340 nm at 30°C for 3 minutes. As a control, mitochondrial samples were treated with 10 µM rotenone after the initial measurement and measured again at 340 nm at 30°C for 3minutes.

The second method was BN-PAGE in-gel activity measurement as previously described (Zerbetto et al., 1997), with minor changes. In brief, mitochondrial sample was loaded onto a native polyacrylamide Novex 3–12% Bis-Tris Gel (Lifescience), and electrophoresis (PAGE) was then conducted. Then, the gel was incubated in 2 mM Tris-Hcl, pH7.4, 0.1 mg/ml NADH and 2.5 mg/ml nitrotetrazolium blue (NTB) (Sigma-Aldrich) for 1hour at room temperature. After incubation, the gel was fixed in fixation reagent containing 50% methanol and 10% acetic acid for 15 minutes at room temperature.

2.18.2 Complex II activity assay

The complex II activity assay was measured by following the protocol as previously described (Dayal et al., 2009), with minor modifications. In brief, this assay measures the colour change of 2, 6-dichloroindophenol (DCPIP) that reflects complex II activity.

Oxidised DCIP that has a blue colour is utilised as the chromophore: once accepting electrons from coenzyme Q, which is an electron carrier, it changes from blue to colourless and leads to the loss of DCPIP absorbance at 600 nm. Firstly, 20 µg purified mitochondria from mouse cerebella were incubated in a cuvette containing assay buffer 1 (0.025 M potassium phosphate buffer, pH=7.2, 5 mM $MgCl_2$, 2 mM sodium succinate (Sigma-Aldrich)) at 30°C for 10 minutes. Then, 10 µl of buffer 2 (0.025 M potassium phosphate buffer, pH=7.2, 600 µM rotenone, 360 µM antimycin A and 5mM DCPIP (Sigma-Aldrich)) were then added to the cuvette and absorbance at 600nm was immediately monitored in a spectrophotometer (Shimadzu) for 1 minute.

2.18.3 Complex III activity assay

Complex III activity was monitored by measuring cytochrome C reduction at 550 nm as described in (Trounce et al., 1996) with changes. Prior to the assay, decylubiquinone was reduced with sodium borohydride ($NaBH_4$) to synthesise decylubiquinonol. Then, 20 µg mitochondria from each sample were incubated in a cuvette of complex III assay buffer (50 mM potassium phosphate, 3 mM sodium azide (NaN_3), 1.5 µM rotenone, 50 µM cytochrome c (Sigma-Aldrich)). Then, decylubiquinol was added to the cuvette to make a final concentration of 50 µM. Reduction of cytochrome *c* was read in a spectrophotometer (Shimadzu) at 550 nm at 30°C for 1 min.

2.18.4 Complex IV activity assay

Complex IV activity was carried out by measuring cytochrome C oxidation at 550nm, a method modified from Wharton et al. (Wharton and Tzagoloff, 1967). Firstly, reduced cytochrome C was synthesised. In Brief, 100 mg cytochrome c (Sigma-Aldrich) was added to 10 ml 0.1M potassium phosphate buffer. Then 10 mg sodium ascorbate was

added. The solution was then transferred to dialysis tubing and submerged in 1 M potassium phosphate buffer. Dialysis against potassium phosphate buffer was carried out at 4°C for 12 to 24 hours. The buffer solution was changed 3 times during the dialysis process. Then, the synthesised reduced cytochrome C was confirmed by spectrophotometry, which showed two peaks at 520 nm and 550 nm respectively. Then, Complex IV assay buffer was made by adding reduced cytochrome C to 0.1 M potassium phosphate buffer to make a final concentration of 50 µM. After that, approximately 100 µg of mitochondria were added and mixed with the Complex IV assay buffer followed by immediate measurement in a spectrophotometer (Shimadzu) at 550 nm at 30°C for 3 minutes.

2.18.5 Citrate synthase activity assay

Citrate synthase activity was assayed by measuring formation of TNB at 412 nm as a result of the reaction between CoA-SH and 5', 5'-Dithiobis 2-nitrobenzoic acid (DTNB) as previously described (Srere et al., 1963), with minor changes. Acetyl CoA was synthesised by dissolving coenzyme A hydrate (Sigma-Aldrich) in ice-cold water to make a 1% solution. Then, 100µl of 1M KHCO3 (Sigma-Aldrich) and 2 µl of acetic anhydride (Sigma-Aldrich) were added, mixed and incubated for 10 minutes followed by another addition of 2 µl acetic anhydride mix and incubated for 10 minutes. Then, the mixture was diluted with 4.416 ml of water. After preparation of Acetyl CoA, 840 µl of water, 100 µl of assay buffer (1mM Dinitrobenzoic acid in 1 M Tris-HCl, pH=8.1), 50 µl of Acetyl CoA and 30 µg of mitochondria were added, mixed and incubated at 30°C for 5 minutes. After incubation, 50 µl of 10 mM Oxaloacetate (Sigma-Aldrich) was added followed by immediate measurement in a spectrophotometer (Shimadzu) at 412 nm at 30°C for 1 minute.

2.19 Mitochondrial stress test

Mitochondrial stress test was carried out using a Seahorse Bioscience XF96 analyser (Seahorse Bioscience Inc.) in 96 well plates at 37°C by following the manufacturer's protocol with minor changes. In brief, GCs at P7 were seeded at $2*10^5$ cells/well in culture medium for granule neurons one week prior to the test. A sensor cartridge was incubated in XF96 Calibrant (Seahorse Bioscience Inc.) in a CO_2 free incubator overnight prior to the test. On the test day, the growth media was removed, washed once and replaced with XF assay media (Seahorse Bioscience Inc.) and the plate was incubated in a CO_2 free incubator for 1 hour at 37°C. The hydrated cartridge was loaded with appropriate volume of mitochondrial inhibitors to achieve final concentrations in each well: port A with oligomycin (3 µM); port B with carbonilcyanide p-triflouromethoxyphenylhydrazone (FCCP) (2 µM) and port C with rotenone and antimycin A (both 2µM). Then, levels of basal respiration, ATP production, proton leak, maximal respiration and non-mitochondrial respiration were measured as described in manufacturer's protocol.

2.20 TUNEL staining

The TUNEL staining was conducted as per the manufacturer's protocol (Roche) with minor modifications. The frozen sections of mouse brain were fixed in 4% PFA in TBS for 20 minutes at room temperature. The slides were then washed in PBS for 30 minutes, followed by incubation in 0.1% sodium citrate and 0.1% Triton X-100 for 2 minutes on ice. The slides were then washed twice for 3 minutes each time in PBS. Then the slides were incubated with TUNEL-Mix (Reagent A and B, 1:1) in a humidified chamber for 60 minutes at 37°C in the dark, followed by washing the slides three times in PBS. The coverslips were then mounted with DAPI.

2.21 Immunohistochemistry

Vibratome sectioned 40 µm free-floating sections were washed with PBS at room temperature for 5 minutes with agitation. Then, endogenous peroxidase was deactivated by incubating in H_2O_2 solution (3% H_2O_2 and 90% methanol) for 15 minutes at room temperature with agitation. After deactivation, sections were washed with PBS and 0.3% Triton X-100 3 times for 5 minutes each time at room temperature followed by incubating in blocking buffer (5% normal goat serum in PBS with 0.3% Triton X-100) for 1 hour at room temperature with agitation. Then, sections were incubated with rabbit anti-tyrosine hydroxylase (TH) (1:750, Abcam) in PBS containing 0.3% Triton X-100, and 5% normal goat serum overnight at 4°C with agitation. The overnight incubation was washed with PBS 3 times for 10 minutes each time at room temperature followed by incubating with biotinylated goat anti-rabbit IgG secondary antibody (1:200, Vector Laboratories) in PBS solution containing 1.5% normal goat serum for 1 hour at room temperature with agitation. The sections were then washed with PBS 3 times for 10 minutes each time at room temperature followed by incubating in an avidin-biotinlyated peroxidase complex (ABC) (Vector Laboratories) for 1 hour at room temperature with agitation. Then, samples were washed with PBS 3 times for 10 minutes each time at room temperature. Immpact 3, 3'-diaminobenzidine (DAB) solution (Vector Laboratories) was added as a substrate of peroxidase to visualise the bound antibodies through immunoreactions. After the reaction, sections were washed with H_2O twice, dehydrated, mounted with hydromount mounting media (National Diagnostics) and coverslipped.

2.22 Stereological quantification of TH positive neurons

Stereological analysis was carried out using the Stereo Investigator software (MBF Bioscience) by following the optical fractionator's settings as described previously (Taylor et al., 2014). The boundaries of substantia nigra pars compacta (SNpc) and ventral tegmental area (VTA) were outlined under a 10 × objective lens using a Leica microscope (Leica) as per the atlas (Paxinos and Franklin, 1997). Dopaminergic neurons, defined as cells with a TH positive cell body and a TH negative nucleus, on vibratome sectioned 40 μm brain slides within the outlined regions were quantified in a blinded fashion under a 40 x objective lens (Leica). Size of counting frames: 50 × 50 μm; size of counting grid: 120 × 160 μm; thickness of optical dissector: 22 μm with 2 μm upper and lower guard zones). Only cells without intersecting forbidden lines were quantified.

2.23 Rotarod test

The accelerating rotarod test was conducted with assistance from Prof. Peter Oliver. Mice aged 12 months and 18 months were placed on a plastic rod of a commercial rotarod apparatus (Ugo Basile) rotating at a default speed of 5 rpm. All mice were facing against the orientation of rotation. The speed was then accelerated from 5 rpm to 40 rpm over a 300 second period. The length of time for mice to stay on the apparatus was determined by either the time latency to fall from the rotating rod, or failure to run on the rotating rod for at least two complete rotations. Mice were tested on 3 consecutive days and a 3-day average was obtained.

2.24 Grip strength test (inverted screen test)

The inverted screen test was conducted with assistance from Prof. Peter Oliver. Mice aged 12 months and 18 months were individually placed in the centre of a wire mesh screen. Then the screen was inverted and then held steady until the mouse had fallen off. The latency to fall from the wire mesh was recorded.

2.25 Statistical analysis

Results were analysed using GraphPad Prism software (GraphPad Software, Inc.). The differences between wild type and mutant or between the various treatments were compared using a Student's t-test or one-way ANOVA or two-way ANOVA test. P-values < 0.05 were considered to be significant. Data were expressed as the mean -/+ S.E.M.

Chapter 3: Investigating the functional consequence of the sub-cellular localisation of Oxr1

3.1. Introduction

Determining the sub-cellular or sub-organellar localisation of a protein is an important step toward understanding its function (Binder et al., 2014). Predicting the sub-cellular and sub-mitochondrial localisation of a protein can be based on its known amino acid sequence using various computational algorithms (Imai and Nakai, 2010). However, the accuracy of prediction remains questionable. So far, the most standard methods for determining sub-cellular protein localisation remain to be cell sub-fractionation and immunostaining cells with markers of different cellular compartments (Rockstroh et al., 2010, Bononi and Pinton, 2015).

Substantial evidence has suggested that the sub-cellular and sub-mitochondrial localisation of various neurodegenerative disease-associated proteins are relevant to their important functions, for example, the Parkinson's disease-related proteins PINK1 and DJ-1 (Gandhi et al., 2006, Narendra et al., 2010, Zhang et al., 2005). PINK1 is mitochondrial OM bound and accumulates at depolarised mitochondria thereby subsequently recruits its downstream interacting partner, Parkin to its mitochondrial localization (Narendra et al., 2010, Okatsu et al., 2015). DJ-1 has been shown to be localised in several mitochondrial compartments such as the IM and MX (Zhang et al., 2005, Kaneko et al., 2014), and its matrix localisation may be involved in oxidative stress or nutrient deprivation response (Calì et al., 2015). In addition, translocation of proteins into and out of mitochondria is sometimes correlated with the stress response and mitochondrial dysfunction. For example, mitochondrial IMS-localised Cyt-C is released

into cytosol during apoptosis (Kluck et al., 1997, Yang et al., 1997), whereas DJ-1 translocates to mitochondria under oxidative stress (Junn et al., 2009).

Accumulating data have demonstrated that up-regulating the endogenous level of mitochondrial anti-oxidative proteins such as SOD and mitochondrial glutathione peroxidase (GPx) is protective against ROS insults (Greco and Fiskum, 2010); while exogenously targeting anti-oxidants such as MitoQ to mitochondria is also capable of preventing ROS damages (Oyewole and Birch-Machin, 2015). However, to date, only a few anti-oxidants, for example, MitoQ have been used to conduct *in vivo* trials with mixed success and potency (Oyewole and Birch-Machin, 2015). Therefore, new anti-oxidative proteins and pathways need to be explored.

High expression level of Oxr1 has been detected in CNS such as brain and spinal cord (Oliver et al., 2011, Finelli, 2010, Liu et al., 2015b). To date, some preliminary data on the localisation of Oxr1 within different cell types have been generated. For example, expressing a GFP-tagged yeast Oxr1 from the endogenous *OXR1* promoter established a mitochondrial localisation in yeast (Elliott and Volkert, 2004). Using an antibody that specifically recognises the C-terminal domain of Oxr1, Elliott *et al.* further showed the mitochondrial localisation of Oxr1 in HeLa, Hep2 and COS cells; whereas at least in yeast and HeLa cells, there is little evidence for the presence of nuclear Oxr1 (Elliott and Volkert, 2004). Several Oxr1 isoforms have been found in mammalian cells (Oliver et al., 2011), and a conserved TLDc domain has been identified in all the isoforms through cDNA cloning, qRT-PCR and western blotting (Oliver et al., 2011, Murphy and Volkert, 2012). However, the sub-cellular and potential sub-mitochondrial localisation of these individual isoforms has not been investigated.

It had been shown previously that under heat stress or H_2O_2 induced oxidative stress, expression of yeast Oxr1 was up-regulated, but whether this up-regulation is

mitochondria- specific remains unclear (Elliott and Volkert, 2004). In HeLa cells, heat or oxidative stress induced OXR1 up-regulation was observed in both mitochondria and cytoplasm (Elliott and Volkert, 2004). Interestingly, under oxidative stress, in mouse GCs and N2a cells, Oxr1 was found to establish a mitochondrial localisation and co-localised with mitochondrial marker COX IV (Oliver et al., 2011). However, which isoform was co-localised with COX IV remains unknown (Oliver et al., 2011). Although a growing body of evidence has shown that Oxr1 plays an important protective role against oxidative stress in several organisms and in the CNS, whether its anti-oxidative role is sub-cellular localisation dependent has also not been systematically studied yet.

Mitochondrial morphological abnormalities, dynamics (fusion, fission and migration) impairments and bioenergetics defects are common features of ALS (Muyderman and Chen, 2014). For example, mutations in mitochondrial Cu/Zn SOD establish genetic linkage to familial ALS (Rosen et al., 1993). Interestingly, mutant SOD1 has been shown to have several mitochondrial localisations including MX, IMS and the cytoplasmic side of OM (Vande Velde et al., 2008, Vijayvergiya et al., 2005, Liu et al., 2004). Mutant SOD1 is believed to be detrimental to both mitochondrial morphology and function; studies based on transgenic G93A mutant ALS mouse model show mitochondrial morphological changes such as swollen shape and structural alteration of cristae (Wong et al., 1995). Defects of mitochondrial Ca^{2+} loading capacity and mitochondrial metabolic abnormality in the CNS before and at onset of the disease have also emerged (Damiano et al., 2006, Mattiazzi et al., 2002).

Apart from SOD1, mutations in several other genes, for example, transcriptional regulator TAR DNA-binding protein 43 (TDP-43) and RNA-binding protein fused in sarcoma (FUS) and chromosome 9 open reading frame 7 (C9ORF72) are thought to be contributing factors of ALS and frontotemporal lobar degeneration (FTLD) (Neumann et

al., 2006, Arai et al., 2006, Kwiatkowski et al., 2009, Vance et al., 2009, DeJesus-Hernandez et al., 2011). Recently, a mouse model expressing a G4C2 repeat expansion in C9ORF72 has been generated and shown to cause TDP-43 pathology, neuronal loss and behavioural deficits (Chew et al., 2015).

The normal subcellular localisation of TDP-43 is in the nucleus, where it establishes potential roles in splicing regulation and genome stability maintenance (Lagier-Tourenne et al., 2010). Nuclear depletion and cytoplasmic aggregation of mutant TDP-43 is one of the most common histopathological features of ALS (Forman et al., 2007). It has been found that cytoplasmic TDP-43 can co-localise with mRNA and mRNA binding protein-containing aggregates called stress granules under oxidative stress (Anderson and Kedersha, 2008, Colombrita et al., 2009). Under stress, stress granules are thought to be formed as a protective structure to limit the translation of mRNAs that are non-essential for cell survival (Lindquist, 1981, Li et al., 2013). However, the exact mechanism of TDP-43 and stress granule interaction still remains unclear.

Importantly, growing evidence has also suggested links between mitochondrial impairments and ALS related TDP-43 mutations such as M337V and Q331K (Sreedharan et al., 2008, Carrì et al., 2015). For example, in mouse NSC-34 motor neuron-like hybrid cells, over-expressing ALS-related mutant TDP-43 (Q331K and M337V) causes mitochondrial distribution abnormalities, increased mitophagy and reduction in mitochondrial membrane potential, one of the key parameters of mitochondrial function (Duan et al., 2010, Hong et al., 2012). It has also been shown in NSC-34 cells and primary motor neurons that mitochondrial morphological abnormalities can be caused by TDP-43 mutants (Q331K and M337V) (Lu et al., 2012, Wang et al., 2013). Of note, previous studies have also demonstrated that *in vitro* over-expression of wild type TDP-43 can also lead to mitochondrial impairments similar to the damage

caused by the mutants (Carrì et al., 2015). Interestingly, in human HEK293 cells and primary motor neurons, over-expressing the M337V mutant is more cytotoxic than the wild type TDP-43 or an A382T mutant (Mutihac et al., 2015). In addition, over-expression of the human M337V mutant in mouse has demonstrated a more severe phenotype compared to over-expression of the wild-type protein (Janssens et al., 2013).

Studies from Kay Davies' group demonstrated that Oxr1-S interacts with both TDP-43 and FUS (Finelli et al., 2015a). Under oxidative stress, Oxr1-S over-expression can reduce wild-type and mutant TDP-43 and FUS recruitment to cytoplasmic inclusion bodies (Finelli et al., 2015a). However, whether Oxr1-S over-expression also has a protective effect on mitochondrial impairments caused by TDP-43 mutations remains unknown.

3.2. Aims of Chapter 3

Therefore, the goals of this chapter were to: (1) investigate the cellular and mitochondrial localisations of different Oxr1 isoforms; (2) determine whether mitochondrial localisation is required for protection against oxidative stress; (3) determine whether Oxr1 over-expression can protect mitochondria from impairments triggered by TDP-43 mutations.

3.3. Results

3.3.1. Different isoforms of Oxr1 are expressed in specific sub-cellular compartments

To date, several Oxr1 isoforms have been found in mammalian cells (Oliver et al., 2011). However, the subcellular localisation of these individual isoforms has not been

studied. To address this important question, total tissue homogenates, cytosolic and mitochondrial fractions from the mouse whole brain, cerebellum and spinal cord were analysed by western blotting using an antibody against an epitope in the TLDc domain of Oxr1 (Oliver et al., 2011).

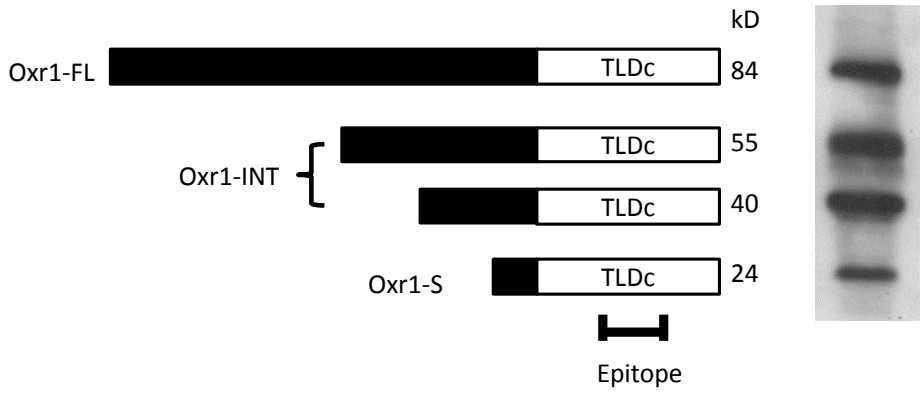

Figure 3.1. Isoforms of Oxr1

(**A**) A schematic illustration of four predicted Oxr1 isoforms in mouse detected by western blot in this study: Oxr1 full-length (FL), approximately 84 kDa; intermediate isoforms: approximately 55kDa and 40kDa, and the shortest (Oxr1-S) isoform: approximately 24kDa. (**B**) Western blot of total adult mouse whole brain homogenate. Total brain homogenate was blotted with anti-Oxr1 antibody that specifically targets an epitope within the shared C- terminal TLDc domain.

In total brain tissue lysate, four main isoforms of Oxr1 were detected in mouse brain at approximately 84, 55, 40 and 24 kDa (**Figure 3.1**). Upon fractionation, however, the shortest isoform (Oxr1-C, approximately 24 kDa) was almost exclusively localised in mitochondria of the brain (**Figure 3.2A**), while the full-length Oxr1 isoform (Oxr-FL, approximately 84kDa) was localised in the cytosolic fraction (**Figure 3.2A**). In addition, the two intermediate isoforms were enriched in the mitochondrial fraction. In the cerebellum and spinal cord, a similar distribution was observed, although Oxr1-C could not be detected (**Figure 3.2B and C**). These data suggest that some, but not all, Oxr1 isoforms are localised to the mitochondria.

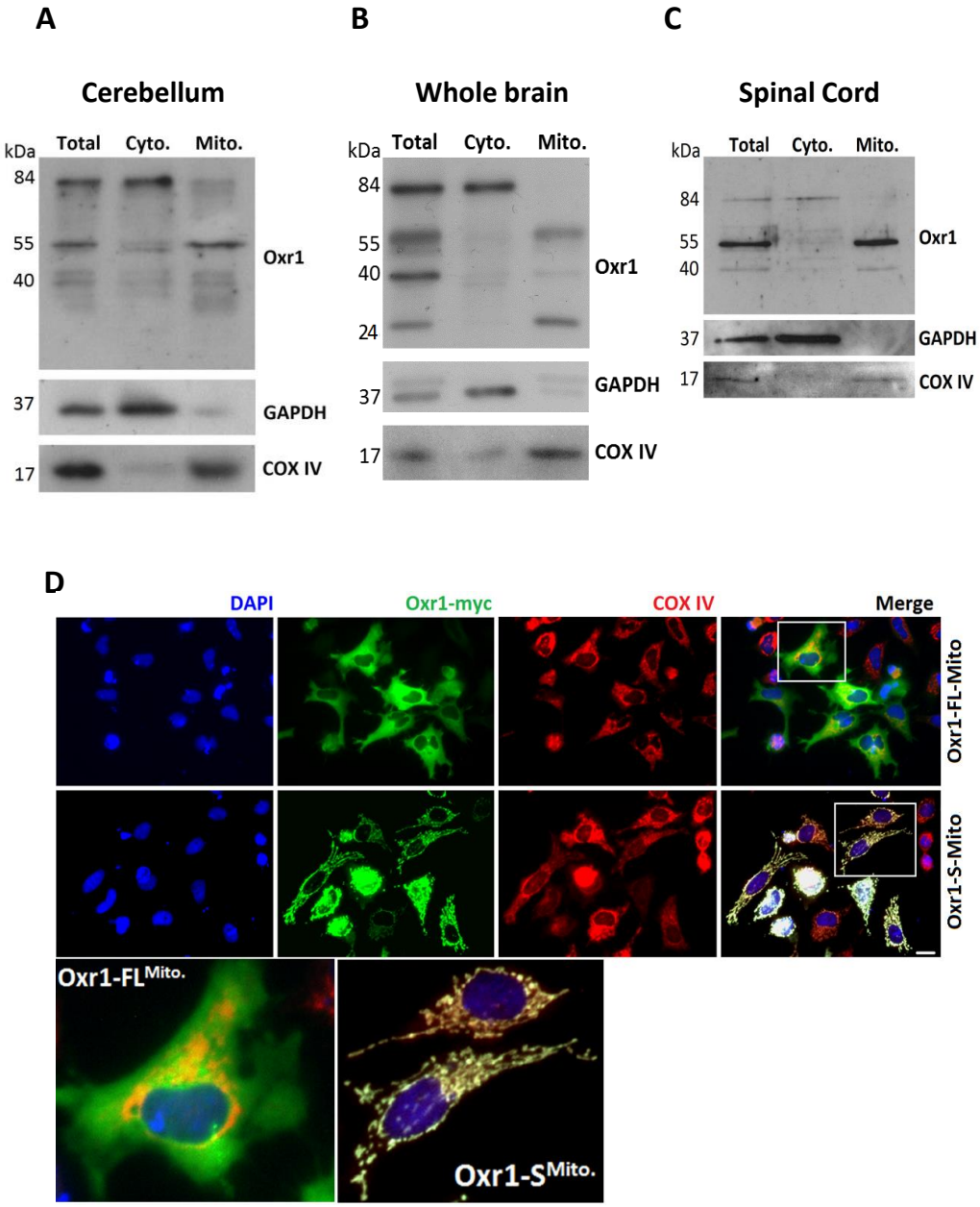

Figure 3.2. Oxr1 isoforms display differential cellular localisation patterns

(A, B and C) Total tissue homogenate, cytoplasmic and mitochondrial fractions from whole brain (B) cerebellum (C) and spinal cord (D) were subjected western blot analysis with anti-Oxr1, anti-GAPDH as a cytoplasmic marker and anti-COX IV as a mitochondrial marker. **(D)** Representative images of HeLa cells transfected with Oxr1-FL-Mito or Oxr1-S-Mito constructs and immunostained with anti-Myc and anti-COX IV. Oxr1-FL-Mito transfected cells displayed a cytoplasmic diffuse pattern, while Oxr1-S-Mito was co-localised with mitochondrial marker COX IV with a typical mitochondrial filamentous morphology, scattered in the cytoplasm. Scale bar = 20 µm.

Predicting the sub-cellular localisation of a protein can be based on its known amino acid sequence using various computational algorithms (Imai and Nakai, 2010). In principle, these computational programmes scan through the amino acid sequence to detect potential nuclear localization signals (NLS) (Cokol et al., 2000), N-terminal targeting sequences (Petsalaki et al., 2006, Small et al., 2004), or localization-specific protein structure (Andrade et al., 1998). To date, several prediction methods have been developed, for example, WoLF PSORT (Horton et al., 2007), MultiLoc2 (Blum et al., 2009) and MitoFates (Fukasawa et al., 2015).

Using an online protein sub-cellular localization prediction programme named PSORT II, it has been postulated that a mitochondrial localisation signal (MLS) is present at the N-terminus of Oxr1 in yeast (scOxr1) (Elliott and Volkert, 2004). However, using the same method, or MitoFates, a more recently developed online analytic method for predicting cleavable N-terminal mitochondrial targeting sequences (Fukasawa et al., 2015), this signal was not found in any of the known isoforms of OXR1 in mouse or human. Since the sub-cellular fractionation results obtained from mouse tissue have demonstrated the mitochondrial localisation of the shorter Oxr1 isoforms, but not the full-length isoform, it was speculated that the presence of Oxr1 in mitochondria is not necessarily dependent on MLS with known features. Therefore, other factors such as the size of protein could limit the cellular distribution pattern.

To examine this further, the shortest Oxr1 isoform (Oxr1-S), which is equivalent to the Oxr1-C, and the full-length Oxr1 (Oxr1-FL) were cloned with an additional N-terminal mitochondrial MLS (Oxr1-S-Mito and Oxr1-FL-Mito). These two constructs were transfected into HeLa cells (**Figure 3.2.D**). If was expected that both Oxr1-FL and Oxr1-S should be detectable in mitochondria by post-transfection immunostaining. However, although Oxr1-S-Mito was indeed co-localised with the mitochondrial marker

COX IV and presented a typical mitochondrial filamentous morphology (**Figure 3.2.D**); Oxr1-FL-Mito did not co-localise with COX IV and established a typical cytoplasmic diffuse pattern (**Figure 3.2.D**). These results suggest that the localisation of the shorter isoforms of Oxr1 to mitochondria may be not only dependent on an MLS, but also facilitated by other factors, such as a maximal size or a potential internal motif for mitochondrial localisation (Bolender et al., 2008, Schmidt et al., 2010).

3.3.2 Mitochondrial Oxr1 is predominantly localised at the cytosolic side of mitochondrial outer membrane

Next, to determine the sub-mitochondrial localisation of Oxr1, mitochondria from mouse cerebellum were separated to the OM, the IMS, the IM and the MX by ultracentrifugation prior to immunoblotting. Interestingly, these results indicate that the mitochondrial isoforms of Oxr1 are localised in the mitochondrial OM and IM, and were barely detectable in the IMS and MX (**Figure 3.3A**). In addition, the specificity of the sub-fractionation was confirmed using a set of specific mitochondrial markers (**Figure 3.3A**). It is noted that the OM marker voltage-dependent anion channel (VDAC) was also observed in the IM, while the IM marker COX IV was also detected in the OM fraction. This is likely due to incomplete OM/IM separation caused by multiple contact points between mitochondrial membranes as previously described (Zhang et al., 2005, Choo et al., 2004, Gandhi et al., 2006).

To further characterise the potential membrane-associated localisation of Oxr1 within mitochondria, a trypsin susceptibility assay was conducted (Choo et al., 2004), where intact mitochondria purified from mouse brain were incubated with increasing concentrations of trypsin (**Figure 3.3B**). All Oxr1 isoforms were digested at the lowest (10 μg/ml) trypsin concentration, apart from the 55 kDa isoform that required 100 μg/ml (**Figure 3.3B**). As a positive control, TOM20, a receptor loosely associated with the cytosolic side of the OM (Schleiff and Turnbull, 1998) was assayed in parallel and this also appeared to have poor resistance to trypsinisation (**Figure 3.3B**) as expected. Conversely, VDAC and COX IV, transmembrane proteins localised in OM and IM, respectively, were not digested even in the presence of high concentration (500 μg/ml) of trypsin (**Figure 3.3B**); while cytochrome C and HSP60, localised in IMS and MX, respectively, were also barely affected (**Figure 3.3B**). Taken together, these data suggest

that the shorter isoforms of Oxr1 are loosely associated with the outer mitochondrial membrane, potentially facing towards the cytosol.

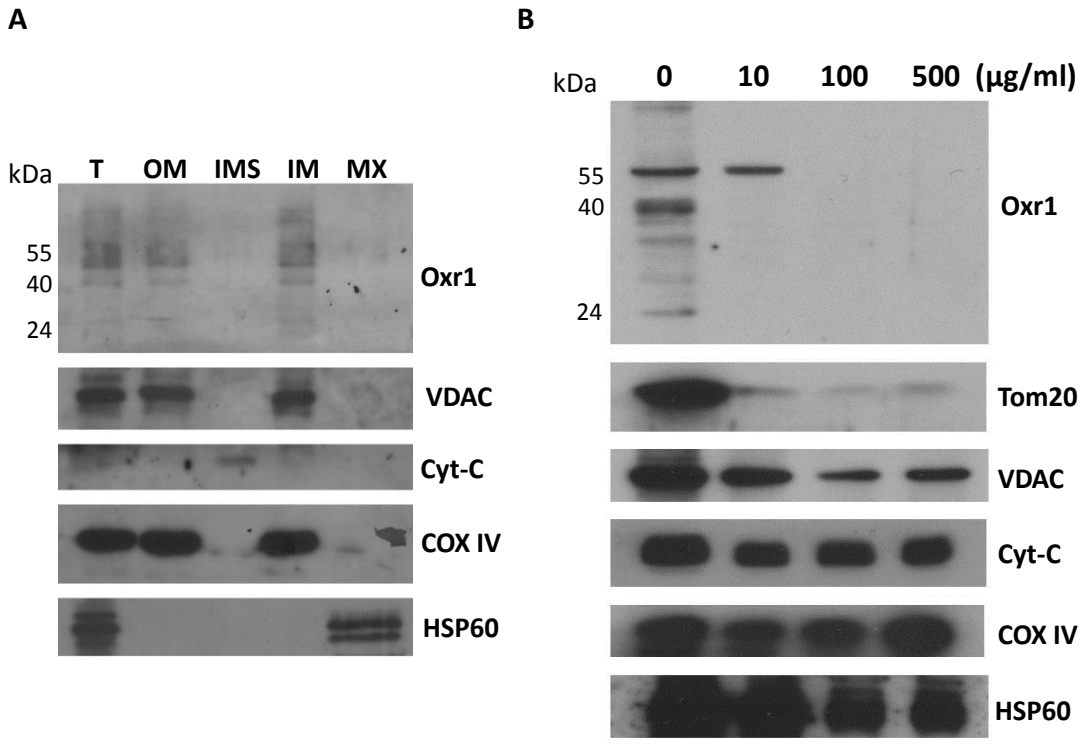

Figure 3. 3. Mitochondrial Oxr1 is associated with mitochondrial outer membrane

(A) Mitochondria purified from mouse cerebellar tissue were sub-fractionated into OM, IMS, IM and MX through ultracentrifugation. Sub-fraction of each compartment as well as the total mitochondrial sample (T) were subjected to western blotting using the anti-Oxr1 antibody and specific markers for individual compartment: TOM20 and VDAC for the OM, Cyt-C and COX IV for the IMS and IM, respectively and HSP-60 for MX. Oxr1 is mainly detected in OM and IM fraction. **(B)** Mitochondria purified from mouse brain were incubated with increasing concentrations of trypsin prior to immunoblotting with mitochondrial marker proteins.

3.3.3 Endogenous levels Oxr1 isoforms remain stable after oxidative stress insult and ageing

The transcriptional level of yeast Oxr1 has been found to be increased under oxidative stress, while in HeLa cells, the protein level of Oxr1 was also up-regulated (Elliott and Volkert, 2004). Interestingly, in N2a cells treated with H_2O_2, the transcriptional levels of Oxr1-FL and Oxr1-C were up-regulated at different times (Finelli et al., 2015a). However, the potential mechanism behind this isoform-specific and transient induction of Oxr1 at mRNA level remains unknown. In addition, whether Oxr1 can translocate between cellular compartments under stress also has not been studied.

Therefore, to examine the localisation of endogenous Oxr1 isoforms in N2a cells under basal conditions or oxidative stress, N2a cells were treated with 250 μM H_2O_2 for 1 or 2 hours. Cells were then harvested and subjected to sub-cellular fractionation. Similar to the sub-cellular fractionation results in mouse tissue, in the untreated group, the Oxr1-FL (84kDa) is localised in cytosolic fraction while the short (24kD) isoform is localised in mitochondria (**Figure 3.4A**), same as the localizations in mouse tissue. After treating with H_2O_2, the sub-cellular levels of Oxr1 isoforms appeared to have a trend towards reduction, but this trend was spastically non-significant within this time frame (**Figure 3.4B**). Taken together, these data suggest that the endogenous Oxr1 does not shuttle from mitochondria to cytoplasm after oxidative stress induction.

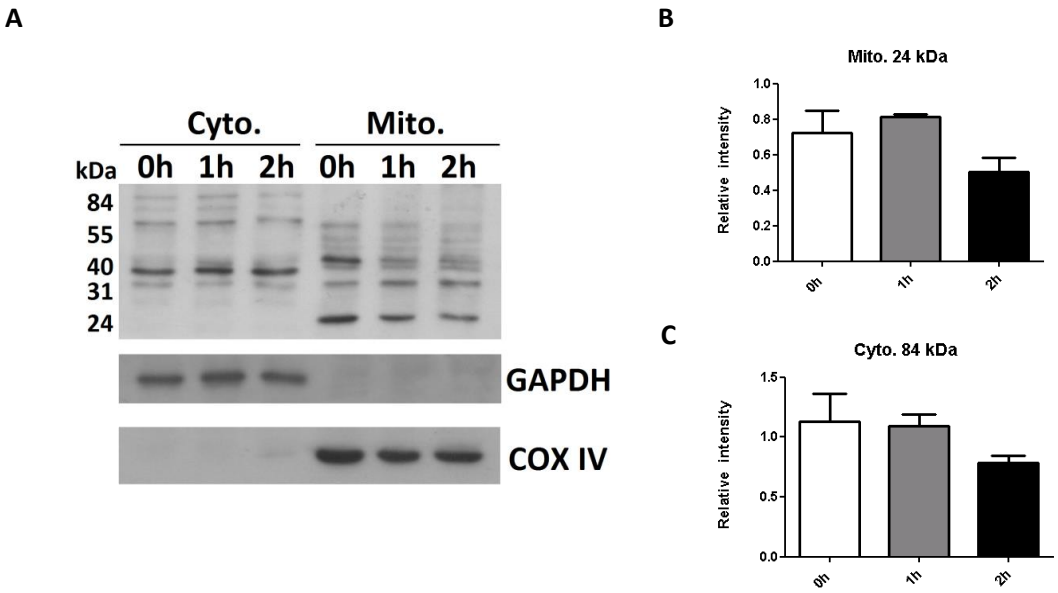

Figure 3.4. Level Oxr1 FL and S isoforms do not translocate between cytoplasm and mitochondria after oxidative stress induction

(A) N2a cells were treated with 0.25mM H_2O_2 for up to 2 h prior to fractionation to cytosolic and mitochondrial fractions. Each sub-cellular sample containing equivalent amount of protein were subjected to Western blot analysis with anti-Oxr1, anti-GAPDH and anti-COX IV. **(B)** Intensity of the 24kD mitochondrial isoform normalised with COX IV. **(C)** Intensity of the cytoplasmic 84kD isoform normalised with GAPDH. Data were from 3 independent repeats, presented as means ± s.e.m. and analysed by one-way analysis of variance (ANOVA) followed by Tukey's multiple comparison test.

It has been widely detected that in tissue, ROS generated by mitochondria accumulates with age (Sawada and Carlson, 1987, Sohal and Sohal, 1991, Capel et al., 2005). Protein levels or activities of several antioxidants such as SOD and GPx have been reported to be increased with age in mouse and rat tissues (Hussain et al., 1995, Oh-Ishi et al., 1995). However, it was previously unknown whether Oxr1 is also up-regulated in the aged wild-type mouse CNS. To investigate whether Oxr1 is also upregulated during ageing, protein levels were compared by between 3-month-old and 27-month-old mice. These data showed that the full-length Oxr1 isoform (Oxr1-FL) was highly expressed in both 27-month-old and 3-month-old samples, whereas the shorter isoforms were expressed in much lower levels comparing to the Oxr1-FL (**Figure 3.5A**). The level of Oxr1-FL in 27-month-old samples was not significantly higher than the 3-month-old group (**Figure 3.5B**), indicating a lack of induction in the protein level of Oxr1-FL during the aging process.

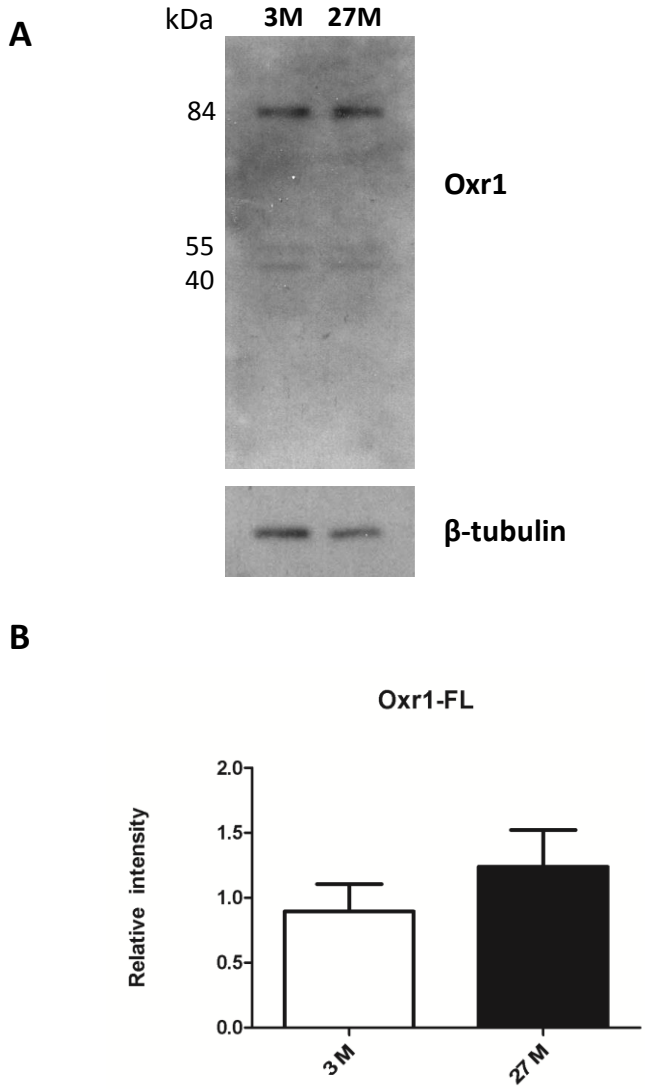

Figure 3.5. Level of Oxr1-FL remains stable in mouse cerebella

(A) Western blot showing stable Oxr1-FL levels in cerebellar homogenates from 3-month-old (3 M) male C57BL/6 mice versus 27-month-old (27 M) C57BL/6 mice. **(B)** Quantification of Oxr1-FL (84 kDa). Oxr1 bands intensity was normalized to β-tubulin used as a control. n=5 for each age group. Tissue was obtained from the SHARM resource, University of Sheffield; mice were housed under identical conditions.

3.3.4 Over-expression of Oxr1 in the cytosol is more protective against oxidative stress-induced cell death than mitochondrial over-expression

We have shown previously that the Oxr1-S isoform, which contains almost exclusively the TLDc domain, is capable of preventing oxidative damage *in vitro* (Oliver et al., 2011); it is noteworthy, however, that these experiments used a promoter that expressed the cloned Oxr1-S protein in the cytoplasm (Oliver et al., 2011). Having demonstrated here that non-full-length isoforms of Oxr1 are likely to be loosely associated to the mitochondrial membrane, next, it was investigated whether cytoplasmic over-expression was more neuroprotective against OS compared to targeted over-expression in mitochondria. Cells were either transfected with Oxr1-S containing a standard CMV promoter with an additional N-terminal mitochondrial localisation signal (MLS) as previously described (Oxr1-S-Mito), Oxr1-S without an additional MLS tag (Oxr1-S-Cyto) or an empty negative control vector (**Figure 3.6**).

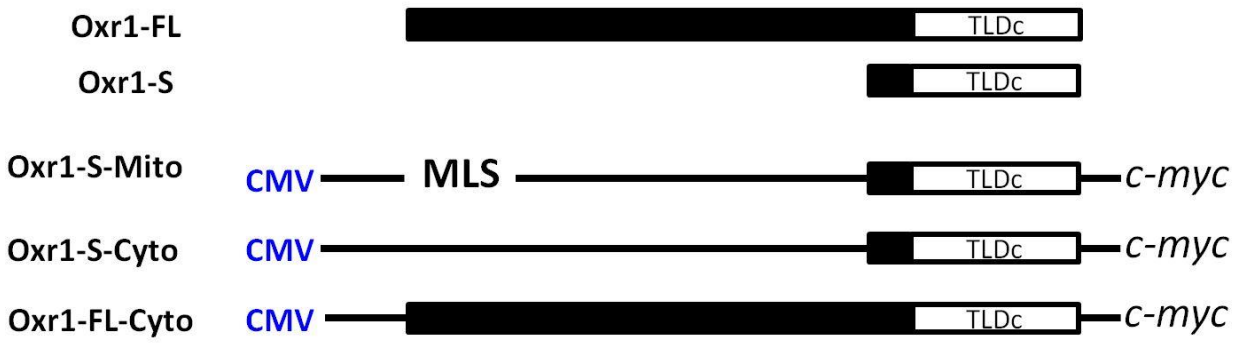

Figure 3.6. Oxr1 endogenous isoforms and constructs

A schematic illustration of the endogenous Oxr1-FL and Oxr1-S isoforms as well as the myc-tagged Oxr1 constructs (Oxr1-S-Mito, Oxr1-S-Cyto and Oxr1-FL-Cyto). MLS: mitochondrial localisation signal; CMV: cytomegalovirus promoter

First, the expression of the myc tagged constructs was confirmed by western blotting in total cell extract (**Figure 3. 7A**) followed by the sub-cellular localisation of each Oxr1-S protein was confirmed by western blotting and co-immonostaining (**Figure 3.7B-C**). Notably, over-expressing cytoplasmic Oxr1-S resulted a band of approximately 30kDa; whereas mitochondrially over-expressed Oxr1-S appeared to have two close bands in the vicinity of 24kDa (**Figure 3.7B**), which may be due to post-translational modification and cleavage of the MLS fragment as expected.

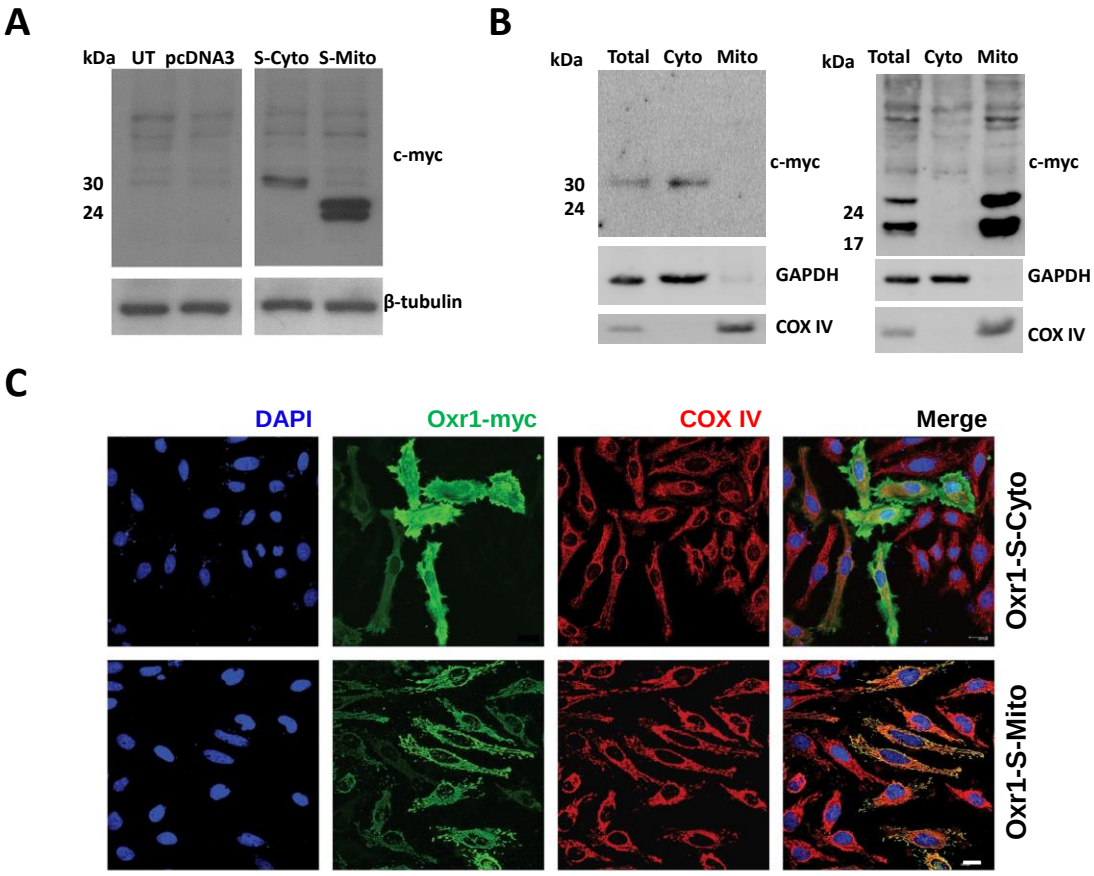

Figure 3.7. Expression of Oxr1 constructs *in vitro*

(A) Representative western blots showing untransfected HeLa cells (UT), cells transfected with empty vector pcDNA3, Oxr1-S-Cyto and Oxr1-S-Mito and cell lysate were labelled with anti-Myc antibody (for Oxr1). β-tubulin was used as a loading control. **(B)** HeLa cells over-expressing Oxr1-S-Cyto or Oxr1-S-Mito were sub-fractionated into cytosolic and mitochondrial fractions and labeled with anti-Myc, cytoplasmic marker GAPDH and mitochondrial marker COX IV. **(C)** Representative image of transfected HeLa cells with Oxr1-S-Cyto or Oxr1-S-Mito constructs. HeLa cells were immunostained with anti-Myc (for Oxr1) and anti-COX IV. Oxr1-S-Mito was co-localised with mitochondrial marker COX IV with a typical mitochondrial filamentous morphology, scattered in the cytoplasm, while Oxr1-S-Cyto had a cytoplasmic diffuse pattern. Nuclei mounted with DAPI. Scale bar=20µm.

To induce OS, cells transfected with Oxr1-S-Cyto and Oxr1-S-Mito were treated with hydrogen peroxide (H_2O_2) (250 μM, 4 hours) 24 hours after transfection and cell death was measured by quantifying cleaved caspase-3, a marker of cell apoptosis, compared to untreated cells (**Figure 3.8A**). After treatment, cells transfected with the control vector showed an increase in the proportion of cell death by approximately 80% (**Figure 3.8B**). In line with previous results, expression of the Oxr1-S-Cyto construct was protective against cell death, and after treatment there was only an approximately 20% increase in cell death, significantly lower than the control vector (**Figure 3.8B**). Interestingly, mitochondrial over-expression of Oxr1-S (Oxr1-S-Mito) did not appear to show any protection against OS, as the percentage increase in cell death was similar to the control vector (an approximately 90% increase) (**Figure 3.8B**). Together, these data indicate that cytoplasmic over-expression of Oxr1-S is potentially more effective at preventing OS-related cell death than mitochondrial over-expression.

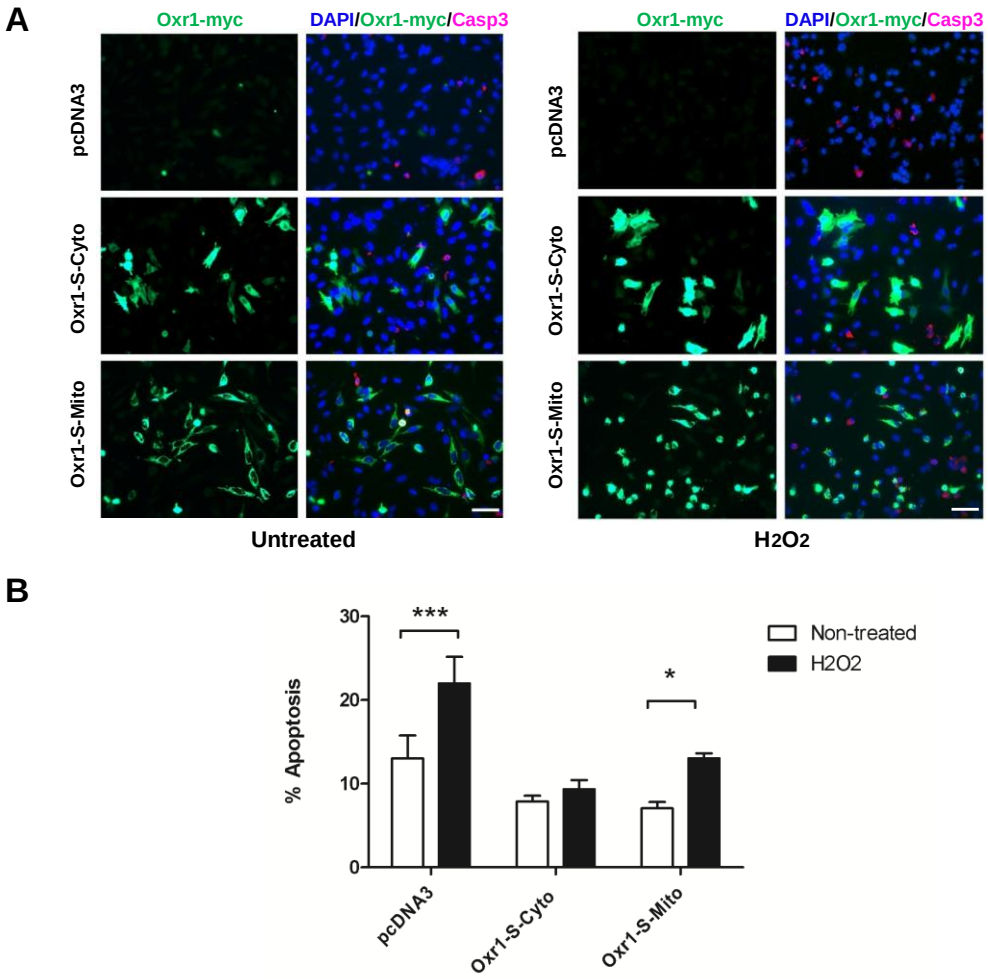

Figure 3. 8. Cytoplasmic Oxr1 has stronger protection against oxidative stress

(A) Representative images of HeLa cells transfected with the control vector, Oxr1-S-Cyto or Oxr1-S-Mito in untreated (UT) conditions or after H_2O_2 treatment (250 μM for 4 hours). Cells were immunostained with anti-myc (for Oxr1) or anti-cleaved caspase-3 (Casp3) to quantify apoptosis. Scale bar = 50μm. **(B)** Cells over-expressing Oxr1-S-Cyto show stronger protection against oxidative insult compared to cells over-expressing Oxr1-S-Mito or the pcDNA3 control vector. Data are shown ± SEM of 4 independent experimental repeats and analysed by ANOVA followed by Bonferroni post-hoc tests, * $p < 0.05$, *** $p < 0.001$

3.3.5 Cytoplasmic but not mitochondrial over-expression of Oxr1 alleviates mitochondrial morphological changes caused by acute rotenone-induced oxidative stress

It is well established that mitochondrial morphology is modified in response to oxidative stress and that these changes can subsequently affect mitochondrial function (Ahmad et al., 2013, Wu et al., 2011, Jendrach et al., 2008). As Oxr1-C was able to provide protection against OS, to further understand the potential role of mitochondria in this process, it was examined whether over-expressing Oxr1 prevents mitochondrial morphological changes induced by OS. For these experiments, rotenone was selected (50 μM for 1 hour) as a specific and potent inhibitor of mitochondrial complex I capable of causing oxidative damage and mitochondrial morphological changes (Ahmad et al., 2013, Koopman et al., 2005, Pham et al., 2004). Prior to treatment, HeLa cells were transfected with either an empty vector, Oxr1-S-Cyto or Oxr1-S-Mito. An Oxr1-FL-Cyto construct was also added to this experiment to complement other studies that have utilised successfully this full-length isoform as a protective protein *in vivo* (Oliver et al., 2011) (**Figure 3.9A**). Consistent with previous findings (Ahmad et al., 2013), by quantifying mitochondria labelled with COX IV, rotenone exposure caused a shift of mitochondrial shape from mainly tubular, which is found in healthy non-treated cells, to non-tubular (‘donut’ or ‘blob’) (**Figure 3.9B**); thus in cells transfected with empty vector, the ratio between tubular and non-tubular mitochondria was significantly reduced by over 2-fold after rotenone exposure (**Figure 3.9C**). In cells over-expressing Oxr1-FL-Cyto or Oxr1-S-Cyto, no significant reduction of this ratio was observed, suggesting a protective role of cytoplasmic Oxr1 against mitochondrial morphological modification induced by rotenone (**Figure 3.9C**). Interestingly, however, expression of the Oxr1-S-Mito construct caused a shift towards non-tubular mitochondria, similar to that observed for cells

transfected with an empty vector. In addition, pair-wise comparisons showed that under rotenone treatment, only cells over-expressing Oxr1-S-Cyto had a significantly higher proportion of tubular mitochondria compared to control cells (**Figure 3.9C**). Next, to exclude the possibility that these ratios were confounded by a change in total number of mitochondria after treatment, the total number of mitochondria per focal plane was quantified, and no differences were observed between the experimental groups (**Figure 3.9D**). In summary, these results suggest that cytosolic over-expression of Oxr1 is more effective at alleviating mitochondrial morphological changes caused by rotenone than over-expression in mitochondria.

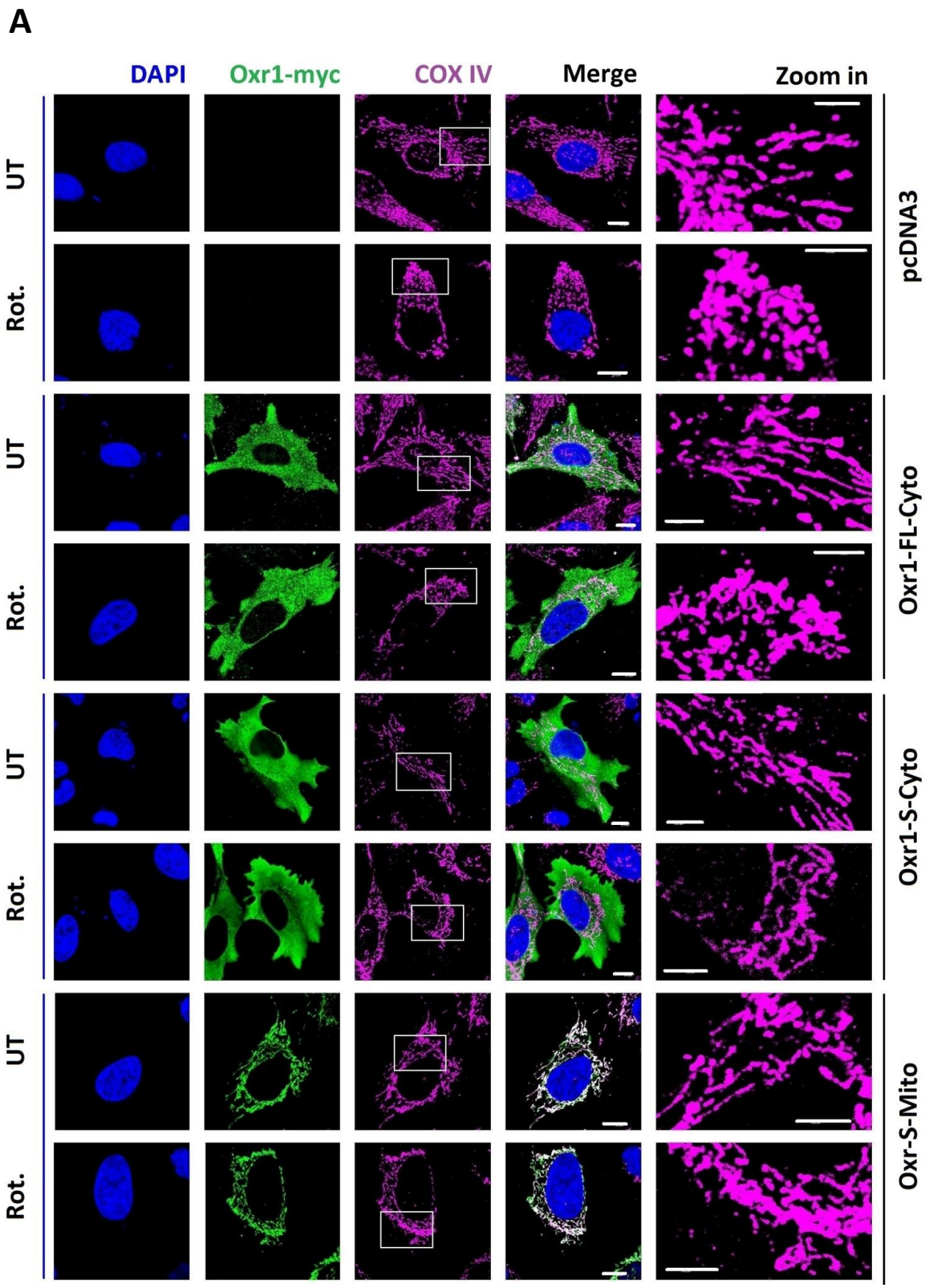
A
DAPI
Oxr1-myc
COX IV
Merge
Zoom in
UT
Rot.
pcDNA3
Oxr1-FL-Cyto
Oxr1-S-Cyto
Oxr-S-Mito

B

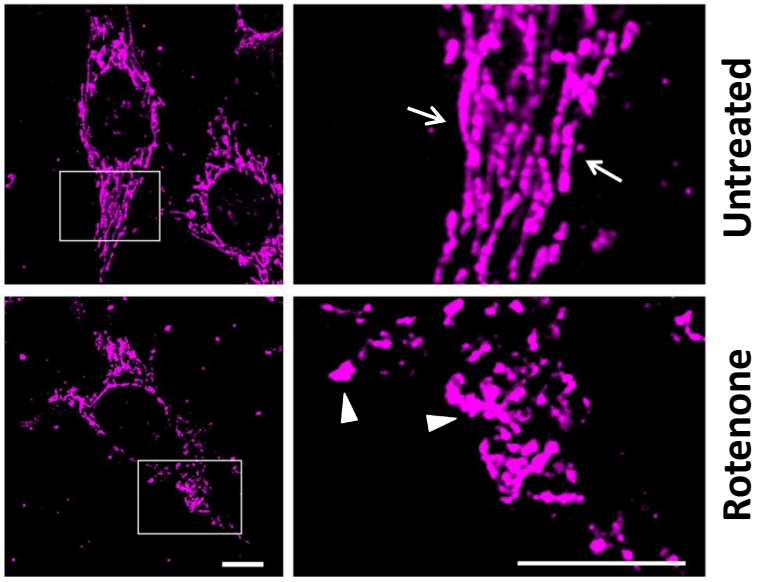
Untreated
Rotenone

C

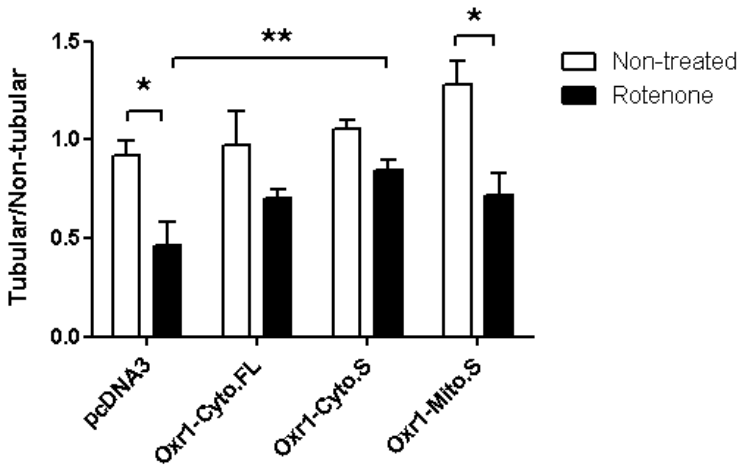
Tubular/Non-tubular
1.5
1.0
0.5
0.0
*
**
*
Non-treated
Rotenone
pcDNA3
Oxr1-Cyto.FL
Oxr1-Cyto.S
Oxr1-Mito.S

D

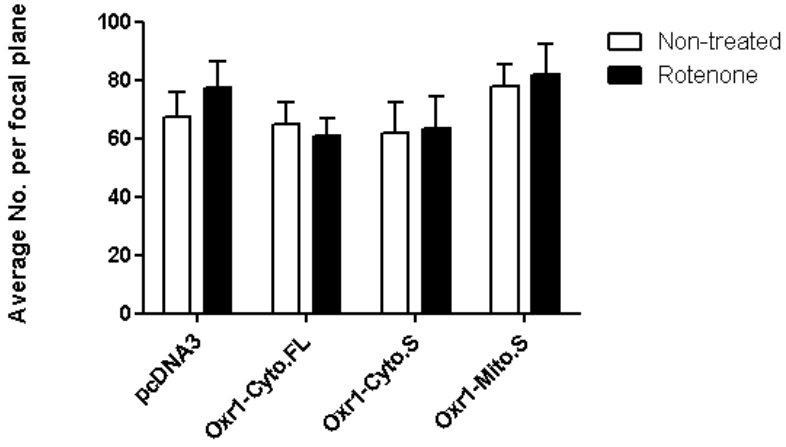
Average No. per focal plane
100
80
60
40
20
0
Non-treated
Rotenone
pcDNA3
Oxr1-Cyto.FL
Oxr1-Cyto.S
Oxr1-Mito.S

Figure 3.9. Cytoplasmic over-expression of Oxr1 alleviates mitochondrial morphological changes induced by acute rotenone treatment

(A) Representative images showing HeLa cells transfected with the control vector, Oxr1-FL-Cyto, Oxr1-S-Cyto or Oxr1-S-Mito, in untreated (UT) or under rotenone treated (50 μM, 1 hour) conditions; Cells were immunostained with anti-myc (for Oxr1) and anti-COX IV. Scale bar = 20 μm. **(B)** Representative images showing tubular mitochondria in untreated control cells (arrows), while non-tubular (donut/blob) mitochondria become predominant after rotenone treatment (arrowheads). Scale bar=10 μm **(C).** Ratio of mitochondria classified as tubular versus non-tubular before and after rotenone treatment. Rotenone treatment significantly reduced the ratio of tubular to non-tubular mitochondria, but over-expression of cytoplasmic and mitochondrial Oxr1 prevented this reduction. **(D)** Total number of mitochondria per focal plane remains unchanged after rotenone treatment. Data are shown as the mean ± S.E.M. from 3 independent replicates of each genotype. A minimum of 15 cells were analysed per group in each repeat. Data were analysed by ANOVA followed by Bonferroni post-hoc tests; * $p < 0.05$, ** $p < 0.01$.

3.3.6 Mitochondrially targeted Oxr1 translocates to the cytoplasm after long term H_2O_2 exposure or reduction of mitochondrial membrane potential

It has been shown above that over-expressing cytosolic but not mitochodnrial Oxr1-S *in vitro* is capable of preventing OS-induced apoptosis and mitochondrial morphological changes. Having demonstrated that the endogenous protein level of Oxr1 isoforms remains stable after induction of oxidative stress, it was then examined whether the exogenously over-expressed Oxr1 isoforms can translocate into or out of mitochondria after oxidative stress induction, HeLa cells were transfected with an Oxr1-FL-Cyto, Oxr1-S-Cyto or Oxr1-S-Mito, and treated with H_2O_2 (250 μM, 4 or 8 hours) 24 hours after transfection. As shown by immunostaining, Oxr1-FL-Cyto and Oxr1-S-Cyto remained in cytoplasm and did not co-localise with the mitochondrial marker COX IV (**Figure 3.10A**), suggesting that these proteins do not directly exert their anti-oxidative role within mitochondria. Oxr1-S-Mito remained in mitochondria and co-localise with COX IV 4 hours after the treatment (**Figure 3.10A**). Interestingly however, Oxr1-S-Mito appeared to be released out of mitochondria 8 hours after treatment (**Figure 3.10B**). Of note, Oxr1-S-Mito appeared to form cytosolic granules once been released from mitochondria and did not tend to form a cytoplasmic diffuse pattern (**Figure 3.10B, the "zoom in" image**).

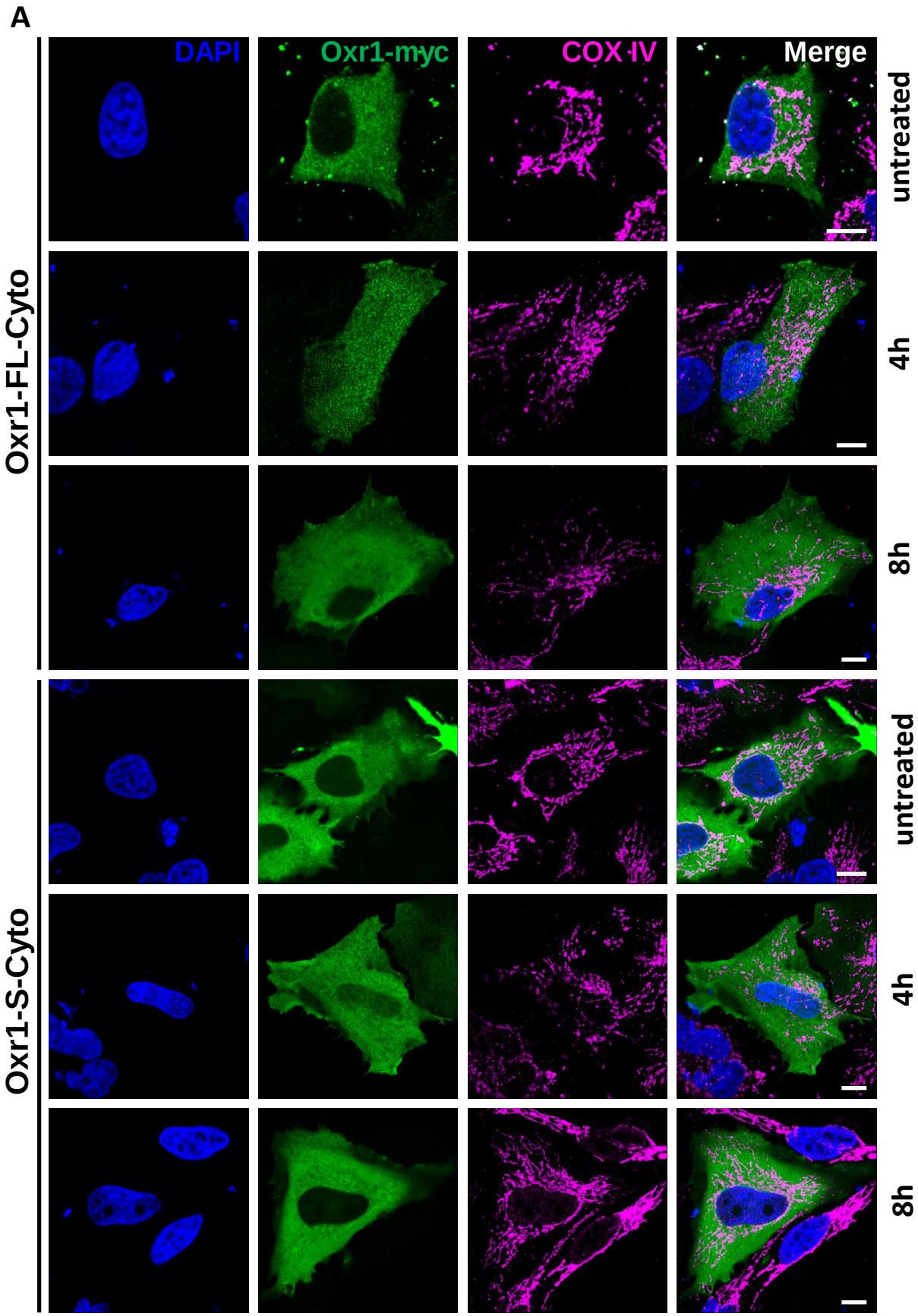
A
DAPI
Oxr1-myc
COX IV
Merge
Oxr1-FL-Cyto
Oxr1-S-Cyto
untreated
4h
8h
untreated
4h
8h

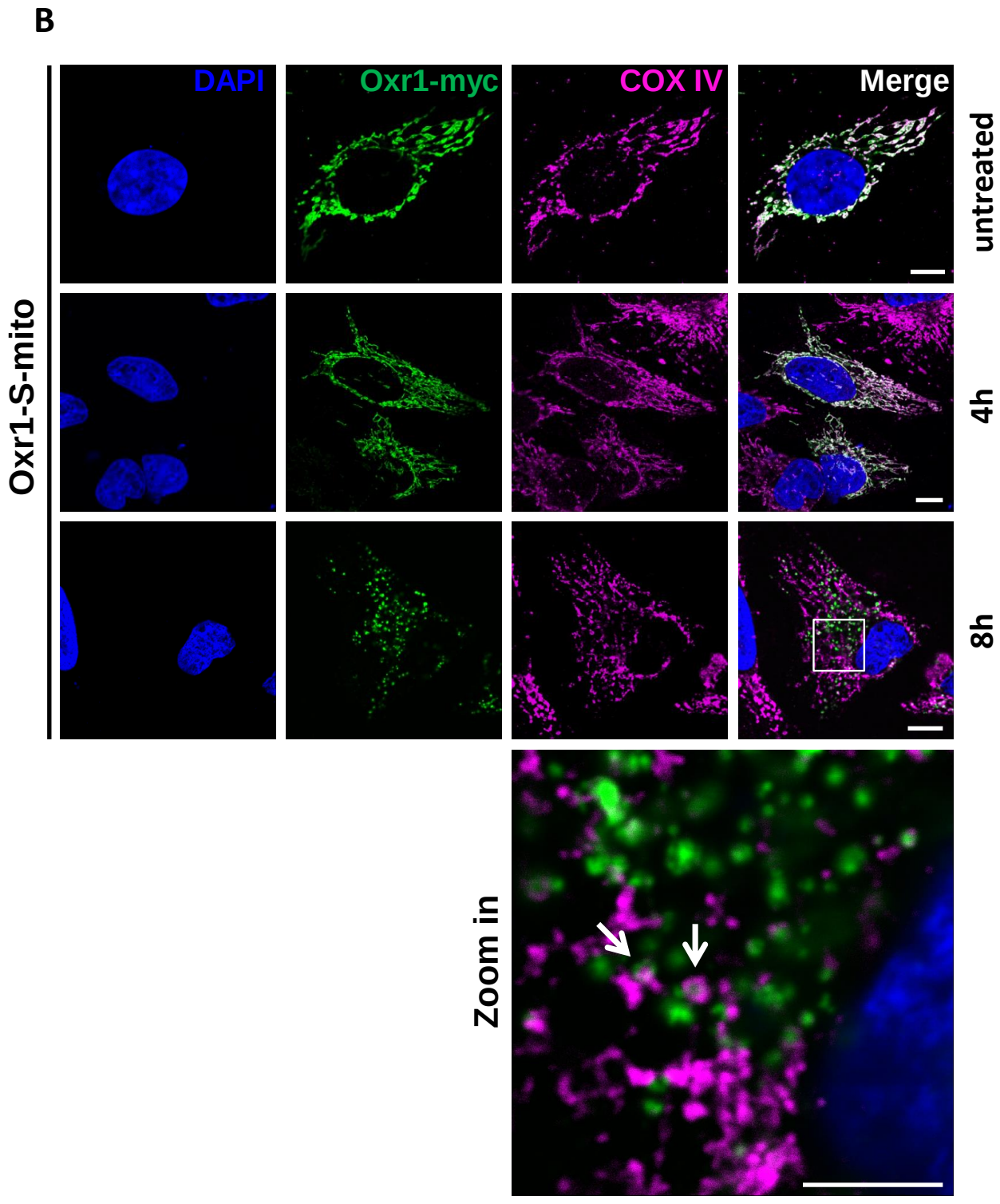
B
DAPI
Oxr1-myc
COX IV
Merge
Oxr1-S-mito
untreated
4h
8h
Zoom in

Figure 3.10. Mitochondrially targeted Oxr1 translocated to the cytoplasm after long term H_2O_2 exposure

(A) Representative images showing HeLa cells transfected with Oxr1-FL-Cyto or Oxr1-S-Cyto, in untreated (UT) or under H_2O_2 (250 μM, 4 or 8 hours) conditions; Cells were immunostained with myc (for Oxr1) and mitochondrial marker COX IV. **(B)** Representative images showing HeLa cells transfected with Oxr1-S-Mito in untreated (UT) or under H_2O_2 (250 μM, 4 or 8 hours) conditions. Arrows indicate separate localisation of COX IV and myc-tagged Oxr1. Scale bar = 10 μm, scale bar for the "zoom in" image=5 μm.

It is well known that several mitochondrial proteins are released into the cytosol during apoptosis, for example, Cyt-C (Kluck et al., 1997, Yang et al., 1997), second mitochondria-derived activator of caspases (Smac) (Du et al., 2000), and HSP60 (Chandra et al., 2007). Reduction of mitochondrial membrane potential ($\Delta\psi m$), which is a voltage difference across the mitochondrial IM (Glynn, 1967), has been found to facilitate the release of mitochondrial proteins such as Cyt-C and Smac from mitochondria to cytosol (Zhou et al., 2005, Gottlieb et al., 2003). To examine whether the release of Oxr1-S-Mito to cytosol also occurs coincidentally with the loss of mitochondrial membrane potential, HeLa cells were transfected with the Oxr1-S-Mito, and treated with mitochondrial uncoupling reagent carbonyl cyanide p-trifluoromethoxyphenylhydrazone (FCCP), (20 μM, 1 or 2 hours) 24 hours after transfection. Mitochondrial membrane potential of the cells was measured by a fluorescent method by quantifying the level fluorescent signal generated by TMRE. As expected, FCCP significantly reduced mitochondrial membrane potential for almost 50% one hour after the treatment (**Figure 3.11A**). Intriguingly, Oxr1-S-Mito was also released from mitochondria to cytosol in a pattern similar to the H_2O_2 treatment one hour after the treatment (**Figure 3.11B**).

Taken together, these results suggest that under oxidative stress, mitochondrially targeted over-expressed Oxr1-S translocates from mitochondria to cytoplasm, likely to be dependent on reduction of mitochondrial membrane potential.

A

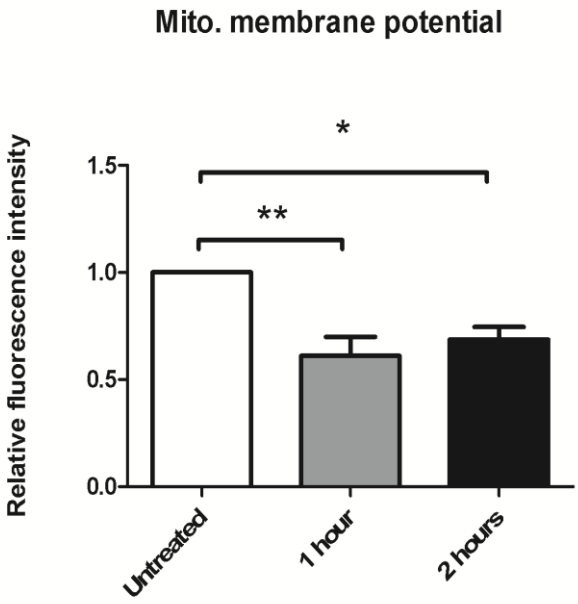
Mito. membrane potential
Relative fluorescence intensity
1.5
1.0
0.5
0.0
*
**
Untreated
1 hour
2 hours

B

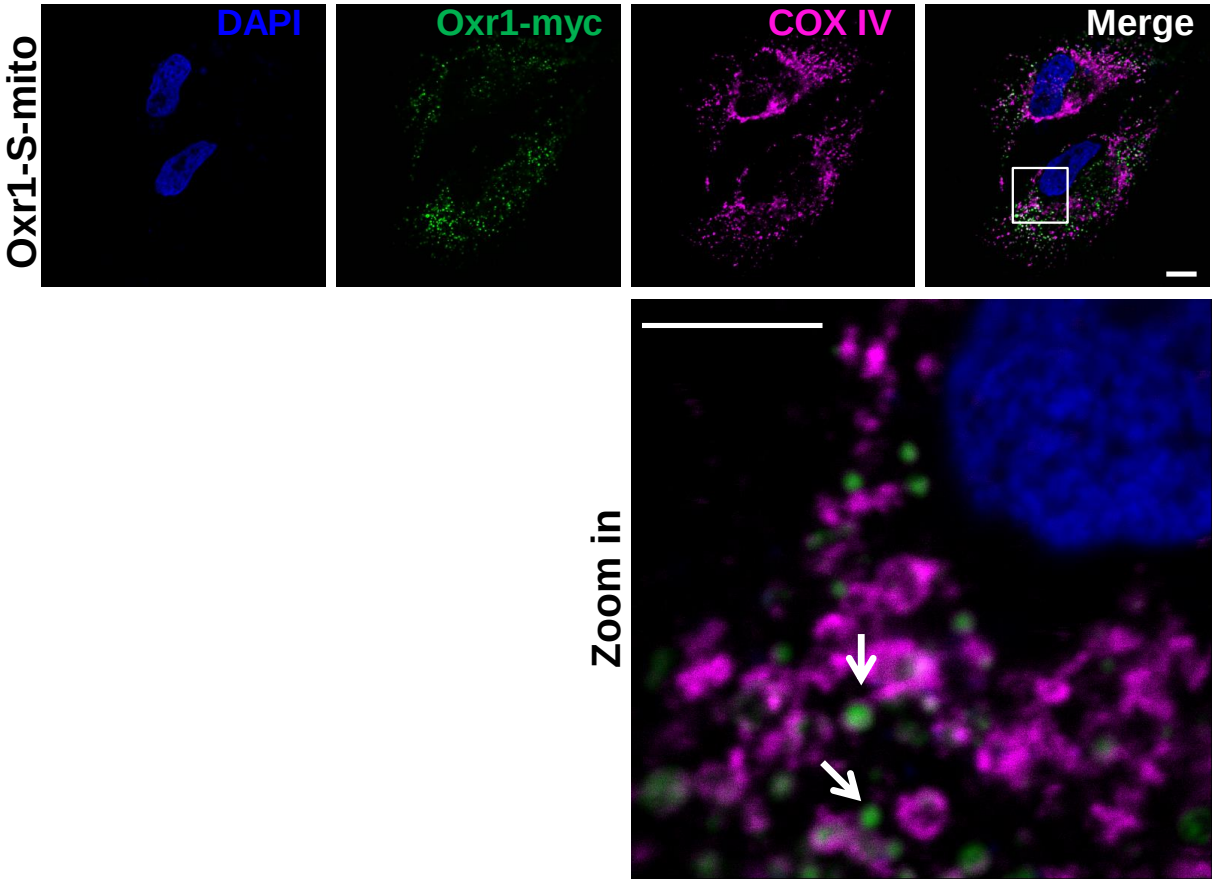
Oxr1-S-mito
DAPI
Oxr1-myc
COX IV
Merge
Zoom in

Figure 3.11. Mitochondrially targeted Oxr1 translocated to the cytoplasm after reduction in mitochondrial membrane potential

(A) Effects of FCCP treatment (20 μM, 1 or 2 hours) on mitochondrial membrane potential in HeLa cells. Data were presented as means ± s.e.m. and analysed by one-way ANOVA followed by Tukey's multiple comparison test. **P* < 0.05 **(B)** Representative images showing HeLa cells transfected with the Oxr1-S-Mito and treated with FCCP (20 μM, 1 hour). Arrows indicate separate localisation of COX IV and myc-tagged Oxr1. Scale bar = 10 μm, scale bar for the "zoom in" image=5 μm.

3.3.7. Oxr1 partially reverses mitochondrial size abnormality and number reduction caused by TDP-43 mutation

In the previous section, it has been demonstrated that cytoplasmic Oxr1-S can prevent mitochondrial morphological changes triggered by acute rotenone induced oxidative stress. Therefore, it was important to determine whether Oxr1-S over-expression has a protective effect on mitochondrial morphological impairments caused by TDP-43 mutations.

It has been shown that under OS conditions, over-expression of WT and mutant TDP-43 results in its localisation to mRNA binding protein T cell-induced antigen 1 (TIA-1)-containing stress granules and Oxr1 interacts with TDP-43 (Finelli et al., 2015a). Therefore, I examined first whether over-expressed Oxr1-S also co-localises with TIA-1 stress granules. To achieve this, mouse motor neuron-like NSC-34 cells were transfected with HA-tagged Oxr1-S. It showed that under oxidative stress (0.1mM sodium arsenite, 30 minute), TIA-1 stress granules were formed, but over-expressed Oxr-S did not co-localise with TIA-1 stress granules (**Figure 3.12**), suggesting that Oxr1 does not interact directly with the TIA-1 stress granules.

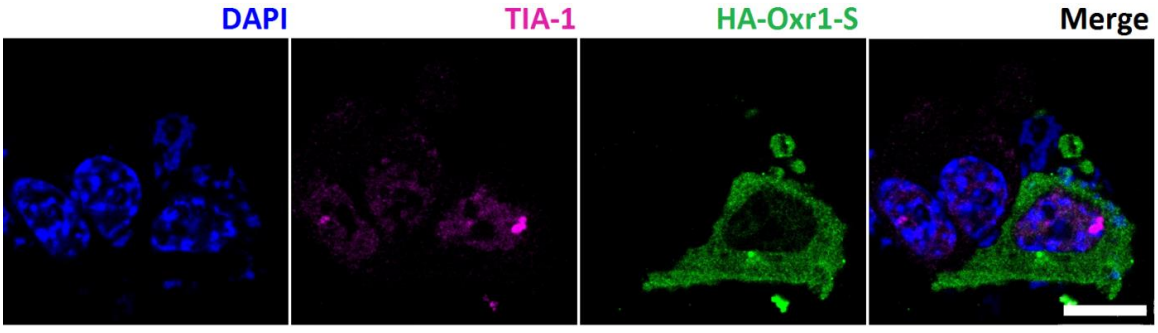

Figure 3. 12. Oxr1 does not co-localise with the TIA-1 stress granules

NSC-34 cells were transfected with and Oxr1-S and immunostained with anti-HA and anti-TIA-1. Scale bar=10µm.

I next examined whether Oxr-1-S over-expression could reverse mitochondrial morphological impairments caused by TDP-43 mutations. NSC-34 cells were transfected with pcDNA3, TDP-43 M337V or Oxr1-S constructs and subjected to confocal microscopy (**Figure3.13.A**). In NSC-43 cells over-expressing TDP-43 M337V, both average mitochondrial size and average number of mitochondria per focal plane were significantly reduced comparing to the control group (**Figure3.13. B-C**), consistent with previous studies (Lu et al., 2012, Wang et al., 2013). In NSC-34 cells co-transfected with TDP-43 M337V and Oxr1-S, increased average mitochondrial size was observed comparing to cells expressing only TDP-43 M337V. However, the average number of mitochondria per focal layer remained unchanged. Under arsenite treated conditions, a trend towards reduction of both mitochondrial size and number in TDP-43 M337V mutant was detected. Whereas, over-expressing Oxr1-S established an increasing trend in comparison with the M337V mutant. These trends were statistically non-significant.

These results suggest that overexpressing Oxr1-S can alleviate abnormalities of mitochondrial size and number caused by TDP-43 mutant over-expression.

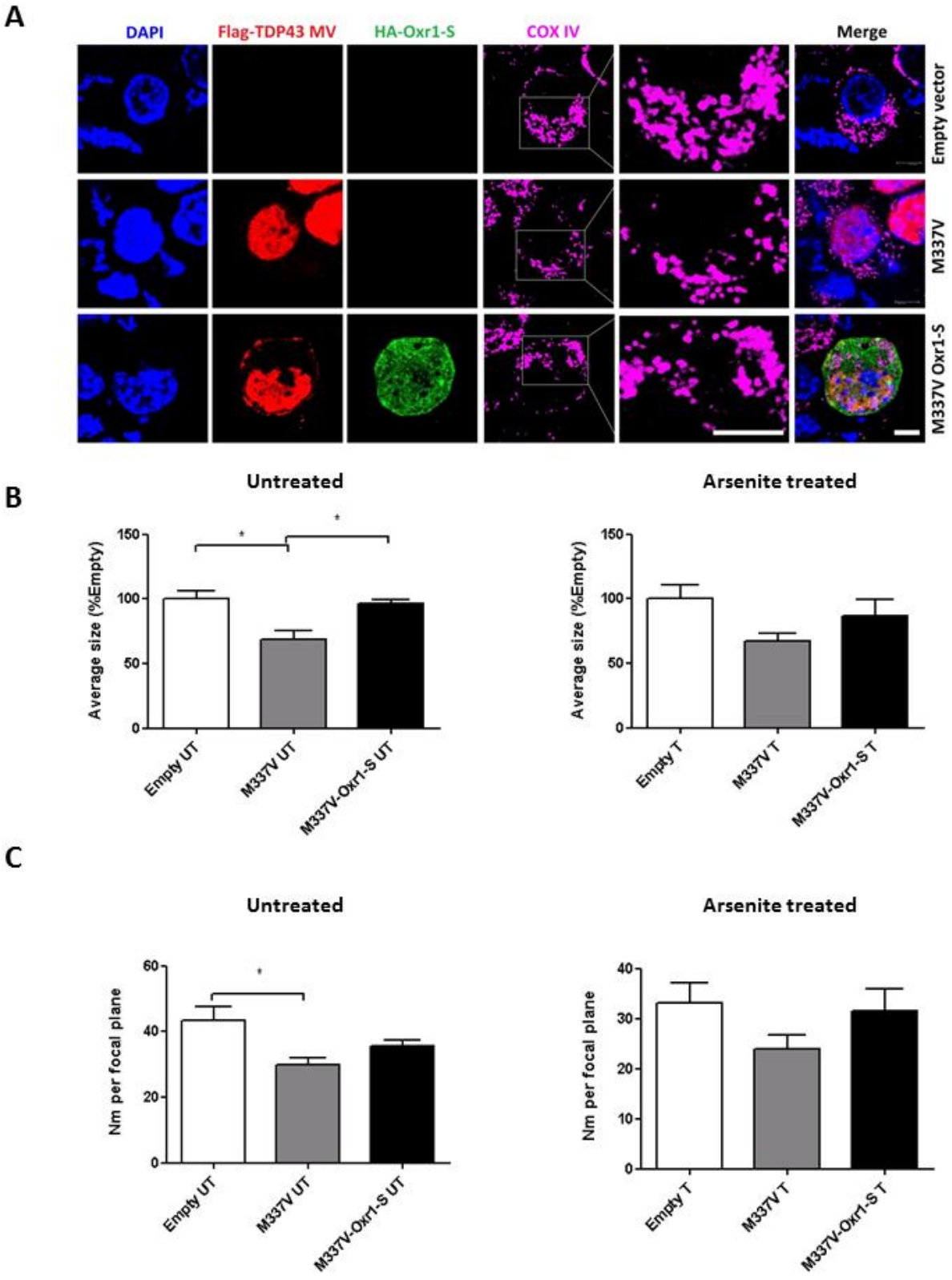
A
DAPI
Flag-TDP43 MV
HA-Oxr1-S
COX IV
Merge
Empty vector
M337V
M337V Oxr1-S
B
Untreated
Arsenite treated
Average size (%Empty)
150
100
50
0
*
*
Empty UT
M337V UT
M337V-Oxr1-S UT
Empty T
M337V T
M337V-Oxr1-S T
C
Untreated
Arsenite treated
Nm per focal plane
60
40
20
0
*
Empty UT
M337V UT
M337V-Oxr1-S UT
40
30
20
10
0
Empty T
M337V T
M337V-Oxr1-S T

Figure 3.13. Oxr1 partially reverses mitochondrial abnormality caused by TDP-43 mutations

(A) Representative picture of transfected NSC-34 cells with pcDNA3, TDP-43 M337V or Oxr1-S constructs. Cells were immunostained with anti-flag, anti-HA and anti-COX IV. Nuclei mounted with DAPI. Scale bar=5µm. **(B, C)** Quantification of mitochondrial average size (B) and average number of mitochondria per cell layer (C). Experiments were carried out in untreated or treated (0.5mM Arsenite, 30minutes) conditions. Experiments were repeated 3 independent times for untreated condition and 4 independent times for treated condition. Data are presented as means ± s.e.m. and analysed by one-way ANOVA followed by Tukey's multiple comparison test. $*P < 0.05$

3.3.8. Oxr1 partially reverses mitochondrial functional abnormality caused by TDP-43 mutations

I then assessed whether the mitochondrial morphological impairment associated with TDP-43 M337V mutation could lead to mitochondrial functional abnormality and, if so, whether Oxr-1-S over-expression could alleviate these abnormalities. To achieve this, mitochondrial oxygen consumption level and mitochondrial membrane potential, -both important parameters of mitochondrial function -were measured. TDP-43 WT and a TDP-43 Q331K mutants were also tested in parallel, as it has been shown that over-expression of wild type TDP43 and Q331K also leads to mitochondrial morphological and functional impairment in motor neurons (Wang et al., 2013).

Oxygen consumption levels of NSC-34 cells transfected with pcDNA3, TDP-43 WT, TDP-43 Q331K, TDP-43 M337V or Oxr1-S constructs in untreated or 10 μM arsenite treated condition were measured by using mitochondrial oxygen consumption assay. As described previously (Hynes et al., 2001), this assay uses a probe of which emission is quenched by O_2 in the surrounding environment under normal conditions. Consumption of O_2 by mitochondria reduces the quenching effect, which leads to an increase in probe signal. The change of probe signal over time indicates the change of oxygen levels consumed by mitochondria. Pairwise study revealed that in the untreated group, cells over-expressing FLAG-tagged TDP-43 M337V had a significantly reduced oxygen consumption rate comparing to the empty vector control. When co-expressing Oxr1-S, oxygen consumption returned to the normal level comparing to the control, indicating a trend towards alleviation **(Figure 3.14A)**. In the treated group, however, such a trend was statistically non-significant **(Figure 3.14A)**.

Mitochondrial membrane potential of NSC-34 cells transfected with pcDNA3, TDP-43 WT, TDP-43 Q331K, TDP-43 M337V or Oxr1-S constructs in untreated or 10 μM arsenite treated condition were measured by a fluorescent TMRM method as described in

Material and Methods. The data showed that over-expression of wild type or mutant TDP-43 did not have any significant impact on mitochondrial membrane potential in both untreated and treated condition **(Figure 3.14B)**.

Taken together, the results show that over-expressing Oxr1-S can partially reverse mitochondrial oxygen consumption abnormality caused by TDP-43 M337V mutation.

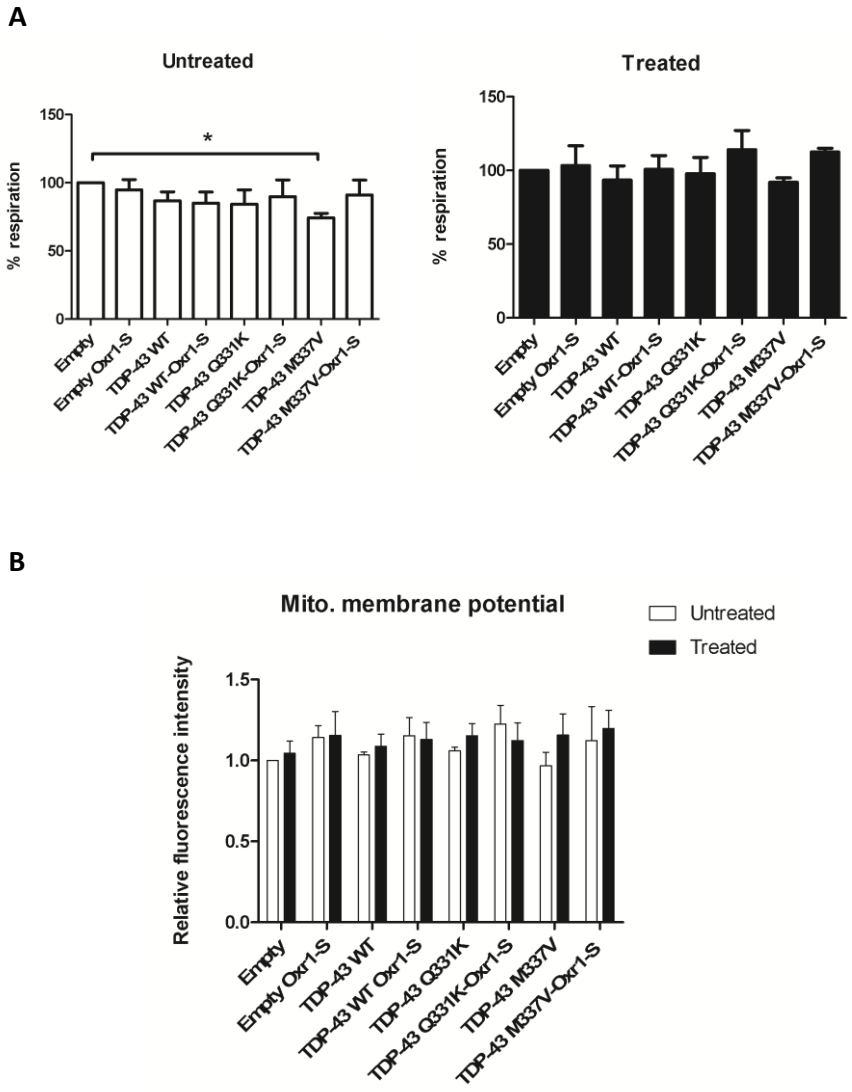

Figure 3.14. Oxr1 partially reverses mitochondrial abnormality caused by TDP-43 mutations

(A) A reduction of mitochondrial oxygen consumption rate (% respiration) was found in cells over-expressing the TDP-43 M337V mutation. Co-expressing with Oxr1-S prevented the reduction. Experiments were carried out in untreated or treated (10 μM Arsenite, 2.5 hours) conditions. Another ALS-associated mutation (Q331K) found to impair mitochondria (Wang et al., 2013) was also added to this experiment. For the untreated condition, data were obtained from 6 independent experiments; for the treated condition, data were obtained from 3 independent experiments. Data were presented as means ± s.e.m. and analysed by one-way ANOVA followed by Tukey's multiple comparison test. *$P < 0.05$ **(B)** No difference in mitochondrial membrane potential was observed in untreated and treated groups. Data were obtained from 3 independent experiments for both untreated and treated conditions. Data were presented as means ± s.e.m. and analysed by two-way ANOVA followed by Bonferroni post hoc test.

3.4 Discussion

In this chapter, it was demonstrated for the first time that Oxr1-FL is localised in cytoplasm, while the shorter Oxr1 isoforms are enriched in mitochondria. These mitochondrial Oxr1 isoforms localised predominantly in the cytosolic side of the outer mitochondrial membrane. It was then investigated whether mitochondrial localisation is required for protection against oxidative stress-induced apoptosis and mitochondrial morphological changes. The data suggest that cytoplasmic over-expression of Oxr1 has a stronger protection against OS induced apoptosis and mitochondrial morphological change compared to the mitochondrial Oxr1. Moreover, over-expression of Oxr1 alleviated mitochondrial morphological changes and mitochondrial oxygen consumption caused by a TDP-43 mutation, indicating a potential role of Oxr1 in maintaining mitochondrial morphology and function.

3.4.1. Isoform specific sub-cellular and sub-mitochondrial localization of Oxr1

Several isoforms of OXR1 and its orthologues have been described in mammalian and non-mammalian systems (Volkert et al., 2000, Elliott and Volkert, 2004, Stowers et al., 1999), and western blot results have indicated a complex differential distribution of isoforms in mouse tissue (Oliver et al., 2011, Liu et al., 2015a). In this study, using our antibody raised against a shared C-terminal epitope (Oliver et al., 2011), the cytosolic localisation of the full-length Oxr1 isoform (84 kDa) and mitochondrial enrichment for the shorter isoforms (55, 40 and 24 kDa) (**Figure 3.2A-C**) was demonstrated. These findings suggest that the mitochondrial localisation of Oxr1 observed previously in mammalian cells by immunofluorescence may have originated from non-full-length isoforms (Elliott and Volkert, 2004, Oliver et al., 2011).

It is still unclear, however, how the shorter Oxr1 isoforms are translocated to the mitochondria. It has been postulated that a mitochondrial localisation signal (MLS) is present at the N-terminus of Oxr1 in yeast (scOxr1) (Elliott and Volkert, 2004). Indeed, in our study, while tagged mouse Oxr1 proteins with an additional MLS are successfully targeted to mitochondria (Oxr1-S-Mito), over-expression of constructs with no additional MLS (both Oxr1-S-Cyto and Oxr1-FL-Cyto) only showed cytosolic localisation. Intriguingly, the full-length Oxr1 protein could not be targeted into mitochondria using the same N-terminal MLS. These findings suggest the association between Oxr1 and mitochondria may be size-selective.

The sub-mitochondrial localisation of Oxr1 had not been investigated before. Using a combination of ultracentrifugation and trypsin digestion assays, the results suggest that that Oxr1 is not likely to be present in the mitochondrial matrix or intermembrane space, but is found at the mitochondrial OM, facing the cytosol. Of note, the anti-oxidative protein DJ-1, mutated in familial Parkinson's disease, has been found to have a similar OM-associated localisation, despite lacking a *bona fide* MLS (Bonifati et al., 2003a, Taira et al., 2004a, Canet-Avilés et al., 2004, Maita et al., 2013). Translocation of DJ-1 into mitochondria is thought to be mediated by interacting with chaperones including heat-shock protein (HSP) 70, C-terminus of heat-shock cognate 71 kDa protein (HSC70)-Interacting Protein (CHIP) and mtHsp70/Grp75 (Li et al., 2005). It is possible that the translocation of Oxr1 to mitochondria occurs via a similar mechanism; for example, our initial results from a protein interaction screen suggest that under OS, Oxr1-S may interact with DnaJ (Hsp40) homolog, subfamily C, member 19 (DNAJC19) (Finelli et al., 2015a), a mitochondrial protein translocase component (Richter-Dennerlein et al., 2014) localised on mitochondrial IM (Richter-Dennerlein et al., 2014). However, the possible mechanism behind this is elusive. In addition, Solute Carrier Family 25 member 3

(SLC25A3) and member 5 (SLC25A5) might also be potential interaction partners of Oxr1-S, but not Oxr1-FL (Finelli et al., 2015a). SLC25A3 is a mitochondrial carrier protein that is in charge of facilitating transportation of phosphate into mitochondrial matrix (Palmieri, 2004). Interestingly, it has both N-terminal and C-terminal protrusions towards cytosol (Palmieri, 2004). The finding of mitochondrial membrane bound, cytosolic facing localisation of mitochondrial Oxr1 provided further possibilities of interactions between the two proteins. Further studies will be required to confirm such associations using methods such as co-immunoprecipitation and understand their functional relevance to OS sensitivity.

3.4.2 Oxr1 localisation and its anti-oxidative role

The cell apoptosis assays revealed that, in contrast to mitochondrially targeted Oxr1-S, cytoplasmic expression of the shortest Oxr1 isoform (Oxr1-S-Cyto), containing almost exclusively the TLDc domain, is protective against OS-induced apoptosis; this is consistent with previous findings that the TLDc domain of Oxr1 is a key feature of its anti-oxidative role (Oliver et al., 2011). Importantly, the MLS used for Oxr1-S-Mito was from subunit VIII of human cytochrome c oxidase that targets proteins to the mitochondrial matrix (Rizzuto et al., 1992); thus my findings suggest that a balance between cytosolic and mitochondrial OM localisation may be required for the anti-oxidative role of Oxr1 in these assays. Interactions of various pro- and anti-apoptotic proteins as well as ROS sensors occur at the interface between the cytosol and the mitochondrial OM, and these binding events are thought to mediate mitochondrial OM permeabilisation (MOMP), one of the hallmarks of the early stage of apoptosis (Chipuk et al., 2006). Moreover, regulation of MOMP is independent from IM and MX proteins (Kuwana et al., 2002). Hence, it will be worthwhile to determine whether the OM-

associated, cytosolic-facing Oxr1 isoforms establish their anti-oxidative role via these pathways.

Oxr1-related proteins localised to other cellular compartments may also confer protection against OS-related insults; for instance, over-expression of Oxr1 from the silk-worm *Bombyx mori* (BmOxr1) was protective against OS in *Drosophila melanogaster* (Kobayashi et al., 2014). Interestingly, when over-expressed, BmOxr1 was found mainly in the nuclei of *Drosophila melanogaster* cells. The sequence alignments provided suggest that this BmOXR1 protein has sequence identity with NCOA7, a known nuclear-expressed TLDc domain-containing protein that is also able to confer protection against OS (Durand et al., 2007).

Of note, mitochondrial over-expression of human OXR1 in a highly peroxide sensitive mutant strain of yeast has shown to be protective against H_2O_2 induced oxidative damage (Elliott and Volkert, 2004). The apparent discrepancy between these results and this study here may relate to differences in the type of assay or species used, the levels of over-expression achieved, or the type of MLS used to tag OXR1 itself. However, the MLS used in the previous study was from yeast Sod2 that should also direct proteins to the mitochondrial matrix. The particular isoforms of Oxr1 used in such OS protection assays must also be considered; it has been focused here on the shortest Oxr1-S isoform that is based on a known cDNA that is expressed in mouse and humans (Oliver et al., 2011), whereas other studies have used longer isoforms containing additional exons outside of the TLDc domain. Those isoforms are likely to be represented by the 44 and/or 55 kDa proteins, which were detected in western blot. It has been suggested that other exons of *OXR1* may also play an important role in OS resistance (Murphy and Volkert, 2012).

With regard to the 30kD band and the double band revealed by the western blot of HeLa cells over-expressing Oxr1-S-Cyto, and Oxr1-S-Mito, respectively (**Figure 3.7A-B**), in Elliott and Volkert's study (Elliott and Volkert, 2004), using an antibody against Oxr1-C (also known as C7C (Fischer et al., 2001)), the smallest Oxr1 isoform that they could detect in HeLa cells was also 30kD. Combining the results, it suggests that in HeLa cells, the smallest and Oxr1-C equivalent cytosolic Oxr1 isoform is 30kDa, which might be due to cytosolic post translational modification (Forte et al., 2011). Mitochondrial protein post translational modification also occurs at a high frequency (Kim et al., 2006). Partial modification of the over-expressed Oxr1-S-Mito such as phosphorylation and acetylation may be the cause of the double band. Notably, the Oxr1-S-Mito construct was cloned with an approximately 3kD N-terminal mitochondrial MLS and the MLS is cleaved once the targeting is complete (Rizzuto et al., 1992). Thus, the double band could also be due to a mixture of cleaved and un-cleaved Oxr1-S-Mito in the cell lysate. Interestingly, in a previous study, FLAG-tagged over-expression of a mitochondrial protein CHCHD10 revealed a double band pattern nearly identical to the Oxr1 results; however, in this case, the lower band was considered to be non-specific (Bannwarth et al., 2014).

3.4.3 The role of Oxr1 in protecting the TDP-43 mutation induced mitochondrial impairments

Multiple lines of evidence has demonstrated that mitochondrial morphological and functional impairment can be caused by mutations in TDP-43 (A315T, Q331K and M337V) (Lu et al., 2012, Wang et al., 2013, Magrané et al., 2014). Studies from our group have demonstrated the interactions between Oxr1-C and TDP-43 as well as FUS (Finelli, 2010). Importantly, my results showed that over-expressing cytoplasmic Oxr1-S

is protective against mitochondrial morphological changes induced by oxidative stress. Therefore, we hypothesised that over-expressing Oxr1 can also protect mitochondria from impairments triggered by TDP-43 mutations. As expected, our results at least partially confirmed the hypothesis, but raised new questions regarding the potential mechanism for the protection.

Oxidative stress is one of the driving forces for TDP-43 and FUS to form stress granules (Bentmann et al., 2012), as well as being a hallmark of ALS (Bentmann et al., 2012). Previous results have also shown that over-expressing mutant TDP-43 is capable of generating oxidative stress (Duan et al., 2010). The data here demonstrated that under basal conditions, expression of the TDP-43 M337V mutation alone was capable of triggering mitochondrial impairment. It is plausible that the role of Oxr1 in protecting the TDP-43 mutation induced mitochondrial impairments is anti-oxidative. In addition, over-expression of Oxr1-S alleviated the reduction of both mitochondrial size and number and conferred a stronger protection under basal conditions comparing to the arsenite treated condition (**Figure 3.13B-C**), suggesting that under treated condition, the gross oxidative stress generated by the mutant TDP-43 and arsenite is beyond the level of Oxr1's anti-oxidative capacity. Nevertheless, it may also indicate a potential involvement of a regulatory role of Oxr1 that is not only dependent on anti-oxidation.

Tdp-43 and FUS are known as splicing regulators (Lagier-Tourenne et al., 2010). Over-expression of WT TDP-43 up-regulated mitochondrial fission regulators Drp1 and Fis1 and down-regulated a fusion regulator Mfn1 (Xu et al., 2010); whereas expression of TDP-43 mutants tend to shift mitochondrial network within motor neurons to a more pro-fission status (Wang et al., 2013), and this effect was reversed by over-expressing mitochondrial fusion protein Mfn2 (Wang et al., 2013). These results suggest a potential

regulatory role of TDP-43 on fusion and fission proteins possibly via its function as a splicing regulator.

Intriguingly, using *in silico* approaches, our lab recently found a potential role of Oxr1-C as a regulator of RNA-post-translational modification. Moreover, under oxidative stress, over-expression of Oxr1-C in cells transfected with Tdp-43 (M337V) abolished the TDP-43 mutation associated splicing alteration of a mitochondrial fission gene, *Mtfr1*, indicating a potential role of Oxr1 in regulating mitochondrial dynamics and a partial involvement of oxidative stress in this complicated unknown mechanism (Finelli et al., 2015a).

It was shown here that co-expression of Oxr1-S was capable of preventing a reduction in oxygen consumption, a key parameter of mitochondrial energy metabolism (**Figure 3.14A**), suggesting a protective role of Oxr1 in maintaining mitochondrial function. However, dysfunction in mitochondrial metabolism can also be caused by mitochondrial morphological changes (Wang et al., 2008b). Therefore, the potential protective role of Oxr1-S in maintaining mitochondrial function may be only a secondary effect of the Oxr1's role in regulating mitochondrial dynamics. Similarly, over-expression of Mfn2 has also been shown to protect cells from mitochondrial dysfunction induced by TDP-43 mutation (Wang et al., 2013), and the mitochondrial dysfunction was indeed found to be caused by mitochondrial morphological abnormalities (Wang et al., 2013).

Nevertheless, our initial results from mass spectrometry indicate Oxr1-S may interact with Atp5b and Slc25a5 (Finelli et al., 2015a), a subunit of the mitochondrial ATP synthase and a mitochondrial adenine nucleotide translocator, respectively (Ohta and Kagawa, 1986, Haitina et al., 2006). This might also suggest a role of Oxr1 in regulating mitochondrial energetic metabolism.

Moreover, the intermediate isoforms of OXR1 (40kDa and 55kDa) were found to be up-regulated in ALS patients' spinal cord biopsy samples (Oliver et al., 2011). Since both isoforms contain the TLDc domain that has a neuroprotective anti-oxidative role (Finelli et al., 2016b, Oliver et al., 2011) and it was found here in mouse spinal cord, the 40kDa and 55kDa isoforms are exclusively localised in mitochondria, these data suggest a potential role of these two mitochondrially localised isoforms in ALS pathology.

In summary, in this chapter, I systematically studied the sub-cellular and sub-mitochodnrial localisation of Oxr1 isoforms and revealed a localisation-specific, anti-oxidative role of Oxr1. Moreover, the mechanisms through which Oxr1 can improve the mitochondrial impairments caused by TDP-43 mutations have been linked with the regulation of mitochondrial fusion and fission. Elucidating these unknown mechanisms may provide potential methods for delay or prevention of TDP-43-related pathology of ALS.

Chapter 4: Investigating the morphological and functional status of mitochondria in Oxr1 knockout (*bella*) mice

4.1. Introduction

In the previous chapter, it was demonstrated that cytoplasmic over-expression of Oxr1 prevented oxidative stress-induced apoptosis. Oxr1 was also able to alleviate aspects of mitochondrial morphology caused by oxidative stress, and partially reversed a mitochondrial oxygen consumption defect that resulted from a pathogenic TDP-43 mutation. These data suggest a protective role of Oxr1 related to mitochondrial function. In contrast to Oxr1 over-expression, the recessive *Oxr1* deletion mutant mouse *bella (bel)* displays a neurodegenerative phenotype associated with oxidative stress (Oliver et al., 2011). Apoptosis in the cerebellar granule cell layer (GCL), severe and progressive ataxia are the phenotypical features of the *bella* mutant (Oliver et al., 2011). Over-expression of Oxr1 *in vitro* is protective against oxidative stress induced apoptosis in primary cerebellar GCs (Oliver et al., 2011). Together, these data suggest an important protective role of Oxr1 against oxidative stress in the CNS. However, the link between *Oxr1* deletion and potential mitochondrial dysfunction has not been fully studied.

Mitochondria play an essential role in oxidative stress generation, which in turn contributes to cell apoptosis (Bhat et al., 2015) Mitochondria are also well known as a key site for apoptosis activation through releasing the IMS protein Cyt-C (Wang and Youle, 2009). Abnormalities in mitochondrial morphology and dynamics as well as dysfunction in mitochondrial bioenergetics are common features of neurodegenerative disorders (Cabezas-Opazo et al., 2015, Su et al., 2010). For example, in a rat neuroblastoma cell line expressing α-synulcein, co-expression of a mutant PD-related, mitophagy regulator PINK1 leads to increased mitochondrial size and abnormal cristae,

suggesting a role of PINK1 in maintaining mitochondrial morphology (Marongiu et al., 2009). In the hippocampus of AD patients, protein levels of mitochondrial fusion regulators OPA1, Mfn1 and Mfn2 as well as the level of a fission protein Drp1 were significantly reduced; whereas the level of another fission regulator, Fis1 was significantly increased, suggesting that the mitochondrial dysfunction and neuronal pathogenesis in AD may be resulted from an alteration in the balance between fusion and fission (Wang et al., 2009). In mitochondria obtained from PD patients' substantia nigra region and platelet, reduced complex I activity or, to a lesser extent, complex III activity have been detected (Schapira et al., 1989, Parker et al., 1989). However, whether these impairments are a direct cause or an effect of neurodegeneration still remains unclear.

Loss of neurodegenerative disease associated genes has been shown to cause mitochondrial abnormalities. For instance, in dopaminergic cells in the substantia nigra, the deletion of the PD associated gene DJ-1, leads to impairment in mitochondrial complex I assembly and a reduction in mitochondrial oxygen consumption (Heo et al., 2012). Knocking out Parkin, an E3 ubiquitin ligase linked with familial PD also causes reductions in protein levels of mitochondrial complex I, complex IV and anti-oxidative protein peroxiredoxin (PRDX) as well as a reduction in mitochondrial respiration, despite an apparently normal mitochondrial morphology (Palacino et al., 2004). The above results suggest that these key neurodegeneration-related genes are likely to exert their regulatory roles via mitochondrial pathways.

Previous studies have demonstrated an anti-oxidative regulatory role of Oxr1, but whether this role is dependent on a mitochondrial pathway is unknown. Based on the finding in chapter 3 that Oxr1 alleviated mitochondrial morphological changes and oxygen consumption defect, it is hypothesised that *Oxr1* deletion may lead to mitochondrial morphological abnormality or dysfunction in bioenergetics.

4.2 Aims of Chapter 4

The aim of this chapter was to examine whether loss of Oxr1 *in vivo* causes mitochondrial morphological disruption or dysfunction in mitochondrial bioenergetics.

4.3 Results

4.3.1 Mitochondrial length is reduced in primary cerebellar GCs from mice lacking *Oxr1*

Since over-expressing cytosolic Oxr1 *in vitro* is able to alleviate OS-induced mitochondrial morphological changes (**Section 3.3.5**), yet the cause of selective neurodegeneration in the *bella Oxr1* deletion mouse is still unclear, it is speculated that the loss of *Oxr1* would influence mitochondrial structural integrity. To examine this hypothesis, primary cerebellar GC neurons were utilised, since this is the only region of the brain where neurodegeneration is detected at disease end-stage in homozygous *bella* mutants ($Oxr1^{bel/bel}$). Primary GCs from *bella* mice and wild-type (WT) littermate controls at P7 were isolated and grown *in vitro* until DIV7 and their identity confirmed by immunostaining with granule neuron marker GABA (A) receptor subunit alpha-6 (GABRA6) (**Figure4.1A**). The differentiation of the primary granule neurons was confirmed by staining with a dendritic marker MAP2 and axonal marker tau (**Figure 4.1B**). Mitochondria were confirmed to be in both dendrite and axon by co-staining with mitochondrial marker COX IV (**Figure 4.1B**).

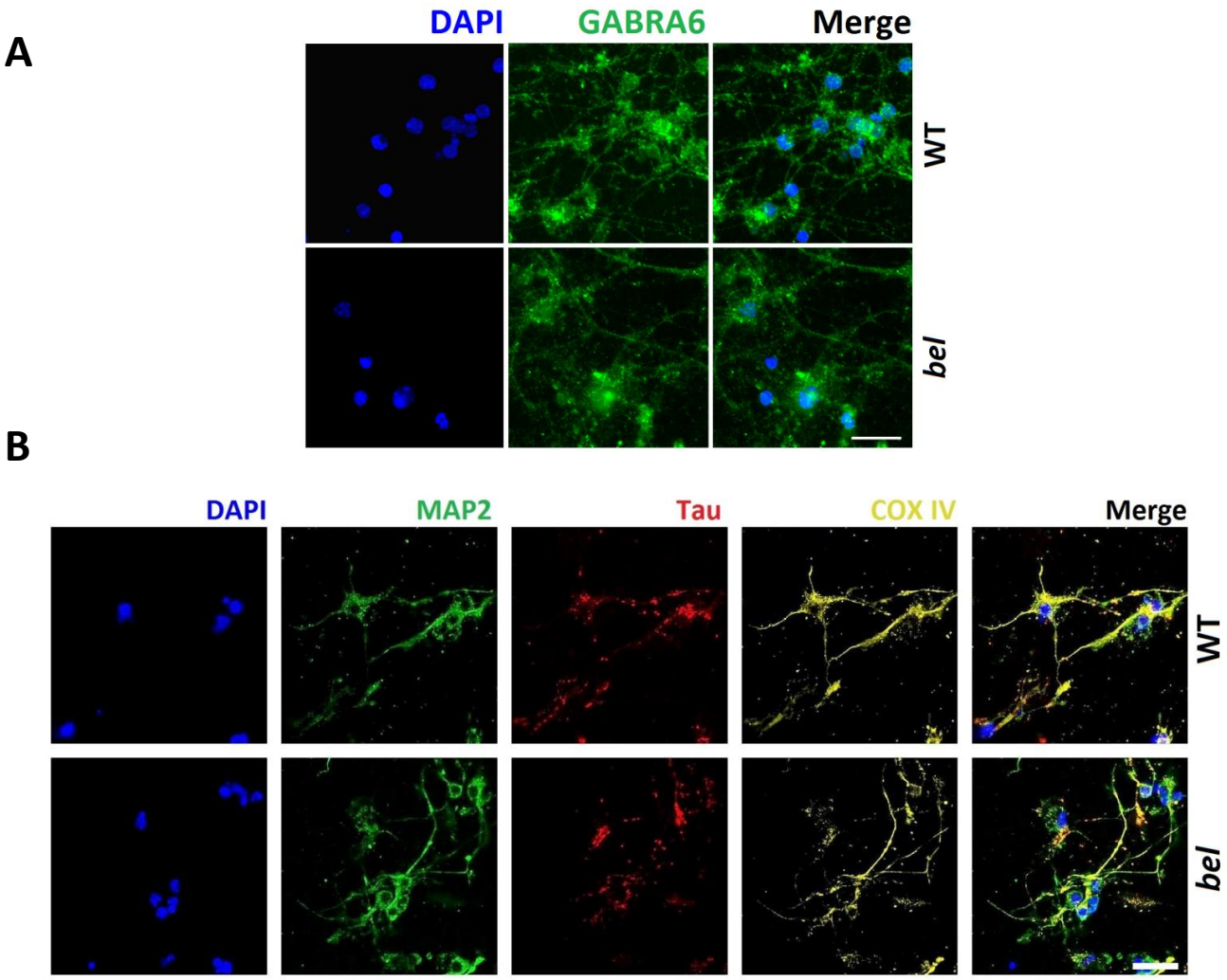

Figure 4.1. Markers for cerebellar granule neuron

(A) Representative images confirming the expression of GABA(A) receptor alpha 6 in granule neurons by immunocytochemistry from primary cerebellar GC culture of WT and *bella* mice. Scale bar = 10µm. **(B)** Primary cerebellar GCs were triple stained for MAP2, a dendritic marker for GC; tau, an axonal marker and COX IV, a mitochondrial marker. Nuclei were mounted with DAPI. Scale bar=20µm

By quantifying mitochondrial structure between primary GCs cultured in parallel from the two genotypes (**Figure 4.2A**), we discovered that mitochondrial length was significantly reduced in primary GCs of *bella* mice in comparison with WT (**Figure 4.2B**). Importantly, there was neither a difference in average size or total number of mitochondria per focal plane between the genotypes (**Figure 4C-D**). These data suggest that the mitochondrial population shifts towards a more non-tubular structure when *oxr1* is deleted.

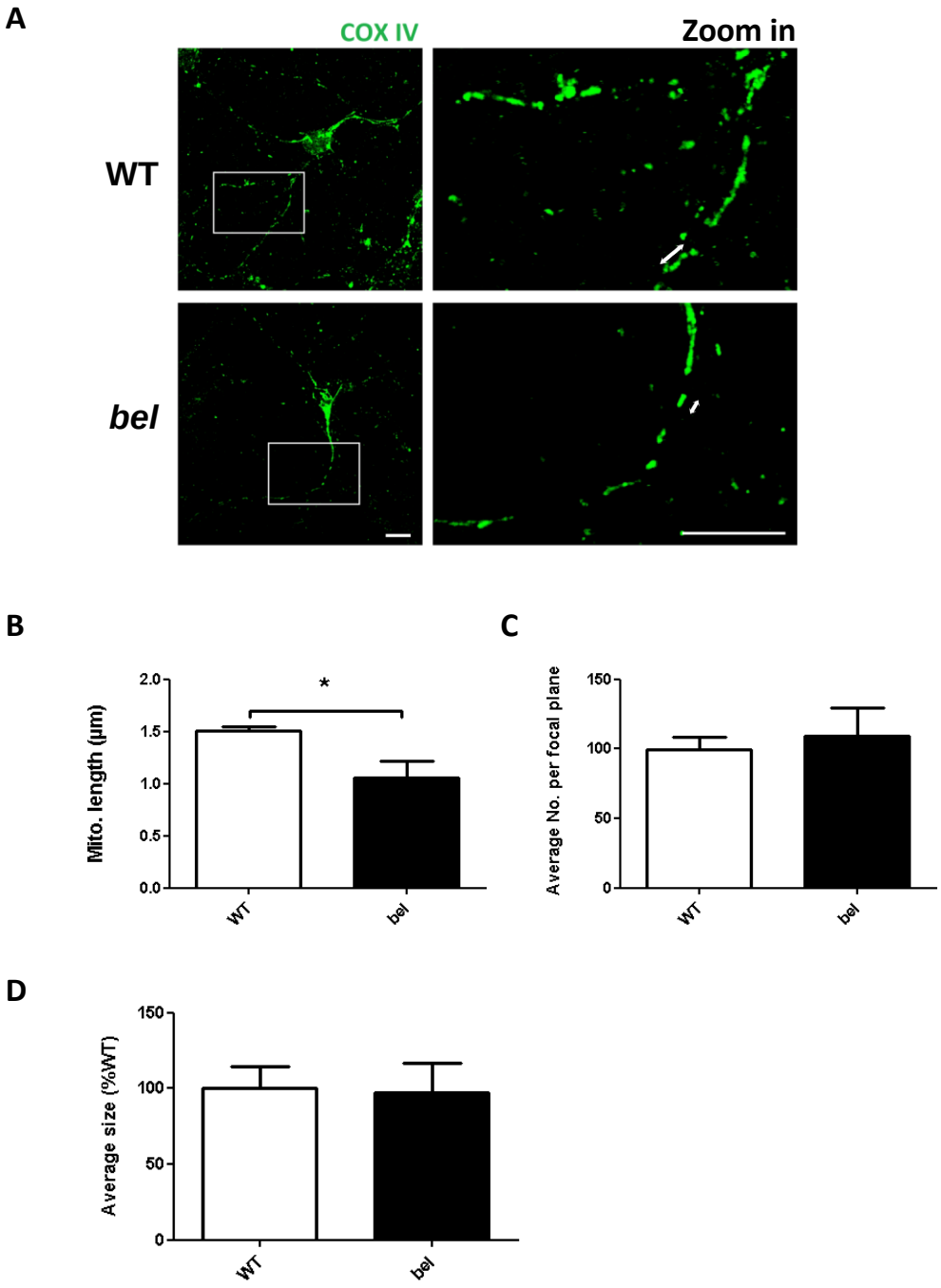

Figure 4.2. Mitochondrial morphological changes in primary cerebellar GCs of *bella* mice

(A) Representative images showing mitochondria in WT and *bella* (*bel*) primary cerebellar GCs. Scale bars = 10µm. **(B)** Mitochondrial length is significantly reduced in *bella* compared to WT GCs. (**C, D**) No difference was observed in the average size or total number of mitochondria per focal plane between WT and *bella* GCs. Mitochondria were quantified in primary GCs of 3 WT and 3 *bella* mice and a minimum of 10 cells were analysed per replicate. Data are shown as mean ± S.E.M. and analysed by Student's t- test; * $p < 0.05$.

4.3.2 Intact mitochondrial ultra-structure in the cerebellum of end-stage *bella* mouse

Mitochondrial ultra-structural changes have been observed in cells under both acute and chronic conditions of oxidative stress. In H_2O_2 treated MEFs, swollen mitochondria with thinner cristae were observed (Cole et al., 2010). In an AD patient specimen, cristae disruptions as well as accumulation of osmophilic substance in mitochondria of Purkinje cells have been detected (Baloyannis, 2013). However, whether lack of Oxr1 can cause mitochondrial ultra-structural alterations is unknown. To address this question, TEM was conducted to detect the ultra-structure of cerebella mitochondria in *bella* and WT mice.

Through visual observation of multiple cerebellar sections, preliminary results showed that the ultra-structure of cerebellar mitochondria from 1 end-stage *bella* and 2 age-matched WT mice appeared to be comparable and intact (**Figure 4.3.**). No rupture of either OM or IM was detected; and neither swelling nor cristae disruption was observed. These results suggest that the loss of Oxr1 does not cause a disruption in mitochondrial ultra-structure.

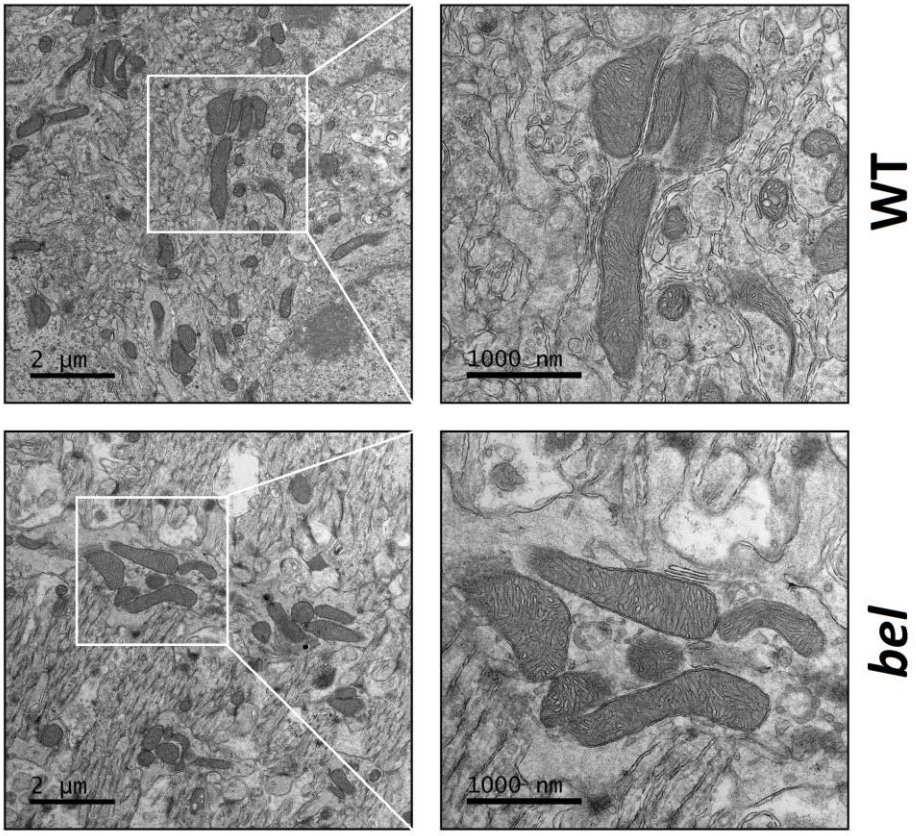

Figure 4.3. Ultra-structure of mitochondria in WT and *bella* cerebellum.

TEM of cerebellar mitochondria from near end-stage *bella* and age-matched WT mice. Mitochondria exhibit normal and comparable ultra-structure from both genotypes.

4.3.3 Deletion of *Oxr1* influences expression of mitochondrial fission regulators

Since mitochondrial shape and morphology are regulated by fusion and fission (Otera et al., 2013), whether deletion of *Oxr1* affects these processes was examined. Protein levels of major known fusion regulators, Mfn1, Mfn2 and OPA1 as well as fission mediators Drp1 and Fis1 were quantified from WT and *bella* cerebellar homogenates taken at end-stage P24 **(Figure 4.4A)**. No differences in expression were detected between genotypes, with the exception of Drp1, that showed a statistically significant increase in *bella* mice compared to WT **(Figure 4.4B)**. Under OS, Drp1 is phosphorylated at Ser616, which activates the protein for recruitment to mitochondria to facilitate the fission process; conversely, dephosphorylation at Ser616 inhibits mitochondrial fission (Qi et al., 2011, Yu et al., 2010). Therefore, whether there is an increase of Drp1 recruitment to mitochondria in the *bella* cerebellum was then tested, although no difference in the levels of Drp1 either in the cytosolic or mitochondrial fractions compared to WT were observed **(Figure 4.4C)**. It was hypothesised, therefore, that there may be an inhibitory effect on the activity of Drp1 in mutant mice, thus we tested the level of phosphorylated (p-) Drp1 S616 **(Figure 4.4D)**. Interestingly, the level of p-Drp1 S616 was significantly lower in cerebella homogenate from *bella* compared to WT mice **(Figure 4.4E)**, indicating an inhibitory effect of Drp1's activity. In addition, it is also known that phosphorylation at Ser637 of Drp1 plays an inhibitory role on the fission process (Chang and Blackstone, 2010, Jahani-Asl and Slack, 2007). To test whether Drp1 S637 is also involved in mitochondrial response to Oxr1 loss, western blotting was carried out. However, the level of phosphorylated (p-) Drp1 S637 was barely detectable, regardless of experiment conditions (data not shown), suggesting a non or less significant role of Drp1 S637 in mitochondrial response to Oxr1 loss. Overall,

these data suggest that the change in mitochondrial morphology observed in *bella* mice may be caused by a compensatory pathway that inhibits the activity of Drp1 through dephosphorylation of Ser616 in response to stress caused by the deletion of *Oxr1*.

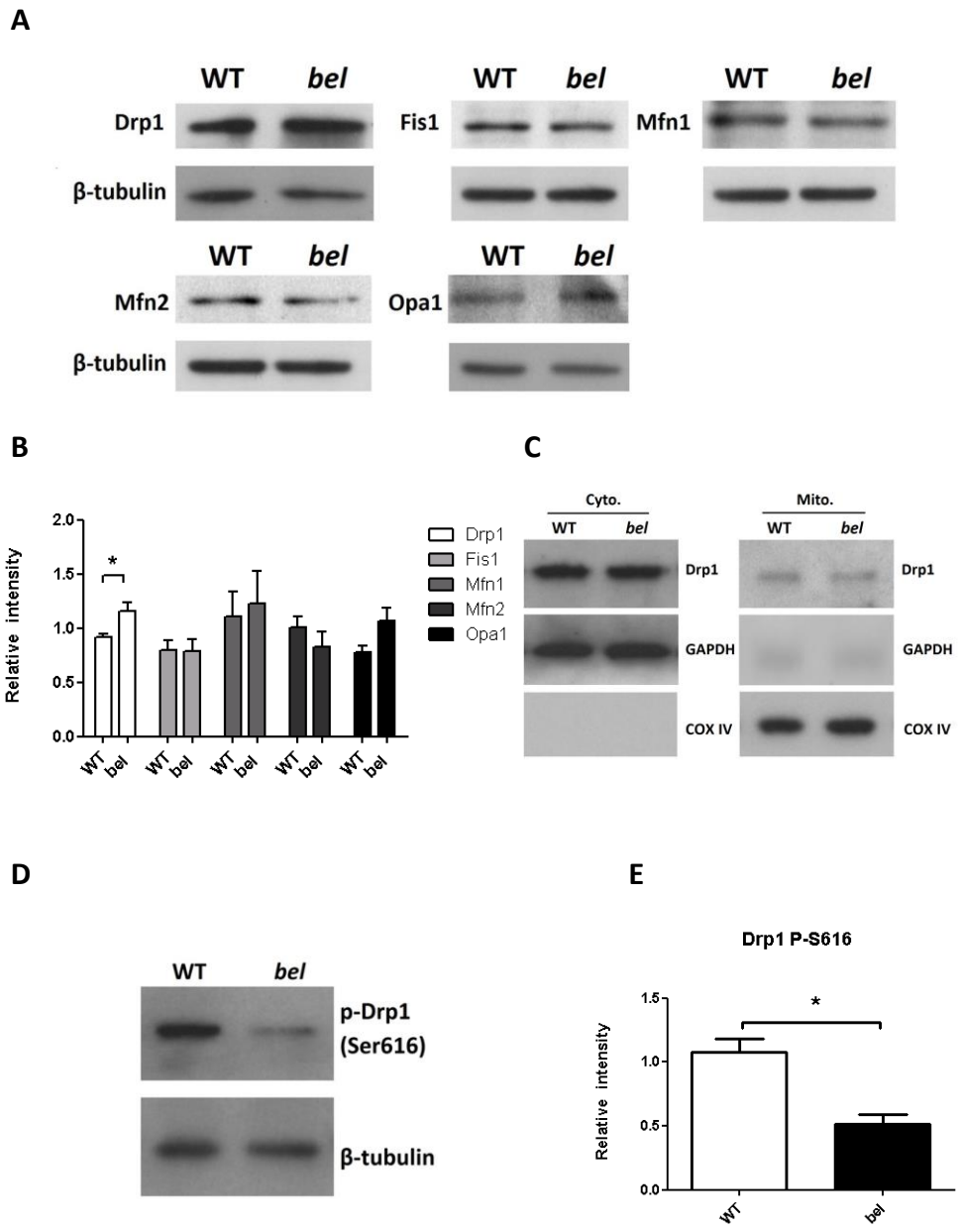

Figure 4.4. Expression level of mitochondrial fusion and fission proteins in cerebella of WT and *bel* mice

(A) Cerebellar homogenates from 6 end-stage *bel* and age-matched WT mice were subjected to western blotting for mediators of mitochondrial fission (Drp1 and Fis1) and fusion (Mfn1 and Mfn2). For fusion regulator Opa1, 3 independent samples of each genotype were measured. **(B)** Quantitative analysis by densitometry; the total level of Drp1 is significantly higher in *bella* comparing to WT tissue. **(C)** Western blot of cytosolic and mitochondrial fractions were labelled with anti-Drp1 cytoplasmic marker anti-GAPDH and mitochondrial marker anti-COX IV. No sub-cellular translocation of Drp1 was observed. **(D)** Western blot of cerebellar homogenate from end-stage *bella* and age-matched WT mice were labeled with p-Drp1 S616, indicating that the expression level in *bella* is significantly lower than WT. (**E**) Phosphorylation of Drp1 relative to β-tubulin loading control. Data are shown as mean ± S.E.M. from 3 independent samples of each genotype and were analysed by Student's t-test; * $p < 0.05$.

4.3.4 Mitochondrial DNA mutations do not accumulate in *bella* mouse

The vulnerability of mitochondrial (mt)DNA to OS has been well-established (Yakes and Van Houten, 1997, Salazar and Van Houten, 1997) and recently, accumulation of mtDNA damage was found in OXR1 depleted (approximately 85% knockdown) HeLa cells treated with H_2O_2 (Yang et al., 2014). Furthermore, it has been shown previously that OS-induced genomic DNA damage occurs in the cerebellar GCL of end-stage *bella* mice using 8-hydroxydeoxyguanosine (8-OHdG), a marker of OS to DNA (Oliver et al., 2011).

To study next whether the deletion of *Oxr1* can cause accumulation of endogenous mtDNA lesions in *in vivo*, DNA was extracted from the cerebella of WT and end-stage (P24) *bella* mice and the mtDNA was subjected to quantitative (q)PCR to amplify a long (10.1 kb) and a short (117 bp) mtDNA fragment (**Figure 4.5A**). Since it becomes less efficient for PCR reactions to amplify long mitochondrial fragments when more lesions appear in mtDNA (Jendrach et al., 2005), level of mtDNA damage can be revealed by comparing relative PCR product. Using this method, no increase in mtDNA lesions was evident in the *bella* cerebellum (**Figure 4.5B**), indicating that loss of Oxr1 does not lead to accumulation of mtDNA damage in the cerebellum.

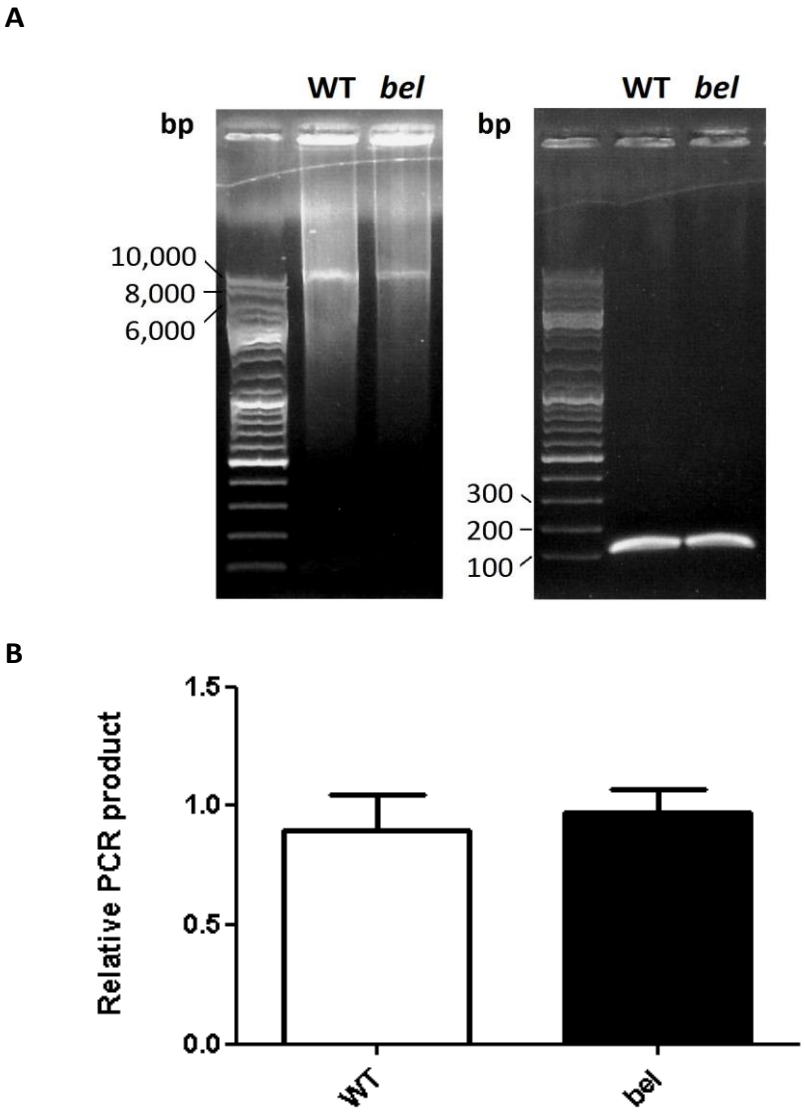

Figure 4. 5. *bella* displays no mitochondrial DNA damage
(**A**) Representative gels showing PCR products of a long (10.1 kb) and a short (117bp) mtDNA fragments from total DNA extracted from cerebellar tissue of 5 WT and end-stage 6 bel mice. (**B**) Quantification was carried out by the PicoGreen method and the relative PCR product number of the long mtDNA fragment (10.1 kb) is normalised to the copy number of the short mtDNA fragment (117bp). There is no difference in the relative PCR product number between WT and *bel* mice. Data are means ± S.E.M. and analysed by Student's t- test.

4.3.5. *bella* mouse has normal mitochondrial ETC expression levels and intact complex assembly

The unique capability of mitochondria for producing energy in the form of ATP is dependent on its ETC embedded in the IM. Previous discoveries have suggested potential association between oxidative phosphorylation (OXPHOS) defects within mitochondria and neurodegenerative diseases (Werner et al., 2012). Both mtDNA mutations and ETC-specific nuclear DNA mutations affect oxidative phosphorylation (OXPHOS) (Trounce, 2000). As an initial investigation into whether lack of Oxr1 *in vivo* can lead to gross alterations of ETC complex protein expression and assembly, expression levels of five ETC complex subunits (Complex I to V) in both WT and *bella* mice were measured by labelling with total OXPHOS antibody cocktail prior to western blot analysis (**Figure 4.6.A**). Results from western blotting displayed similar expression levels of the five ETC complex subunits between the WT and *bel* mice. These results suggested that Oxr1 does not play an essential role in regulating the translation of the subunits of the ETC complex.

Proper function of the ETC relies on the appropriate assembly of mitochondrial ETC complexes. Whether loss of Oxr1 had an impact on mitochondrial complex assembly pathways was then tested by conducting BN PAGE analysis to detect formation of the 5 complexes. BN results revealed no difference in mitochondrial ETC complex formation between WT and *bella* mice (**Figure 4.6.B**), which indicated that Oxr1 does not participate in the assembly process of mitochondrial ETC complex.

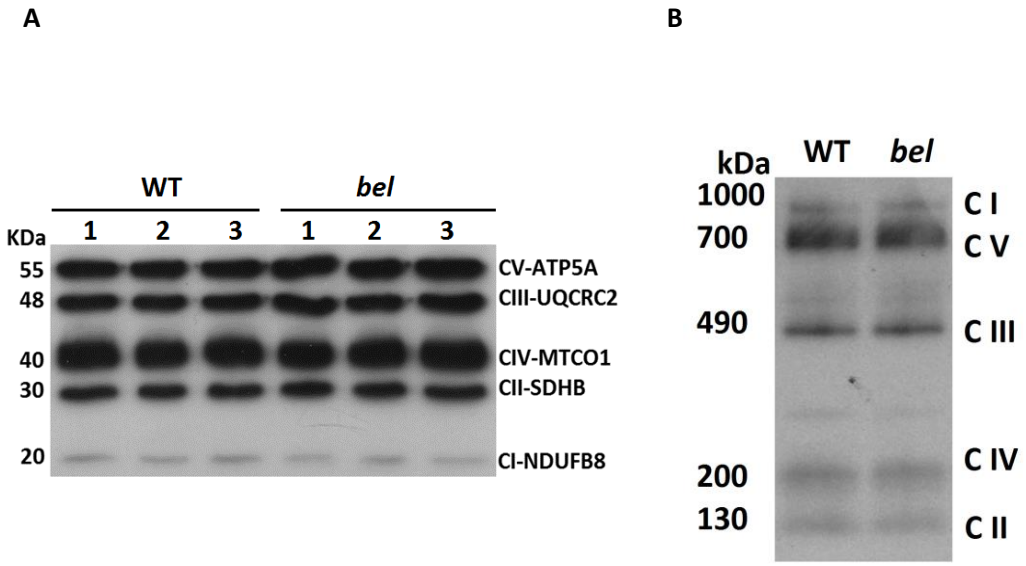

Figure 4.6. Expression levels of five ETC complexes and ETC complex assembly in WT and *bel* mice

(A) Equal amount (30 μg) of mitochondria purified from cerebella of 3 end stage *bella* and 3 age-matched WT mice were immunoblotted with an antibody cocktail against subunits of five ETC complexes: CI-NDUFB8, CII-SDHB, CIII-UQCRC2, CIV-MTCO1 and CV-ATP5A. No differences in expression were observed. **(B)** End-stage *bella* and age-matched WT cerebellar tissue were subjected to BN-PAGE analysis to resolve purified mitochondrial proteins solubilised by the detergent n-dodecyl-β-D-maltopyranoside (DDM). A representative image is shown of samples probed using an anti-OxPhos Complex antibody indicating no defects in complex assembly in *bella* mice.

4.3.6. Loss of Oxr1 does not affect enzymatic activities of mitochondrial electron transport system (ETS)

Having shown similar levels of ETC protein translation and intact complex assembly between the genotypes, the potential effect of Oxr1 loss on the mitochondrial ETS (C I to C IV) activities was then evaluated. To achieve this, mitochondria isolated from cerebella of end-stage *bella* (P24) and age-matched controls were subjected to spectrophotometric or in-gel activity assays.

The activity of mitochondrial Complex I was detected by measuring rotenone-sensitive NADH oxidation at 340 nm. It showed no difference between WT and *bella* (**Figure 4.7A**). The result was verified by C I in-gel activity assay: bands representing C I also revealed no difference between the genotypes (**Figure 4.7B**). The activity of C II was then assayed by measuring the colour change of DCPIP at 600nm. Results showed no difference between WT and *bella* (**Figure 4.7C**). The activity of C III was also assayed by measuring Cyt-C reduction at 550nm; comparable activities were observed between the genotypes (**Figure 4.7D**). C IV activity was measured by detecting Cyt-C oxidation at 550 nm. Mitochondria in *bella* also appeared to have a similar CI activity in comparison with the WT (**Figure 4.7E**). Finally, as a control, citric synthase activity was examined by measuring formation of TNB at 412 nm as a result of a reaction between CoA-SH and 5', 5'-Dithiobis 2-nitrobenzoic acid (DTNB). No difference between the two genotypes was discovered (**Figure 4.7E**).

Taken together, the data suggest that the *Oxr1* deletion has no overt impact on mitochondrial ETC complex activities (C I to C IV).

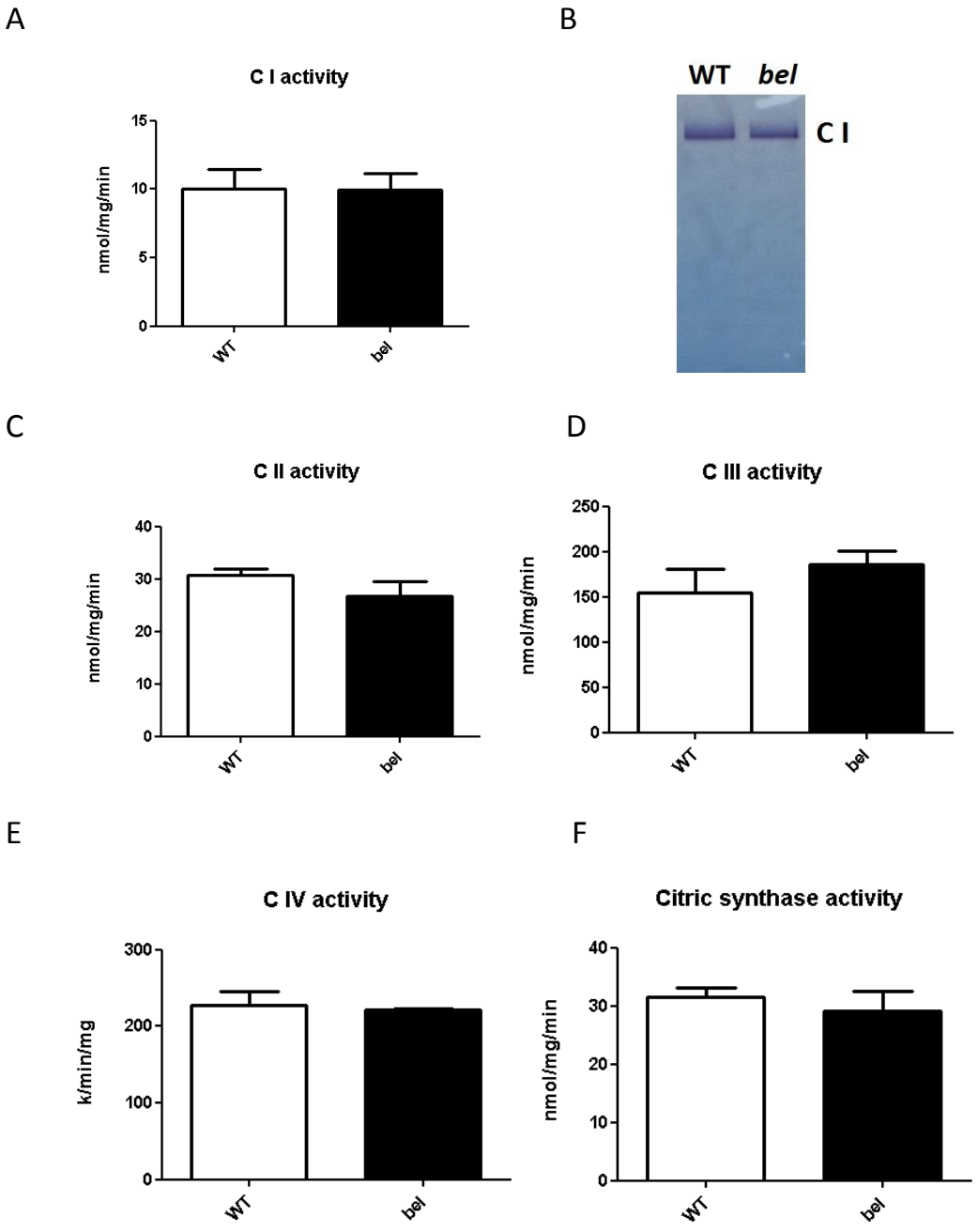

Figure 4.7. Mitochondrial ETC complex activities in *bella* and WT mice

No differences in ETC activities between *bella* and WT mice were observed. Measurement of complex activities was conducted using spectrophotometry and BN-PAGE gel electrophoresis for in-gel CI assay. All activity results were obtained from mitochondrial extractions of end stage *bella* and age-matched WT mice **(A)** CI activity **(B)** in-gel activity of CI **(C)** CII activity **(D)** CIII activity **(E)** CIV activity **(F)** Citric synthase activity. Data are shown as the mean ± S.E.M. from 3-6 replicates of each genotype and analysed by Student's t- test.

4.3.7 Primary cerebellar GCs from *bella* mice display normal mitochondrial membrane potential

Having shown similar mitochondrial ETS activities (CI to C IV) between WT and *bella* tissue samples, the functional status of ATP synthase (C V) needs to be investigated. Initially, attempts to directly measure the activity of C V were made by using an in-gel method as previously described (Zerbetto et al., 1997). However, the bands representing the C V activity were barely detectable (data not shown), indicating that the sensitivity of this in-gel method previously used for measuring heart and skeletal muscle C V activities (Zerbetto et al., 1997) was insufficient in detecting the cerebellar C V activity. Therefore, mitochondrial membrane potential, the electrical gradient of proton motive force that drives protons across the IM through ATP-synthase was measured as an indirect way to reveal the functional status of C V and overall mitochondrial energy metabolism (Perry et al., 2011).

Using a TMRM fluorescent method, mitochondrial membrane potential was measured in primary cerebellar GCs culture. The GCs were isolated from cerebella of the WT and *bella* mice at P7 and cultured for 7 days. It showed that mitochondrial membrane potential measured by TMRM fluorescence remained the same between the genotypes, indicating once again that Oxr1 loss does not lead to impairment in mitochondrial energetic metabolism (**Figure 4.8**).

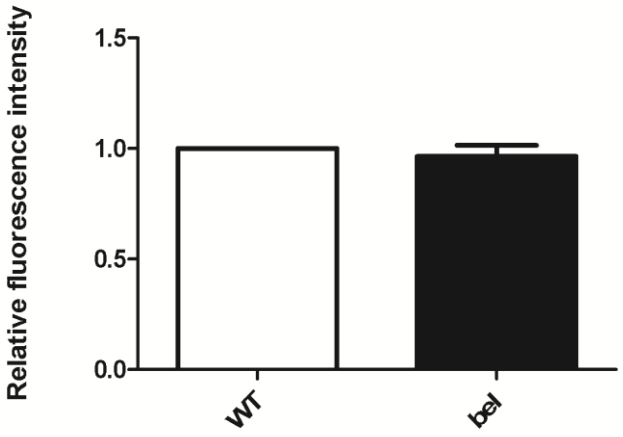

Figure 4.8. No difference in mitochondrial membrane potential between *bella* and WT mice

Pulled primary GCs obtained from 2-3 WT and *bella* mice were measured in each experiment and the data were obtained from 3 independent experiments. No difference in mitochondrial membrane potential was observed between *bella* and the age-matched wild type control. Data were presented as means ± s.e.m. and analysed by Student's t-test.

4.3.8 Primary cerebellar GCs from *bella* mice display normal mitochondrial oxygen consumption levels

To date, loss or disruption of a number of antioxidant proteins such as SOD1 and DJ-1 has been found to influence mitochondrial oxygen consumption as part of a potential neurodegenerative pathway in the SOD1 (G93A) mutant mouse tissue and DJ-1 knockout dopaminergic neurons (Heo et al., 2012, Mattiazzi et al., 2002). Whether deletion of *Oxr1* can cause similar defects was therefore studied by measuring mitochondrial oxygen consumption and other respiratory parameters from WT and *bella* primary GCs at P7 cultured for 7 days using the Seahorse metabolic analyser that utilises fluorescently sensitive probe to measure the concentration of oxygen. Basal respiration level was first measured prior to addition of any mitochondrial stressors, and no difference was observed between genotypes at any of the time points measured (**Figure 4. 9A**). After adding mitochondrial complex V inhibitor oligomycin, a marked decline of oxygen consumption level (approximately 100 pmol/min) was observed in both WT and *bella* GCs, indicating the same amount of oxygen was used for ATP production. Then the mitochondrial uncoupler FCCP was added that immediately triggered a marked induction of oxygen consumption (approximately 150 pmol/min) in both WT and *bella*, suggesting the spare oxygen consumption capacity of GCs from both genotypes was equivalent (**Figure 4. 9A**). Finally, rotenone and antimycin A, which inhibit CI and CIII respectively, were added to the assays causing a considerable reduction in oxygen consumption as expected. The remaining oxygen consumption level indicated the amount of oxygen available for non-mitochondrial respiration, approximately 50 pmol/min for both genotypes. By subtracting non-mitochondrial O_2 consumption level, the normalised data suggest that there was no significant difference of mitochondrial oxygen

consumption in basal level, proton leak stage or maximum respiration between WT and *bella* GCs (**Figure 4. 9B**).

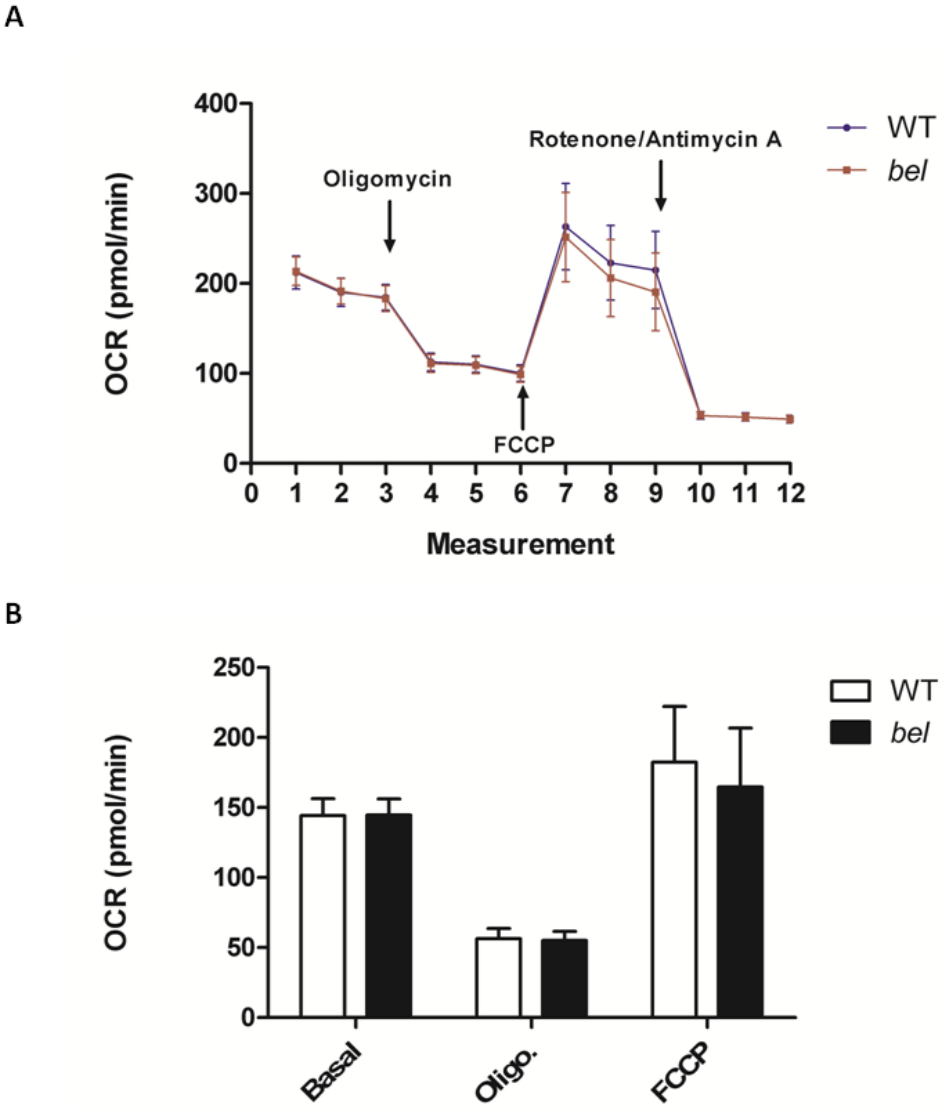

Figure 4.9. Oxygen consumption in primary GCs is not affected by deletion of *Oxr1*

(A) Oxygen consumption rate (OCR) profiles are expressed as pmol of O_2 consumed per minute in primary GCs of WT and *bel*. Arrows indicate the time point of adding mitochondrial inhibitors/stressors: oligomycin (3 µM), FCCP (2 µM) and rotenone and antimycin (2µM, each). **(B)** Normalized OCRs after subtraction of rotenone/antimycin treated OCR (non-mitochondrial respiration), under basal condition, after adding oligomycin (3 µM, proton leak) or FCCP (2 µM, maximal respiration). The data were obtained from 3 independent experiments using primary GCs obtained from 6 WT and 5 *bella* mice. Data are shown as the mean ± S.E.M. and analysed by Student's t-test.

Discussion

In this chapter, to investigate whether the loss of Oxr1 causes mitochondrial morphological abnormalities or functional defects, the primary GCs or cerebellar tissue from *bella* mice and the age-matched WT control were studied. It was found that *Oxr1* deletion leads to a mild mitochondrial gross shape change compared to the WT in primary GCs, but normal ultra-structure *in vivo*. No differences in protein levels of major fusion and fission regulators were detected between the genotypes, except the levels of Drp1 and phosphorylated Drp1 (S616). In terms of mitochondrial bioenergetics, the levels of protein expression and post-translational assembly of mitochondrial ETC complexes appeared to be unchanged in the end-stage *bella* mouse in comparison with the age-matched control. ETC complex activities, mitochondrial membrane potential and mitochondrial respiratory capacities in *bella* mouse were also comparable to the control. These experiments suggest that the *Oxr1* deletion alone is unlikely to trigger overt mitochondrial dysfunction prior to the activation of cerebellar GC apoptosis.

4.4.1 Oxr1 loss and mitochondrial morphology and dynamics

Mitochondrial dynamics is constantly regulated by fusion and fission processes, and plays a key role in determining mitochondrial morphology (Otera et al., 2013). Loss of anti-oxidative proteins such as DJ-1 can lead to abnormalities in both mitochondrial morphology and dynamics. For example, in DJ-1 null dopaminergic neuronal cells, both mitochondrial size and numbers are reduced comparing to the control (Heo et al., 2012). In mouse embryonic fibroblasts (MEFs), loss of DJ-1 leads to reduced mitochondrial length (Irrcher et al., 2010); while using the same cell type, Krebiehl, Ruckerbauer *et al* not only confirmed a reduced mitochondrial length but also showed a reduced level in mitochondrial branching (Krebiehl et al., 2010). In MEFs, loss of DJ-1 leads to

fragmented mitochondria with reduced fusion rates and a reduction in the protein level of mitochondrial fusion regulator Mfn1, but not the fission regulator Drp1 (Irrcher et al., 2010). Importantly, the mitochondrial fragmentation was found to be linked with elevated ROS levels (Irrcher et al., 2010). Together, these results indicate that oxidative stress plays an important role in facilitating mitochondrial fragmentation.

It was therefore hypothesised that there would be a shift in the mitochondrial population towards a more pro-fission status in cerebella of end-stage *bella* mice due to an increased level of OS in this region as detected previously (Oliver et al., 2011). The confocal microscopy here showed mitochondria with reduced length, but normal size and number (Figure **4.2B- D**), and TEM showed cerebellar mitochondria of near-end stage *bella* mice displayed normal ultra-structure (**Figure 4.3**). Of note, the TEM images obtained in this study were two-dimensional (2D). Since different mitochondrial three-dimensional (3D) projections (0.2-2 μm) exist and the mitochondrial 2D images taken from the ultrathin (50-100 nm) tissue sections cannot accurately reflect those 3D projections (Nathaly Rigoglio et al., 2012), TEM is not considered as a suitable method for measuring the length of mitochondria. Using the confocal method for mitochondrial length observation and quantification in neurons has been well established (Cheng et al., 2012, Silva-Alvarez et al., 2013, Wang et al., 2013). The TEM method here was therefore only used for observing potential mitochondrial ultra-structural abnormalities such as matrix swelling and membrane damage, in order to complement the incapability of confocal microscopy in studying mitochondrial ultra-structures.

Screening the protein level of major known fusion regulators, Mfn1, Mfn2 and OPA1 as well as fission mediators Drp1 and Fis1 found no difference between the *bella* and age-matched WT mice, apart from a small but statistically significant increase in the Drp1 (**Figure 4.4B**), suggesting a pro-fission protein up-regulation towards

mitochondrial fission in response to the loss of Oxr1. Unexpectedly, the level of phospho-Drp1 (Ser616) was found to be significantly reduced in cerebellar homogenate of *bella* mouse (**Figure 4.4E**). Multiple lines of evidence have shown that under OS, once phosphorylated at Ser616, the fission protein Drp1 is activated to facilitate mitochondrial fragmentation (Taguchi et al., 2007, Qi et al., 2011). Intriguingly, reduction of phosphor-Drp1 S616 is also observed in cells upon starvation (Rambold et al., 2011), indicating a protective pathway against stress. My results are therefore in favour of an unknown pathway involved in regulating the phosphorylation of Drp1 to inhibit mitochondrial fission and compensate the stress caused by the loss of Oxr1.

4.4.2 Oxr1 loss and mitochondrial DNA integrity

mtDNA damage has been detected in several neurodegenerative diseases and can subsequently lead to mitochondrial dysfunction (Cha et al., 2015). For example, in substantia nigra neurons of PD patients, high levels of mtDNA mutations were detected (Bender et al., 2006); while in the motor cortex of sporadic ALS patients, the level of a mtDNA deletion mutation was significantly higher comparing to the temporal cortex of the patients, but not in the same brain regions of the healthy controls (Dhaliwal and Grewal, 2000). However, using quantitative (q) PCR, no evident increase of mtDNA lesions in the cerebella of *bella* mice was detected (**Figure 4.5B**); while Yang *et al.* also showed no accumulation of mtDNA damage in OXR1 depleted (85% knockdown) HeLa cells (Yang et al., 2014). However, when treated with hydrogen peroxide, accumulation of mtDNA damage occurs (Yang et al., 2014). Together, these results suggest that the loss of OXR1 alone does not lead to mtDNA damage, but increases the susceptibility of mtDNA to oxidative stress. Furthermore, by staining with oxidative DNA damage marker 8-OHdG, Kay Davies' lab had demonstrated that OS induced DNA damage is

exclusively detectable in cerebellar GCL of end-stage *bel* mice (Oliver et al., 2011). Since the GCL comprises only a small proportion of the whole cell population, it could be that the levels of mtDNA damage between the genotypes at the disease end-point are below the detection threshold of the most sensitive techniques used in the experiment.

4.4.3 Oxr1 loss and mitochondrial metabolic functions

Defects in the expression and assembly of OXPHOS complexes have been reported in several neurodegenerative disorder-related gene knockout cell types and animal models. For instance, a defect in complex I assembly has been detected in PINK1 knockout flies and DJ-1 null substantia nigra dopaminergic cells (Liu et al., 2011, Heo et al., 2012). In PINK1 knockout flies, this defect subsequently leads to a reduction in complex I activity (Liu et al., 2011); while in DJ-1 null cells, the defect further causes a reduction in mitochondrial respiration (Heo et al., 2012). Recently, it has been demonstrated that a loss of function in *vacuolar protein sorting 13C* (*VPS13C*) leads to autosomal-recessive early-onset PD (Lesage et al., 2016). Knockdown of this gene (approximately 75%) in monkey fibroblast-like COS-7 cell line leads to a reduction in mitochondrial membrane potential and an increase in mitochondrial respiration rates (Lesage et al., 2016). However, results here showed that loss of Oxr1 did not lead to alterations in mitochondrial ETC protein levels (**Figure 4.6A**), complex assembly (**Figure 4.6B**) and the subsequent mitochondrial bioenergetics (**Figures 4.7-9.**), indicating that the deletion of *Oxr1* in the mouse cerebellum or cultured GCs does not trigger a profound mitochondrial functional alteration. Moreover, using RNA sequencing, Yang *et al.* recently found a large number of genes including anti-oxidative genes, transcription factors and apoptosis regulators that were up- or down-regulated in OXR1 depleted HeLa cells under basal or oxidative stress conditions (Yang et al., 2015).

However, only very few genes were mitochondria-related including Cyt-C, which plays a key regulatory role in apoptosis (Yang et al., 2015). Together, these results further indicate that Oxr1 might not exert its anti-oxidative role directly via mitochondrial bioenergetics pathways.

Interestingly, proteomic interaction studies from Kay Davies' group indicate Oxr1-S may interact with mitochondrial protein Atp5b and Slc25a5 (Finelli et al., 2015a), a subunit of the mitochondrial ATP synthase and a mitochondrial adenine nucleotide translocator, respectively (Ohta and Kagawa, 1986, Haitina et al., 2006). Of note, both proteins are localised in mitochondrial IM (Vyssokikh et al., 2001, Alberts et al., 2008). Since the mitochondrial sub-mitochondrial localisation data in the previous chapter revealed that Oxr1 is likely to be associated with OM, and multiple contact points have been shown between IM and OM (Reichert and Neupert, 2002), these findings can potentially indicate a role of Oxr1 in regulating mitochondrial metabolism. Since previous results suggested that only a small neuronal population within cerebella of the end-stage mutant is affected (Oliver et al., 2011), it could be that the mitochondrial functional differences between the genotypes at disease end-point are below the detection threshold of the most sensitive techniques used for GCs, cerebellar tissue homogenate or isolated mitochondria, further indicating that mitochondrial dysfunction is at least not a major contributor to apoptosis and neurodegeneration caused by *Oxr1* knockout. To address mitochondrial assay sensitivity, however, further studies could be more focused on the mitochondrial bioenergetics of individual cells within the cerebellar GCL of *bella* mutants. For instance, using the immunohistochemical complex II/complex IV double-labelling method to specifically visualise ETC activities in fresh frozen brain sections (Ross, 2011). Of note, complex II and IV are preferable among other ETC complex candidates are mainly because the assay conditions for histochemical analysis have long

been developed and proven to be amenable (Ross, 2011, Old and Johnson, 1989). Yet it is clear that further experiments where the mitochondria are under additional functional pressure, such as under oxidative stress induced by H_2O_2 or arsenite, might reveal more regarding the significance of Oxr1.

Several discrepancies have emerged when investigating potential alterations in mitochondrial oxidative metabolism caused by neurodegeneration-related gene knockout or mutations. For instance, significant reductions in complex I activity and mitochondrial respiration have been observed in DJ-1 null dopaminergic neuronal cells (Kwon et al., 2011, Heo et al., 2012); whereas in DJ-1 knockout MEFs, the mitochondrial respiration level and mitochondrial complex activities are unchanged comparing to the control (Giaime et al., 2012). In mitochondria isolated from the cerebral cortex of DJ-1 knockout mouse, mitochondrial respiration level is also similar to the control, suggesting that DJ-1 may not directly regulate mitochondrial respiration through its anti-oxidative role (Giaime et al., 2012). A recent study of the oxidative metabolism in a HD mouse model carrying mutant huntingtin (mHtt) has shown similar levels of nuclear-encoded subunits of complex I, II, IV, and V comparing to the control (Hamilton et al., 2015). Mitochondrial respiration levels and ATP levels are also comparable between the genotypes (Hamilton et al., 2015). These discrepancies may be due to differences in model systems and assay protocols used in these studies. This evidence also suggests that impairments in mitochondrial oxidative metabolism may not be the causal effect in neurodegenerative diseases.

In summary, apart from normal mitochondrial ultra-structure and functions, loss of *Oxr1* can lead to a mild modification of mitochondrial gross shape and an alteration in mitochondrial fission regulators. It is plausible that the *Oxr1* deletion-related cerebellar GC apoptosis could be resulted from mitochondria-unrelated oxidative stress, for

example, the ROS produced by the cell membrane-associated NADPH oxidase complex (Hernandes and Britto, 2012). Interestingly, recent data have indeed shown that NADPH oxidase 4 (NOX4), one of the homologues of the NADPH oxidase family, plays an essential contributing role in the pathogenesis of an oxidative stress-related, cerebellar neurodegenerative disease called Ataxia telangiectasia (A-T) (Weyemi et al., 2015). A-T is caused by a defect or loss of a protein kinase named ataxia telangiectasia mutated (ATM) (Savitsky et al., 1995). ATM also establishes a role as a ROS sensor and is protective against ROS accumulation (Guo et al., 2010, Cosentino et al., 2011). Cerebellar ataxia, a progressive loss of cerebellar GCs and Purkinje cells as well as an increased expression level of NOX4 are pathological features of A-T patients (Barzilai et al., 2002, Weyemi et al., 2015). Whether NOX4 also plays a role in the *bella* pathology could be examined in order to gain an insight into the mechanism of cerebellar GCs degeneration caused by *Oxr1* deletion.

Chapter 5: Characterisation of conditional dopaminergic *Oxr1* knockout mouse

5.1 Introduction

Parkinson's disease (PD) is the second most common adult onset neurodegenerative disease after AD (Pankratz and Foroud, 2007). Progressive loss of dopaminergic neurons in substantia nigra (SNc) and the formation of α-synuclein containing aggregates (Lewy bodies) in neurons are major pathological hallmarks of the disease (Baba et al., 1998, Forno, 1996, Braak and Braak, 2000). At early stages of PD, dopamine deficiency is the major contributor that leads to symptoms such as rigidity, tremor and bradykinesia (Connolly and Lang, 2014, Samii et al., 2004). So far, PD is incurable and available treatments are still restricted to symptom relief. For example, utilising the dopamine precursor, levodopa, or dopamine agonists, which activate dopamine receptors, to complement the loss of dopamine (Connolly and Lang, 2014). Therefore, in order to search for a more effective treatment for this disease, the causal mechanisms as well as new therapeutic candidates need to be identified.

Oxidative stress (OS) and mitochondrial dysfunction are common features of PD (Moon and Paek, 2015). In the SNc region of PD patients, a reduction in mitochondrial complex I activity has been observed (Mann VM, 1994, Schapira et al., 1989). Complex I deficiency can contribute to an increase in excessive ROS production, which further damages mitochondria (Tretter et al., 2004). In addition to mitochondrial complex I defect, multiple lines of evidence have demonstrated that mtDNA mutation is also involved in PD. For example, fusing platelets from PD patients that contains mtDNA mutations with cells without mtDNA led to complex I impairment (Gu et al., 1998).

Moreover, levels of mtDNA mutations in neurons from the substantia nigra were also found to be markedly increased at early stage of PD (Lin et al., 2012).

To date, mutations in several genes involved in mitochondrial-related pathways have been identified in familial PD. For example, mutations in mitophagy pathway-related genes such as *PINK1* and *PARK2* that encode a serine/threonine protein kinase named PINK1 and its downstream interaction partner Parkin respectively, lead to autosomal recessive, early onset PD (Bonifati et al., 2005, Kitada et al., 1998, Clark et al., 2006). In primary fibroblasts of PD patients with PINK1 mutations, mitochondrial morphological abnormalities such as an increase in mitochondria fragmentation has been observed (Exner et al., 2007). In a *PINK1* knockout mouse, mitochondrial respiration level was found to be reduced (Gautier et al., 2008). These data indicate that loss or mutation in PINK1 leads to mitochondrial dysfunction. Similarly, mitochondrial dysfunction such as reduced mitochondrial membrane potential has also been detected in primary fibroblasts from patients with Parkin mutations (Mortiboys et al., 2008), while mitochondria isolated from striatum of *Parkin* knockout mice exhibit reduced respiration (Palacino et al., 2004). Moreover, mutation in PARK7 that encodes a redox-sensitive chaperone DJ-1 also contributes to PD (Bonifati et al., 2003a). Interestingly, DJ-1 has an anti-oxidative role that protects human neuroblastoma cell lines (SH-SY5Y and SK-N-BE(2)C) from H_2O_2-induced cell death and this protective role was found to be related to its mitochondrial localisation (Taira et al., 2004b, Zhang et al., 2005, Junn et al., 2009). Furthermore, very recently, it has been demonstrated that a loss of function in *vacuolar protein sorting 13C* (*VPS13C*) leads to autosomal-recessive early-onset PD (Lesage et al., 2016). Knockdown of this gene (approximately 75%) in monkey fibroblast-like COS-7 cell line resulted in decreased mitochondrial membrane potential and higher mitochondrial respiration rates (Lesage et al., 2016). Combining these results, it is plausible that identifying new PD-

related genes and studying their potential functions in mitochondria and anti-oxidative pathways could deepen the understanding of the pathological mechanism of PD and shed light on potential treatments.

So far, there is still a lack of human disease-associated OXR1 mutations. Importantly, however, differential expression of OXR1 has been implicated in neurodegenerative disease. For example, in spinal cord biopsy samples of ALS patients and spinal cord tissue of pre-symptomatic ALS mouse (SOD1 G93A), intermediate or full-length isoforms of Oxr1 were up-regulated, respectively (Oliver et al., 2011). Interestingly, in the posterior cingulated cortex of PD patients without dementia, *OXR1* has been shown to be down-regulated by 3-fold at the RNA level (Stamper et al., 2008). Together, this evidence above suggests a potential role of OXR1 as an early indicator of neurodegenerative disorders such as PD and ALS.

Dopaminergic neurons in the substantia nigra pars compacta (SNc) are the neuronal population vulnerable in PD (Double, 2012), whereas cerebella granule neurons are the only neuronal population affected at the end-stage of the *bella* mouse (Oliver et al., 2011). Therefore, it is unknown loss of *Oxr1* would influence the cell survival in neuronal populations outside of the cerebellum, such as dopaminergic neurons, as the mice reach end-stage at such a young age; as such it is not a good model for examining slowly progressive neurodegenerative disorders such as PD. Given the potentially important role of OS in PD, it was decided that conditional deletion of Oxr1 in dopaminergic neurons would be a new and valuable model for assessing selective vulnerability in the midbrain.

5.2 Aims of Chapter 5

The aim of this chapter was to characterise conditional dopaminergic *Oxr1* knockout mouse in order to examine whether Oxr1 has a potential protective role in dopaminergic neurons.

5.3 Results

5.3.1 Generation of dopaminergic *Oxr1* conditional knockout mouse

As has been demonstrated in Chapter 3, the shortest isoforms of Oxr1 can be fully functional, therefore in order to disrupt the gene genetically, it was necessary to design a strategy that would affect all isoforms. Therefore, it was decided to target the TLDc domain. In this strategy, the Cre-mediated deletion of two coding exons of Oxr1 leads to a truncated protein (**Figure 5.1A**). In summary, Oxr1$^{tm1a(EUCOMM)Wtsi}$ knockout-first conditional allele (tm1a) mice (Oxr1$^{tm1a/+}$) were generated by the Wellcome Trust Sanger Institute using a previously described gene targeting method (Skarnes et al., 2011). This particular allele leads to expression of a truncated Oxr1 allele with a lacZ trapping element and a floxed promoter-driven neo cassette (Skarnes et al., 1992, Skarnes et al., 2011) (**Figure 5.1B**). The successful functional disruption of Oxr1 in the tm1a allele was confirmed by generating Oxr1$^{tm1a/tm1a}$ animals; these displayed an identical phenotype to the bella mutants (Finelli et al. JBC 2016). Heterozygous Oxr1$^{tm1a/+}$ mice were then crossed with a transgenic Flpe mouse line (Flp) to remove the lacZ elements as well as the floxed promoter-driven neo cassette using a β-actin-driven FLPe variant recombinase from the Flpe mouse (**Figure 5.1B**). The offspring of this cross generate the conditional-ready allele (tm1c) that contains exons 15 and 16 of Oxr1 flanked by loxP sites

recognisable by the Cre recombinase (**Figure 5.1B**). Importantly, the tm1c allele expresses Oxr1 normally, and thus homozygous animals are viable.

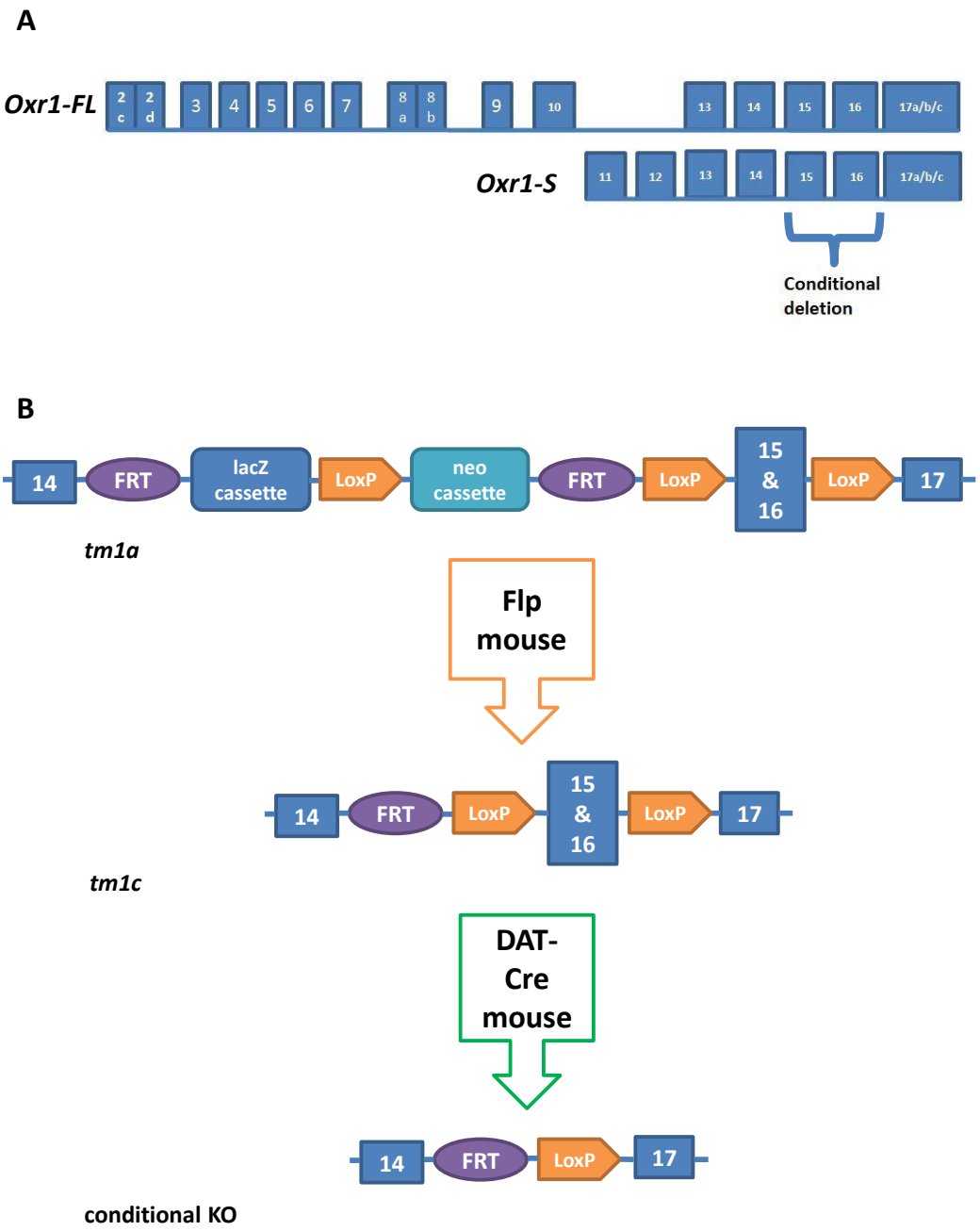

Figure 5.1. Generation of dopaminergic Oxr1 conditional knockout mouse

(A) A schematic illustration of the full-length (Oxr1-FL) and the shortest (Oxr1-S). Both exons 15 and 16 were targeted to knockout all isoforms of Oxr1. **(B)** A schematic illustration of the tm1a allele that contains a neo and a lacZ cassettes located between the exons 14 and 17 of *Oxr1*. These cassettes are removed by crossing the tmla mouse with an Flp mouse line. The β-actin driven FLPe variant recombinase specifically recognises the flippase recominase target (FRT) sites and the cutting generates a conditional tm1c allele. Crossing this mouse line that contains the conditional tm1c allele with the DAT promoter driven Cre mouse generates a dopaminergic *Oxr1* conditional knockout mouse.

Next, to further confirm that the Cre-mediated disruption of the tm1c allele was fully effective, Oxr1$^{tm1c/tm1c}$ mice were crossed with SRY-box containing gene 2 (Sox2)-Cre+ mice, thus generating a constitutive disruption of *Oxr1* (Hayashi et al., 2002). It was expected, therefore, that the Oxr1$^{tm1c/tm1c}$/Sox2-Cre+ mouse would display neurodegeneration similar to the *Oxr1* knockout *bella* mouse. As expected, Oxr1$^{tm1c/tm1c}$/Sox2-Cre+ mice showed rapid, progressive ataxia from P18 and TUNEL staining showed cell death in the cerebellar GCL, while in age-matched Oxr1$^{tm1c/tm1c}$/Sox2-Cre- mice, cell death was not detectable (**Figure 5.2**). These results confirm the functional disruption of the *Oxr1* conditional allele.

To generate the dopaminergic *Oxr1* conditional knockout mouse, homozygous Oxr1$^{tm1c/tm1c}$ mice were crossed with a transgenic line where the expression of Cre recombinase is controlled by a dopamine transporter (DAT) promoter (Zhuang et al., 2005) (**Figure 5.1B**). Firstly, however, the specificity of Cre expression by the DAT-driven transgene was confirmed by crossing the DAT-Cre mice with Rosa26 locus lacZ reporter (R26R (lacZ)) mice. It was expected that the offspring should co-express lacZ with Cre-expressing neurons (Zhuang et al., 2005). Indeed, it was found that Cre recombinase co-expressed with lacZ in dopaminergic neurons in the SNc and ventral tegmental area (VTA) of mouse midbrain (**Figure 5.3A) (**Peter Oliver, unpublished data**).**

Next, the disruption of *Oxr1* in the midbrain in Oxr1$^{tm1c/tm1c}$ / DAT-Cre+ mice was confirmed by *in situ* hybridization using a probe specific to the deleted exons. These data showed that the expression level of *Oxr1* in the SNc and VTA regions of the Oxr1$^{tm1c/tm1c}$ / DAT-Cre+ mouse was barely detectable comparing to the Oxr1$^{tm1c/tm1c}$ / DAT-Cre- mouse (**Figure 5.3B**) **(**Peter Oliver, unpublished data**)**. Together, these results confirm that the Oxr1 disruption in the SNc had been achieved successfully and that the Cre-mediated deletion allele is non-functional.

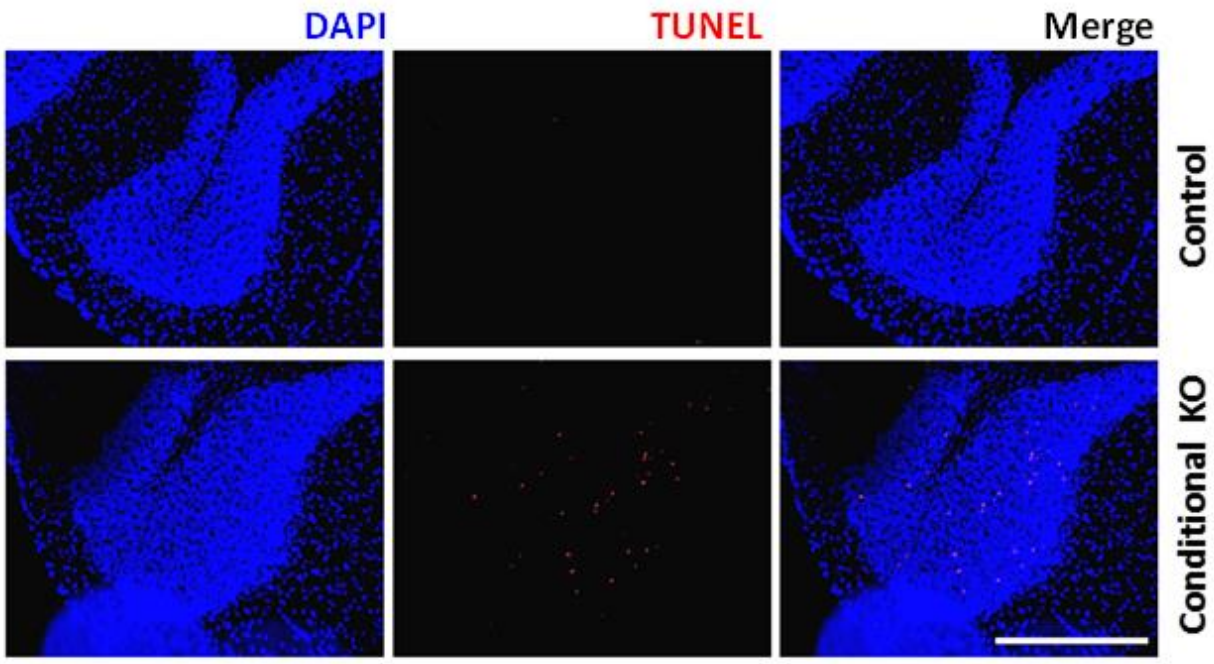

Figure 5.2. TUNEL staining of the GCL region

TUNEL staining shows GCL apoptosis in conditional knockout ($Oxr1^{tm1c/tm1c}$/Sox2-Cre+) mouse, but not in age-matched tm1c/tm1c control ($Oxr1^{tm1c/tm1c}$/Sox2-Cre−) mouse. Nuclei mounted with DAPI. Scale bar=400 μm.

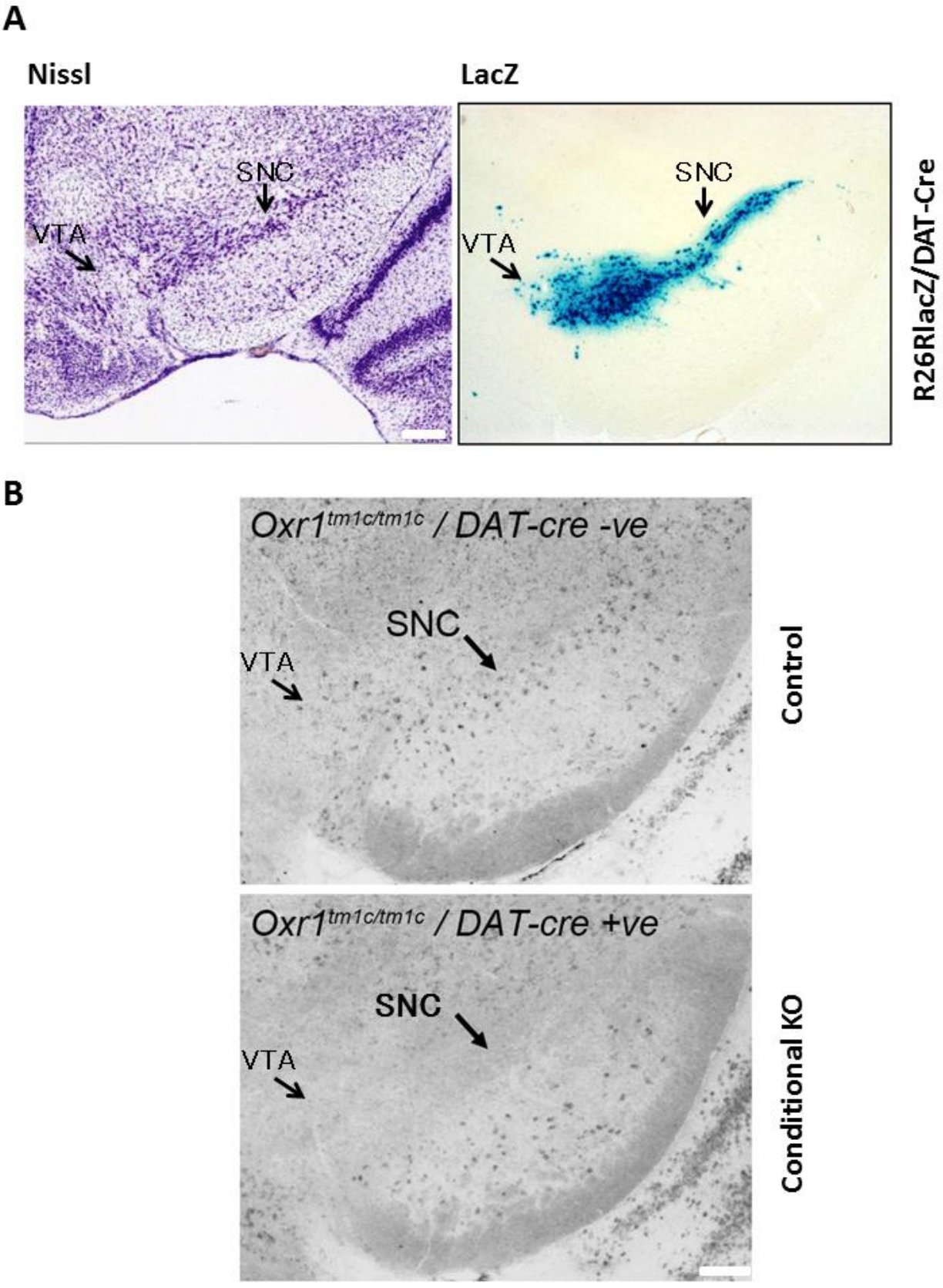
A
Nissl
LacZ
SNC
VTA
SNC
VTA
R26RlacZ/DAT-Cre
B
Oxr1tm1c/tm1c / DAT-cre -ve
SNC
VTA
Control
Oxr1tm1c/tm1c / DAT-cre +ve
SNC
VTA
Conditional KO

Figure 5.3. Expression of *Oxr1* in DAT-positive neurons is specifically deleted in Oxr1$^{tm1c/tm1c}$/DAT-cre mice

(A) Left: Nissl staining shows the neuronal population in substantia nigra (SNc) and ventral tegmental area (VTA). Right: LacZ staining demonstrates the co-expression of Cre with lacZ in dopaminergic neurons in the SNc and VTA of mouse midbrain. Images were taken by Prof. Peter Oliver. Scale bar=100 μm (**B**) *In situ* hybridisation showed that the expression level of *Oxr1* in the SNc and VTA regions of the Oxr1$^{tm1c/tm1c}$/DAT-Cre+ mouse (conditional knockout (KO)) was barely detectable comparing to the Ox1$^{tm1c/tm1c}$ /DAT-Cre- (control) mouse. Images were taken by Prof. Peter Oliver. Scale bar=100 μm

5.3.2 Selective loss of *Oxr1* in dopaminergic neurons does not affect rotarod performance and grip strength

PD patients display motor symptoms such as movement slowness and rigidity (Mazzoni et al., 2012). In the mouse, behavioural tests can be used to assess these parameters and others related to dopaminergic cell dysfunction (Taylor et al., 2010). To examine whether selective loss of Oxr1 in dopaminergic neurons also leads to these defects as a preliminary screen, motor function, muscle strength and weight were measured in a cohort of 12-month-old Oxr1$^{tm1c/tm1c}$/DAT-Cre+ and age-matched control Oxr1$^{tm1c/tm1c}$/DAT-Cre- mice.

Using accelerating rotarod to examine the motor co-ordination and motor function, no difference in latency to fall between the genotypes was observed (**Figure 5.4A**). Using the inverted screen test for the grip strength measurement, there was also no difference found between the genotypes (**Figure 5.4B**). Moreover, there was no significant difference in weight between the genotypes (**Figure 5.4C**). Together, these data indicate that the selective loss of *Oxr1* in dopaminergic neurons does not have a major effect on aspects of motor function.

Nevertheless, it was found that female mice in general had better rotarod and grip strength test performance in comparison with the age-matched males (**Figure 5.4A-B**). Whereas the male mice generally have a higher weight comparing to the females (**Figure 5.4C**), suggesting that weight can potentially affect the performance in rotarod and grip strength tests.

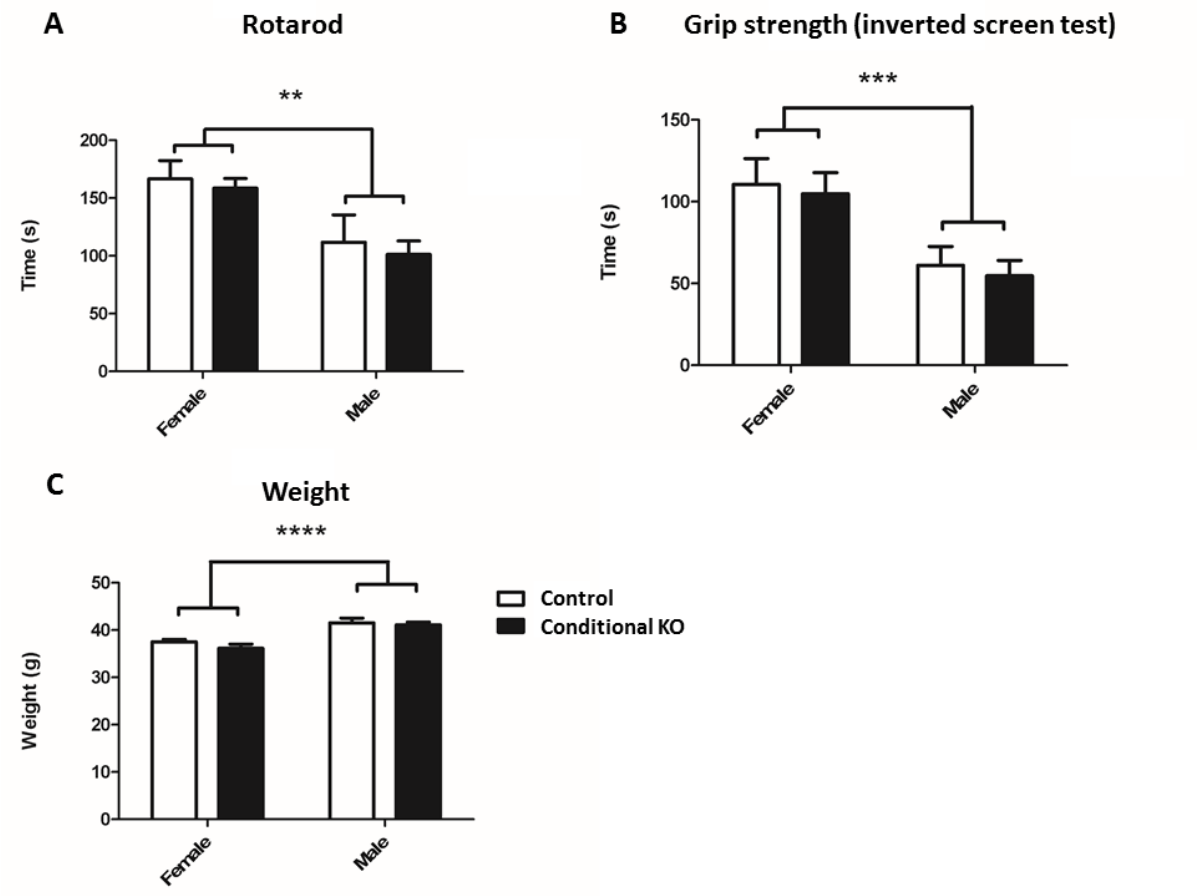

Figure 5.4. Selective loss of *Oxr1* in dopaminergic neurons does not affect rotarod performance and grip strength in 12-month old mice

(A) No difference in motor function between the conditional KO ($Oxr1^{tm1c/tm1c}$/DAT-Cre+) and age matched control ($Oxr1^{tm1c/tm1c}$/DAT-Cre−) mice. However, the latency to fall was significantly different between the sexes. **(B)** No difference in grip strength (inverted screen test) between the conditional KO and age matched control mice. However, the grip strength also was significantly different between the sexes. **(C)** No difference in weight between the conditional KO and age matched control mice. However, the weight was significantly different between the sexes. n=8-14 for each sex and genotype. Data are means ± S.E.M. and Pairwise analysis was analysed by Student's t- test. To determine whether there is a significant difference between the sexes in weight, grip strength and latency to fall, two-way ANOVA followed by Bonferroni post-hoc tests were conducted. (**P<0.01, ***p<0.001 and ****p<0.0001).

5.3.3 Selective loss of Oxr1 in dopaminergic neurons does not reduce the number of TH+ cells

Loss of dopaminergic neurons in SNpc region is one of the pathological hallmarks of PD (Forno, 1996). Loss of Oxr1 in *bella* mouse at end stage leads to a significant induction of apoptosis in cerebellar GCL comparing to the age-matched control (Oliver et al., 2011). It is therefore investigated whether the conditional *Oxr1* knockout reduces the total number of dopaminergic neurons by quantifying the number of cells expressing a dopaminergic neuron marker tyrosine hydroxylase (TH).

In contrast to *bella* mice, which only have a short lifespan of P26 (Oliver et al., 2011), we found that Oxr1$^{tm1c/tm1c}$/DAT-Cre+ could be aged up to 18 months, meaning that neuropathology at a late-stage could be assessed; this approach might be suitable for modeling age-related cellular stress relevant to PD (Varçin et al., 2012). Serial midbrain sections obtained from 18-month old conditional knockout and control mice were stained with an anti-TH antibody (**Figure 5.5A**) and subjected to stereological quantification of both the SNpc and VTA regions. Only cells with a TH positive cell body and a TH negative nucleus were counted (**Figure 5.5B**). However, no significant difference in the total number between the genotype was observed (**Figure 5.5C**), suggesting that selective loss of *Oxr1* in dopaminergic neurons does not lead to overt neurodegeneration in SNc and VTA by 18 months of age.

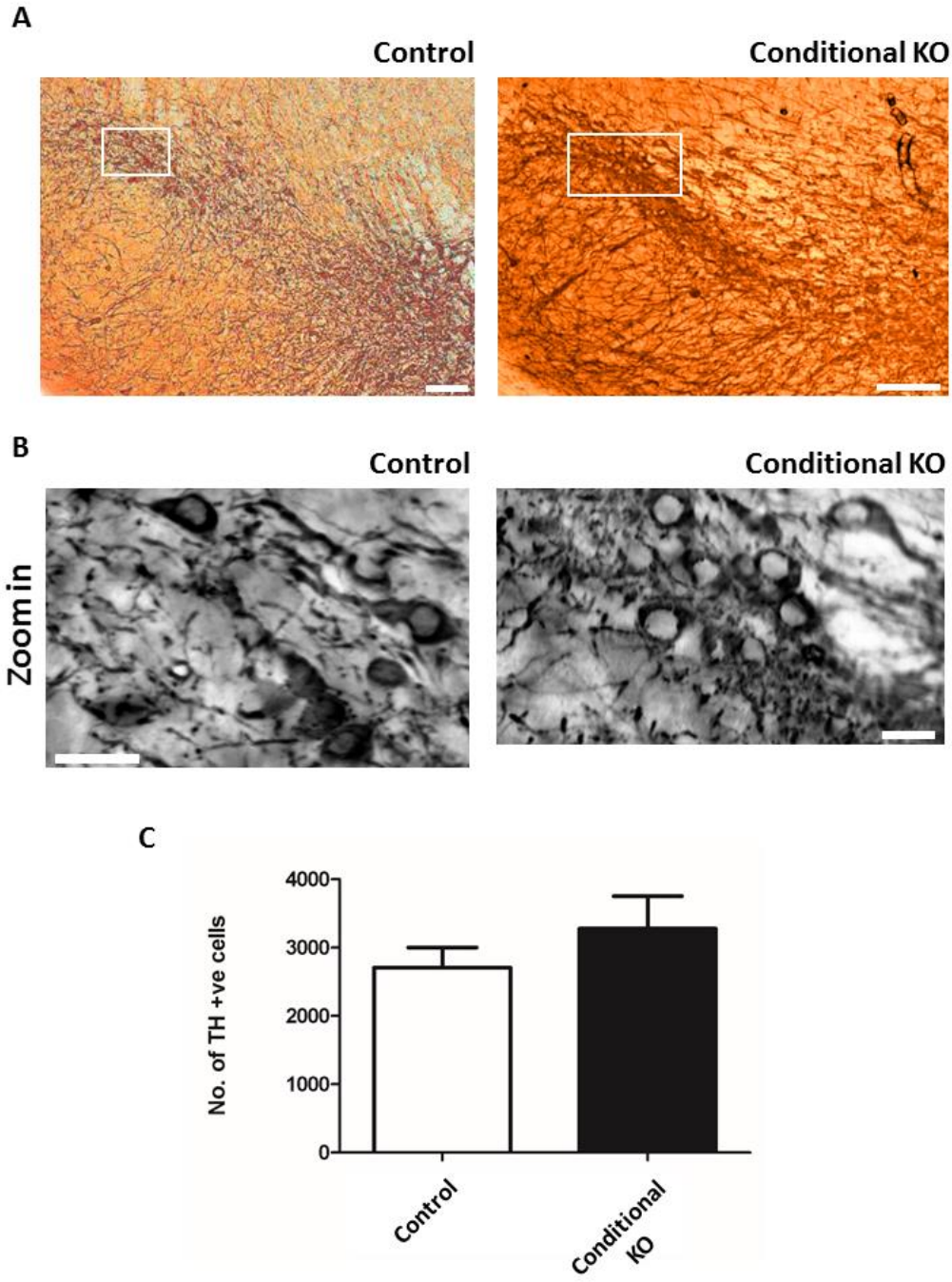

Figure 5.5. Conditional Oxr1 knockout in dopaminergic neurons does not reduce the number of TH+ cells

(A) Representative images showing sections obtained from 18-month control ($Oxr1^{tm1c/tm1c}$/DAT-Cre−) and conditional KO ($Oxr1^{tm1c/tm1c}$/DAT-Cre+) mice stained for TH. Scale bar=100 µm. **(B)** "Zoom in" images for dopaminergic neurons, defined as cells with a TH positive (dark) cell body and a TH negative nucleus (bright). Scale bar=25 µm. **(C)** Total TH + cell number sterologically counted in serial immunohistological sections of 18-month old mice stained for TH. 7 sections were counted per animal. Mouse brain was sectioned at 40 µm and counted sections were spaced at 240 µm apart; n=4 animals per group; Data are means ± S.E.M. and analysed by Student's t- test.

5.4 Discussion

In this chapter, a mouse model in which *Oxr1* is selectively deleted in dopaminergic neurons was generated and characterised. The conditional knockout Oxr1$^{tm1c/tm1c}$/DAT-Cre+ mice displayed no differences in survival and no reduction in the number of dopaminergic neurons within the SNc and VTA regions in comparison with the age-matched control up to 18 months of age. It was also demonstrated here that up to 12 months, no loss of motor function, muscle strength or weight was observed in Oxr1$^{tm1c/tm1c}$/DAT-Cre+ mice comparing to the age-matched controls. Together, these preliminary results indicate that this *Oxr1* conditional deletion does not lead to the selective vulnerability of dopaminergic neurons to neurodegeneration.

Importantly, it was demonstrated successfully that *Oxr1* had been disrupted in the dopaminergic neurons predominantly located in the SNc and VTA regions in Oxr1$^{tm1c/tm1c}$/DAT-Cre+, an essential control for any new conditional mouse study. Alternative cre recombinase drivers are used to selectively target midbrain neuronal populations. For example, using an alternative TH-Cre driven method, a dopaminergic conditional knockout mouse has been used to study neuronal signalling mechanisms in the VTA region (Stamatakis et al., 2013). However, a recent intensive study comparing different Cre-driver transgenic mouse lines at anatomical, molecular and functional levels have demonstrated that when regulated by TH, considerable non-dopaminergic cell expression patterns were discovered in the VTA compared to the DAT-cre driver. This indicates a potential confound in experiments that have used the TH-cre (Lammel et al., 2015). These data therefore support the use of the DAT-cre transgene for modeling dopaminergic cell function.

As introduced in the previous chapters, deletion of *Oxr1* in mice causes oxidative damage and cerebellar neurodegeneration (Oliver et al., 2011), whereas over-expression

of OXR1 has been found to be neuroprotective in cellular and mouse models of amyotrophic lateral sclerosis (ALS) (Finelli et al., 2015a, Liu et al., 2015b). This evidence indicates an anti-oxidative role that Oxr1 plays in the CNS. Intriguingly, transcriptomic studies have shown that the protective role of Oxr1 against SOD1-mediated ALS may be associated with anti-inflammatory pathways (Liu et al., 2015b), while accumulating evidence has shown that neuroinflammation is an important feature of PD. For example, in the SNc, an increasing level of pro-inflammation mediators such as interleukin-1β (IL-1β), tumour necrosis factor-α (TNF-α) and inducible nitric oxide synthase (iNOS) have been detected in PD, (Hirsch et al., 2012, Herrero et al., 2015), while a macrophage marker, cluster of differentiation 68 (CD68) has been found to be associated with PD in post-mortem SNc of PD patients (Croisier et al., 2005). Therefore, in the future, it will be important to determine whether there are changes in neuroinflammation in the SNc region of the *Oxr1* conditional knockout by immunocytochemical labelling brain tissue sections for inflammatory markers; for example, the CD68 and glial fibrillary acidic protein (GFAP), a marker for astrogliosis that is recently found to be inversely correlated with the progression of PD in the SNc (Hatfield and Skoff, 1982, Tong et al., 2015).

In addition, since multiple lines of evidence has shown that Oxr1 is an early marker of stress (Oliver et al., 2011, Stamper et al., 2008), the transcriptional and transactional level of Oxr1 in the PD affected regions such as SNc should be measured in the future. However, since mouse dopaminergic neurons predominantly located in the SNc and VTA regions are very difficult to be isolated, it is hard to carry out qPCR or western blotting to directly study the transcriptional and translational levels of Oxr1 in these cells. More sophisticated methods need to be ultilised. For example, using laser capture micro-dissection technique, Kummari *et al*. recently isolated individual dopaminergic neurons

and the whole VTA region from mouse brain (Kummari et al., 2015). Our future studies can therefore be potentially benefited from this technique. Furthermore, in contrast to the cerebellar GCs death detected in the end-stage *bella* mutant, our preliminary results could not find dopaminergic cell loss in the midbrain of the conditional knockout mice, suggesting the loss of Oxr1 does not lead to dopaminergic cell loss. Of note, in end-stage *bella* mice, oxidative stress markers such as 8-OHdG were detected in the GCL (Oliver et al., 2011). However, stress markers have not been tested on the *Oxr1* conditional knockout mice. Therefore, in the future, oxidative stress markers such as 8-OHdG should be tested in the SNc and VTA regions.

One important feature of the *bella* mutant is the apparent selective vulnerability of cells in the cerebellar GCL at disease end-stage (P24) versus the rest of the CNS (Oliver et al., 2011). So far, the reason behind this specific susceptibility is unknown, although it has been shown that cerebellar GCs were more vulnerable from oxidative stress-related cell death than primary cortical cells (Oliver et al., 2011). Hence, it was hoped that deletion of *Oxr1* in dopaminergic cells would lead to neurodegeneration due to ageing-related factors that do not occur in the midbrain of *bella* mice at P24. However, no indication of selective degeneration of cells in the SNc or VTA was detected at 18 months of age in DAT-Cre *Oxr1* conditional knockouts. Therefore, more detailed pathological analyses of this line at the behavioural, pathological and physiological level is required to be studied in the future. For example, the level of dopamine within mouse brain can be measured in real time using the fast-scan voltammetry with carbon-fibre microelectrodes to reflect the status of dopaminergic neurotransmission (Robinson et al., 2003). Previously, using this technique, Senior *et al.* found that the extracellular concentration of dopamine in an α- and γ-synulcein double- knockout mouse was significantly elevated after discretely stimulating the striatum using the microelectrodes

(Senior et al., 2008). Of note, the double knockout mice that they studied only displayed a subtle phenotype with hyper-dopaminergic-like behaviour (Senior et al., 2008), suggesting that the fast-scan voltammetry method may be useful to capture transient neuronal changes resulted from genetic changes. Therefore, this method can potentially be used in our future studies on the *Oxr1* conditional knockout mice.

For dopaminergic cells in the mouse midbrain, there are several pharmacological tools available to model the PD-related cell death. For example, the neurotoxin MPTP can be applied to the *Oxr1* conditional knockouts. Once in the brain, MPTP is converted to MPP+, which specifically inhibits the activity of mitochondrial complex I and causes dopaminergic neuron death in midbrain regions such as SNc (Langston et al., 1983, Nicklas et al., 1985). In addition, the selectivity of MPP+-induced damage to dopaminergic neurons is also mainly affected in PD and can acutely trigger PD symptoms (Nicklas et al., 1985, German et al., 1996, Langston et al., 1983). Therefore, MPTP is considered as an ideal pharmacological tool to unveil the potential pathological mechanism of PD and MPTP mouse model for PD has been developed through intraperitoneal or subcutaneous injections (Jackson-Lewis and Przedborski, 2007). Several parameters can be studied in the MPTP treated mice, for example, studying the potential pathological effect of MPTP treated mouse midbrain by quantifying the number of TH-positive neurons in the SNc region (Muthane et al., 1994, Taylor et al., 2014) or investigating potential physiological and behavioural changes in MPTP treated mice by rotarod or grip coordination test (Sedelis et al., 2001).

In summary, in this chapter, we preliminarily characterised the $Oxr1^{tm1c/tm1c}$/DAT-Cre mice to examine whether specific loss of *Oxr1* in dopaminergic neuron populations would lead to potential selective vulnerability in the midbrain regions. Despite no change was detected between the genotypes, the work here is still at a preliminary stage and as

introduced in the discussion section, more parameters such as transient dopamine release, cell death, oxidative stress and neuroinflammation markers need to be systematically studied in the future.

Chapter 6: *In vitro* characterisation of an ENU-induced mutation (Y644H) in Oxr1

6.1 Introduction

It was introduced in previous chapters that the deletion or mutation of many genes could lead to neurodegenerative phenotypes, including those that encode anti-oxidative proteins. Point mutations can cause impairment of a protein's function and may subsequently lead to neurodegenerative disorders. Studying point mutations can therefore help further understand the potential biological function of a protein that may not be possible from the study of a gene deletion (Oliver and Davies, 2012).

N-ethyl-N-nitrosourea (ENU) mutagenesis, which uses the potent alkylating compound ENU as a mutagen has been widely applied as a useful tool in screening potential mutations and studying function of genes in the mouse (Acevedo-Arozena et al., 2008). ENU transfers its ethyl group to the nucleobases thereby randomly induces base substitutions primarily in AT base pairs in DNA, and consequently triggers mainly missense mutations (Justice et al., 1999). So far, there are two main types of ENU mutagenesis screening: a phenotype-driven screen and a gene-driven screen (Acevedo-Arozena et al., 2008). The phenotype-driven screen identifies genes, which mutations within them were previously unknown to be linked with the phenotype of interest resulted from ENU mutagenesis; whereas the gene-driven screen is focused on potential ENU-induced mutations within a selected gene (Quwailid et al., 2004).

Through studying point mutations generated by ENU mutagenesis, new functions of a number of proteins, which were unable to be discovered from studying gene deletion, has been identified. For example, homozygous deletion of synaptosomal-associated protein 25 (Snap-25) in mouse is embryonic lethal, whereas heterozygous mice do not have apparent phenotype (Washbourne et al., 2002, Schoch et al., 2001), which makes

these mice not suitable for phenotypic characterisation. Interestingly, mice with a mutation in a highly conserved domain of Snap-25 showed alteration in behavior and protein functions at both molecular and cellular level (Jeans et al., 2007). Of note, these mutant mice were first identified using a large-scale, phenotype-driven dominant mutagenesis screen (Jeans et al., 2007, Nolan et al., 2000).

The gene-driven screen is also a useful tool to study potential functional alterations of a gene in consequence of amino acid changes (Quwailid et al., 2004). This can be carried out by two complementary methods: the first approach uses mutagenised embryonic stem (ES) cells to construct a library by either freezing the clones or extracting the DNA (Chen et al., 2000, Munroe et al., 2000); while the second method uses sperm achieves from the offspring (G1) of the ENU-treated male mouse (Quwailid et al., 2004, Coghill et al., 2002).The DNA obtained from either method is sequenced and mutations of interest can then be introduced into live mice for phenotypic characterisation (Quwailid et al., 2004).

To date, the function of Oxr1 is still unknown. As described in the previous chapter (**Section 1.3.4)**, it has been found that recessive *Oxr1* deletion mutant mouse *bella (bel)* displays a severe neurodegenerative phenotype associated with oxidative stress (Oliver et al., 2011). However, Oxr1 mutant mice with an intermediate phenotype have not been generated. In addition, potential functional consequences of ENU mutations identified in Oxr1 can be investigated *in vitro* before generating the mutant mouse, which is efficient and cost-effective.

6.2 Aim of Chapter 6

The aims of this chapter were to identify and characterise ENU mutations in Oxr1 as well as predicting the phenotype in mouse.

6.3 Results

6.3.1 Identifying ENU-induced Oxr1 mutation in mouse

Much of the amino acid sequence of Oxr1 is highly conserved in evolution (Volkert et al., 2000). Moreover, BLASTP analysis (Altschul et al., 1997, Altschul et al., 2005) showed that the amino acid sequences of mouse Oxr1 are highly similar to human OXR1 (84% identical). Together, these results suggest that Oxr1 is an ideal candidate for ENU screening.

To identify potential point mutations in Oxr1, ENU mutagenesis screening was conducted by MRC Harwell using the denaturing high-performance liquid chromatography (DHPLC). Through screening mutations in mouse genomic DNA, several point mutations and 3 single nucleotide polymorphisms (SNPs) in *Oxr1* (Transcript: Oxr1-201) on mouse chromosome 15 were identified (**Table 6.1**).

Table 6.1. ENU-induced mutations in mouse Oxr1

Base change	**Location**	**Amino acid (AA) change**	**Comments**
A>T	Exon 5	E117D	Both are negatively charged AAs (acidic)
G>A	Exon 5	S101S	Silent
T>G	Exon 6	M181R	AA with hydrophobic side chain to positively charged

			(basic)
A>C (SNP)	Exon 7	T347P	AA with a polar uncharged side chain to cyclic
G>A (SNP)	Exon 7	V349I	Both are AA with a hydrophobic side chain
C>T (SNP)	Exon 7	S363L	AA with a polar uncharged side chain to a hydrophobic side chain
A>G	Exon 8	K473E	Positively charged AA (basic) to negatively charged AA (acidic)
C>T	Exon 9	A509A	Silent
A>C	Exon 10	E574D	Both are negatively charged AAs (acidic)
A>G	Exon 10	T578T	Silent
A>G	Exon 10	R581R	Silent
C>T	Exon 11	D602D	Silent
C>T	Exon 11	P610L	Changed to AA with a hydrophobic side chain (aliphatic)
C>T	Exon 12	T641M	AA with a polar uncharged side chain to a hydrophobic side chain
T>C	Exon 12	Y644H	AA with a hydrophobic side chain (aromatic) to positively charged (basic)

Among the mutations identified in the ENU screen, a threonine-to-methionine (T641M) and a tyrosine-to-histidine (Y644H) were found in exon 12, which are within the well-conserved TLDc domain of Oxr1 spanning from exon 12 to 16 (Durand et al., 2007, Doerks et al., 2002). Specifically, the tyrosine 644 but not threonine 641 within the TLDc domain is highly conserved through evolution (**Figure 6.1.**). Importantly, alignment studies revealed that the tyrosine 644 (tyrosine 740 in humans) corresponds to phenylalanine 667 in the TLDc domain of the OXR1A from zebrafish. Based on the crystal structure of the TLDc domain of zebrafish OXR1A (PDB-ID: 4ACJ) (Blaise et al., 2012), the phenylalanine 667 is part of the hydrophobic core of the TLDc domain and is in close interaction with leucine 679 (leucine 752 in humans) (**Figure 6.2.)**. Of note, both tyrosine and phenylalanine are aromatic amino acids with hydrophobic side chains. Changing from tyrosine or phenylalanine to the positively charged basic amino acid histidine is unlikely to maintain the hydrophobic core, and may destabilise the TLDc domain. In addition, using PolyPhen-2, which is a computational tool for predicting potential structural and functional impact of an amino acid substitution on a protein, it suggested that changing from tyrosine to histidine is likely to damage the TLDc domain with a score of 0.999 (Sanchez-Pulido, unpublished data). Since multiple lines of evidence has demonstrated an anti-oxidative role of the TLDc domain (Oliver et al., 2011, Finelli et al., 2016b), it is speculated that the Oxr1 Y644H mutation could cause structural alterations in Oxr1 and have a negative impact on its anti-oxidative role.

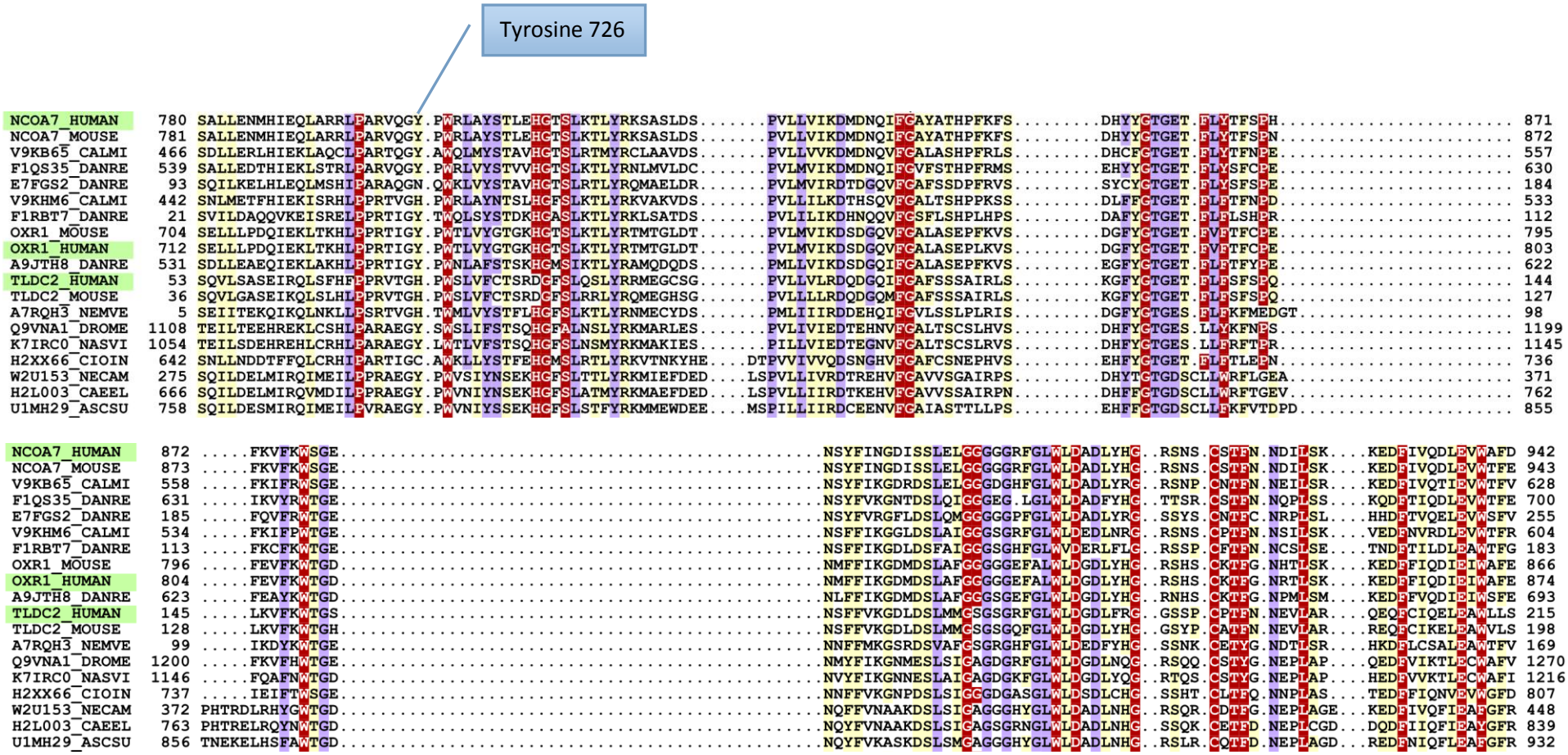

Figure 6.1. The tyrosine in the TLDc domain is highly conserved across species

Alignment of TLDc domain-containing proteins across species. Colours correspond to the amino acid conservation of each alignment column: red (highly conserved), purple (mildly conserved), and light yellow (poorly conserved) based on BLOSUM62 scores. Residues mutated in this study are labelled according to reference protein sequences for human NCOA7-B (red), human NCOA7-(FL) (magenta) and the zebrafish OXR1A-TLDc sequence (PDB-ID: 4ACJ, purple) (Blaise et al., 2012). Of note, the tyrosine 644 is tyrosine 726 in mouse Oxr1 on this alignment. Protein sequences are shown by name or by Uniprot identifier. abbreviations: ASCSU, *Ascaris suum* (pig roundworm); CAEEL,

Caenorhabditis elegans; CALMI, *Callorhinchus milii* (ghost shark); CIOIN, Ciona intestinalis; DANRE, Danio rerio (zebrafish); DROME, Drosophila melanogaster (fruit fly); HUMAN, Homo sapiens; MOUSE, Mus musculus; NASVI, Nasonia vitripennis (wasp); NECAM, Necator americanus (human hookworm); NEMVE, Nematostella vectensis (starlet sea anemone). The figure is adapted from Finelli, M. J., L. Sanchez-Pulido, K. X. Liu, K. E. Davies and P. L. Oliver (2016). "The evolutionarily conserved Tre2/Bub2/Cdc16 (TBC), Lysin motif (LysM), Domain catalytic (TLDc) domain is neuroprotective against oxidative stress." Journal of Biological Chemistry, 291: 2751-2763.

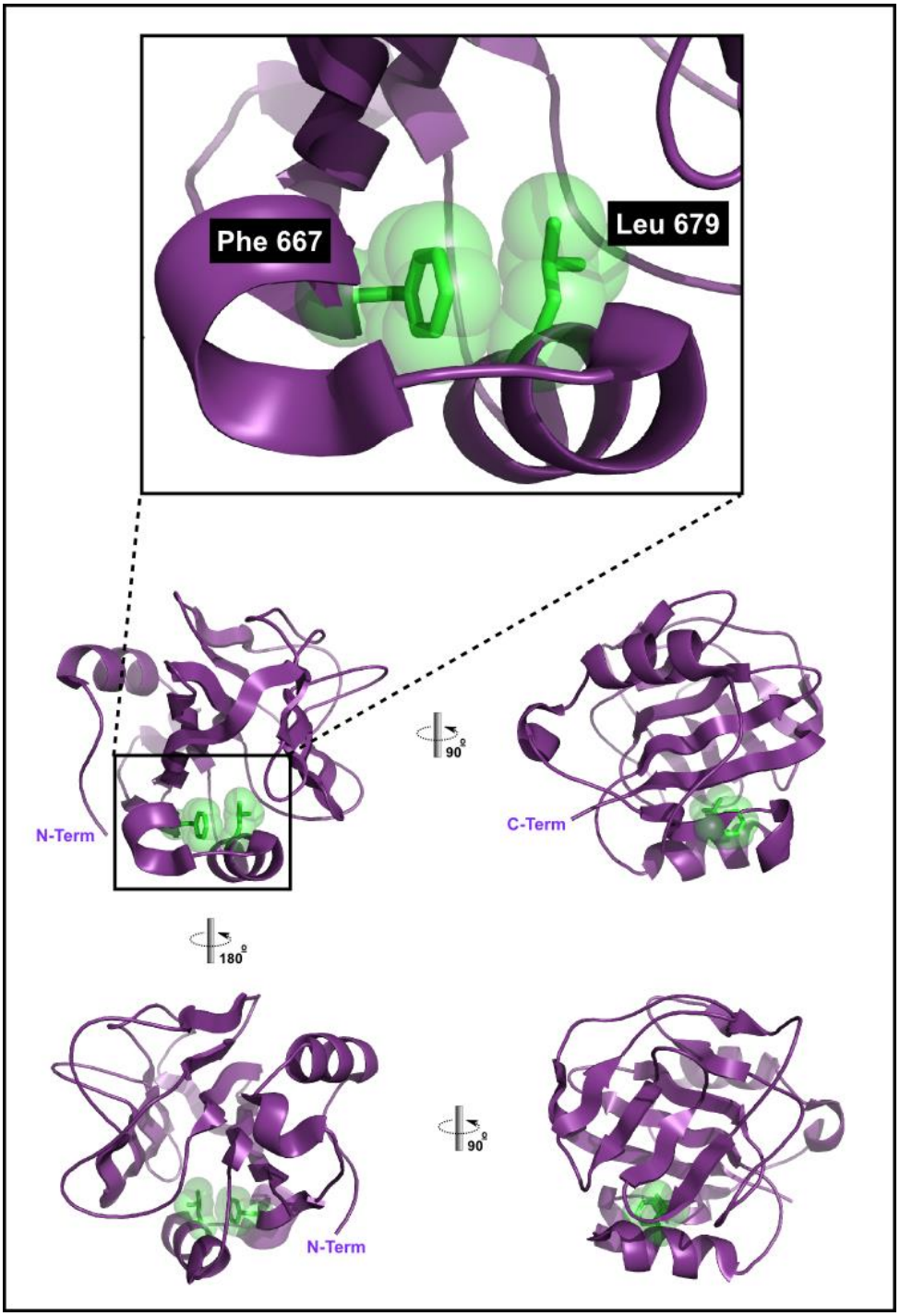

Figure 6.2. Conserved phenylalanine 667 (Phe 667) in the TLDc domain of zebrafish OXR1A

Crystal structure of the TLDc domain of zebrafish OXR1A (PDB-ID: 4ACJ). The visualisation of the structure was made by Pymol. Phe 667 is part of the hydrophobic core of the TLDc domain and is in close interaction with leucine 679 (Leu 679).
Taken from Sanchez-Pulido, unpublished data.

6.3.2 Over-expression of Oxr1-S Y644H causes more severe oxidative stress-related protein aggregation

It has been found that transgenic over-expression of proteins can cause abnormal cellular accumulations. For example, over-expressing a PD-related αSYN mutant (A30P) causes abnormal protein accumulation in neuronal cells of mouse brain (Kahle et al., 2000); over-expressing both wild-type and mutant TDP-43 in cultured motor neurons also leads to abnormal cytoplasmic accumulation (Wang et al., 2013). To examine whether over-expression of the mutant Oxr1 Y644H also triggers any abnormal cellular accumulation, Oxr1-S WT and Oxr-S-Y644H containing almost exclusively the TLDc domain (Oliver et al., 2011) were constructed, since the Y644H is within the conserved TLDc domain.

Lysate from un-transfected HeLa cells, cells transfected with pCX-GFP, cells over-expressing HA-tagged Oxr1-S WT or Oxr1-S Y644H were subjected to western blotting. Cells transfected with WT and Y644H demonstrated similar levels of Oxr1-S and HA (**Figure 6.3A-B**). Interestingly, confocal images showed that the majority of cells transfected with Oxr1-S-WT exhibited a cytosolic diffuse pattern; whereas in cells over-expressing the Y644H mutation, aggregate-like puncta were observed to be scattered in cytoplasm (**Figure 6.3C**). The percentage of cells with such punctate form was two-fold higher in cells over-expressing the mutant comparing to the cells over-expressing the wild-type protein (**Figure 6.3D**). Moreover, when treating cells with 0.25 mM H_2O_2, an aggravated effect was found on both WT and Y644H groups (**Figure 6.3D**), indicating that the aggregates were oxidative stress-related.

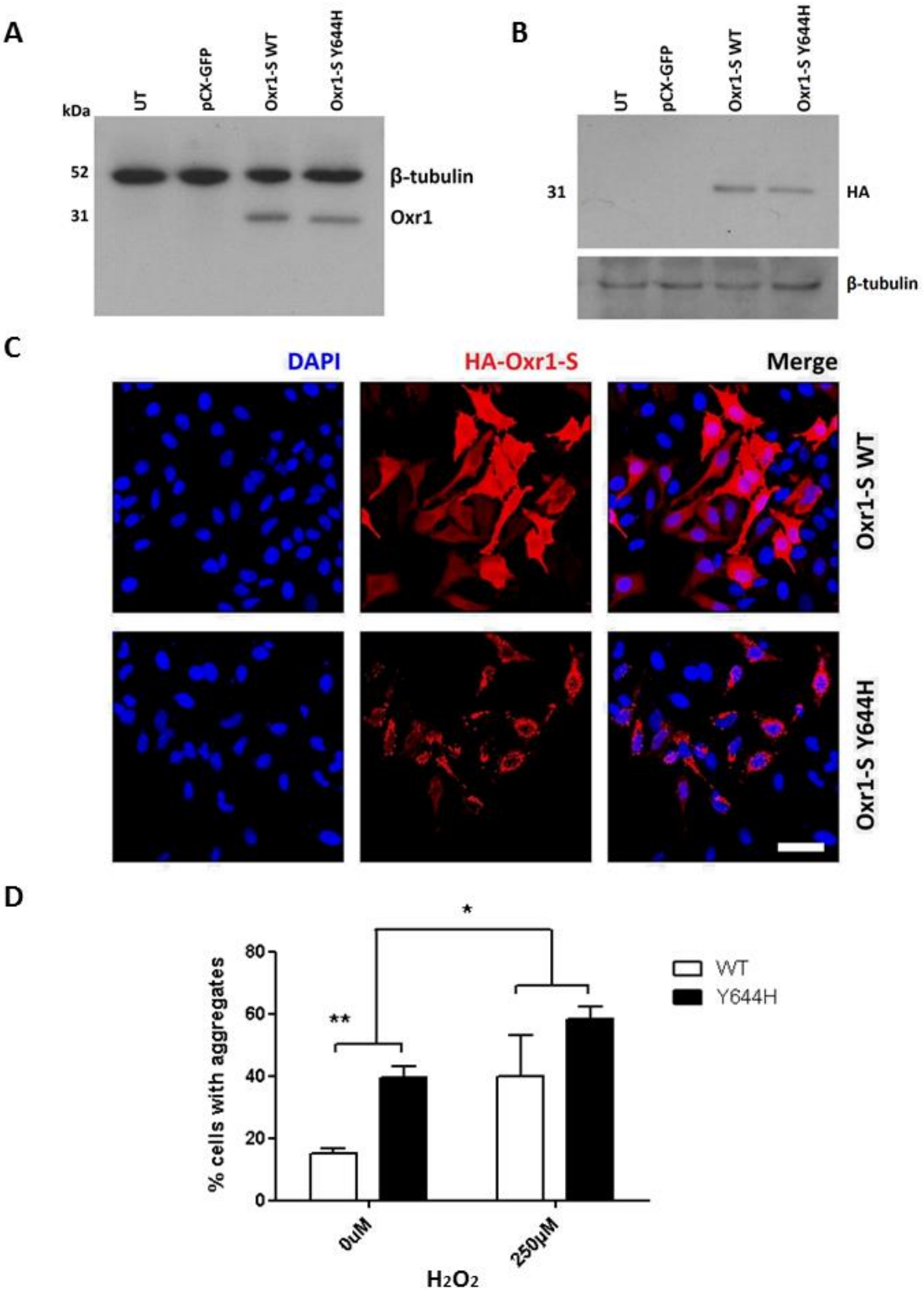
A
kDa
UT
pCX-GFP
Oxr1-S WT
Oxr1-S Y644H
52
31
β-tubulin
Oxr1
B
UT
pCX-GFP
Oxr1-S WT
Oxr1-S Y644H
31
HA
β-tubulin
C
DAPI
HA-Oxr1-S
Merge
Oxr1-S WT
Oxr1-S Y644H
D
% cells with aggregates
80
60
40
20
0
**
*
WT
Y644H
0uM
250μM
H2O2

Figure 6.3. Over-expression of Oxr1-S Y644H causes more severe oxidative stress-related protein aggregation

(A) HeLa cells were transfected with pcX-GFP, pcX-Oxr1-S WT and pcX-Oxr1-S Y644H. Cell lysate were labelled with anti-Oxr1 antibody. β-tubulin was used as a loading control. **(B)** Cells were labeled with anti-HA antibody. β-tubulin was used as a loading control. **(C)** HeLa cells were transfected with pCX-Oxr1-S WT and pCX-Oxr1-S Y644H constructs and immunostained with mouse anti-HA. Nuclei were mounted with DAPI. Scale bar=50 μm **(D)** In untreated condition, cells over-expressing Oxr1-S Y644H has significant higher percentage of cells with aggregates; Treating with 250 μM H_2O_2 had an aggravated impact. Data are means ± S.E.M. of 3 independent repeats and analysed by two-way ANOVA followed by Bonferroni Test, * $p < 0.05$. Pairwise comparisons in untreated or treated groups were made by Student's t test, ** $p < 0.01$

6.3.3 The oxidative stress-related protein aggregates are co-localised with cytoplasmic ubiquitin

Since the punctuate aggregate-like sub-cellular distribution of Oxr1-S was similar to the distribution pattern of mitochondria within cells, it was examined whether these aggregates were co-localised with mitochondria. However, neither Oxr1-S WT nor Oxr1-S Y644H was co-localised with the mitochondrial marker COX IV (**Figure 6.4A**), indicating the aggregates were not mitochondrially associated.

Since the degradation of misfolded proteins can be carried out via the ubiquitin-proteasome pathway (Wilkinson, 2000), to test whether these aggregates are ubiquitinated, cells were immunostained with an anti-ubiquitin antibody that specifically recognises ubiquitinated cytoplasmic inclusion bodies. It showed that the aggregates co-localised with the ubiquitin antibody (**Figure 6.4B)**, indicating that the mutant Oxr1-S is more likely to be targeted by ubiquitin and subjected to degradation.

A

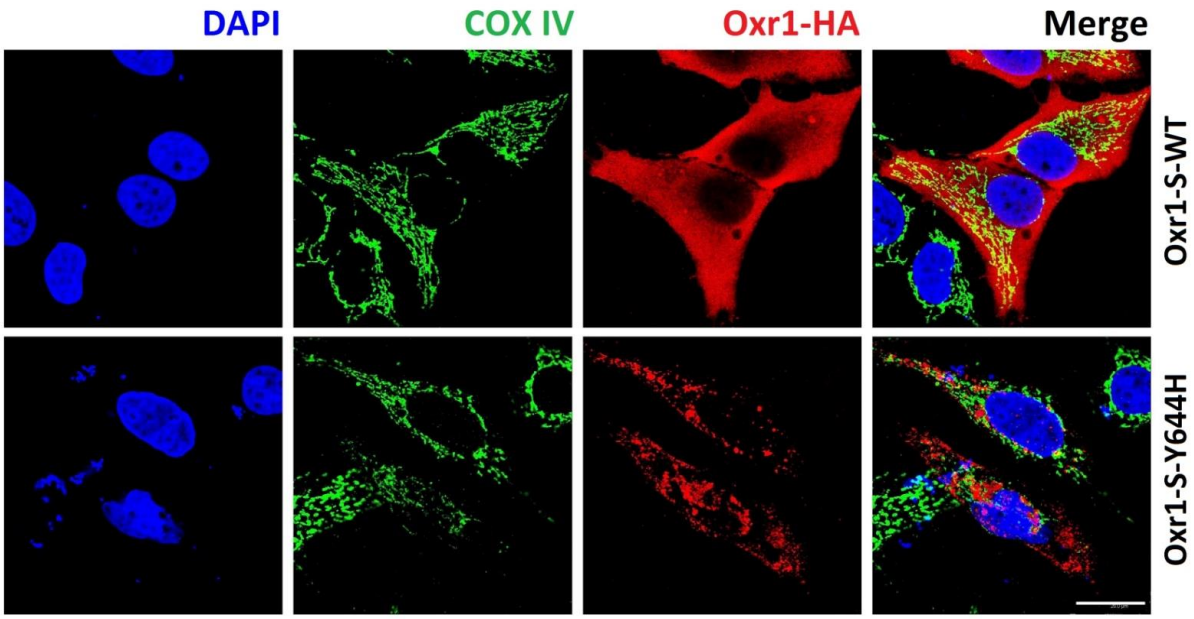
DAPI
COX IV
Oxr1-HA
Merge
Oxr1-S-WT
Oxr1-S-Y644H

B

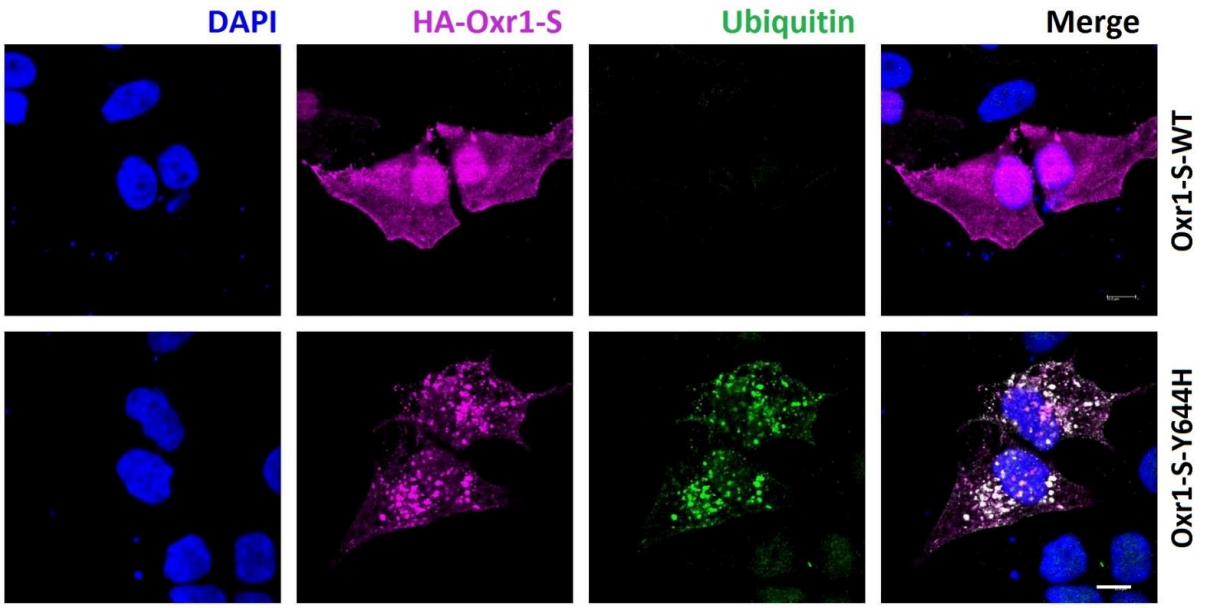
DAPI
HA-Oxr1-S
Ubiquitin
Merge
Oxr1-S-WT
Oxr1-S-Y644H

Figure 6.4. Oxr1-S Y644H aggregates are stress dependent and co-localise with ubiquitin

(A) Oxr1-S WT did not co-localise with mitochondrial marker COX IV and displayed a diffuse pattern; Oxr1-S Y644H also did not co-localise with COX IV. Nuclei were mounted with DAPI. Scale bar=20µm. **(B)** Cells were labelled with antibody specifically against cytoplasmic ubiquitin aggregates. Ubiquitin aggregates were not detectable in cells over-expressing Oxr1-S WT that had a diffuse pattern, but co-localised with cells over-expressing Oxr1-S Y644H that had a punctuate aggregate-like sub-cellular distribution.

6.3.4 Oxr1-S Y644H over-expression increases cell death under OS

It has been demonstrated previously that in Oxr1 knockout and knockdown primary GCs, H_2O_2-induced oxidative stress significantly increases the level of apoptosis (Oliver et al., 2011). However, whether over-expressing the mutant Oxr1 can also lead to increased cell apoptosis had not been studied.

To address this question, a hydrogen peroxide stress assay on HeLa cells was carried out. Hela cells were transfected with pCX-GFP, HA tagged pCX-Oxr1-S WT or pCX-Oxr1-S Y644H constructs, then exposed to 250 μM H_2O_2 for 4 hours. Cell death was measured by labelling cells with anti-cleaved Caspase-3, a marker of cell apoptosis (**Figure 6.5A**). The percentage of cell death was calculated as the number of cells with cleaved Caspase-3 positive nucleus versus the number of transfected cells. In untreated condition, all groups exhibited similar apoptosis levels (**Figure 6.5B**). In the group over-expressing mutant Oxr1, it manifested a significant induction of cell death after the treatment (**Figure 6.5B**). Conversely, all other groups exhibited no statistically significant increase in cell death after treating with H_2O_2 despite an increasing trend. The data suggest that over-expression of mutant Oxr1-S Y644H rendered cells more susceptible to oxidative stress.

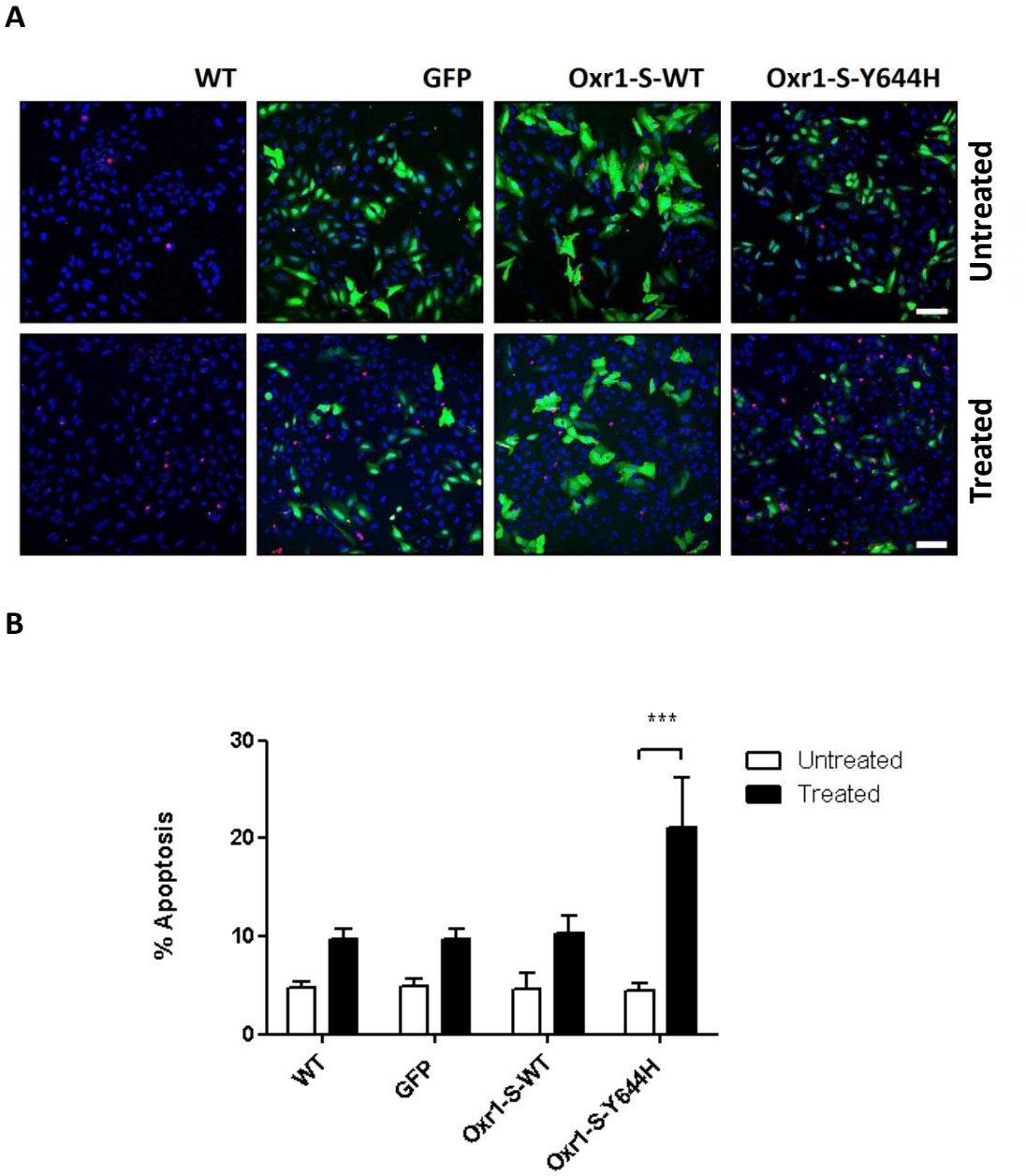

Figure 6.5. Oxr1-S Y644H over-expression significantly increases apoptosis under OS

(A) Stably transfected HeLa cells were exposed to 250 µM H_2O_2 for 4 hours, and apoptosis was measured by labelling with anti-cleaved Caspase-3. Scale bar=50µm **(B)** When treated with 250 µM H_2O_2, cells over-expressing Oxr1-S Y644H had significantly higher percentage of cell death in comparison with untransfected cell, cells over-expressing GFP and cells over-expressing Oxr1-S WT. Data are means ± S.E.M. of 3 independent repeats and analysed by two-way ANOVA followed by Bonferroni Test, *** $p < 0.001$.

6.3.5 Oxr1-S Y644H over-expression does not cause mitochondrial functional abnormalities

It has been shown that Y644H over-expression alone cannot lead to an increase in cell apoptosis. Since apoptosis is a severe cellular response to stress and damage, and I have observed formation of ubiquitin co-localised aggregates under basal conditions, whether Y644H over-expression also causes other cellular responses under basal condition should also be examined. To achieve this, mitochondrial membrane potential, which is an important parameter of mitochondrial function as well as an early indicator of apoptosis, was measured by the TMRE assay. It showed that there was no statistically significant difference in mitochondrial membrane potential among cells untransfected or transfected with different constructs, in both untreated and FCCP treated conditions, although the uncoupling reagent FCCP caused a significant reduction in the membrane potential (**Figure 6.6A**).

Oxygen consumption levels of untransfected HeLa cells and cells over-expressing GFP, Oxr1-S-WT or Oxr1-S-Y644H constructs were measured by using Luxcel mitochondrial oxygen consumption assay as introduced in Material and Methods. No statistically significant difference was observed among cells (**Figure 6.6B**).

Taken together, these results suggest that the over-expression of neither Oxr1-S-WT nor the Y644H mutant caused mitochondrial functional abnormalities.

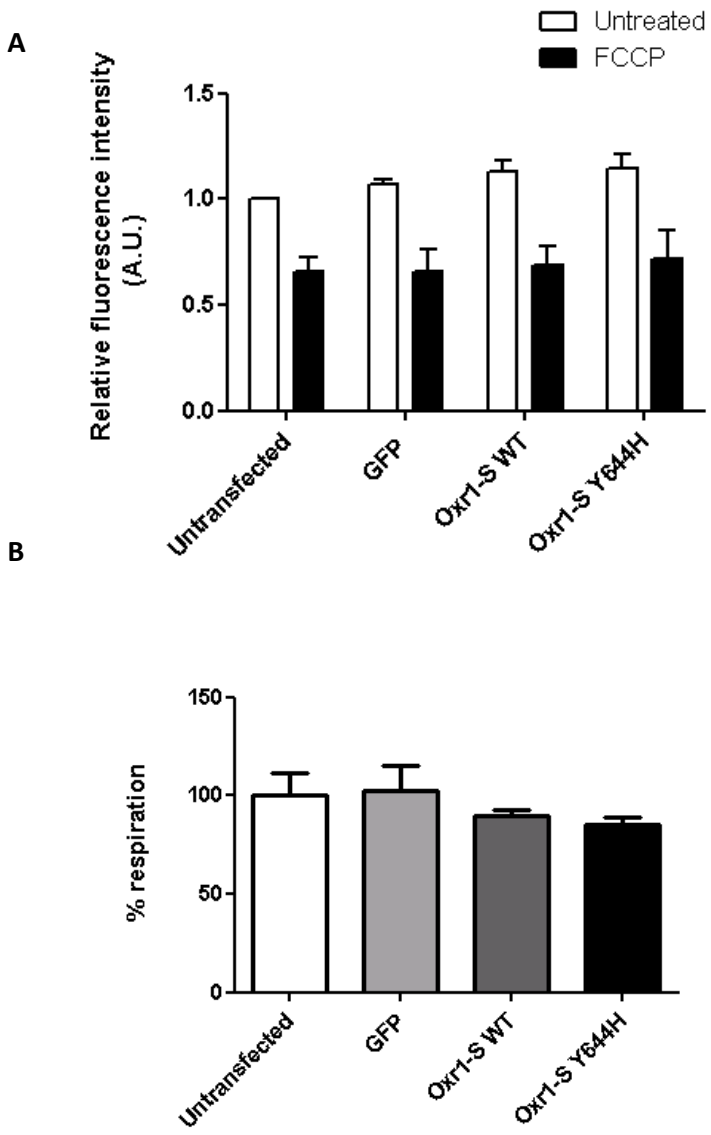

Figure 6.6. Oxr1-S Y644H over-expression does not cause mitochondrial functional abnormalities

(A) Stably transfected HeLa cells under basal condition or treated with 20 µM FCCP for 10 minutes were subjected to TMRE assay. FCCP treatment significantly reduced mitochondrial membrane potential ($p<0.0001$), but no difference was detected among cells under the same condition (treated or untreated). Data are means ± S.E.M. of 4 independent repeats and analysed by two-way ANOVA followed by Bonferroni post-hoc tests; pairwise comparisons in untreated or treated groups were made by one-way ANOVA followed by Bonferroni post-hoc tests. **(B)** Stably transfected HeLa cells were subjected to Luxcel mitochondrial oxygen consumption assay; no difference was detected among groups. Data are means ± S.E.M. of 3 independent repeats and analysed by one-way ANOVA followed by Bonferroni post-hoc tests.

6.3.6 Rederivation of Oxr1 mutant (Y644H) mice

Having shown potential structural and functional consequences of ENU mutations identified in Oxr1 by *in vitro* studies, an Oxr1 mutant (Y644H) mouse ought to be generated for phenotypic characterisation.

Three separate attempts were made to rederive the Y644H mouse from frozen sperm using the *in vitro* fertilisation (IVF) method by MRC Harwell. However, no live pups were born, which is likely due to poor sperm quality of the ENU-treated mice.

6.4 Discussion

In this chapter, from an ENU gene-driven screen, an Oxr1 mutant (Y644H) was identified. Over-expression of Oxr1-S-Y644H led to a much higher percentage of cells with abnormal cytoplasmic puncta comparing to over-expression of the wild-type Oxr1-S. These aggregates were found to be oxidative stress-dependent and targeted by ubiquitin. Moreover, over-expression of Y644H alone neither induced apoptosis nor triggered mitochondrial functional abnormality; whereas under oxidative stress, it significantly increased the level of apoptosis. Together, these results suggest that the over-expression of mutant Oxr1-S Y644H rendered cells more vulnerable to oxidative stress.

6.4.1 Pros and cons of ENU mutagenesis

In the past decade, ENU mutagenesis has been widely applied as an important tool to study the biological function of genes and generate mouse models of human diseases (Acevedo-Arozena et al., 2008). One of the major advantages of ENU mutagenesis is its unbiased approach to discover gene functions (Justice et al., 1999). Randomly generated mutations can lead to a wide range of effect at molecular and cellular levels, which enables mouse phenotypic diversity (Acevedo-Arozena et al., 2008). However, several drawbacks of ENU mutagenesis have also been revealed. For instance, the cost of large gene screening is high (Kile and Hilton, 2005). Moreover, taken our study as an example, it is occasionally unable to rederive mutant mice with newly identified mutations due to unknown factors, which prevents further characterisation of the mutations *in vivo*. Furthermore, ENU treated mice always carry multiple mutations and sometimes have to be backcrossed for several generations (Gondo, 2008), which is time-consuming and expensive. Nevertheless, due to its unbiased and versatile features, ENU mutagenesis will still remain an important tool of studying mouse genetics in the near future.

6.4.2 The potential structural impact of Y644H mutation on Oxr1

Expression of mutant proteins can cause protein misfolding and mislocalisation (Valastyan and Lindquist, 2014); and these abnormalities are hallmarks of neurodegenerative diseases (Hung and Link, 2011, Ramdzan et al., 2012). For example, over-expression of a PD-associated mutant DJ-1 (L166P) causes protein accumulation and loss of function (Bonifati et al., 2003b, Olzmann et al., 2004). Of note, according to the crystal structure of DJ-1, the leucine 166 is located in a helix that is important to the dimerisation of the protein (Tao and Tong, 2003, Wilson et al., 2003); changing from the aliphatic leucine to the cyclic proline can therefore affect the assembly of the dimer and subsequently affects its function. Interestingly, it was shown here that over-expression of Oxr1 with a mutation (Y644H) in the hydrophobic core of the TLDc domain (Blaise et al., 2012) also leads to the formation of cellular aggregates; and these aggregates were co-localised with ubiquitin (**Figure 6.4B**), which targets misfolded proteins for degradation (Wilkinson, 2000). These results suggest that changing from the aromatic tyrosine to the basic histidine in the hydrophobic core of the TLDc domain may trigger a structural alteration of Oxr1.

6.4.3 The potential functional impact of Y644H mutation on Oxr1

It was also found here that the cytoplasmic aggregates of Oxr1 were oxidative stress-related. In untreated condition, a significantly higher percentage of cells with the Oxr1 aggregates were detected in the mutant group in comparison with the WT group, indicating that over-expression of the mutant Oxr1 alone may lead to an imbalance between ROS and anti-oxidative activities within the cell. Over-expressing mutant anti-oxidative proteins under oxidative stress has been shown to cause increased level of cell death, for example, overexpression of PD-related mutant DJ-1 (R98Q, D149A and

L166P) in human dopaminergic neuroblastoma M17 cells showed significant elevation of cell death in H_2O_2 treated condition comparing to the over-expression of the WT and empty vector control (Wang et al., 2012a). Results here showed that over-expression of Oxr1-S-Y644H also caused a significant induction in apoptosis after treating with H_2O_2 (**Figure 6.5B**). Since multiple lines of evidence has shown that Oxr1 is anti-oxidative (Oliver et al., 2011, Elliott and Volkert, 2004), the incapability of mutant Oxr1 in protecting cells against oxidative stress suggests a potential alteration in the anti-oxidative role of Oxr1.

In addition, previous results demonstrated that under basal condition, Oxr1 knockout or knockdown is insufficient to induce apoptosis *in vitro* (Oliver et al., 2011), whereas under H_2O_2-induced oxidative stress the level of apoptosis is significantly increased (Oliver et al., 2011). Here, over-expression of mutant Oxr1 also did not show any induction of apoptosis under basal condition (**Figure 6.5B**); whereas under H_2O_2-induced oxidative stress, the level of apoptosis was significantly elevated, consistent with previous findings in the Oxr1 knockout or knockdown cells (Oliver et al., 2011). In addition, over-expression of the Y644H mutant did not lead to any impairment in mitochondrial oxygen consumption and mitochondrial membrane potential, which is consistent with previous studies in the chapter 4 using the Oxr1 knockout primary GCs. These results further indicate that Oxr1 deletion or mutation alone is unlikely to trigger mitochondrial dysfunction. Together, these data indicate that the Y644H mutation caused an impairment of the anti-oxidative role of Oxr1, similar to the effect resulted from the loss of Oxr1 (Oliver et al., 2011).

In summary, in this chapter, *in vitro* characterisation of the ENU-induced mutation (Y644H) in Oxr1 revealed both potentially structural and functional changes to Oxr1, further suggesting the structural and functional significance of the TLDc domain in Oxr1.

It has been demonstrated that Oxr1-S interacts with ALS-related genes TDP-43 and FUS (Finelli et al., 2015a). It is worthwhile to study in the future whether the Oxr1 mutation could influence the protein-protein interaction. Moreover, it has also been found that over-expression of Oxr1 *in vitro* is protective against oxidative stress induced apoptosis in *Oxr1* knockout primary cerebellar GCs; a genetic rescue of *Oxr1* expression in the brain prevented the establishment of *bella* phenotype (Oliver et al., 2011). Therefore, it also needs to be studied whether over-expressing the mutant Oxr1 in *Oxr1* knockout primary GCs or in *bella* mouse could rescue the oxidative stress induced cytotoxicity or phenotype.

Chapter 7: Discussion

7.1 Summary of results

The overall goal of this thesis was to investigate the potential role of Oxr1 in mitochondria and to understand more regarding the function of the gene in the oxidative stress response *in vitro* and *in vivo*. The results demonstrated that different isoforms of Oxr1 are expressed in specific sub-cellular compartments and those mitochondrial Oxr1 isoforms are associated with mitochondrial OM, facing toward cytosol. In addition, over-expression of cytoplasmic Oxr1-S is protective against oxidative stress-induced apoptosis as well as TDP-43 mutation-related gross mitochondrial morphological changes and dysfunction. These results indicate a potential role of Oxr1 in maintaining mitochondrial morphology and function. Following on from these data, it was shown that mitochondrial ultra-structure and bioenergetic metabolism were not affected in the cerebellar tissue of *Oxr1* knockout (*bella*) mice, although a reduction in mitochondrial length was observed in primary GCs. Analysis of mitochondrial fusion and fission proteins indicated that the level of the fission regulator p-Drp1 S616 was altered in *bella* tissue. These results suggest that *Oxr1* deletion alone does not trigger overt mitochondrial dysfunction but it may influence aspects of mitochondrial morphology.

Conditional deletion of *Oxr1* in mouse dopaminergic neurons *in vivo* showed no motor or pathological abnormalities compared to age-matched controls, suggesting that this conditional deletion does not lead to the selective vulnerability of dopaminergic neurons to neurodegeneration. Regarding the ENU mutagenesis screening, a mutation in the highly-conserved TLDc domain of Oxr1 (Y644H) was identified and over-expression of this mutation *in vitro* rendered cells more vulnerable to oxidative stress, demonstrating that this region of the protein is functionally important.

7.2 Role of Oxr1 in mitochondria

Because mitochondria are critically involved in the generation of ROS, anti-oxidative defence mechanisms and neurodegeneration, and Oxr1 is known to be protective against OS-induced neurodegeneration (Oliver et al., 2011), we first hypothesised that Oxr1 may play an important role in mitochondria. The data in this thesis demonstrated that although specific Oxr1 isoforms are associated with mitochondria, no overt defects in mitochondrial function can be detected in *Oxr1* knockout tissue apart from subtle structural alterations in primary cells. These findings are somewhat surprising, given that the early OXR1 studies had focused on the role of the gene in mitochondria (Elliot 2004). Importantly, however, using fractionation and western blotting, I was able to reveal the complex distribution of Oxr1 isoforms and their relevance to cellular survival that had not been addressed before. Although these findings have provided important, new information regarding Oxr1, the direct functional significance of the gene in mitochondria, if any, is still unclear.

To investigate the function of OXR1 in more detail in the presence and absence of oxidative stress in an *in vitro* context, a very recent study applied RNAseq to HeLa cells where OXR1 had been knocked-down by approximately 85% (Yang et al., 2015). Results showed that many (807) genes were differentially expressed in *OXR1* knockdown cells comparing to the control cells under the H_2O_2 treated or non-treated conditions (Yang et al., 2015). Of note, under non-treated condition alone, a large number of genes (679) were differentially expressed and more than 50% of those differentially expressed genes found under non-treated condtion are still similarly regulated after treating with H_2O_2, indicating an important regulatory role of OXR1 in regulating gene expression under normal or stressed conditions (Yang et al., 2015).

Interestingly, combining basal and H_2O_2-treated conditions with *OXR1* knockdown, from these data only 8 differentially expressed genes identified were mitochondria-related (Yang et al., 2015). For example, cytochrome C (Cyt-C), an early indicator of apoptosis (Zou et al., 1999), was up-regulated (Yang et al., 2015). It is well known that immediately prior to apoptosis, Cyt-C is released from mitochondria to cytosol, thereby triggering the downstream apoptotic cascade in cytosol (Kluck et al., 1997). From my work in Chapter 3, it was shown that over expression of cytosolic, but not mitochondrial Oxr1-S in HeLa cells prevented oxidative stress-induced apoptosis; while in the RNAseq study, knockdown of *OXR1* was also found to regulate the protein level and activation of the mainly cytosolic, pro-apoptotic caspase-9 (Yang et al., 2015, van Loo et al., 2002, Chandra and Tang, 2003). Taken together, these data suggest that the Cyt-C expression changes observed by RNAseq are due to the triggering of cell death pathways as opposed to defects in the mitochondrial, electron transport chain-related function of this Complex IV protein.

It appears that two mitochondrial genes, proline dehydrogenase (oxidase) 1 (PRODH) and oxoglutarate dehydrogenase-like protein (OGDHL) involved in metabolic pathways and stress response were down-regulated in *OXR1* knockdown HeLa cells (Yang et al., 2015, Phang et al., 2010, McLain et al., 2011). Therefore, I suggested that there was a potential association between Oxr1 and mitochondrial bioenergetics. However, in Chapter 4, I showed that *Oxr1* deletion alone does not trigger overt mitochondrial dysfunction. This notion is supported by early studies of primary GCs from the *bella* mutant, where under basal conditions no differences in cell death were observed in culture. However after exogenous oxidative stress, the *bella* GCs were more susceptible to degeneration (Oliver et al., 2011). Moreover, as discussed in Chapter 4, previous proteomic interaction studies showed that specific interactors such as a subunit of the

mitochondrial ATP synthase named Atp5b (Ohta and Kagawa, 1986, Finelli et al., 2015a), were identified under H_2O_2-induced oxidative stress. These data further support the hypothesis that key functional aspects of Oxr1 can only be identified under such stress conditions.

Hence, future work is required to determine the bioenergetic status of mitochondria under oxidative stress in the context of Oxr1, for example, measuring mitochondrial respiration, ATP synthesis and mitochondrial membrane potential in H_2O_2 or arsenite-treated primary GCs from wild-type and *bella* mice.

7.3 Oxr1 level and its anti-oxidative role

It was proposed initially that the expression of OXR1 itself is induced under both oxidative and heat stress (Elliott and Volkert, 2004, Oliver et al., 2011). Differential expression in several endogenous anti-oxidative genes has been found under oxidative stress. For example, induction of the anti-oxidative protein DJ-1 at both mRNA and protein levels was detected in human neuroblastoma cells treated with oxidative stress-inducing reagents such as 6-hydroxydopamine or rotenone (Lev et al., 2008). However, studies on the expression of endogenous Oxr1 under oxidative stress have generated mixed results. For example, data from Elliott *et al.* indicated an up-regulation of certain isoforms of OXR1 under heat or oxidative stress at the mRNA or protein level (Elliott and Volkert, 2004), whereas my data from Chapter 3 neither observed an induction of endogenous Oxr1 isoforms at protein level nor a significant shift in the sub-cellular re-localisation of these isoforms in N2a cells under H_2O_2-induced oxidative stress.

Recent evidence has indicated that the response of Oxr1 to oxidative stress may be transient and cell-type specific. For instance, in H_2O_2 treated N2a cells, transcriptional levels of the full-length and shortest Oxr1 isoforms were induced at different time points

(Finelli et al., 2015a), whereas in arsenite treated mouse primary cortical neurons, only the transcriptional level of the shortest Oxr1 isoform was induced (Finelli et al., 2016b) and in HeLa cells treated with H_2O_2, no induction of Oxr1 at mRNA level was observed (Yang et al., 2015).

Importantly, induction of a number of anti-oxidative proteins has been found to be regulated by nuclear factor erythroid-derived 2-like 2 **(**Nrf2)-mediated OS-response pathways through the binding of Nrf2/small Maf protein complex to anti-oxidant response elements (AREs) in the promoter region of the downstream anti-oxidative genes (Wang et al., 2007, Itoh et al., 1997). Intriguingly, neither the shortest nor longest *OXR1* isoforms contains a predicted or experimentally determined (ARE), suggesting that the gene is not downstream of the classical Nrf2-mediated OS-response pathways (Wang et al., 2007, Kuosmanen et al., 2016). In addition, other anti-oxidation-related proteins such as SOD1 and DJ-1 have been found to be closely associated with the Nrf2 pathway, and DJ-1 is believed to be an upstream activator (Milani et al., 2013). The possibility for Oxr1 to be an upstream regulator of the Nrf2 pathway still cannot be ruled out, despite a lack of supportive evidence. Recently, Yang *et al*. detected the activation of stress-response P53 pathway-related apoptosis regulators in the same *OXR1* knockdown RNAseq study introduced above (Yang et al., 2015). The authors therefore suggested a potential transcriptional regulatory role of Oxr1 on anti-oxidative stress-related pathways in cytosol, which is supported by my findings in Chapter 3 that over-expressing cytoplasmic Oxr1 is more protective against oxidative stress comparing to the mitochondrial Oxr1.

Therefore, the complexities and functional importance of Oxr1 up-regulation in response to oxidative stress and neurodegenerative diseases needs to be further studied. For instance, a more detailed study on Oxr1 at mRNA and protein levels across a range

of stressors such as mitochondrial complex inhibitors (rotenone and antimycin A) and more time points corresponded to the transcriptional studies should be considered**.**

7.4 Potential links between Oxr1 and mitochondrial protein import

Recent RNAseq data from Yang *et al.* showed that the translocase of outer mitochondrial membrane 22 homolog (TOM22) was the only gene found to be up-regulated in both untreated and treated conditions (Yang et al., 2015). TOM22 is a mitochondrial import receptor localised to mitochondrial OM with a cytosolic domain that interacts with mitochondrial import receptor TOM20 (Yano et al., 2000). In Chapter 3, it was demonstrated that mitochondrial Oxr1 is OM-associated and cytosolic-facing, similar to the localisation of TOM20 and TOM22. This raises the possibility of a potential functional interaction between Oxr1 and TOM22.

Disruption of mitochondrial protein import has been found to be associated with neurodegeneration. For example, primary cortical neurons of pre-symptomatic HD mouse model that express mutant HTT with an abnormal polyglutamine expansion display an impairment in mitochondrial protein import and increased susceptibility to oxidative stress (Yano et al., 2014b). These results suggested a direct association between mitochondrial protein import defect, vulnerability of cells to oxidative insult and HD pathogenesis (Yano et al., 2014b). Interestingly, however, mitochondria with the impairment in protein import obtained from both pre-symptomatic and mid-stage disease mice appeared to have normal mitochondrial respiratory function and membrane potential (Yano et al., 2014b), suggesting that the defect in import system was not in conjunction with mitochondrial bioenergetic dysfunction. Notably, my work in Chapter 4 also demonstrated normal mitochondrial respiratory function and membrane potential in *Oxr1* knockout mice. Therefore, this evidence cannot exclude a possibility of

mitochondrial protein import dysfunction resulted from Oxr1 loss and should be independently investigated.

In addition, as discussed in Chapter 3 and 4, results from a protein interaction screen have shown that under OS, Oxr1-S may interact with mitochondrial IM protein translocase component DNAJC19 as well as mitochondrial carrier protein SLC25A3 and SLC25A5 (Finelli et al., 2015a, Richter-Dennerlein et al., 2014, Palmieri, 2004). However, this protein interaction screen did not detect an interaction between Oxr1 and TOM22 (Finelli et al., 2015a). These data, in combination with the RNA sequencing data (Yang et al., 2015), indicate a potentially direct or indirect relationship between Oxr1 and mitochondrial import. Of note, these studies were carried out using tagged, exogenously expressed Oxr1 constructs that may not reflect the specific three-dimensional structural features or expression levels of certain mitochondrial membrane associations.

Therefore, in the future, it would be interesting to conduct studies to validate the potential relationship between endogenous Oxr1 and mitochondria protein import. Previously, interaction between TOM22 and other mitochondrial membrane associated partners such as TOM20 was demonstrated by using co-immunoprecipitation (van Wilpe et al., 1999, Alconada et al., 1995). The potential interaction between endogenous Oxr1 and those mitochondrial import regulators (DNAJC19, SLC25A3, SLC25A5 and TOM22) could therefore be validated by using co-immunoprecipitation from mouse brain tissue homogenate. In addition, an established radiolabelled precursor matrix protein-based protein import assay can be used to test the mitochondrial protein import activities in *bella* mouse and age-matched controls to search for defects that might contribute to cell death (Yano et al., 2000, Terada et al., 1997, Yano et al., 2014b).

7.5 Using CRISPR technique to investigate potential mutations in conserved regions of Oxr1

In Chapter 6, a point mutation in a tyrosine amino acid within the TLDc domain of Oxr1 (Y644H) was identified through ENU mutagenesis screening. This mutant was selected for further study due to the conservation of this amino acid in the TLDc domain of *scOxr1*. *In vitro* characterisation of this mutation revealed an increasing susceptibility of cells to oxidative stress compared to cells over-expressing the wild-type Oxr1. Since these data were collected, and based on the predicted three-dimensional structure of the TLDc domain from zebrafish (Blaise et al., 2012), mutations in other highly conserved amino acids in the C-terminal of TLDc domain have been characterised *in vitro* (Finelli et al., 2016a). For example, a C-terminal glutamic acid in Oxr1 is conserved in all TLDc domain-containing proteins and over-expressing these mutations (Oxr1-FL E773A and Oxr1-C E293A) significantly impaired the anti-oxidative role of the protein (Finelli et al., 2016a), indicating an important function of certain structural positions within the TLDc domain in maintaining its anti-oxidative role. However, whether expression of these mutations *in vivo* leads to a phenotype in the mouse CNS, for example one that is less severe than the *bella* deletion mutant, has not been investigated.

In the past three decades, development of new embryonic manipulation techniques, such as gene knockout, conditional knockout, as well as ENU-based gene-driven mutagenesis have meant that the mouse is well-established as a key model organism to study biological function of genes and potential mechanism of human diseases (Gondo, 2010). More recently, the RNA-guided endonuclease Cas9 from type II clustered regulatory interspaced short palindromic repeat (CRISPR) systems have been widely implemented for gene editing *in vitro* and *in vivo* (Hsu et al., 2014). For example, CRISPR-Cas9-mediated methods for genome editing have been shown to be highly

capable of conducting *in vivo* genome manipulation (Platt et al., 2014). In the case of generating mice with subtle genetic mutations, for example, substitution of crucial amino-acids of a protein, using the CRISPR-Cas9 targeted approach can bypass the multiple manipulation steps in the ES cells used by the traditional methods based on homologous recombination (Menke, 2013, Singh et al., 2015). Moreover, since the crystal structure of the conserved TLDc domain in zebrafish has been determined (Blaise et al., 2012), based on this structure and alignment studies, potential point mutations that may cause structural or functional alteration within this conserved TLDc domain can be predicted. Comparing the ENU mutagenesis approach used in Chapter 6 that randomly induces a large number of point mutations *in vivo* before identifying and selecting potentially important mutations to the targeted CRISPR-Cas9 approach, the later method enables a direct modification to the amino acid predicted to be structurally or functionally important. As the result, it bypasses the mutation selection step and the IVF in the ENU-mutagenesis method, which is more efficient and cost-effective.

Therefore, in the future, the CRISPR technique could be used to study those Oxr1 mutations (Y644H, E773A and E293A) *in vivo*.

7.6 The therapeutic potential of Oxr1

In recent years, delivering antioxidant proteins to mitochondria or cytoplasm to directly or indirectly regulate mitochondria-related functions has been considered as a potentially effective way of treating disease where OS is thought to be an important contributing factor to pathology, for example, PD (Jin et al., 2014, Smith et al., 2012). Although results here have confirmed several mitochondrial isoforms in mouse tissue and cells, my *in vitro* and *in vivo* work indicates that Oxr1 might not exert its anti-oxidative role directly via mitochondrial bioenergetics pathways. This evidence suggests that if

Oxr1 is indeed a viable protective factor in diseases such as neurodegeneration, it would be different from drug candidates such as MitoQ that directly manipulates mitochondrial metabolic activities (Smith et al., 2012).

Interestingly, my *in vitro* work here has demonstrated that over-expression of Oxr1 in cytoplasm is protective against cellular and mitochondrial damage resulted from oxidative stress and ALS-related TDP-43 mutation. Importantly, the cytoplasmic over-expression does not induce cytotoxicity such as apoptosis, or mitochondrial impairments such as alteration in mitochondrial morphology and function. Moreover, a neuronal Oxr1 over-expression transgenic mouse exhibited no pathological or phenotypic abnormality, while crossing this mouse with the ALS mouse model (SOD1 G93A) significantly delayed the disease onset and improved neurodegenerative phenotype such as motor deficits (Liu et al., 2015b). These *in vitro* and *in vivo* results indicate that Oxr1 can be a potential drug candidate that indirectly alleviates cellular and mitochondrial impairments. Indeed, injection of mouse bone marrow-derived mesenchymal stem cells (MSCs) over-expressing hOXR1 into mouse kidney has been shown to be protective against experimentally-induced renal injury and inflammation (Li et al., 2014), while mutations in an *Oxr1* homologue in *Drosophila melanogaster* show increased tolerance to *Vibrio cholerae* infection (Wang et al., 2012d). Together, these findings deepen the understanding of Oxr1 as a novel antioxidant protein and offer new and important insights into its role in the OS-response and its potential use in future antioxidant therapies.

References:

ACEVEDO-AROZENA, A., WELLS, S., POTTER, P., KELLY, M., COX, R. D. & BROWN, S. D. M. 2008. ENU Mutagenesis, a Way Forward to Understand Gene Function. *Annual Review of Genomics and Human Genetics,* 9**,** 49-69.

AHMAD, T., AGGARWAL, K., PATTNAIK, B., MUKHERJEE, S., SETHI, T., TIWARI, B. K., KUMAR, M., MICHEAL, A., MABALIRAJAN, U., GHOSH, B., SINHA ROY, S. & AGRAWAL, A. 2013. Computational classification of mitochondrial shapes reflects stress and redox state. *Cell Death Dis,* 4**,** e461.

ALBERTS, B., JOHNSON, A., LEWIS, J., RAFF, M., ROBERTS, K. & WALTER, P. 2008. The Mitochondrion *Molecular Biology of the Cell.* 5th ed. New York: Garland Publishing Inc.

ALCONADA, A., GÄRTNER, F., HÖNLINGER, A., KÜBRICH, M. & PFANNER, N. 1995. [19] Mitochondrial receptor complex from Neurospora crassa and Saccharomyces cerevisiae. *Methods in Enzymology.* Academic Press.

ALEXANDER, C., VOTRUBA, M., PESCH, U. E. A., THISELTON, D. L., MAYER, S., MOORE, A., RODRIGUEZ, M., KELLNER, U., LEO-KOTTLER, B., AUBURGER, G., BHATTACHARYA, S. S. & WISSINGER, B. 2000. OPA1, encoding a dynamin-related GTPase, is mutated in autosomal dominant optic atrophy linked to chromosome 3q28. *Nat Genet,* 26**,** 211-215.

ALEXEYEV, M., SHOKOLENKO, I., WILSON, G. & LEDOUX, S. 2013. The Maintenance of Mitochondrial DNA Integrity—Critical Analysis and Update. *Cold Spring Harbor Perspectives in Biology,* 5.

ALLAN BUTTERFIELD, D., CASTEGNA, A., LAUDERBACK, C. M. & DRAKE, J. 2002. Evidence that amyloid beta-peptide-induced lipid peroxidation and its sequelae in Alzheimer's disease brain contribute to neuronal death. *Neurobiology of Aging,* 23**,** 655-664.

ALTSCHUL, S. F., MADDEN, T. L., SCHÄFFER, A. A., ZHANG, J., ZHANG, Z., MILLER, W. & LIPMAN, D. J. 1997. Gapped BLAST and PSI-BLAST: a new generation of protein database search programs. *Nucleic Acids Research,* 25**,** 3389-3402.

ALTSCHUL, S. F., WOOTTON, J. C., GERTZ, E. M., AGARWALA, R., MORGULIS, A., SCHÄFFER, A. A. & YU, Y.-K. 2005. Protein Database Searches Using Compositionally Adjusted Substitution Matrices. *The FEBS journal,* 272**,** 5101-5109.

ANDERSON, P. & KEDERSHA, N. 2008. Stress granules: the Tao of RNA triage. *Trends in Biochemical Sciences,* 33**,** 141-150.

ANDERSON, S., BANKIER, A. T., BARRELL, B. G., DE BRUIJN, M. H. L., COULSON, A. R., DROUIN, J., EPERON, I. C., NIERLICH, D. P., ROE, B. A., SANGER, F., SCHREIER, P. H., SMITH, A. J. H., STADEN, R. & YOUNG, I. G. 1981. Sequence and organization of the human mitochondrial genome. *Nature,* 290**,** 457-465.

ANDRADE, M. A., O'DONOGHUE, S. I. & ROST, B. 1998. Adaptation of protein surfaces to subcellular location1. *Journal of Molecular Biology,* 276**,** 517-525.

ARAI, T., HASEGAWA, M., AKIYAMA, H., IKEDA, K., NONAKA, T., MORI, H., MANN, D., TSUCHIYA, K., YOSHIDA, M., HASHIZUME, Y. & ODA, T. 2006. TDP-43 is a component of ubiquitin-positive tau-negative inclusions in frontotemporal lobar degeneration and amyotrophic lateral sclerosis. *Biochemical and Biophysical Research Communications,* 351**,** 602-611.

ARITA, Y., HARKNESS, S. H., KAZZAZ, J. A., KOO, H.-C., JOSEPH, A., MELENDEZ, J. A., DAVIS, J. M., CHANDER, A. & LI, Y. 2006. Mitochondrial localization of catalase provides optimal protection from H2O2-induced cell death in lung epithelial cells. *American Journal of Physiology - Lung Cellular and Molecular Physiology,* 290**,** L978-L986.

ARMSTRONG, J. S. 2007. Mitochondrial Medicine: Pharmacological targeting of mitochondria in disease. *British Journal of Pharmacology,* 151**,** 1154-1165.

BABA, M., NAKAJO, S., TU, P., TOMITA, T., NAKAYA, K., LEE, V. M.-Y., TROJANOWSKI, J. Q. & IWATSUBO, T. 1998. Aggregation of a-Synuclein in Lewy Bodies of Sporadic Parkinson's Disease and Dementia with Lewy Bodies. *Am J Pathol.,* 152**,** 879-884.

BALOYANNIS, S. J. 2013. Alterations of Mitochondria and Golgi Apparatus Are Related to Synaptic Pathology in Alzheimer's Disease. *Neurodegenerative Diseases.*

BANNWARTH, S., AIT-EL-MKADEM, S., CHAUSSENOT, A., GENIN, E. C., LACAS-GERVAIS, S., FRAGAKI, K., BERG-ALONSO, L., KAGEYAMA, Y., SERRE, V., MOORE, D. G., VERSCHUEREN, A., ROUZIER, C., LE BER, I., AUGÉ, G., COCHAUD, C., LESPINASSE, F., N'GUYEN, K., DE SEPTENVILLE, A., BRICE, A., YU-WAI-MAN, P., SESAKI, H., POUGET, J. & PAQUIS-FLUCKLINGER, V. 2014. A mitochondrial origin for frontotemporal dementia and amyotrophic lateral sclerosis through CHCHD10 involvement. *Brain,* 137**,** 2329-2345.

BARBER, S. C. & SHAW, P. J. 2010. Oxidative stress in ALS: Key role in motor neuron injury and therapeutic target. *Free Radical Biology and Medicine,* 48**,** 629-641.

BARNHAM, K. J., MASTERS, C. L. & BUSH, A. I. 2004. Neurodegenerative diseases and oxidative stress. *Nat Rev Drug Discov,* 3**,** 205-214.

BARSOUM, M. J., YUAN, H., GERENCSER, A. A., LIOT, G., KUSHNAREVA, Y., GRÄBER, S., KOVACS, I., LEE, W. D., WAGGONER, J., CUI, J., WHITE, A. D., BOSSY, B., MARTINOU, J.-C., YOULE, R. J., LIPTON, S. A., ELLISMAN, M. H., PERKINS, G. A. & BOSSY-WETZEL, E. 2006. Nitric oxide-induced mitochondrial fission is regulated by dynamin-related GTPases in neurons. *The EMBO Journal,* 25**,** 3900-3911.

BARZILAI, A., ROTMAN, G. & SHILOH, Y. 2002. ATM deficiency and oxidative stress: a new dimension of defective response to DNA damage. *DNA Repair,* 1**,** 3-25.

BAUER, M. F. & NEUPERT, W. 2001. Import of proteins into mitochondria: A novel pathomechanism for progressive neurodegeneration. *Journal of Inherited Metabolic Disease,* 24**,** 166-180.

BECKER, T., BÖTTINGER, L. & PFANNER, N. 2011. Mitochondrial protein import: from transport pathways to an integrated network. *Trends in Biochemical Sciences,* 37**,** 85-91.

BEER, S. M., TAYLOR, E. R., BROWN, S. E., DAHM, C. C., COSTA, N. J., RUNSWICK, M. J. & MURPHY, M. P. 2004. Glutaredoxin 2 Catalyzes the Reversible Oxidation and Glutathionylation of Mitochondrial Membrane Thiol Proteins: IMPLICATIONS FOR MITOCHONDRIAL REDOX REGULATION AND ANTIOXIDANT DEFENSE. *Journal of Biological Chemistry,* 279**,** 47939-47951.

BEHL, C., DAVIS, J. B., LESLEY, R. & SCHUBERT, D. 1994. Hydrogen peroxide mediates amyloid β protein toxicity. *Cell,* 77**,** 817-827.

BENCHOUA, A., TRIOULIER, Y., ZALA, D., GAILLARD, M.-C., LEFORT, N., DUFOUR, N., SAUDOU, F., ELALOUF, J.-M., HIRSCH, E., HANTRAYE, P., DÉGLON, N. & BROUILLET, E. 2006. Involvement of Mitochondrial Complex II Defects in

Neuronal Death Produced by N-Terminus Fragment of Mutated Huntingtin. *Molecular Biology of the Cell,* 17**,** 1652-1663.
BENDER, A., KRISHNAN, K. J., MORRIS, C. M., TAYLOR, G. A., REEVE, A. K., PERRY, R. H., JAROS, E., HERSHESON, J. S., BETTS, J., KLOPSTOCK, T., TAYLOR, R. W. & TURNBULL, D. M. 2006. High levels of mitochondrial DNA deletions in substantia nigra neurons in aging and Parkinson disease. *Nat Genet,* 38**,** 515-517.
BENTMANN, E., NEUMANN, M., TAHIROVIC, S., RODDE, R., DORMANN, D. & HAASS, C. 2012. Requirements for Stress Granule Recruitment of Fused in Sarcoma (FUS) and TAR DNA-binding Protein of 43 kDa (TDP-43). *Journal of Biological Chemistry,* 287**,** 23079-23094.
BEREITER-HAHN, J. & VOTH, M. 1994. Dynamics of mitochondria in living cells: shape changes,dislocations, fusion, and fission of mitochondria. *Microsc. Res. Tech.,* 27**,** 198–219.
BERLETT, B. S. & STADTMAN, E. R. 1997. Protein Oxidation in Aging, Disease, and Oxidative Stress. *Journal of Biological Chemistry,* 272**,** 20313-20316.
BHAT, A. H., DAR, K. B., ANEES, S., ZARGAR, M. A., MASOOD, A., SOFI, M. A. & GANIE, S. A. 2015. Oxidative stress, mitochondrial dysfunction and neurodegenerative diseases; a mechanistic insight. *Biomedicine & Pharmacotherapy,* 74**,** 101-110.
BILIMORIA, P. M. & BONNI, A. 2008. Cultures of Cerebellar Granule Neurons. *Cold Spring Harbor Protocols,* 2008**,** pdb.prot5107.
BILLIA, F., HAUCK, L., GROTHE, D., KONECNY, F., RAO, V., KIM, R. H. & MAK, T. W. 2013. Parkinson-susceptibility gene DJ-1/PARK7 protects the murine heart from oxidative damage in vivo. *Proceedings of the National Academy of Sciences,* 110**,** 6085-6090.
BINDER, J. X., PLETSCHER-FRANKILD, S., TSAFOU, K., STOLTE, C., O'DONOGHUE, S. I., SCHNEIDER, R. & JENSEN, L. J. 2014. COMPARTMENTS: unification and visualization of protein subcellular localization evidence. *Database,* 2014.
BISKUP, S., MOORE, D. J., CELSI, F., HIGASHI, S., WEST, A. B., ANDRABI, S. A., KURKINEN, K., YU, S.-W., SAVITT, J. M., WALDVOGEL, H. J., FAULL, R. L. M., EMSON, P. C., TORP, R., OTTERSEN, O. P., DAWSON, T. M. & DAWSON, V. L. 2006. Localization of LRRK2 to membranous and vesicular structures in mammalian brain. *Annals of Neurology,* 60**,** 557-569.
BLAISE, M., ALSARRAF, H. M. A. B., WONG, J. E. M. M., MIDTGAARD, S. R., LAROCHE, F., SCHACK, L., SPAINK, H., STOUGAARD, J. & THIRUP, S. 2012. Crystal structure of the TLDc domain of oxidation resistance protein 2 from zebrafish. *Proteins: Structure, Function, and Bioinformatics,* 80**,** 1694-1698.
BLUM, T., BRIESEMEISTER, S. & KOHLBACHER, O. 2009. MultiLoc2: integrating phylogeny and Gene Ontology terms improves subcellular protein localization prediction. *BMC Bioinformatics,* 10**,** 1-11.
BOHR, V. A. 2002. Repair of oxidative DNA damage in nuclear and mitochondrial DNA, and some changes with aging in mammalian cells. *Free Radical Biology and Medicine,* 32**,** 804-812.
BOLENDER, N., SICKMANN, A., WAGNER, R., MEISINGER, C. & PFANNER, N. 2008. Multiple pathways for sorting mitochondrial precursor proteins. *EMBO Reports,* 9**,** 42-49.
BONIFATI, V., RIZZU, P., SQUITIERI, F., KRIEGER, E., VANACORE, N., VAN SWIETEN, J. C., BRICE, A., VAN DUIJN, C. M., OOSTRA, B., MECO, G. & HEUTINK, P. 2003a. DJ-

1(PARK7), a novel gene for autosomal recessive, early onset parkinsonism. *Neurological Sciences,* 24**,** 159-160.

BONIFATI, V., RIZZU, P., VAN BAREN, M. J., SCHAAP, O., BREEDVELD, G. J., KRIEGER, E., DEKKER, M. C. J., SQUITIERI, F., IBANEZ, P., JOOSSE, M., VAN DONGEN, J. W., VANACORE, N., VAN SWIETEN, J. C., BRICE, A., MECO, G., VAN DUIJN, C. M., OOSTRA, B. A. & HEUTINK, P. 2003b. Mutations in the DJ-1 Gene Associated with Autosomal Recessive Early-Onset Parkinsonism. *Science,* 299**,** 256-259.

BONIFATI, V., ROHÉ, C. F., BREEDVELD, G. J., FABRIZIO, E., DE MARI, M., TASSORELLI, C., TAVELLA, A., MARCONI, R., NICHOLL, D. J., CHIEN, H. F., FINCATI, E., ABBRUZZESE, G., MARINI, P., DE GAETANO, A., HORSTINK, M. W., MAAT-KIEVIT, J. A., SAMPAIO, C., ANTONINI, A., STOCCHI, F., MONTAGNA, P., TONI, V., GUIDI, M., LIBERA, A. D., TINAZZI, M., DE PANDIS, F., FABBRINI, G., GOLDWURM, S., DE KLEIN, A., BARBOSA, E., LOPIANO, L., MARTIGNONI, E., LAMBERTI, P., VANACORE, N., MECO, G., OOSTRA, B. A. & NETWORK, T. I. P. G. 2005. Early-onset parkinsonism associated with PINK1 mutations: Frequency, genotypes, and phenotypes. *Neurology,* 65**,** 87-95.

BONONI, A. & PINTON, P. 2015. Study of PTEN subcellular localization. *Methods (San Diego, Calif.),* 77-78**,** 92-103.

BRAAK, H. & BRAAK, E. 2000. Pathoanatomy of Parkinson's disease. *Journal of Neurology,* 247**,** II3-II10.

BUTTERFIELD, D. A., SWOMLEY, A. M. & SULTANA, R. 2013. Amyloid β-Peptide (1–42)-Induced Oxidative Stress in Alzheimer Disease: Importance in Disease Pathogenesis and Progression. *Antioxidants & Redox Signaling,* 19**,** 823-835.

CABEZAS-OPAZO, F. A., VERGARA-PULGAR, K., PÉREZ, M. J., JARA, C., OSORIO-FUENTEALBA, C. & QUINTANILLA, R. A. 2015. Mitochondrial Dysfunction Contributes to the Pathogenesis of Alzheimer's Disease. *Oxidative Medicine and Cellular Longevity,* 2015**,** 12.

CALÌ, T., OTTOLINI, D., SORIANO, M. E. & BRINI, M. 2015. A new split-GFP-based probe reveals DJ-1 translocation into the mitochondrial matrix to sustain ATP synthesis upon nutrient deprivation. *Human Molecular Genetics,* 24**,** 1045-1060.

CANET-AVILÉS, R. M., WILSON, M. A., MILLER, D. W., AHMAD, R., MCLENDON, C., BANDYOPADHYAY, S., BAPTISTA, M. J., RINGE, D., PETSKO, G. A. & COOKSON, M. R. 2004. The Parkinson's disease protein DJ-1 is neuroprotective due to cysteine-sulfinic acid-driven mitochondrial localization. *Proceedings of the National Academy of Sciences of the United States of America,* 101**,** 9103-9108.

CAPEL, F., RIMBERT, V., LIOGER, D., DIOT, A., ROUSSET, P., MIRAND, P. P., BOIRIE, Y., MORIO, B. & MOSONI, L. 2005. Due to reverse electron transfer, mitochondrial H2O2 release increases with age in human vastus lateralis muscle although oxidative capacity is preserved. *Mechanisms of Ageing and Development,* 126**,** 505-511.

CARRÌ, M. T., VALLE, C., BOZZO, F. & COZZOLINO, M. 2015. Oxidative stress and mitochondrial damage: importance in non-SOD1 ALS. *Frontiers in Cellular Neuroscience,* 9**,** 41.

CASPERSEN, C., WANG, N., YAO, J., SOSUNOV, A., CHEN, X., LUSTBADER, J. W., XU, H. W., STERN, D., MCKHANN, G. & YAN, S. D. 2005. Mitochondrial Aβ: a potential focal point for neuronal metabolic dysfunction in Alzheimer's disease. *The FASEB Journal,* 19**,** 2040-2041.

CHA, M.-Y., KIM, D. K. & MOOK-JUNG, I. 2015. The role of mitochondrial DNA mutation on neurodegenerative diseases. *Exp Mol Med,* 47**,** e150.

CHANDRA, D., CHOY, G. & TANG, D. G. 2007. Cytosolic Accumulation of HSP60 during Apoptosis with or without Apparent Mitochondrial Release: EVIDENCE THAT ITS PRO-APOPTOTIC OR PRO-SURVIVAL FUNCTIONS INVOLVE DIFFERENTIAL INTERACTIONS WITH CASPASE-3. *Journal of Biological Chemistry,* 282**,** 31289-31301.

CHANDRA, D. & TANG, D. G. 2003. Mitochondrially Localized Active Caspase-9 and Caspase-3 Result Mostly from Translocation from the Cytosol and Partly from Caspase-mediated Activation in the Organelle: LACK OF EVIDENCE FOR Apaf-1-MEDIATED PROCASPASE-9 ACTIVATION IN THE MITOCHONDRIA. *Journal of Biological Chemistry,* 278**,** 17408-17420.

CHANG, C.-R. & BLACKSTONE, C. 2010. Dynamic regulation of mitochondrial fission through modification of the dynamin-related protein Drp1. *Annals of the New York Academy of Sciences,* 1201**,** 34-39.

CHEN, H., DETMER, S. A., EWALD, A. J., GRIFFIN, E. E., FRASER, S. E. & CHAN, D. C. 2003. Mitofusins Mfn1 and Mfn2 coordinately regulate mitochondrial fusion and are essential for embryonic development. *The Journal of Cell Biology,* 160**,** 189-200.

CHEN, Y., YEE, D., DAINS, K., CHATTERJEE, A., CAVALCOLI, J., SCHNEIDER, E., OM, J., WOYCHIK, R. P. & MAGNUSON, T. 2000. Genotype-based screen for ENU-induced mutations in mouse embryonic stem cells. *Nat Genet,* 24**,** 314-317.

CHENG, A., WAN, R., YANG, J.-L., KAMIMURA, N., SON, T. G., OUYANG, X., LUO, Y., OKUN, E. & MATTSON, M. P. 2012. Involvement of PGC-1α in the formation and maintenance of neuronal dendritic spines. *Nat Commun,* 3**,** 1250.

CHEW, J., GENDRON, T. F., PRUDENCIO, M., SASAGURI, H., ZHANG, Y.-J., CASTANEDES-CASEY, M., LEE, C. W., JANSEN-WEST, K., KURTI, A., MURRAY, M. E., BIENIEK, K. F., BAUER, P. O., WHITELAW, E. C., ROUSSEAU, L., STANKOWSKI, J. N., STETLER, C., DAUGHRITY, L. M., PERKERSON, E. A., DESARO, P., JOHNSTON, A., OVERSTREET, K., EDBAUER, D., RADEMAKERS, R., BOYLAN, K. B., DICKSON, D. W., FRYER, J. D. & PETRUCELLI, L. 2015. C9ORF72 repeat expansions in mice cause TDP-43 pathology, neuronal loss, and behavioral deficits. *Science,* 348**,** 1151-1154.

CHIPUK, J. E., BOUCHIER-HAYES, L. & GREEN, D. R. 2006. Mitochondrial outer membrane permeabilization during apoptosis: the innocent bystander scenario. *Cell Death Differ,* 13**,** 1396-1402.

CHIPUK, J. E. & GREEN, D. R. 2008. How do BCL-2 proteins induce mitochondrial outer membrane permeabilization? *Trends in Cell Biology,* 18**,** 157-164.

CHOO, Y. S., JOHNSON, G. V. W., MACDONALD, M., DETLOFF, P. J. & LESORT, M. 2004. Mutant huntingtin directly increases susceptibility of mitochondria to the calcium-induced permeability transition and cytochrome c release. *Human Molecular Genetics,* 13**,** 1407-1420.

CIPOLAT, S., DE BRITO, O. M., DAL ZILIO, B. & SCORRANO, L. 2004. OPA1 requires mitofusin 1 to promote mitochondrial fusion. *Proceedings of the National Academy of Sciences of the United States of America,* 101**,** 15927-15932.

CIPOLAT, S., RUDKA, T., HARTMANN, D., COSTA, V., SERNEELS, L., CRAESSAERTS, K., METZGER, K., FREZZA, C., ANNAERT, W., D'ADAMIO, L., DERKS, C., DEJAEGERE, T., PELLEGRINI, L., D'HOOGE, R., SCORRANO, L. & DE STROOPER, B. 2006.

Mitochondrial Rhomboid PARL Regulates Cytochrome c Release during Apoptosis via OPA1-Dependent Cristae Remodeling. *Cell,* 126**,** 163-175.
CLARK, I. E., DODSON, M. W., JIANG, C., CAO, J. H., HUH, J. R., SEOL, J. H., YOO, S. J., HAY, B. A. & GUO, M. 2006. Drosophila pink1 is required for mitochondrial function and interacts genetically with parkin. *Nature,* 441**,** 1162-1166.
CLEREN, C., YANG, L., LORENZO, B., CALINGASAN, N. Y., SCHOMER, A., SIRECI, A., WILLE, E. J. & BEAL, M. F. 2008. Therapeutic effects of coenzyme Q10 (CoQ10) and reduced CoQ10 in the MPTP model of Parkinsonism. *Journal of Neurochemistry,* 104**,** 1613-1621.
COGHILL, E. L., HUGILL, A., PARKINSON, N., DAVISON, C., GLENISTER, P., CLEMENTS, S., HUNTER, J., COX, R. D. & BROWN, S. D. M. 2002. A gene-driven approach to the identification of ENU mutants in the mouse. *Nat Genet,* 30**,** 255-256.
COKOL, M., NAIR, R. & ROST, B. 2000. Finding nuclear localization signals. *EMBO Reports,* 1**,** 411-415.
COLE, N. B., DANIELS, M. P., LEVINE, R. L. & KIM, G. 2010. Oxidative stress causes reversible changes in mitochondrial permeability and structure. *Experimental gerontology,* 45**,** 596-602.
COLOMBRITA, C., ZENNARO, E., FALLINI, C., WEBER, M., SOMMACAL, A., BURATTI, E., SILANI, V. & RATTI, A. 2009. TDP-43 is recruited to stress granules in conditions of oxidative insult. *Journal of Neurochemistry,* 111**,** 1051-1061.
CONNOLLY, B. S. & LANG, A. E. 2014. Pharmacological treatment of parkinson disease: A review. *JAMA,* 311**,** 1670-1683.
CORBETT, M. A., BAHLO, M., JOLLY, L., AFAWI, Z., GARDNER, A. E., OLIVER, K. L., TAN, S., COFFEY, A., MULLEY, J. C., DIBBENS, L. M., SIMRI, W., SHALATA, A., KIVITY, S., JACKSON, G. D., BERKOVIC, S. F. & GECZ, J. 2010. A Focal Epilepsy and Intellectual Disability Syndrome Is Due to a Mutation in TBC1D24. *American Journal of Human Genetics,* 87**,** 371-375.
COSENTINO, C., GRIECO, D. & COSTANZO, V. 2011. ATM activates the pentose phosphate pathway promoting anti‐oxidant defence and DNA repair. *The EMBO Journal,* 30**,** 546-555.
CROISIER, E., MORAN, L. B., DEXTER, D. T., PEARCE, R. K. & GRAEBER, M. B. 2005. Microglial inflammation in the parkinsonian substantia nigra: relationship to alpha-synuclein deposition. *Journal of Neuroinflammation,* 2**,** 1-8.
DALFÓ, E., PORTERO-OTÍN, M., AYALA, V., MARTÍNEZ, A., PAMPLONA, R. & FERRER, I. 2005. Evidence of Oxidative Stress in the Neocortex in Incidental Lewy Body Disease. *Journal of Neuropathology & Experimental Neurology,* 64**,** 816-830.
DAMIANO, M., STARKOV, A. A., PETRI, S., KIPIANI, K., KIAEI, M., MATTIAZZI, M., FLINT BEAL, M. & MANFREDI, G. 2006. Neural mitochondrial Ca2+ capacity impairment precedes the onset of motor symptoms in G93A Cu/Zn-superoxide dismutase mutant mice. *Journal of Neurochemistry,* 96**,** 1349-1361.
DAVID, D. C., OLLIKAINEN, N., TRINIDAD, J. C., CARY, M. P., BURLINGAME, A. L. & KENYON, C. 2010. Widespread Protein Aggregation as an Inherent Part of Aging in <italic>C. elegans</italic>. *PLoS Biol,* 8**,** e1000450.
DAYAL, D., MARTIN, S. M., OWENS, K. M., AYKIN-BURNS, N., ZHU, Y., BOOMINATHAN, A., PAIN, D., LIMOLI, C. L., GOSWAMI, P. C., DOMANN, F. E. & SPITZ, D. R. 2009. Mitochondrial Complex II Dysfunction Can Contribute Significantly to Genomic Instability after Exposure to Ionizing Radiation. *Radiation research,* 172**,** 737-745.

DE GIORGI, F., LARTIGUE, L., BAUER, M. K. A., SCHUBERT, A., GRIMM, S., HANSON, G. T., REMINGTON, S. J., YOULE, R. J. & ICHAS, F. 2002. The permeability transition pore signals apoptosis by directing Bax translocation and multimerization. *The FASEB Journal*.

DE SOUZA-PINTO, N. C., MASON, P. A., HASHIGUCHI, K., WEISSMAN, L., TIAN, J., GUAY, D., LEBEL, M., STEVNSNER, T. V., RASMUSSEN, L. J. & BOHR, V. A. 2009. Novel DNA mismatch-repair activity involving YB-1 in human mitochondria. *DNA Repair,* 8**,** 704-719.

DEJESUS-HERNANDEZ, M., MACKENZIE, I. R., BOEVE, B. F., BOXER, A. L., BAKER, M., RUTHERFORD, N. J., NICHOLSON, A. M., FINCH, N. A., GILMER, H. F., ADAMSON, J., KOURI, N., WOJTAS, A., SENGDY, P., HSIUNG, G.-Y. R., KARYDAS, A., SEELEY, W. W., JOSEPHS, K. A., COPPOLA, G., GESCHWIND, D. H., WSZOLEK, Z. K., FELDMAN, H., KNOPMAN, D., PETERSEN, R., MILLER, B. L., DICKSON, D., BOYLAN, K., GRAFF-RADFORD, N. & RADEMAKERS, R. 2011. Expanded GGGGCC hexanucleotide repeat in non-coding region of C9ORF72 causes chromosome 9p-linked frontotemporal dementia and amyotrophic lateral sclerosis. *Neuron,* 72**,** 245-256.

DELETTRE, C., LENAERS, G., GRIFFOIN, J.-M., GIGAREL, N., LORENZO, C., BELENGUER, P., PELLOQUIN, L., GROSGEORGE, J., TURC-CAREL, C., PERRET, E., ASTARIE-DEQUEKER, C., LASQUELLEC, L., ARNAUD, B., DUCOMMUN, B., KAPLAN, J. & HAMEL, C. P. 2000. Nuclear gene OPA1, encoding a mitochondrial dynamin-related protein, is mutated in dominant optic atrophy. *Nat Genet,* 26**,** 207-210.

DENG, H., DODSON, M. W., HUANG, H. & GUO, M. 2008. The Parkinson's disease genes pink1 and parkin promote mitochondrial fission and/or inhibit fusion in Drosophila. *Proceedings of the National Academy of Sciences,* 105**,** 14503-14508.

DEVI, L., PRABHU, B. M., GALATI, D. F., AVADHANI, N. G. & ANANDATHEERTHAVARADA, H. K. 2006. Accumulation of Amyloid Precursor Protein in the Mitochondrial Import Channels of Human Alzheimer's Disease Brain Is Associated with Mitochondrial Dysfunction *The Journal of Neuroscience,* 26**,** 9057-9068.

DEVI, L., RAGHAVENDRAN, V., PRABHU, B. M., AVADHANI, N. G. & ANANDATHEERTHAVARADA, H. K. 2008. Mitochondrial Import and Accumulation of α-Synuclein Impair Complex I in Human Dopaminergic Neuronal Cultures and Parkinson Disease Brain. *Journal of Biological Chemistry,* 283**,** 9089-9100.

DHALIWAL, G. K. & GREWAL, R. P. 2000. Mitochondrial DNA deletion mutation levels are elevated in ALS brains. *NeuroReport,* 11**,** 2507-2509.

DOERKS, T., COPLEY, R. R., SCHULTZ, J., PONTING, C. P. & BORK, P. 2002. Systematic Identification of Novel Protein Domain Families Associated with Nuclear Functions. *Genome Research,* 12**,** 47-56.

DOLEZAL, P., LIKIC, V., TACHEZY, J. & LITHGOW, T. 2006. Evolution of the Molecular Machines for Protein Import into Mitochondria. *Science,* 313**,** 314-318.

DOUBLE, K. L. 2012. Neuronal vulnerability in Parkinson's disease. *Parkinsonism & Related Disorders,* 18, Supplement 1**,** S52-S54.

DU, C., FANG, M., LI, Y., LI, L. & WANG, X. 2000. Smac, a Mitochondrial Protein that Promotes Cytochrome c–Dependent Caspase Activation by Eliminating IAP Inhibition. *Cell,* 102**,** 33-42.

DUAN, W., LI, X., SHI, J., GUO, Y., LI, Z. & LI, C. 2010. Mutant TAR DNA-binding protein-43 induces oxidative injury in motor neuron-like cell. *Neuroscience,* 169**,** 1621-1629.

DUBOFF, B., GÖTZ, J. & FEANY, MEL B. 2012. Tau Promotes Neurodegeneration via DRP1 Mislocalization In Vivo. *Neuron,* 75**,** 618-632.

DUDEK, J., REHLING, P. & VAN DER LAAN, M. 2013. Mitochondrial protein import: Common principles and physiological networks. *Biochimica et Biophysica Acta (BBA) - Molecular Cell Research,* 1833**,** 274-285.

DURAND, M., KOLPAK, A., FARRELL, T., ELLIOTT, N., SHAO, W., BROWN, M. & VOLKERT, M. 2007. The OXR domain defines a conserved family of eukaryotic oxidation resistance proteins. *BMC Cell Biology,* 8**,** 13.

ELLIOTT, N. A. & VOLKERT, M. R. 2004. Stress Induction and Mitochondrial Localization of Oxr1 Proteins in Yeast and Humans. *Molecular and Cellular Biology,* 24**,** 3180-3187.

ERNSTER, L. & DALLNER, G. 1995. Biochemical, physiological and medical aspects of ubiquinone function. *Biochim Biophys Acta.,* 1271**,** 195-204.

ESTERBAUER, H., SCHAUR, R. J. & ZOLLNER, H. 1991. Chemistry and biochemistry of 4-hydroxynonenal, malonaldehyde and related aldehydes. *Free Radical Biology and Medicine,* 11**,** 81-128.

EXNER, N., TRESKE, B., PAQUET, D., HOLMSTRÖM, K., SCHIESLING, C., GISPERT, S., CARBALLO-CARBAJAL, I., BERG, D., HOEPKEN, H.-H., GASSER, T., KRÜGER, R., WINKLHOFER, K. F., VOGEL, F., REICHERT, A. S., AUBURGER, G., KAHLE, P. J., SCHMID, B. & HAASS, C. 2007. Loss-of-Function of Human PINK1 Results in Mitochondrial Pathology and Can Be Rescued by Parkin. *The Journal of Neuroscience,* 27**,** 12413-12418.

FALACE, A., FILIPELLO, F., LA PADULA, V., VANNI, N., MADIA, F., DE PIETRI TONELLI, D., DE FALCO, F. A., STRIANO, P., DAGNA BRICARELLI, F., MINETTI, C., BENFENATI, F., FASSIO, A. & ZARA, F. 2010. TBC1D24, an ARF6-Interacting Protein, Is Mutated in Familial Infantile Myoclonic Epilepsy. *The American Journal of Human Genetics,* 87**,** 365-370.

FAYET, G., JANSSON, M., STERNBERG, D., MOSLEMI, A.-R., BLONDY, P., LOMBÈS, A., FARDEAU, M. & OLDFORS, A. 2002. Ageing muscle: clonal expansions of mitochondrial DNA point mutations and deletions cause focal impairment of mitochondrial function. *Neuromuscular Disorders,* 12**,** 484-493.

FERNANDEZ-CHECA, J. C. F., A.; MORALES, A.; MARI, M.; GARCIA-RUIZ, C.; COLELL, A. 2010. Oxidative Stress and Altered Mitochondrial Function in Neurodegenerative Diseases: Lessons From Mouse Models. *CNS Neurol Disord Drug Targets,* 9**,** 439-454.

FERREIRA, I. L., NASCIMENTO, M. V., RIBEIRO, M., ALMEIDA, S., CARDOSO, S. M., GRAZINA, M., PRATAS, J., SANTOS, M. J., JANUÁRIO, C., OLIVEIRA, C. R. & REGO, A. C. 2010. Mitochondrial-dependent apoptosis in Huntington's disease human cybrids. *Experimental Neurology,* 222**,** 243-255.

FINELLI, M. J. 2010. *Study of two mouse mutants to identify novel neurodegenerative pathways. .* University of Oxford.

FINELLI, M. J., LIU, K. X., WU, Y., OLIVER, P. L. & DAVIES, K. E. 2015a. Oxr1 improves pathogenic cellular features of ALS-associated FUS and TDP-43 mutations. *Human Molecular Genetics,* 24**,** 3529-3544.

FINELLI, M. J., SANCHEZ-PULIDO, L., LIU, K. X., DAVIES, K. E. & OLIVER, P. L. 2015b. The evolutionarily conserved Tre2/Bub2/Cdc16 (TBC), Lysin motif (LysM), Domain

catalytic (TLDc) domain is neuroprotective against oxidative stress. *Journal of Biological Chemistry*.

FINELLI, M. J., SANCHEZ-PULIDO, L., LIU, K. X., DAVIES, K. E. & OLIVER, P. L. 2016a. The Evolutionarily Conserved Tre2/Bub2/Cdc16 (TBC), Lysin Motif (LysM), Domain Catalytic (TLDc) Domain Is Neuroprotective against Oxidative Stress. *Journal of Biological Chemistry,* 291**,** 2751-2763.

FINELLI, M. J., SANCHEZ-PULIDO, L., LIU, K. X., DAVIES, K. E. & OLIVER, P. L. 2016b. The evolutionarily conserved Tre2/Bub2/Cdc16 (TBC), Lysin motif (LysM), Domain catalytic (TLDc) domain is neuroprotective against oxidative stress. *Journal of Biological Chemistry,* 291**,** 2751-2763.

FINSTERER, J. 2008. Leigh and Leigh-Like Syndrome in Children and Adults. *Pediatric Neurology,* 39**,** 223-235.

FISCHER, H., ZHANG, X. U., O'BRIEN, K. P., KYLSTEN, P. & ENGVALL, E. 2001. C7, a Novel Nucleolar Protein, Is the Mouse Homologue of the Drosophila Late Puff Product L82 and an Isoform of Human OXR1. *Biochemical and Biophysical Research Communications,* 281**,** 795-803.

FISCHER, L. R., IGOUDJIL, A., MAGRANÉ, J., LI, Y., HANSEN, J. M., MANFREDI, G. & GLASS, J. D. 2011. SOD1 targeted to the mitochondrial intermembrane space prevents motor neuropathy in the Sod1 knockout mouse. *Brain,* 134**,** 196-209.

FORMAN, M. S., TROJANOWSKI, J. Q. & LEE, V. M. Y. 2007. TDP-43: a novel neurodegenerative proteinopathy. *Current Opinion in Neurobiology,* 17**,** 548-555.

FORNO, L. S. 1996. Neuropathology of Parkinson's Disease. *Journal of Neuropathology & Experimental Neurology,* 55**,** 259-272.

FORTE, G. M. A., POOL, M. R. & STIRLING, C. J. 2011. N-Terminal Acetylation Inhibits Protein Targeting to the Endoplasmic Reticulum. *PLoS Biology* 9**,** e1001073.

FUKASAWA, Y., TSUJI, J., FU, S.-C., TOMII, K., HORTON, P. & IMAI, K. 2015. MitoFates: Improved Prediction of Mitochondrial Targeting Sequences and Their Cleavage Sites. *Molecular & Cellular Proteomics : MCP,* 14**,** 1113-1126.

GANDHI, S. & ABRAMOV, A. Y. 2012. Mechanism of Oxidative Stress in Neurodegeneration. *Oxidative Medicine and Cellular Longevity,* 2012**,** 11.

GANDHI, S., MUQIT, M. M. K., STANYER, L., HEALY, D. G., ABOU-SLEIMAN, P. M., HARGREAVES, I., HEALES, S., GANGULY, M., PARSONS, L., LEES, A. J., LATCHMAN, D. S., HOLTON, J. L., WOOD, N. W. & REVESZ, T. 2006. PINK1 protein in normal human brain and Parkinson's disease. *Brain,* 129**,** 1720-1731.

GARRIDO, N., GRIPARIC, L., JOKITALO, E., WARTIOVAARA, J., VAN DER BLIEK, A. M. & SPELBRINK, J. N. 2003. Composition and Dynamics of Human Mitochondrial Nucleoids. *Molecular Biology of the Cell,* 14**,** 1583-1596.

GÁSPÁR, T., DOMOKI, F., LENTI, L., INSTITORIS, Á., SNIPES, J. A., BARI, F. & BUSIJA, D. W. 2009. Neuroprotective effect of adenoviral catalase gene transfer in cortical neuronal cultures. *Brain research,* 1270**,** 1-9.

GAUTIER, C. A., KITADA, T. & SHEN, J. 2008. Loss of PINK1 causes mitochondrial functional defects and increased sensitivity to oxidative stress. *Proceedings of the National Academy of Sciences,* 105**,** 11364-11369.

GEISLER, S., HOLMSTROM, K. M., SKUJAT, D., FIESEL, F. C., ROTHFUSS, O. C., KAHLE, P. J. & SPRINGER, W. 2010. PINK1/Parkin-mediated mitophagy is dependent on VDAC1 and p62/SQSTM1. *Nat Cell Biol,* 12**,** 119-131.

GERMAN, D. C., NELSON, E. L., LIANG, C. L., SPECIALE, S. G., SINTON, C. M. & SONSALLA, P. K. 1996. The Neurotoxin MPTP Causes Degeneration of Specific Nucleus A8, A9 and A10 Dopaminergic Neurons in the Mouse. *Neurodegeneration,* 5**,** 299-312

GIAIME, E., YAMAGUCHI, H., GAUTIER, C. A., KITADA, T. & SHEN, J. 2012. Loss of DJ-1 Does Not Affect Mitochondrial Respiration but Increases ROS Production and Mitochondrial Permeability Transition Pore Opening. *PLoS ONE,* 7**,** e40501.

GLYNN, I. M. 1967. Involvement of a Membrane Potential in the Synthesis of ATP by Mitochondria. *Nature,* 216**,** 1318-1319.

GONDO, Y. 2008. Trends in large-scale mouse mutagenesis: from genetics to functional genomics. *Nat Rev Genet,* 9**,** 803-810.

GONDO, Y. 2010. Now and future of mouse mutagenesis for human disease models. *Journal of Genetics and Genomics,* 37**,** 559-572.

GOTTLIEB, E., ARMOUR, S. M., HARRIS, M. H. & THOMPSON, C. B. 2003. Mitochondrial membrane potential regulates matrix configuration and cytochrome c release during apoptosis. *Cell Death Differ,* 10**,** 709-717.

GRECO, T. & FISKUM, G. 2010. Neuroprotection through Stimulation of Mitochondrial Antioxidant Protein Expression. *Journal of Alzheimer's Disease,* 20**,** 427-437.

GREEN, D. R. & LLAMBI, F. 2015. Cell Death Signaling. *Cold Spring Harbor Perspectives in Biology,* 7.

GU, M., COOPER, J. M., TAANMAN, J. W. & SCHAPIRA, A. H. 1998. Mitochondrial DNA transmission of the mitochondrial defect in Parkinson's disease. *ANN NEUROL,* 44**,** 177-186.

GUO, Z., KOZLOV, S., LAVIN, M. F., PERSON, M. D. & PAULL, T. T. 2010. ATM Activation by Oxidative Stress. *Science,* 330**,** 517-521.

GUVEN, A. & TOLUN, A. 2013. TBC1D24 truncating mutation resulting in severe neurodegeneration. *Journal of Medical Genetics,* 50**,** 199-202.

HAITINA, T., LINDBLOM, J., RENSTRÖM, T. & FREDRIKSSON, R. 2006. Fourteen novel human members of mitochondrial solute carrier family 25 (SLC25) widely expressed in the central nervous system. *Genomics,* 88**,** 779-790.

HALLIWELL, B. & CHIRICO, S. 1993. Lipid peroxidation: its mechanism, measurement, and significance. *The American Journal of Clinical Nutrition,* 57**,** 715S-724S.

HAMILTON, J., PELLMAN, J. J., BRUSTOVETSKY, T., HARRIS, R. A. & BRUSTOVETSKY, N. 2015. Oxidative metabolism in YAC128 mouse model of Huntington's disease. *Human Molecular Genetics,* 24**,** 4862-4878.

HANSSON PETERSEN, C. A., ALIKHANI, N., BEHBAHANI, H., WIEHAGER, B., PAVLOV, P. F., ALAFUZOFF, I., LEINONEN, V., ITO, A., WINBLAD, B., GLASER, E. & ANKARCRONA, M. 2008. The amyloid β-peptide is imported into mitochondria via the TOM import machinery and localized to mitochondrial cristae. *Proceedings of the National Academy of Sciences,* 105**,** 13145-13150.

HARTMANN, A., MICHEL, P. P., TROADEC, J.-D., MOUATT-PRIGENT, A., FAUCHEUX, B. A., RUBERG, M., AGID, Y. & HIRSCH, E. C. 2001. Is Bax a mitochondrial mediator in apoptotic death of dopaminergic neurons in Parkinson's disease? *Journal of Neurochemistry,* 76**,** 1785-1793.

HASHIMOTO, M., HSU, L. J., XIA, Y., TAKEDA, A., SISK, A., SUNDSMO, M. & MASLIAH, E. 1999. Oxidative stress induces amyloid-like aggregate formation of NACP/α-synuclein in vitro. *Neuroreport,* 10**,** 717–721.

HASSON, S. A., KANE, L. A., YAMANO, K., HUANG, C.-H., SLITER, D. A., BUEHLER, E., WANG, C., HEMAN-ACKAH, S. M., HESSA, T., GUHA, R., MARTIN, S. E. & YOULE, R. J. 2013. High-content genome-wide RNAi screens identify regulators of parkin upstream of mitophagy. *Nature,* 504**,** 291-295.

HATFIELD, J. S. & SKOFF, R. P. 1982. FAP immunoreactivity reveals astrogliosis in females heterozygous for jimpy. . *Brain research* 250**,** 123-131.

HAYASHI, S., LEWIS, P., PEVNY, L. & MCMAHON, A. P. 2002. RETRACTED: Efficient gene modulation in mouse epiblast using a Sox2Cre transgenic mouse strain. *Gene Expression Patterns,* 2**,** 93-97.

HAYES, J. D. & MCLELLAN, L. I. 1999. Glutathione and glutathione-dependent enzymes represent a co-ordinately regulated defence against oxidative stress. *Free Radical Research,* 31**,** 273-300.

HEO, J. Y., PARK, J. H., KIM, S. J., SEO, K. S., HAN, J. S., LEE, S. H., KIM, J. M., PARK, J. I., PARK, S. K., LIM, K., HWANG, B. D., SHONG, M. & KWEON, G. R. 2012. DJ-1 Null Dopaminergic Neuronal Cells Exhibit Defects in Mitochondrial Function and Structure: Involvement of Mitochondrial Complex I Assembly. *PLoS ONE,* 7**,** e32629.

HERNANDES, M. S. & BRITTO, L. R. G. 2012. NADPH Oxidase and Neurodegeneration. *Current Neuropharmacology,* 10**,** 321-327.

HERRERO, M.-T., ESTRADA, C., MAATOUK, L. & VYAS, S. 2015. Inflammation in Parkinson's disease: role of glucocorticoids. *Frontiers in Neuroanatomy,* 9**,** 32.

HIRSCH, E. C., VYAS, S. & HUNOT, S. 2012. Neuroinflammation in Parkinson's disease. *Parkinsonism & Related Disorders,* 18, Supplement 1**,** S210-S212.

HOLT, I. J., HE, J., MAO, C.-C., BOYD-KIRKUP, J. D., MARTINSSON, P., SEMBONGI, H., REYES, A. & SPELBRINK, J. N. 2007. Mammalian mitochondrial nucleoids: Organizing an independently minded genome. *Mitochondrion,* 7**,** 311-321.

HONG, K., LI, Y., DUAN, W., GUO, Y., JIANG, H., LI, W. & LI, C. 2012. Full-length TDP-43 and its C-terminal fragments activate mitophagy in NSC34 cell line. *Neuroscience Letters,* 530**,** 144-149.

HOPPINS, S., LACKNER, L. & NUNNARI, J. 2007. The Machines that Divide and Fuse Mitochondria. *Annual Review of Biochemistry,* 76**,** 751-780.

HORTON, P., PARK, K.-J., OBAYASHI, T., FUJITA, N., HARADA, H., ADAMS-COLLIER, C. J. & NAKAI, K. 2007. WoLF PSORT: protein localization predictor. *Nucleic Acids Research,* 35**,** W585-W587.

HOVIUS, R., LAMBRECHTS, H., NICOLAY, K. & DE KRUIJFF, B. 1990. Improved methods to isolate and subfractionate rat liver mitochondria. Lipid composition of the inner and outer membrane. *Biochimica et Biophysica Acta (BBA) - Biomembranes,* 1021**,** 217-226.

HROUDOVÁ, J., SINGH, N. & FIŠAR, Z. 2014. Mitochondrial Dysfunctions in Neurodegenerative Diseases: Relevance to Alzheimer’s Disease. *BioMed Research International,* 2014**,** 9.

HSU, L. J., SAGARA, Y., ARROYO, A., ROCKENSTEIN, E., SISK, A., MALLORY, M., WONG, J., TAKENOUCHI, T., HASHIMOTO, M. & MASLIAH, E. 2000. α-Synuclein Promotes Mitochondrial Deficit and Oxidative Stress. *The American Journal of Pathology,* 157**,** 401-410.

HSU, PATRICK D., LANDER, ERIC S. & ZHANG, F. 2014. Development and Applications of CRISPR-Cas9 for Genome Engineering. *Cell,* 157**,** 1262-1278.

HUANG, X., ATWOOD, C. S., HARTSHORN, M. A., MULTHAUP, G., GOLDSTEIN, L. E., SCARPA, R. C., CUAJUNGCO, M. P., GRAY, D. N., LIM, J., MOIR, R. D., TANZI, R. E. & BUSH, A. I. 1999. The Aβ Peptide of Alzheimer's Disease Directly Produces Hydrogen Peroxide through Metal Ion Reduction. *Biochemistry,* 38**,** 7609-7616.

HUNG, M.-C. & LINK, W. 2011. Protein localization in disease and therapy. *Journal of Cell Science,* 124**,** 3381-3392.

HUSSAIN, S., SLIKKER JR, W. & ALI, S. F. 1995. Age-related changes in antioxidant enzymes, superoxide dismutase, catalase, glutathione peroxidase and glutathione in different regions of mouse brain. *International Journal of Developmental Neuroscience,* 13**,** 811-817.

HYNES, J., NATOLI, E. & WILL, Y. 2001. Fluorescent pH and Oxygen Probes of the Assessment of Mitochondrial Toxicity in Isolated Mitochondria and Whole Cells. *Current Protocols in Toxicology.* John Wiley & Sons, Inc.

IMAI, K. & NAKAI, K. 2010. Prediction of subcellular locations of proteins: Where to proceed? *PROTEOMICS,* 10**,** 3970-3983.

IMAI, Y., SODA, M. & TAKAHASHI, R. 2000. Parkin Suppresses Unfolded Protein Stress-induced Cell Death through Its E3 Ubiquitin-protein Ligase Activity. *Journal of Biological Chemistry,* 275**,** 35661-35664.

IRRCHER, I., ALEYASIN, H., SEIFERT, E. L., HEWITT, S. J., CHHABRA, S., PHILLIPS, M., LUTZ, A. K., ROUSSEAUX, M. W. C., BEVILACQUA, L., JAHANI-ASL, A., CALLAGHAN, S., MACLAURIN, J. G., WINKLHOFER, K. F., RIZZU, P., RIPPSTEIN, P., KIM, R. H., CHEN, C. X., FON, E. A., SLACK, R. S., HARPER, M. E., MCBRIDE, H. M., MAK, T. W. & PARK, D. S. 2010. Loss of the Parkinson's disease-linked gene DJ-1 perturbs mitochondrial dynamics. *Human Molecular Genetics,* 19**,** 3734-3746.

ISHIHARA, N., FUJITA, Y., OKA, T. & MIHARA, K. 2006. *Regulation of mitochondrial morphology through proteolytic cleavage of OPA1*.

ITOH, K., CHIBA, T., TAKAHASHI, S., ISHII, T., IGARASHI, K., KATOH, Y., OYAKE, T., HAYASHI, N., SATOH, K., HATAYAMA, I., YAMAMOTO, M. & NABESHIMA, Y.-I. 1997. An Nrf2/Small Maf Heterodimer Mediates the Induction of Phase II Detoxifying Enzyme Genes through Antioxidant Response Elements. *Biochemical and Biophysical Research Communications,* 236**,** 313-322.

JACKSON-LEWIS, V. & PRZEDBORSKI, S. 2007. Protocol for the MPTP mouse model of Parkinson's disease. *Nat. Protocols,* 2**,** 141-151.

JAHANI-ASL, A. & SLACK, R. S. 2007. The phosphorylation state of Drp1 determines cell fate. *EMBO Reports,* 8**,** 912-913.

JAMES, A. M., SHARPLEY, M. S., MANAS, A.-R. B., FRERMAN, F. E., HIRST, J., SMITH, R. A. J. & MURPHY, M. P. 2007. Interaction of the Mitochondria-targeted Antioxidant MitoQ with Phospholipid Bilayers and Ubiquinone Oxidoreductases. *Journal of Biological Chemistry,* 282**,** 14708-14718.

JANSSENS, J., WILS, H., KLEINBERGER, G., JORIS, G., CUIJT, I., CEUTERICK-DE GROOTE, C., VAN BROECKHOVEN, C. & KUMAR-SINGH, S. 2013. Overexpression of ALS-Associated p.M337V Human TDP-43 in Mice Worsens Disease Features Compared to Wild-type Human TDP-43 Mice. *Molecular Neurobiology,* 48**,** 22-35.

JARAMILLO-GUTIERREZ, G., MOLINA-CRUZ, A., KUMAR, S. & BARILLAS-MURY, C. 2010. The <italic>Anopheles gambiae</italic> Oxidation Resistance 1 (OXR1) Gene Regulates Expression of Enzymes That Detoxify Reactive Oxygen Species. *PLoS ONE,* 5**,** e11168.

JAUSLIN, M. L., MEIER, T., SMITH, R. A. J. & MURPHY, M. P. 2003. Mitochondria-targeted antioxidants protect Friedreich Ataxia fibroblasts from endogenous oxidative stress more effectively than untargeted antioxidants. *The FASEB Journal*.

JAWORSKI, J. 2007. ARF6 in the nervous system. *European Journal of Cell Biology,* 86**,** 513-524.

JEANS, A. F., OLIVER, P. L., JOHNSON, R., CAPOGNA, M., VIKMAN, J., MOLNÁR, Z., BABBS, A., PARTRIDGE, C. J., SALEHI, A., BENGTSSON, M., ELIASSON, L., RORSMAN, P. & DAVIES, K. E. 2007. A dominant mutation in Snap25 causes impaired vesicle trafficking, sensorimotor gating, and ataxia in the blind-drunk mouse. *Proceedings of the National Academy of Sciences,* 104**,** 2431-2436.

JENDRACH, M., MAI, S., POHL, S., VÖTH, M. & BEREITER-HAHN, J. 2008. Short- and long-term alterations of mitochondrial morphology, dynamics and mtDNA after transient oxidative stress. *Mitochondrion,* 8**,** 293-304.

JENDRACH, M., POHL, S., VÖTH, M., KOWALD, A., HAMMERSTEIN, P. & BEREITER-HAHN, J. 2005. Morpho-dynamic changes of mitochondria during ageing of human endothelial cells. *Mechanisms of Ageing and Development,* 6-7**,** 813 – 821.

JIN, H., KANTHASAMY, A., GHOSH, A., ANANTHARAM, V., KALYANARAMAN, B. & KANTHASAMY, A. G. 2014. Mitochondria-targeted antioxidants for treatment of Parkinson's disease: Preclinical and clinical outcomes. *Biochimica et Biophysica Acta (BBA) - Molecular Basis of Disease,* 1842**,** 1282-1294.

JUNG, C., HIGGINS, C. M. J. & XU, Z. 2002. Mitochondrial electron transport chain complex dysfunction in a transgenic mouse model for amyotrophic lateral sclerosis. *Journal of Neurochemistry,* 83**,** 535-545.

JUNN, E., JANG, W. H., ZHAO, X., JEONG, B. S. & MOURADIAN, M. M. 2009. Mitochondrial localization of DJ-1 leads to enhanced neuroprotection. *Journal of Neuroscience Research,* 87**,** 123-129.

JUSTICE, M. J., NOVEROSKE, J. K., WEBER, J. S., ZHENG, B. & BRADLEY, A. 1999. Mouse ENU Mutagenesis. *Human Molecular Genetics,* 8**,** 1955-1963.

KAHLE, P. J., NEUMANN, M., OZMEN, L., MÜLLER, V., JACOBSEN, H., SCHINDZIELORZ, A., OKOCHI, M., LEIMER, U., VAN DER PUTTEN, H., PROBST, A., KREMMER, E., KRETZSCHMAR, H. A. & HAASS, C. 2000. Subcellular Localization of Wild-Type and Parkinson's Disease-Associated Mutant α-Synuclein in Human and Transgenic Mouse Brain. *The Journal of Neuroscience,* 20**,** 6365-6373.

KANE, L. A., LAZAROU, M., FOGEL, A. I., LI, Y., YAMANO, K., SARRAF, S. A., BANERJEE, S. & YOULE, R. J. 2014. PINK1 phosphorylates ubiquitin to activate Parkin E3 ubiquitin ligase activity. *The Journal of Cell Biology,* 205**,** 143-153.

KANEKO, Y., SHOJO, H., BURNS, J., STAPLES, M., TAJIRI, N. & BORLONGAN, C. V. 2014. DJ-1 ameliorates ischemic cell death in vitro possibly via mitochondrial pathway. *Neurobiology of Disease,* 62**,** 56-61.

KEHREIN, K., SCHILLING, R., MÖLLER-HERGT, BRAULIO V., WURM, CHRISTIAN A., JAKOBS, S., LAMKEMEYER, T., LANGER, T. & OTT, M. 2015. Organization of Mitochondrial Gene Expression in Two Distinct Ribosome-Containing Assemblies. *Cell Reports,* 10**,** 843-853.

KHAIDAKOV, M., HEFLICH, R. H., MANJANATHA, M. G., MYERS, M. B. & AIDOO, A. 2003. Accumulation of point mutations in mitochondrial DNA of aging mice. *Mutation Research/Fundamental and Molecular Mechanisms of Mutagenesis,* 526**,** 1-7.

KHALIL, B., EL FISSI, N., AOUANE, A., CABIROL-POL, M. J., RIVAL, T. & LIEVENS, J. C. 2015. PINK1-induced mitophagy promotes neuroprotection in Huntington/'s disease. *Cell Death Dis,* 6**,** e1617.

KILE, B. T. & HILTON, D. J. 2005. The art and design of genetic screens: mouse. *Nat Rev Genet,* 6**,** 557-567.

KIM, S. C., SPRUNG, R., CHEN, Y., XU, Y., BALL, H., PEI, J., CHENG, T., KHO, Y., XIAO, H., XIAO, L., GRISHIN, N. V., WHITE, M., YANG, X.-J. & ZHAO, Y. 2006. Substrate and Functional Diversity of Lysine Acetylation Revealed by a Proteomics Survey. *Molecular Cell,* 23**,** 607-618.

KITADA, T., ASAKAWA, S., HATTORI, N., MATSUMINE, H., YAMAMURA, Y., MINOSHIMA, S., YOKOCHI, M., MIZUNO, Y. & SHIMIZU, N. 1998. Mutations in the parkin gene cause autosomal recessive juvenile parkinsonism. *Nature,* 392**,** 605-608.

KLUCK, R. M., BOSSY-WETZEL, E., GREEN, D. R. & NEWMEYER, D. D. 1997. The Release of Cytochrome c from Mitochondria: A Primary Site for Bcl-2 Regulation of Apoptosis. *Science,* 275**,** 1132-1136.

KOBAYASHI, N., TAKAHASHI, M., KIHARA, S., NIIMI, T., YAMASHITA, O. & YAGINUMA, T. 2014. Cloning of cDNA encoding a Bombyx mori homolog of human oxidation resistance 1 (OXR1) protein from diapause eggs, and analyses of its expression and function. *Journal of Insect Physiology,* 68**,** 58-68.

KOOPMAN, W. J. H., VERKAART, S., VISCH, H.-J., VAN DER WESTHUIZEN, F. H., MURPHY, M. P., VAN DEN HEUVEL, L. W. P. J., SMEITINK, J. A. M. & WILLEMS, P. H. G. M. 2005. Inhibition of complex I of the electron transport chain causes O2−·-mediated mitochondrial outgrowth. *American Journal of Physiology - Cell Physiology,* 288**,** C1440-C1450.

KOPEIKINA, K. J., CARLSON, G. A., PITSTICK, R., LUDVIGSON, A. E., PETERS, A., LUEBKE, J. I., KOFFIE, R. M., FROSCH, M. P., HYMAN, B. T. & SPIRES-JONES, T. L. 2011. Tau Accumulation Causes Mitochondrial Distribution Deficits in Neurons in a Mouse Model of Tauopathy and in Human Alzheimer's Disease Brain. *The American Journal of Pathology,* 179**,** 2071-2082.

KORSHUNOV, S. S., KRASNIKOV, B. F., PEREVERZEV, M. O. & SKULACHEV, V. P. 1999. The antioxidant functions of cytochrome c. *FEBS Letters,* 462**,** 192-198.

KOYANO, F., OKATSU, K., KOSAKO, H., TAMURA, Y., GO, E., KIMURA, M., KIMURA, Y., TSUCHIYA, H., YOSHIHARA, H., HIROKAWA, T., ENDO, T., FON, E. A., TREMPE, J.-F., SAEKI, Y., TANAKA, K. & MATSUDA, N. 2014a. Ubiquitin is phosphorylated by PINK1 to activate parkin. *Nature,* 510**,** 162-166.

KOYANO, F., OKATSU, K., KOSAKO, H., TAMURA, Y., GO, E., KIMURA, M., KIMURA, Y., TSUCHIYA, H., YOSHIHARA, H., HIROKAWA, T., ENDO, T., FON, E. A., TREMPE, J.-F., SAEKI, Y., TANAKA, K. & MATSUDA, N. 2014b. Ubiquitin is phosphorylated by PINK1 to activate parkin. *Nature,* advance online publication.

KRAYTSBERG, Y., KUDRYAVTSEVA, E., MCKEE, A. C., GEULA, C., KOWALL, N. W. & KHRAPKO, K. 2006. Mitochondrial DNA deletions are abundant and cause functional impairment in aged human substantia nigra neurons. *Nat Genet,* 38**,** 518-520.

KREBIEHL, G., RUCKERBAUER, S., BURBULLA, L. F., KIEPER, N., MAURER, B., WAAK, J., WOLBURG, H., GIZATULLINA, Z., GELLERICH, F. N., WOITALLA, D., RIESS, O., KAHLE, P. J., PROIKAS-CEZANNE, T. & KRÜGER, R. 2010. Reduced Basal

Autophagy and Impaired Mitochondrial Dynamics Due to Loss of Parkinson's Disease-Associated Protein DJ-1. *PloS One,* 5**,** e9367.
KUMMARI, E., GUO-ROSS, S. X. & EELLS, J. B. 2015. Laser Capture Microdissection - A Demonstration of the Isolation of Individual Dopamine Neurons and the Entire Ventral Tegmental Area. e52336.
KUOSMANEN, S. M., VIITALA, S., LAITINEN, T., PERÄKYLÄ, M., PÖLÖNEN, P., KANSANEN, E., LEINONEN, H., RAJU, S., WIENECKE-BALDACCHINO, A., NÄRVÄNEN, A., POSO, A., HEINÄNIEMI, M., HEIKKINEN, S. & LEVONEN, A.-L. 2016. The Effects of Sequence Variation on Genome-wide NRF2 Binding—New Target Genes and Regulatory SNPs. *Nucleic Acids Research,* 44**,** 1760-1775.
KUWANA, T., MACKEY, M. R., PERKINS, G., ELLISMAN, M. H., LATTERICH, M., SCHNEITER, R., GREEN, D. R. & NEWMEYER, D. D. 2002. Bid, Bax, and Lipids Cooperate to Form Supramolecular Openings in the Outer Mitochondrial Membrane. *Cell,* 111**,** 331-342.
KWIATKOWSKI, T. J., BOSCO, D. A., LECLERC, A. L., TAMRAZIAN, E., VANDERBURG, C. R., RUSS, C., DAVIS, A., GILCHRIST, J., KASARSKIS, E. J., MUNSAT, T., VALDMANIS, P., ROULEAU, G. A., HOSLER, B. A., CORTELLI, P., DE JONG, P. J., YOSHINAGA, Y., HAINES, J. L., PERICAK-VANCE, M. A., YAN, J., TICOZZI, N., SIDDIQUE, T., MCKENNA-YASEK, D., SAPP, P. C., HORVITZ, H. R., LANDERS, J. E. & BROWN, R. H. 2009. Mutations in the FUS/TLS Gene on Chromosome 16 Cause Familial Amyotrophic Lateral Sclerosis. *Science,* 323**,** 1205-1208.
KWON, H. J., HEO, J. Y., SHIM, J. H., PARK, J. H., SEO, K. S., RYU, M. J., HAN, J. S., SHONG, M., SON, J. H. & KWEON, G. R. 2011. DJ-1 mediates paraquat-induced dopaminergic neuronal cell death. *Toxicology Letters,* 202**,** 85-92.
LAGIER-TOURENNE, C., POLYMENIDOU, M. & CLEVELAND, D. W. 2010. TDP-43 and FUS/TLS: emerging roles in RNA processing and neurodegeneration. *Human Molecular Genetics,* 19**,** R46-R64.
LAMMEL, S., STEINBERG, ELIZABETH E., FÖLDY, C., WALL, NICHOLAS R., BEIER, K., LUO, L. & MALENKA, ROBERT C. 2015. Diversity of Transgenic Mouse Models for Selective Targeting of Midbrain Dopamine Neurons. *Neuron,* 85**,** 429-438.
LANGSTON, J., BALLARD, P., TETRUD, J. & IRWIN, I. 1983. Chronic Parkinsonism in humans due to a product of meperidine-analog synthesis. *Science,* 219**,** 979-980.
LANSBURY, P. T. 1996. A Reductionist View of Alzheimer's Disease. *Accounts of Chemical Research,* 29**,** 317-321.
LAZAROU, M., SLITER, D. A., KANE, L. A., SARRAF, S. A., WANG, C., BURMAN, J. L., SIDERIS, D. P., FOGEL, A. I. & YOULE, R. J. 2015. The ubiquitin kinase PINK1 recruits autophagy receptors to induce mitophagy. *Nature,* 524**,** 309-314.
LEMASTERS, J. J. 2005. Selective Mitochondrial Autophagy, or Mitophagy, as a Targeted Defense Against Oxidative Stress, Mitochondrial Dysfunction, and Aging. *Rejuvenation Research,* 8**,** 3-5.
LESAGE, S., DROUET, V., MAJOUNIE, E., DERAMECOURT, V., JACOUPY, M., NICOLAS, A., CORMIER-DEQUAIRE, F., HASSOUN, SIDI M., PUJOL, C., CIURA, S., ERPAPAZOGLOU, Z., USENKO, T., MAURAGE, C.-A., SAHBATOU, M., LIEBAU, S., DING, J., BILGIC, B., EMRE, M., ERGINEL-UNALTUNA, N., GUVEN, G., TISON, F., TRANCHANT, C., VIDAILHET, M., CORVOL, J.-C., KRACK, P., LEUTENEGGER, A.-L., NALLS, MICHAEL A., HERNANDEZ, DENA G., HEUTINK, P., GIBBS, J. R., HARDY, J., WOOD, NICHOLAS W., GASSER, T., DURR, A., DELEUZE, J.-F., TAZIR, M., DESTÉE,

A., LOHMANN, E., KABASHI, E., SINGLETON, A., CORTI, O., BRICE, A., AGID, Y., ANHEIM, M., BONNET, A.-M., BORG, M., BROUSSOLLE, E., DAMIER, P., DÜRR, A., DURIF, F., KLEBE, S., MARTINEZ, M., POLLAK, P., RASCOL, O., VÉRIN, M., VIALLET, F., CORVOL, JEAN C., AREPALLI, S., BARKER, ROGER A., BEN-SHLOMO, Y., BERG, D., BETTELLA, F., BHATIA, K., DE BIE, ROB M. A., BIFFI, A., BLOEM, BASTIAAN R., BOCHDANOVITS, Z., BONIN, M., BRAS, JOSE M., BROCKMANN, K., BROOKS, J., BURN, DAVID J., CHARLESWORTH, G., CHEN, H., CHINNERY, PATRICK F., CHONG, S., CLARKE, CARL E., COOKSON, MARK R., COUNSELL, C., DARTIGUES, J.-F., DELOUKAS, P., DEUSCHL, G., DEXTER, DAVID T., VAN DIJK, KARIN D., DILLMAN, A., DONG, J., DURIF, F., EDKINS, S., ESCOTT-PRICE, V., EVANS, JONATHAN R., FOLTYNIE, T., GAO, J., GARDNER, M., GOATE, A., GRAY, E., GUERREIRO, R., HARRIS, C., VAN HILTEN, JACOBUS J., HOFMAN, A., HOLLENBECK, A., et al. 2016. Loss of VPS13C Function in Autosomal-Recessive Parkinsonism Causes Mitochondrial Dysfunction and Increases PINK1/Parkin-Dependent Mitophagy. *The American Journal of Human Genetics,* 98**,** 500-513.

LEV, N., ICKOWICZ, D., MELAMED, E. & OFFEN, D. 2008. Oxidative insults induce DJ-1 upregulation and redistribution: Implications for neuroprotection. *NeuroToxicology,* 29**,** 397-405.

LI, H. M., NIKI, T., TAIRA, T., IGUCHI-ARIGA, S. M. M. & ARIGA, H. 2005. Association of DJ-1 with chaperones and enhanced association and colocalization with mitochondrial Hsp70 by oxidative stress. *Free Radical Research,* 39**,** 1091-1099.

LI, W.-W., YANG, R., GUO, J.-C., REN, H.-M., ZHA, X.-L., CHENG, J.-S. & CAI, D.-F. 2007. Localization of α-synuclein to mitochondria within midbrain of mice. *NeuroReport,* 18**,** 1543-1546 10.1097/WNR.0b013e3282f03db4.

LI, Y., LI, W., LIU, C., YAN, M., RAMAN, I., DU, Y., FANG, X., ZHOU, X. J., MOHAN, C. & LI, Q.-Z. 2014. Delivering Oxidation Resistance-1 (OXR1) to Mouse Kidney by Genetic Modified Mesenchymal Stem Cells Exhibited Enhanced Protection against Nephrotoxic Serum Induced Renal Injury and Lupus Nephritis. *Journal of stem cell research & therapy,* 4**,** 231.

LI, Y. R., KING, O. D., SHORTER, J. & GITLER, A. D. 2013. Stress granules as crucibles of ALS pathogenesis. *The Journal of Cell Biology,* 201**,** 361-372.

LIN, M. T. & BEAL, M. F. 2006. Mitochondrial dysfunction and oxidative stress in neurodegenerative diseases. *Nature,* 443**,** 787-795.

LIN, M. T., CANTUTI-CASTELVETRI, I., ZHENG, K., JACKSON, K. E., TAN, Y. B., ARZBERGER, T., LEES, A. J., BETENSKY, R. A., BEAL, M. F. & SIMON, D. K. 2012. Somatic mitochondrial DNA mutations in early parkinson and incidental lewy body disease. *Annals of Neurology,* 71**,** 850-854.

LINDQUIST, S. 1981. Regulation of protein synthesis during heat shock. *Nature,* 293**,** 311-314.

LIU, J., LILLO, C., JONSSON, P. A., VELDE, C. V., WARD, C. M., MILLER, T. M., SUBRAMANIAM, J. R., ROTHSTEIN, J. D., MARKLUND, S., ANDERSEN, P. M., BRÄNNSTRÖM, T., GREDAL, O., WONG, P. C., WILLIAMS, D. S. & CLEVELAND, D. W. 2004. Toxicity of Familial ALS-Linked SOD1 Mutants from Selective Recruitment to Spinal Mitochondria. *Neuron,* 43**,** 5-17.

LIU, K. X., EDWARDS, B., LEE, S., FINELLI, M. J., DAVIES, B., DAVIES, K. E. & OLIVER, P. L. 2015a. Neuron-specific antioxidant OXR1 extends survival of a mouse model of amyotrophic lateral sclerosis. *Brain,* 138**,** 1167-1181.

LIU, K. X., EDWARDS, B., LEE, S., FINELLI, M. J., DAVIES, B., DAVIES, K. E. & OLIVER, P. L. 2015b. Neuron-specific antioxidant OXR1 extends survival of a mouse model of amyotrophic lateral sclerosis. *Brain*.

LIU, W., ACÍN-PERÉZ, R., GEGHMAN, K. D., MANFREDI, G., LU, B. & LI, C. 2011. Pink1 regulates the oxidative phosphorylation machinery via mitochondrial fission. *Proceedings of the National Academy of Sciences,* 108**,** 12920-12924.

LU, C., ZHANG, D., WHITEMAN, M. & ARMSTRONG, J. S. 2007. Is Antioxidant Potential of the Mitochondrial Targeted Ubiquinone Derivative MitoQ Conserved in Cells Lacking mtDNA? *Antioxidants & Redox Signaling,* 10**,** 651-660.

LU, J., DUAN, W., GUO, Y., JIANG, H., LI, Z., HUANG, J., HONG, K. & LI, C. 2012. Mitochondrial dysfunction in human TDP-43 transfected NSC34 cell lines and the protective effect of dimethoxy curcumin. *Brain Research Bulletin,* 89**,** 185-190.

LUSTBADER, J. W., CIRILLI, M., LIN, C., XU, H. W., TAKUMA, K., WANG, N., CASPERSEN, C., CHEN, X., POLLAK, S., CHANEY, M., TRINCHESE, F., LIU, S., GUNN-MOORE, F., LUE, L.-F., WALKER, D. G., KUPPUSAMY, P., ZEWIER, Z. L., ARANCIO, O., STERN, D., YAN, S. S. & WU, H. 2004. ABAD Directly Links Aß to Mitochondrial Toxicity in Alzheimer's Disease. *Science,* 304**,** 448-452.

MAGRANÉ, J., CORTEZ, C., GAN, W.-B. & MANFREDI, G. 2014. Abnormal mitochondrial transport and morphology are common pathological denominators in SOD1 and TDP43 ALS mouse models. *Human Molecular Genetics,* 23**,** 1413-1424.

MAITA, C., MAITA, H., IGUCHI-ARIGA, S. M. M. & ARIGA, H. 2013. Monomer DJ-1 and Its N-Terminal Sequence Are Necessary for Mitochondrial Localization of DJ-1 Mutants. *PLoS ONE,* 8**,** e54087.

MAKI, H. 2002. Origins of Spontaneous Mutations: Specificity and Directionality of Base-Substitution, Frameshift, and Sequence-Substitution Mutageneses. *Annual Review of Genetics,* 36**,** 279-303.

MANCZAK, M., MAO, P., CALKINS, M., CORNEA, A., ARUBALA, R. P., MURPHY, M. P., SZETO, H. H., PARK, B. & REDDY, P. H. 2010. Mitochondria-targeted antioxidants protect against Abeta toxicity in Alzheimer's disease neurons. *Journal of Alzheimer's disease : JAD,* 20**,** S609-S631.

MANN VM, C. J., DANIEL SE, SRAI K, JENNER P, MARSDEN CD, SCHAPIRA AH. 1994. Complex I, iron, and ferritin in Parkinson's disease substantia nigra. *Annals of Neurology,* 36**,** 876-881.

MARONGIU, R., SPENCER, B., CREWS, L., ADAME, A., PATRICK, C., TREJO, M., DALLAPICCOLA, B., VALENTE, E. M. & MASLIAH, E. 2009. Mutant Pink1 induces mitochondrial dysfunction in a neuronal cell model of Parkinson's disease by disturbing calcium flux. *Journal of Neurochemistry,* 108**,** 1561-1574.

MARRIAGE, B. J., CLANDININ, M. T., MACDONALD, I. M. & GLERUM, D. M. 2004. Cofactor treatment improves ATP synthetic capacity in patients with oxidative phosphorylation disorders. *Molecular Genetics and Metabolism,* 81**,** 263-272.

MATSUDA, N., SATO, S., SHIBA, K., OKATSU, K., SAISHO, K., GAUTIER, C. A., SOU, Y.-S., SAIKI, S., KAWAJIRI, S., SATO, F., KIMURA, M., KOMATSU, M., HATTORI, N. & TANAKA, K. 2010. PINK1 stabilized by mitochondrial depolarization recruits Parkin to damaged mitochondria and activates latent Parkin for mitophagy. *The Journal of Cell Biology,* 189**,** 211-221.

MATTHEWS, R. T., YANG, L., BROWNE, S., BAIK, M. & BEAL, M. F. 1998. Coenzyme Q10 administration increases brain mitochondrial concentrations and exerts

neuroprotective effects. *Proceedings of the National Academy of Sciences,* 95**,** 8892-8897.
MATTIAZZI, M., D'AURELIO, M., GAJEWSKI, C. D., MARTUSHOVA, K., KIAEI, M., BEAL, M. F. & MANFREDI, G. 2002. Mutated Human SOD1 Causes Dysfunction of Oxidative Phosphorylation in Mitochondria of Transgenic Mice. *Journal of Biological Chemistry,* 277**,** 29626-29633.
MAZZONI, P., SHABBOTT, B. & CORTÉS, J. C. 2012. Motor Control Abnormalities in Parkinson's Disease. *Cold Spring Harbor Perspectives in Medicine,* 2**,** a009282.
MCLAIN, A. L., SZWEDA, P. A. & SZWEDA, L. I. 2011. α-Ketoglutarate dehydrogenase: A mitochondrial redox sensor. *Free Radical Research,* 45**,** 29-36.
MEEUSEN, S., DEVAY, R., BLOCK, J., CASSIDY-STONE, A., WAYSON, S., MCCAFFERY, J. M. & NUNNARI, J. 2006. Mitochondrial Inner-Membrane Fusion and Crista Maintenance Requires the Dynamin-Related GTPase Mgm1. *Cell,* 127**,** 383-395.
MENKE, D. B. 2013. Engineering subtle targeted mutations into the mouse genome. *genesis,* 51**,** 605-618.
MILANI, P., AMBROSI, G., GAMMOH, O., BLANDINI, F. & CEREDA, C. 2013. SOD1 and DJ-1 Converge at Nrf2 Pathway: A Clue for Antioxidant Therapeutic Potential in Neurodegeneration. *Oxidative Medicine and Cellular Longevity,* 2013**,** 1-12.
MISHRA, P. & CHAN, D. C. 2014. Mitochondrial dynamics and inheritance during cell division, development and disease. *Nat Rev Mol Cell Biol,* 15**,** 634-646.
MOON, H. E. & PAEK, S. H. 2015. Mitochondrial Dysfunction in Parkinson's Disease. *Experimental Neurobiology,* 24**,** 103-116.
MOREIRA, P. I., ZHU, X., WANG, X., LEE, H.-G., NUNOMURA, A., PETERSEN, R. B., PERRY, G. & SMITH, M. A. 2010. Mitochondria: A therapeutic target in neurodegeneration. *Biochimica et Biophysica Acta (BBA) - Molecular Basis of Disease,* 1802**,** 212-220.
MORTIBOYS, H., THOMAS, K. J., KOOPMAN, W. J. H., KLAFFKE, S., ABOU-SLEIMAN, P., OLPIN, S., WOOD, N. W., WILLEMS, P. H. G. M., SMEITINK, J. A. M., COOKSON, M. R. & BANDMANN, O. 2008. Mitochondrial function and morphology are impaired in parkin-mutant fibroblasts. *Annals of Neurology,* 64**,** 555-565.
MUCHA, B. E., HENNEKAM, R. C. M., SISODIYA, S. & CAMPEAU, P. M. 2015. TBC1D24-Related Disorders. *In:* PAGON, R. A., ADAM, M. P., ARDINGER, H. H., WALLACE, S. E., AMEMIYA, A., BEAN, L. J. H., BIRD, T. D., FONG, C. T., MEFFORD, H. C., SMITH, R. J. H. & STEPHENS, K. (eds.) *GeneReviews [Internet].* Seattle: University of Washington, http://www.ncbi.nlm.nih.gov/books/NBK274566/.
MULLER, F. L., LIU, Y. & VAN REMMEN, H. 2004. Complex III Releases Superoxide to Both Sides of the Inner Mitochondrial Membrane. *Journal of Biological Chemistry,* 279**,** 49064-49073.
MUNROE, R. J., BERGSTROM, R. A., Y ZHENG, Q., LIBBY, B., SMITH, R., JOHN, S. W. M., SCHIMENTI, K. J., BROWNING, V. L. & SCHIMENTI, J. C. 2000. Mouse mutants from chemically mutagenized embryonic stem cells. *Nat Genet,* 24**,** 318-321.
MUONA, M., BERKOVIC, S. F., DIBBENS, L. M., OLIVER, K. L., MALJEVIC, S., BAYLY, M. A., JOENSUU, T., CANAFOGLIA, L., FRANCESCHETTI, S., MICHELUCCI, R., MARKKINEN, S., HERON, S. E., HILDEBRAND, M. S., ANDERMANN, E., ANDERMANN, F., GAMBARDELLA, A., TINUPER, P., LICCHETTA, L., SCHEFFER, I. E., CRISCUOLO, C., FILLA, A., FERLAZZO, E., AHMAD, J., AHMAD, A., BAYKAN, B., SAID, E., TOPCU, M., RIGUZZI, P., KING, M. D., OZKARA, C., ANDRADE, D. M., ENGELSEN, B. A.,

CRESPEL, A., LINDENAU, M., LOHMANN, E., SALETTI, V., MASSANO, J., PRIVITERA, M., ESPAY, A. J., KAUFFMANN, B., DUCHOWNY, M., MOLLER, R. S., STRAUSSBERG, R., AFAWI, Z., BEN-ZEEV, B., SAMOCHA, K. E., DALY, M. J., PETROU, S., LERCHE, H., PALOTIE, A. & LEHESJOKI, A.-E. 2015. A recurrent de novo mutation in KCNC1 causes progressive myoclonus epilepsy. *Nat Genet,* 47**,** 39-46.

MURPHY, K. & VOLKERT, M. 2012. Structural/functional analysis of the human OXR1 protein: identification of exon 8 as the anti-oxidant encoding function. *BMC Molecular Biology,* 13**,** 26.

MUTHANE, U., RAMSAY, K. A., JIANG, H., JACKSON-LEWIS, V., DONALDSON, D., FERNANDO, S., FERREIRA, M. & PRZEDBORSKI, S. 1994. Differences in Nigral Neuron Number and Sensitivity to 1-Methyl-4-phenyl-1,2,3,6-tetrahydropyridine in C57/bl and CD-1 Mice. *Experimental Neurology,* 126**,** 195-204.

MUTIHAC, R., ALEGRE-ABARRATEGUI, J., GORDON, D., FARRIMOND, L., YAMASAKI-MANN, M., TALBOT, K. & WADE-MARTINS, R. 2015. TARDBP pathogenic mutations increase cytoplasmic translocation of TDP-43 and cause reduction of endoplasmic reticulum Ca2 + signaling in motor neurons. *Neurobiology of Disease,* 75**,** 64-77.

MUYDERMAN, H. & CHEN, T. 2014. Mitochondrial dysfunction in amyotrophic lateral sclerosis – a valid pharmacological target? *British Journal of Pharmacology,* 171**,** 2191-2205.

NARENDRA, D., TANAKA, A., SUEN, D.-F. & YOULE, R. J. 2008. Parkin is recruited selectively to impaired mitochondria and promotes their autophagy. *The Journal of Cell Biology,* 183**,** 795-803.

NARENDRA, D. P., JIN, S. M., TANAKA, A., SUEN, D.-F., GAUTIER, C. A., SHEN, J., COOKSON, M. R. & YOULE, R. J. 2010. PINK1 Is Selectively Stabilized on Impaired Mitochondria to Activate Parkin. *PLoS Biol,* 8**,** e1000298.

NATHALY RIGOGLIO, N., MENDES SILVA, M. V., PAVANELO JUNIOR, V., FERREIRA LIMA, S. A., LUIZ NOGUEIRA, J., AVANCINI FERNANDES, R. & MIGLINO, M. A. 2012. Ultrastructural morphometric analysis by transmission electron microscopy associated with stereology methods. *Current Microscopy Contributions to Advances in Science and Technology***,** 309-315.

NEUMANN, M., SAMPATHU, D. M., KWONG, L. K., TRUAX, A. C., MICSENYI, M. C., CHOU, T. T., BRUCE, J., SCHUCK, T., GROSSMAN, M., CLARK, C. M., MCCLUSKEY, L. F., MILLER, B. L., MASLIAH, E., MACKENZIE, I. R., FELDMAN, H., FEIDEN, W., KRETZSCHMAR, H. A., TROJANOWSKI, J. Q. & LEE, V. M.-Y. 2006. Ubiquitinated TDP-43 in Frontotemporal Lobar Degeneration and Amyotrophic Lateral Sclerosis. *Science,* 314**,** 130-133.

NICKLAS, W., VYAS, I. & HEIKKILA, R. E. 1985. Inhibition of NADH-linked oxidation in brain mitochondria by 1-methyl-4-phenyl-pyridine, a metabolite of the neurotoxin, 1-methyl-4-phenyl-1,2,5,6-tetrahydropyridine. *Life Sciences,* 36**,** 2503-2508.

NOLAN, P. M., PETERS, J., STRIVENS, M., ROGERS, D., HAGAN, J., SPURR, N., GRAY, I. C., VIZOR, L., BROOKER, D., WHITEHILL, E., WASHBOURNE, R., HOUGH, T., GREENAWAY, S., HEWITT, M., LIU, X., MCCORMACK, S., PICKFORD, K., SELLEY, R., WELLS, C., TYMOWSKA-LALANNE, Z., ROBY, P., GLENISTER, P., THORNTON, C., THAUNG, C., STEVENSON, J.-A., ARKELL, R., MBURU, P., HARDISTY, R., KIERNAN, A., ERVEN, A., STEEL, K. P., VOEGELING, S., GUENET, J.-L., NICKOLS, C., SADRI, R.,

NAASE, M., ISAACS, A., DAVIES, K., BROWNE, M., FISHER, E. M. C., MARTIN, J., RASTAN, S., BROWN, S. D. M. & HUNTER, J. 2000. A systematic, genome-wide, phenotype-driven mutagenesis programme for gene function studies in the mouse. *Nat Genet,* 25**,** 440-443.

O'DONNELL, E. & LYNCH, M. A. 1998. Dietary antioxidant supplementation reverses age-related neuronal changes. *Neurobiology of Aging,* 19**,** 461-467.

OH-ISHI, S., KIZAKI, T., YAMASHITA, H., NAGATA, N., SUZUKI, K., TANIGUCHI, N. & OHNO, H. 1995. Alterations of superoxide dismutase iso-enzyme activity, content, and mRNA expression with aging in rat skeletal muscle. *Mechanisms of Ageing and Development,* 84**,** 65-76.

OHTA, S. & KAGAWA, Y. 1986. Human F1-ATPase: molecular cloning of cDNA for the beta subunit. *Journal of Biochemistry,* 99**,** 135-141.

OKADO-MATSUMOTO, A. & FRIDOVICH, I. 2001. Subcellular Distribution of Superoxide Dismutases (SOD) in Rat Liver: Cu,Zn-SOD IN MITOCHONDRIA. *Journal of Biological Chemistry,* 276**,** 38388-38393.

OKATSU, K., KIMURA, M., OKA, T., TANAKA, K. & MATSUDA, N. 2015. Unconventional PINK1 localization to the outer membrane of depolarized mitochondria drives Parkin recruitment. *Journal of Cell Science,* 128**,** 964-978.

OKOUCHI, M., EKSHYYAN, O., MARACINE, M. & AW, T. Y. 2007. Neuronal Apoptosis in Neurodegeneration. *Antioxidants & Redox Signaling,* 9**,** 1059-1096.

OLD, S. L. & JOHNSON, M. A. 1989. Methods of microphotometric assay of succinate dehydrogenase and cytochromec oxidase activities for use on human skeletal muscle. *The Histochemical Journal,* 21**,** 545-555.

OLIVER, P. L. & DAVIES, K. E. 2012. New insights into behaviour using mouse ENU mutagenesis. *Human Molecular Genetics,* 21**,** R72-R81.

OLIVER, P. L., FINELLI, M. J., EDWARDS, B., BITOUN, E., BUTTS, D. L., BECKER, E. B. E., CHEESEMAN, M. T., DAVIES, B. & DAVIES, K. E. 2011. Oxr1 Is Essential for Protection against Oxidative Stress-Induced Neurodegeneration. *PLoS Genet,* 7**,** e1002338.

OLZMANN, J. A., BROWN, K., WILKINSON, K. D., REES, H. D., HUAI, Q., KE, H., LEVEY, A. I., LI, L. & CHIN, L.-S. 2004. Familial Parkinson's Disease-associated L166P Mutation Disrupts DJ-1 Protein Folding and Function. *Journal of Biological Chemistry,* 279**,** 8506-8515.

ORRENIUS, S., GOGVADZE, V. & ZHIVOTOVSKY, B. 2007. Mitochondrial Oxidative Stress: Implications for Cell Death. *Annual Review of Pharmacology and Toxicology,* 47**,** 143-183.

OTERA, H., ISHIHARA, N. & MIHARA, K. 2013. New insights into the function and regulation of mitochondrial fission. *Biochimica et Biophysica Acta (BBA) - Molecular Cell Research,* 1833**,** 1256-1268.

OYEWOLE, A. O. & BIRCH-MACHIN, M. A. 2015. Mitochondria-targeted antioxidants. *The FASEB Journal,* 29**,** 4766-4771.

PALACINO, J. J., SAGI, D., GOLDBERG, M. S., KRAUSS, S., MOTZ, C., WACKER, M., KLOSE, J. & SHEN, J. 2004. Mitochondrial Dysfunction and Oxidative Damage in parkin-deficient Mice. *Journal of Biological Chemistry,* 279**,** 18614-18622.

PALMIERI, F. 2004. The mitochondrial transporter family (SLC25): physiological and pathological implications. *Pflügers Archiv,* 447**,** 689-709.

PANKRATZ, N. & FOROUD, T. 2007. Genetics of Parkinson disease. *Genet Med,* 9**,** 801-811.

PARIHAR, M. S., PARIHAR, A., FUJITA, M., HASHIMOTO, M. & GHAFOURIFAR, P. 2008. Mitochondrial association of alpha-synuclein causes oxidative stress. *Cellular and Molecular Life Sciences,* 65**,** 1272-1284.

PARKER, W. D., BOYSON, S. J. & PARKS, J. K. 1989. Abnormalities of the electron transport chain in idiopathic parkinson's disease. *Annals of Neurology,* 26**,** 719-723.

PAXINOS, G. & FRANKLIN, K. B. J. 1997. *The Mouse Brain in Stereotaxic Coordinates.,* San Diego, Academic Press.

PAXINOU, E., CHEN, Q., WEISSE, M., GIASSON, B. I., NORRIS, E. H., RUETER, S. M., TROJANOWSKI, J. Q., LEE, V. M.-Y. & ISCHIROPOULOS, H. 2001. Induction of α-Synuclein Aggregation by Intracellular Nitrative Insult. *The Journal of Neuroscience,* 21**,** 8053-8061.

PEREVERZEV, M. O., VYGODINA, T. V., KONSTANTINOV, A. A. & SKULACHEV, V. P. 2003. Cytochrome c, an ideal antioxidant. *Biochemical Society Transactions,* 31**,** 1312-1315.

PERRY, S. W., NORMAN, J. P., BARBIERI, J., BROWN, E. B. & GELBARD, H. A. 2011. Mitochondrial membrane potential probes and the proton gradient: a practical usage guide. *BioTechniques,* 50**,** 98-115.

PETSALAKI, E. I., BAGOS, P. G., LITOU, Z. I. & HAMODRAKAS, S. J. 2006. PredSL: A Tool for the N-terminal Sequence-based Prediction of Protein Subcellular Localization. *Genomics, Proteomics & Bioinformatics,* 4**,** 48-55.

PHAM, N.-A., RICHARDSON, T., CAMERON, J., CHUE, B. & ROBINSON, B. H. 2004. Altered Mitochondrial Structure and Motion Dynamics in Living Cells with Energy Metabolism Defects Revealed by Real Time Microscope Imaging. *Microscopy and Microanalysis,* 10**,** 247-260.

PHANG, J. M., LIU, W. & ZABIRNYK, O. 2010. Proline Metabolism and Microenvironmental Stress. *Annual Review of Nutrition,* 30**,** 441-463.

PLATT, RANDALL J., CHEN, S., ZHOU, Y., YIM, MICHAEL J., SWIECH, L., KEMPTON, HANNAH R., DAHLMAN, JAMES E., PARNAS, O., EISENHAURE, THOMAS M., JOVANOVIC, M., GRAHAM, DANIEL B., JHUNJHUNWALA, S., HEIDENREICH, M., XAVIER, RAMNIK J., LANGER, R., ANDERSON, DANIEL G., HACOHEN, N., REGEV, A., FENG, G., SHARP, PHILLIP A. & ZHANG, F. 2014. CRISPR-Cas9 Knockin Mice for Genome Editing and Cancer Modeling. *Cell,* 159**,** 440-455.

PORTERA-CAILLIAU, C., HEDREEN, J. C., PRICE, D. L. & KOLIATSOS, V. E. 1995. Evidence for apoptotic cell death in Huntington disease and excitotoxic animal models. *J Neurosci.,* 15**,** 3775-3787.

QI, X., DISATNIK, M.-H., SHEN, N., SOBEL, R. A. & MOCHLY-ROSEN, D. 2011. Aberrant mitochondrial fission in neurons induced by protein kinase Cδ under oxidative stress conditions in vivo. *Molecular Biology of the Cell,* 22**,** 256-265.

QUWAILID, M. M., HUGILL, A., DEAR, N., VIZOR, L., WELLS, S., HORNER, E., FULLER, S., WEEDON, J., MCMATH, H., WOODMAN, P., EDWARDS, D., CAMPBELL, D., RODGER, S., CAREY, J., ROBERTS, A., GLENISTER, P., LALANNE, Z., PARKINSON, N., COGHILL, E. L., MCKEONE, R., COX, S., WILLAN, J., GREENFIELD, A., KEAYS, D., BRADY, S., SPURR, N., GRAY, I., HUNTER, J., BROWN, S. D. M. & COX, R. D. 2004.

A gene-driven ENU-based approach to generating an allelic series in any gene. *Mammalian Genome,* 15**,** 585-591.

RADAK, Z., ZHAO, Z., GOTO, S. & KOLTAI, E. 2011. Age-associated neurodegeneration and oxidative damage to lipids, proteins and DNA. *Molecular Aspects of Medicine,* 32**,** 305-315.

RAGAN, C. I., WILSON, M. T., DARLEY-USMAR & V. M.; LOWE, P. N. 1987. Subfractionation of mitochondria, and isolation of the proteins of oxidative phosphorylation, in mitochondria, a practical approach. *In:* DARLEY-USMAR V.M., RICKWOOD D. & M.T., W. (eds.) *Mitochondria: a practical approach.* Oxford: IRL Press.

RAMBOLD, A. S., KOSTELECKY, B., ELIA, N. & LIPPINCOTT-SCHWARTZ, J. 2011. Tubular network formation protects mitochondria from autophagosomal degradation during nutrient starvation. *Proceedings of the National Academy of Sciences of the United States of America,* 108**,** 10190-10195.

RAMDZAN, Y. M., POLLING, S., CHIA, C. P. Z., NG, I. H. W., ORMSBY, A. R., CROFT, N. P., PURCELL, A. W., BOGOYEVITCH, M. A., NG, D. C. H., GLEESON, P. A. & HATTERS, D. M. 2012. Tracking protein aggregation and mislocalization in cells with flow cytometry. *Nat Meth,* 9**,** 467-470.

REICHERT, A. S. & NEUPERT, W. 2002. Contact sites between the outer and inner membrane of mitochondria—role in protein transport. *Biochimica et Biophysica Acta (BBA) - Molecular Cell Research,* 1592**,** 41-49.

RICHTER-DENNERLEIN, R., KORWITZ, A., HAAG, M., TATSUTA, T., DARGAZANLI, S., BAKER, M., DECKER, T., LAMKEMEYER, T., RUGARLI, ELENA I. & LANGER, T. 2014. DNAJC19, a Mitochondrial Cochaperone Associated with Cardiomyopathy, Forms a Complex with Prohibitins to Regulate Cardiolipin Remodeling. *Cell Metabolism,* 20**,** 158-171.

RIZZUTO, R., SIMPSON, A. W. M., BRINI, M. & POZZAN, T. 1992. Rapid changes of mitochondrial Ca2+ revealed by specifically targeted recombinant aequorin. *Nature,* 358**,** 325-327.

ROBINSON, D. L., VENTON, B. J., HEIEN, M. L. A. V. & WIGHTMAN, R. M. 2003. Detecting Subsecond Dopamine Release with Fast-Scan Cyclic Voltammetry in Vivo. *Clinical Chemistry,* 49**,** 1763-1773.

ROCKSTROH, M., MÜLLER, S., JENDE, C., KERZHNER, A., VON BERGEN, M. & TOMM, J. M. 2010. Cell fractionation - an important tool for compartment proteomics. *Journal of Integrated Omics,* 1**,** 135-143.

ROSEN, D. R., SIDDIQUE, T., PATTERSON, D., FIGLEWICZ, D. A., SAPP, P., HENTATI, A., DONALDSON, D., GOTO, J., O'REGAN, J. P., DENG, H.-X., RAHMANI, Z., KRIZUS, A., MCKENNA-YASEK, D., CAYABYAB, A., GASTON, S. M., BERGER, R., TANZI, R. E., HALPERIN, J. J., HERZFELDT, B., VAN DEN BERGH, R., HUNG, W.-Y., BIRD, T., DENG, G., MULDER, D. W., SMYTH, C., LAING, N. G., SORIANO, E., PERICAK-VANCE, M. A., HAINES, J., ROULEAU, G. A., GUSELLA, J. S., HORVITZ, H. R. & BROWN, R. H. 1993. Mutations in Cu/Zn superoxide dismutase gene are associated with familial amyotrophic lateral sclerosis. *Nature,* 362**,** 59-62.

ROSS, J. M. 2011. Visualization of Mitochondrial Respiratory Function using Cytochrome C Oxidase / Succinate Dehydrogenase (COX/SDH) Double-labeling Histochemistry. *Journal of Visualized Experiments : JoVE***,** 3266.

ROWE, L. A., DEGTYAREVA, N. & DOETSCH, P. W. 2008. DNA damage-induced reactive oxygen species (ROS) stress response in Saccharomyces cerevisiae. *Free Radical Biology and Medicine,* 45**,** 1167-1177.

RYAN, B. J., HOEK, S., FON, E. A. & WADE-MARTINS, R. 2015. Mitochondrial dysfunction and mitophagy in Parkinson's: from familial to sporadic disease. *Trends in Biochemical Sciences,* 40**,** 200-210.

SALAZAR, J. J. & VAN HOUTEN, B. 1997. Preferential mitochondrial DNA injury caused by glucose oxidase as a steady generator of hydrogen peroxide in human fibroblasts. *Mutation Research/DNA Repair,* 385**,** 139-149.

SAMII, A., NUTT, J. G. & RANSOM, B. R. 2004. Parkinson's disease. *The Lancet,* 363**,** 1783-1793.

SANADA, Y., ASAI, S., IKEMOTO, A., MORIWAKI, T., NAKAMURA, N., MIYAJI, M. & ZHANG-AKIYAMA, Q.-M. 2014. Oxidation resistance 1 is essential for protection against oxidative stress and participates in the regulation of aging in Caenorhabditis elegans. *Free Radical Research,* 48**,** 919-928.

SARASTE, M. 1999. Oxidative Phosphorylation at the fin de siècle. *Science,* 283**,** 1488-1493.

SAVITSKY, K., BAR-SHIRA, A., GILAD, S., ROTMAN, G., ZIV, Y., VANAGAITE, L., TAGLE, D., SMITH, S., UZIEL, T., SFEZ, S. & AL., E. 1995. A single ataxia telangiectasia gene with a product similar to PI-3 kinase. *Science,* 268**,** 1749-1753.

SAWADA, M. & CARLSON, J. C. 1987. Changes in superoxide radical and lipid peroxide formation in the brain, heart and liver during the lifetime of the rat. *Mechanisms of Ageing and Development,* 41**,** 125-137.

SAXENA, S. & CARONI, P. 2011. Selective Neuronal Vulnerability in Neurodegenerative Diseases: from Stressor Thresholds to Degeneration. *Neuron,* 71**,** 35-48.

SCHAPIRA, A. H. V., COOPER, J. M., DEXTER, D., JENNER, P., CLARK, J. B. & MARSDEN, C. D. 1989. Mitochondrial complex I deficiency in Parkinson's disease. *The Lancet,* 333**,** 1269.

SCHLEIFF, E. & TURNBULL, J. L. 1998. Functional and Structural Properties of the Mitochondrial Outer Membrane Receptor Tom20. *Biochemistry,* 37**,** 13043-13051.

SCHMIDT, O., PFANNER, N. & MEISINGER, C. 2010. Mitochondrial protein import: from proteomics to functional mechanisms. *Nat Rev Mol Cell Biol,* 11**,** 655-667.

SCHOCH, S., DEÁK, F., KÖNIGSTORFER, A., MOZHAYEVA, M., SARA, Y., SÜDHOF, T. C. & KAVALALI, E. T. 2001. SNARE Function Analyzed in Synaptobrevin/VAMP Knockout Mice. *Science,* 294**,** 1117-1122.

SCHRINER, S. E., LINFORD, N. J., MARTIN, G. M., TREUTING, P., OGBURN, C. E., EMOND, M., COSKUN, P. E., LADIGES, W., WOLF, N., VAN REMMEN, H., WALLACE, D. C. & RABINOVITCH, P. S. 2005. Extension of Murine Life Span by Overexpression of Catalase Targeted to Mitochondria. *Science,* 308**,** 1909-1911.

SEDELIS, M., SCHWARTING, R. K. W. & HUSTON, J. P. 2001. Behavioral phenotyping of the MPTP mouse model of Parkinson's disease. *Behavioural Brain Research,* 125**,** 109-125.

SENIOR, S. L., NINKINA, N., DEACON, R., BANNERMAN, D., BUCHMAN, V. L., CRAGG, S. J. & WADE-MARTINS, R. 2008. Increased striatal dopamine release and hyperdopaminergic-like behaviour in mice lacking both alpha-synuclein and gamma-synuclein. *The European journal of neuroscience,* 27**,** 947-957.

SHAO, W., HALACHMI, S. & BROWN, M. 2002. ERAP140, a Conserved Tissue-Specific Nuclear Receptor Coactivator. *Molecular and Cellular Biology,* 22**,** 3358-3372.
SHIMURA, H., HATTORI, N., KUBO, S.-I., MIZUNO, Y., ASAKAWA, S., MINOSHIMA, S., SHIMIZU, N., IWAI, K., CHIBA, T., TANAKA, K. & SUZUKI, T. 2000. Familial Parkinson disease gene product, parkin, is a ubiquitin-protein ligase. *Nat Genet,* 25**,** 302-305.
SHKOLNIK, K., BEN-DOR, S., GALIANI, D., HOURVITZ, A. & DEKEL, N. 2008. Molecular characterization and bioinformatics analysis of Ncoa7B, a novel ovulation-associated and reproduction system-specific Ncoa7 isoform. *Reproduction,* 135**,** 321-333.
SILVA-ALVAREZ, C., ARRAZOLA, M., GODOY, J. A., ORDENES, D. & INESTROSA, N. C. 2013. Canonical Wnt Signaling Protects Hippocampal Neurons from Aβ Oligomers: Role of Non-Canonical Wnt-5a/Ca2+ in Mitochondrial Dynamics. *Frontiers in Cellular Neuroscience,* 7.
SINGH, P., SCHIMENTI, J. C. & BOLCUN-FILAS, E. 2015. A Mouse Geneticist's Practical Guide to CRISPR Applications. *Genetics,* 199**,** 1-15.
SKARNES, W. C., AUERBACH, B. A. & JOYNER, A. L. 1992. A gene trap approach in mouse embryonic stem cells: the lacZ reported is activated by splicing, reflects endogenous gene expression, and is mutagenic in mice. *Genes & Development,* 6**,** 903-918.
SKARNES, W. C., ROSEN, B., WEST, A. P., KOUTSOURAKIS, M., BUSHELL, W., IYER, V., MUJICA, A. O., THOMAS, M., HARROW, J., COX, T., JACKSON, D., SEVERIN, J., BIGGS, P., FU, J., NEFEDOV, M., DE JONG, P. J., STEWART, A. F. & BRADLEY, A. 2011. A conditional knockout resource for the genome-wide study of mouse gene function. *Nature,* 474**,** 337-342.
SMALL, I., PEETERS, N., LEGEAI, F. & LURIN, C. 2004. Predotar: A tool for rapidly screening proteomes for N-terminal targeting sequences. *PROTEOMICS,* 4**,** 1581-1590.
SMIRNOVA, E., GRIPARIC, L., SHURLAND, D.-L. & VAN DER BLIEK, A. M. 2001. Dynamin-related Protein Drp1 Is Required for Mitochondrial Division in Mammalian Cells. *Molecular Biology of the Cell,* 12**,** 2245-2256.
SMITH, R. A. J., HARTLEY, R. C., COCHEMÉ, H. M. & MURPHY, M. P. 2012. Mitochondrial pharmacology. *Trends in Pharmacological Sciences,* 33**,** 341-352.
SOHAL, R. S. & SOHAL, B. H. 1991. Hydrogen peroxide release by mitochondria increases during aging. *Mechanisms of Ageing and Development,* 57**,** 187-202.
SOMAYAJULU, M., MCCARTHY, S., HUNG, M., SIKORSKA, M., BOROWY-BOROWSKI, H. & PANDEY, S. 2005. Role of mitochondria in neuronal cell death induced by oxidative stress; neuroprotection by Coenzyme Q10. *Neurobiology of Disease,* 18**,** 618-627.
SONG, W., CHEN, J., PETRILLI, A., LIOT, G., KLINGLMAYR, E., ZHOU, Y., POQUIZ, P., TJONG, J., POULADI, M. A., HAYDEN, M. R., MASLIAH, E., ELLISMAN, M., ROUILLER, I., SCHWARZENBACHER, R., BOSSY, B., PERKINS, G. & BOSSY-WETZEL, E. 2011. Mutant huntingtin binds the mitochondrial fission GTPase dynamin-related protein-1 and increases its enzymatic activity. *Nat Med,* 17**,** 377-382.
SOROLLA, M. A., REVERTER-BRANCHAT, G., TAMARIT, J., FERRER, I., ROS, J. & CABISCOL, E. 2008. Proteomic and oxidative stress analysis in human brain samples of Huntington disease. *Free Radical Biology and Medicine,* 45**,** 667-678.

SREEDHARAN, J., BLAIR, I. P., TRIPATHI, V. B., HU, X., VANCE, C., ROGELJ, B., ACKERLEY, S., DURNALL, J. C., WILLIAMS, K. L., BURATTI, E., BARALLE, F., DE BELLEROCHE, J., MITCHELL, J. D., LEIGH, P. N., AL-CHALABI, A., MILLER, C. C., NICHOLSON, G. & SHAW, C. E. 2008. TDP-43 Mutations in Familial and Sporadic Amyotrophic Lateral Sclerosis. *Science,* 319**,** 1668-1672.

SRERE, P. A., BRAZIL, H., GONEN, L. & TAKAHASHI, M. 1963. The Citrate Condensing Enzyme of Pigeon Breast Muscle and Moth Flight Muscle. *Acta Chemica Scandinavica,* 17 supl.**,** 129-134.

ST-PIERRE, J., BUCKINGHAM, J. A., ROEBUCK, S. J. & BRAND, M. D. 2002. Topology of Superoxide Production from Different Sites in the Mitochondrial Electron Transport Chain. *Journal of Biological Chemistry,* 277**,** 44784-44790.

STAMATAKIS, ALICE M., JENNINGS, JOSHUA H., UNG, RANDALL L., BLAIR, GRACE A., WEINBERG, RICHARD J., NEVE, RACHAEL L., BOYCE, F., MATTIS, J., RAMAKRISHNAN, C., DEISSEROTH, K. & STUBER, GARRET D. 2013. A Unique Population of Ventral Tegmental Area Neurons Inhibits the Lateral Habenula to Promote Reward. *Neuron,* 80**,** 1039-1053.

STAMPER, C., SIEGEL, A., LIANG, W. S., PEARSON, J. V., STEPHAN, D. A., SHILL, H., CONNOR, D., CAVINESS, J. N., SABBAGH, M., BEACH, T. G., ADLER, C. H. & DUNCKLEY, T. 2008. Neuronal Gene Expression Correlates of Parkinson's Disease with Dementia. *Movement disorders : official journal of the Movement Disorder Society,* 23**,** 1588-1595.

STEFANOVA, N. A., MURALEVAA, N. A., SKULACHEV, V. P. & KOLOSOVA, N. G. 2014. Alzheimer's Disease-Like Pathology in Senescence-Accelerated OXYS Rats can be Partially Retarded with Mitochondria-Targeted Antioxidant SkQ1. *Journal of Alzheimer's Disease,* 38**,** 681–694.

STOWERS, R. S., RUSSELL, S. & GARZA, D. 1999. The 82F Late Puff Contains the L82 Gene, an Essential Member of a Novel Gene Family. *Developmental Biology,* 213**,** 116-130.

STUDER, ROMAIN A., DESSAILLY, BENOIT H. & ORENGO, CHRISTINE A. 2013. Residue mutations and their impact on protein structure and function: detecting beneficial and pathogenic changes. *Biochemical Journal,* 449**,** 581-594.

STURTZ, L. A., DIEKERT, K., JENSEN, L. T., LILL, R. & CULOTTA, V. C. 2001. A fraction of yeast Cu/Zn superoxide dismutase and its metallochaperone, CCS, localize to the intermembrane space of mitochondria: A physiological role for SOD1 in guarding against mitochondrial oxidative damage. *Journal of Biological Chemistry*.

SU, B., WANG, X., ZHENG, L., PERRY, G., SMITH, M. A. & ZHU, X. 2010. Abnormal Mitochondrial Dynamics and Neurodegenerative Diseases. *Biochimica et biophysica acta,* 1802**,** 135-142.

TAGUCHI, N., ISHIHARA, N., JOFUKU, A., OKA, T. & MIHARA, K. 2007. Mitotic Phosphorylation of Dynamin-related GTPase Drp1 Participates in Mitochondrial Fission. *Journal of Biological Chemistry,* 282**,** 11521-11529.

TAIRA, T., SAITO, Y., NIKI, T., IGUCHI-ARIGA, S. M. M., TAKAHASHI, K. & ARIGA, H. 2004a. DJ-1 has a role in antioxidative stress to prevent cell death. *EMBO reports,* 5**,** 213-218.

TAIRA, T., SAITO, Y., NIKI, T., IGUCHI‐ARIGA, S. M. M., TAKAHASHI, K. & ARIGA, H. 2004b. *DJ‐1 has a role in antioxidative stress to prevent cell death*.

TAO, X. & TONG, L. 2003. Crystal Structure of Human DJ-1, a Protein Associated with Early Onset Parkinson's Disease. *Journal of Biological Chemistry,* 278**,** 31372-31379.

TATUCH, Y., CHRISTODOULOU, J., FEIGENBAUM, A., CLARKE, J. T., WHERRET, J., SMITH, C., RUDD, N., PETROVA-BENEDICT, R. & ROBINSON, B. H. 1992. Heteroplasmic mtDNA mutation (T----G) at 8993 can cause Leigh disease when the percentage of abnormal mtDNA is high. *American Journal of Human Genetics,* 50**,** 852-858.

TAYLOR, T. N., GREENE, J. G. & MILLER, G. W. 2010. Behavioral phenotyping of mouse models of Parkinson's Disease. *Behavioural brain research,* 211**,** 1-10.

TAYLOR, T. N., POTGIETER, D., ANWAR, S., SENIOR, S. L., JANEZIC, S., THRELFELL, S., RYAN, B., PARKKINEN, L., DELTHEIL, T., CIOROCH, M., LIVIERATOS, A., OLIVER, P. L., JENNINGS, K. A., DAVIES, K. E., ANSORGE, O., BANNERMAN, D. M., CRAGG, S. J. & WADE-MARTINS, R. 2014. Region-specific deficits in dopamine, but not norepinephrine, signaling in a novel A30P α-synuclein BAC transgenic mouse. *Neurobiology of Disease,* 62**,** 193-207.

TERADA, K., KANAZAWA, M., YANO, M., HANSON, B., HOOGENRAAD, N. & MORI, M. 1997. Participation of the import receptor Tom20 in protein import into mammalian mitochondria: analyses in vitro and in cultured cells. *FEBS Letters,* 403**,** 309-312.

TIPTON, K. F. 1968. The prosthetic groups of pig brain mitochondrial monoamine oxidase. *Biochimica et Biophysica Acta (BBA) - Enzymology,* 159**,** 451-459.

TONG, J., ANG, L.-C., WILLIAMS, B., FURUKAWA, Y., FITZMAURICE, P., GUTTMAN, M., BOILEAU, I., HORNYKIEWICZ, O. & KISH, S. J. 2015. Low levels of astroglial markers in Parkinson's disease: relationship to α-synuclein accumulation. *Neurobiology of Disease,* 82**,** 243-253.

TRETTER, L., SIPOS, I. & ADAM-VIZI, V. 2004. Initiation of Neuronal Damage by Complex I Deficiency and Oxidative Stress in Parkinson's Disease. *Neurochemical Research,* 29**,** 569–577.

TROUNCE, I. 2000. Genetic control of oxidative phosphorylation and experimental models of defects. *Human Reproduction,* 15**,** 18-27.

TROUNCE, I. A., KIM, Y. L., JUN, A. S. & WALLACE, D. C. 1996. [42]Assessment of mitochondrial oxidative phosphorylation in patient muscle biopsies, lymphoblasts, and transmitochondrial cell lines. *In:* GIUSEPPE M. ATTARDI, A. C. (ed.) *Methods in Enzymology.* Academic Press.

TUPPEN, H. A. L., BLAKELY, E. L., TURNBULL, D. M. & TAYLOR, R. W. 2010. Mitochondrial DNA mutations and human disease. *Biochimica et Biophysica Acta (BBA) - Bioenergetics,* 1797**,** 113-128.

TURRENS, J. F. 2003. Mitochondrial formation of reactive oxygen species. *The Journal of Physiology,* 552**,** 335-344.

TURRENS, J. F. & BOVERIS, A. 1980. Generation of superoxide anion by the NADH dehydrogenase of bovine heart mitochondria. *Biochem. J.,* 191**,** 421–427.

UTTARA, B., SINGH, A. V., ZAMBONI, P. & MAHAJAN, R. T. 2009. Oxidative Stress and Neurodegenerative Diseases: A Review of Upstream and Downstream Antioxidant Therapeutic Options. *Current Neuropharmacology,* 7**,** 65-74.

VALASTYAN, J. S. & LINDQUIST, S. 2014. Mechanisms of protein-folding diseases at a glance. *Disease Models and Mechanisms,* 7**,** 9-14.

VALENTE, E. M., ABOU-SLEIMAN, P. M., CAPUTO, V., MUQIT, M. M. K., HARVEY, K., GISPERT, S., ALI, Z., DEL TURCO, D., BENTIVOGLIO, A. R., HEALY, D. G., ALBANESE, A., NUSSBAUM, R., GONZÁLEZ-MALDONADO, R., DELLER, T., SALVI, S., CORTELLI, P., GILKS, W. P., LATCHMAN, D. S., HARVEY, R. J., DALLAPICCOLA, B., AUBURGER, G. & WOOD, N. W. 2004. Hereditary Early-Onset Parkinson's Disease Caused by Mutations in PINK1. *Science,* 304**,** 1158-1160.

VAN LOO, G., SAELENS, X., MATTHIJSSENS, F., SCHOTTE, P., BEYAERT, R., DECLERCQ, W. & VANDENABEELE, P. 2002. Caspases are not localized in mitochondria during life or death. *Cell Death and Differentiation,* 9**,** 1207-1211.

VAN WILPE, S., RYAN, M. T., HILL, K., MAARSE, A. C., MEISINGER, C., BRIX, J., DEKKER, P. J. T., MOCZKO, M., WAGNER, R., MEIJER, M., GUIARD, B., HONLINGER, A. & PFANNER, N. 1999. Tom22 is a multifunctional organizer of the mitochondrial preprotein translocase. *Nature,* 401**,** 485-489.

VANCE, C., ROGELJ, B., HORTOBÁGYI, T., DE VOS, K. J., NISHIMURA, A. L., SREEDHARAN, J., HU, X., SMITH, B., RUDDY, D., WRIGHT, P., GANESALINGAM, J., WILLIAMS, K. L., TRIPATHI, V., AL-SARAJ, S., AL-CHALABI, A., LEIGH, P. N., BLAIR, I. P., NICHOLSON, G., DE BELLEROCHE, J., GALLO, J.-M., MILLER, C. C. & SHAW, C. E. 2009. Mutations in FUS, an RNA Processing Protein, Cause Familial Amyotrophic Lateral Sclerosis Type 6. *Science,* 323**,** 1208-1211.

VANDE VELDE, C., MILLER, T. M., CASHMAN, N. R. & CLEVELAND, D. W. 2008. Selective association of misfolded ALS-linked mutant SOD1 with the cytoplasmic face of mitochondria. *Proceedings of the National Academy of Sciences,* 105**,** 4022-4027.

VARÇIN, M., BENTEA, E., MICHOTTE, Y. & SARRE, S. 2012. Oxidative Stress in Genetic Mouse Models of Parkinson’s Disease. *Oxidative Medicine and Cellular Longevity,* 2012**,** 25.

VENDEROVA, K. & PARK, D. S. 2012. Programmed Cell Death in Parkinson's Disease. *Cold Spring Harbor Perspectives in Medicine,* 2.

VIJAYVERGIYA, C., BEAL, M. F., BUCK, J. & MANFREDI, G. 2005. Mutant Superoxide Dismutase 1 Forms Aggregates in the Brain Mitochondrial Matrix of Amyotrophic Lateral Sclerosis Mice. *The Journal of Neuroscience,* 25**,** 2463–2470.

VOLKERT, M. R., ELLIOTT, N. A. & HOUSMAN, D. E. 2000. Functional genomics reveals a family of eukaryotic oxidation protection genes. *Proceedings of the National Academy of Sciences of the United States of America,* 97**,** 14530-14535.

VYSSOKIKH, M. Y., KATZ, A., RUECK, A., WUENSCH, C., DÖRNER, A., ZOROV, D. B. & BRDICZKA, D. 2001. Adenine nucleotide translocator isoforms 1 and 2 are differently distributed in the mitochondrial inner membrane and have distinct affinities to cyclophilin D. *Biochemical Journal,* 358**,** 349-358.

WANG, C. & YOULE, R. J. 2009. The Role of Mitochondria in Apoptosis. *Annual Review of Genetics,* 43**,** 95-118.

WANG, H.-Q., NAKAYA, Y., DU, Z., YAMANE, T., SHIRANE, M., KUDO, T., TAKEDA, M., TAKEBAYASHI, K., NODA, Y., NAKAYAMA, K. I. & NISHIMURA, M. 2005. Interaction of presenilins with FKBP38 promotes apoptosis by reducing mitochondrial Bcl-2. *Human Molecular Genetics,* 14**,** 1889-1902.

WANG, W., LI, L., LIN, W.-L., DICKSON, D. W., PETRUCELLI, L., ZHANG, T. & WANG, X. 2013. The ALS disease-associated mutant TDP-43 impairs mitochondrial dynamics and function in motor neurons. *Human Molecular Genetics,* 22**,** 4706-4719.

WANG, W., WANG, L., LU, J., SIEDLAK, S. L., FUJIOKA, H., LIANG, J., JIANG, S., MA, X., JIANG, Z., DA ROCHA, E. L., SHENG, M., CHOI, H., LEROU, P. H., LI, H. & WANG, X. 2016. The inhibition of TDP-43 mitochondrial localization blocks its neuronal toxicity. *Nat Med,* advance online publication.

WANG, X., PETRIE, T. G., LIU, Y., LIU, J., FUJIOKA, H. & ZHU, X. 2012a. Parkinson's disease-associated DJ-1 mutations impair mitochondrial dynamics and cause mitochondrial dysfunction. *Journal of Neurochemistry,* 121**,** 830-839.

WANG, X., SU, B., LEE, H.-G., LI, X., PERRY, G., SMITH, M. A. & ZHU, X. 2009. Impaired Balance of Mitochondrial Fission and Fusion in Alzheimer's Disease. *The Journal of Neuroscience,* 29**,** 9090-9103.

WANG, X., SU, B., SIEDLAK, S. L., MOREIRA, P. I., FUJIOKA, H., WANG, Y., CASADESUS, G. & ZHU, X. 2008a. Amyloid-β overproduction causes abnormal mitochondrial dynamics via differential modulation of mitochondrial fission/fusion proteins. *Proceedings of the National Academy of Sciences of the United States of America,* 105**,** 19318-19323.

WANG, X., SU, B., SIEDLAK, S. L., MOREIRA, P. I., FUJIOKA, H., WANG, Y., CASADESUS, G. & ZHU, X. 2008b. Amyloid-β overproduction causes abnormal mitochondrial dynamics via differential modulation of mitochondrial fission/fusion proteins. *Proceedings of the National Academy of Sciences,* 105**,** 19318-19323.

WANG, X., TOMSO, D. J., CHORLEY, B. N., CHO, H.-Y., CHEUNG, V. G., KLEEBERGER, S. R. & BELL, D. A. 2007. Identification of polymorphic antioxidant response elements in the human genome. *Human Molecular Genetics,* 16**,** 1188-1200.

WANG, X., YAN, M. H., FUJIOKA, H., LIU, J., WILSON-DELFOSSE, A., CHEN, S. G., PERRY, G., CASADESUS, G. & ZHU, X. 2012b. LRRK2 regulates mitochondrial dynamics and function through direct interaction with DLP1. *Human Molecular Genetics*.

WANG, Z., BERKEY, C. D. & WATNICK, P. I. 2012c. The Drosophila protein Mustard tailors the innate immune response activated by the IMD pathway. *Journal of Immunology (Baltimore, Md. : 1950),* 188**,** 3993-4000.

WANG, Z., BERKEY, C. D. & WATNICK, P. I. 2012d. The Drosophila Protein Mustard Tailors the Innate Immune Response Activated by the Immune Deficiency Pathway. *The Journal of Immunology,* 188**,** 3993-4000.

WASHBOURNE, P., THOMPSON, P. M., CARTA, M., COSTA, E. T., MATHEWS, J. R., LOPEZ-BENDITO, G., MOLNAR, Z., BECHER, M. W., VALENZUELA, C. F., PARTRIDGE, L. D. & WILSON, M. C. 2002. Genetic ablation of the t-SNARE SNAP-25 distinguishes mechanisms of neuroexocytosis. *Nat Neurosci,* 5**,** 19-26.

WEISIGER, R. A. & FRIDOVICH, I. 1973. Superoxide Dismutase: ORGANELLE SPECIFICITY. *Journal of Biological Chemistry,* 248**,** 3582-3592.

WERNER, J. H. K., FELIX, D., JAN, A. M. S. & PETER, H. G. M. W. 2012. OXPHOS mutations and neurodegeneration. *The EMBO Journal,* 32**,** 9-29.

WESTERMANN, B. 2012. Bioenergetic role of mitochondrial fusion and fission. *Biochimica et Biophysica Acta (BBA) - Bioenergetics,* 1817**,** 1833-1838.

WEYEMI, U., REDON, C. E., AZIZ, T., CHOUDHURI, R., MAEDA, D., PAREKH, P. R., BONNER, M. Y., ARBISER, J. L. & BONNER, W. M. 2015. NADPH oxidase 4 is a critical mediator in Ataxia telangiectasia disease. *Proceedings of the National Academy of Sciences,* 112**,** 2121-2126.

WHARTON, D. C. & TZAGOLOFF, A. 1967. Cytochrome oxidase from beef heart mitochondria. *Methods Enzymol.,* 10**,** 245–250.

WILKINSON, K. D. 2000. Ubiquitination and deubiquitination: Targeting of proteins for degradation by the proteasome. *Seminars in Cell & Developmental Biology,* 11**,** 141-148.

WILSON, M. A., COLLINS, J. L., HOD, Y., RINGE, D. & PETSKO, G. A. 2003. The 1.1-Å resolution crystal structure of DJ-1, the protein mutated in autosomal recessive early onset Parkinson's disease. *Proceedings of the National Academy of Sciences,* 100**,** 9256-9261.

WOLTER, K. G., HSU, Y.-T., SMITH, C. L., NECHUSHTAN, A., XI, X.-G. & YOULE, R. J. 1997. Movement of Bax from the Cytosol to Mitochondria during Apoptosis. *The Journal of Cell Biology,* 139**,** 1281-1292.

WONG, P. C., PARDO, C. A., BORCHELT, D. R., LEE, M. K., COPELAND, N. G., JENKINS, N. A., SISODIA, S. S., CLEVELAND, D. W. & PRICE, D. L. 1995. An adverse property of a familial ALS-linked SOD1 mutation causes motor neuron disease characterized by vacuolar degeneration of mitochondria. *Neuron,* 14**,** 1105-1116.

WU, S., ZHOU, F., ZHANG, Z. & XING, D. 2011. Mitochondrial oxidative stress causes mitochondrial fragmentation via differential modulation of mitochondrial fission–fusion proteins. *FEBS Journal,* 278**,** 941-954.

XIAO, L., CHEN, D., HU, P., WU, J., LIU, W., ZHAO, Y., CAO, M., FANG, Y., BI, W., ZHENG, Z., REN, J., JI, G., WANG, Y. & YUAN, Z. 2011. The c-Abl-MST1 Signaling Pathway Mediates Oxidative Stress-Induced Neuronal Cell Death. *The Journal of Neuroscience,* 31**,** 9611-9619.

XU, Y.-F., GENDRON, T. F., ZHANG, Y.-J., LIN, W.-L., D'ALTON, S., SHENG, H., CASEY, M. C., TONG, J., KNIGHT, J., YU, X., RADEMAKERS, R., BOYLAN, K., HUTTON, M., MCGOWAN, E., DICKSON, D. W., LEWIS, J. & PETRUCELLI, L. 2010. Wild-Type Human TDP-43 Expression Causes TDP-43 Phosphorylation, Mitochondrial Aggregation, Motor Deficits, and Early Mortality in Transgenic Mice. *The Journal of Neuroscience,* 30**,** 10851-10859.

YAKES, F. M. & VAN HOUTEN, B. 1997. Mitochondrial DNA damage is more extensive and persists longer than nuclear DNA damage in human cells following oxidative stress. *Proceedings of the National Academy of Sciences,* 94**,** 514-519.

YANG, J., LIU, X., BHALLA, K., KIM, C. N., IBRADO, A. M., CAI, J., PENG, T.-I., JONES, D. P. & WANG, X. 1997. Prevention of Apoptosis by Bcl-2: Release of Cytochrome c from Mitochondria Blocked. *Science,* 275**,** 1129-1132.

YANG, M., LIN, X., ROWE, A., ROGNES, T., EIDE, L. & BJØRÅS, M. 2015. Transcriptome analysis of human OXR1 depleted cells reveals its role in regulating the p53 signaling pathway. *Scientific Reports,* 5**,** 17409.

YANG, M., LUNA, L., SØRBØ, J. G., ALSETH, I., JOHANSEN, R. F., BACKE, P. H., DANBOLT, N. C., EIDE, L. & BJØRÅS, M. 2014. Human OXR1 maintains mitochondrial DNA integrity and counteracts hydrogen peroxide-induced oxidative stress by regulating antioxidant pathways involving p21. *Free Radical Biology and Medicine,* 77**,** 41-48.

YANO, H., BARANOV, S. V., BARANOVA, O. V., KIM, J., PAN, Y., YABLONSKA, S., CARLISLE, D. L., FERRANTE, R. J., KIM, A. H. & FRIEDLANDER, R. M. 2014a. Inhibition of mitochondrial protein import by mutant huntingtin. *Nat Neurosci,* 17**,** 822-831.

YANO, H., BARANOV, S. V., BARANOVA, O. V., KIM, J., PAN, Y., YABLONSKA, S., CARLISLE, D. L., FERRANTE, R. J., KIM, A. H. & FRIEDLANDER, R. M. 2014b. Inhibition of

mitochondrial protein import by mutant huntingtin. *Nature neuroscience,* 17**,** 822-831.

YANO, M., HOOGENRAAD, N., TERADA, K. & MORI, M. 2000. Identification and Functional Analysis of Human Tom22 for Protein Import into Mitochondria. *Molecular and Cellular Biology,* 20**,** 7205-7213.

YOON, Y., KRUEGER, E. W., OSWALD, B. J. & MCNIVEN, M. A. 2003. The Mitochondrial Protein hFis1 Regulates Mitochondrial Fission in Mammalian Cells through an Interaction with the Dynamin-Like Protein DLP1. *Molecular and Cellular Biology,* 23**,** 5409-5420.

YU, T., JHUN, B. S. & YOON, Y. 2010. High-Glucose Stimulation Increases Reactive Oxygen Species Production Through the Calcium and Mitogen-Activated Protein Kinase-Mediated Activation of Mitochondrial Fission. *Antioxidants & Redox Signaling,* 14**,** 425-437.

ZERBETTO, E., VERGANI, L. & DABBENI-SALA, F. 1997. Quantification of muscle mitochondrial oxidative phosphorylation enzymes via histochemical staining of blue native polyacrylamide gels. *Electrophoresis,* 18**,** 2059-2064.

ZHANG, L., SHIMOJI, M., THOMAS, B., MOORE, D. J., YU, S.-W., MARUPUDI, N. I., TORP, R., TORGNER, I. A., OTTERSEN, O. P., DAWSON, T. M. & DAWSON, V. L. 2005. Mitochondrial localization of the Parkinson's disease related protein DJ-1: implications for pathogenesis. *Human Molecular Genetics,* 14**,** 2063-2073.

ZHANG, Y. & CHAN, D. C. 2007. Structural basis for recruitment of mitochondrial fission complexes by Fis1. *Proceedings of the National Academy of Sciences of the United States of America,* 104**,** 18526-18530.

ZHAO, K., LUO, G., GIANNELLI, S. & SZETO, H. H. 2005. Mitochondria-targeted peptide prevents mitochondrial depolarization and apoptosis induced by tert-butyl hydroperoxide in neuronal cell lines. *Biochemical Pharmacology,* 70**,** 1796-1806.

ZHAO, K., ZHAO, G.-M., WU, D., SOONG, Y., BIRK, A. V., SCHILLER, P. W. & SZETO, H. H. 2004. Cell-permeable Peptide Antioxidants Targeted to Inner Mitochondrial Membrane inhibit Mitochondrial Swelling, Oxidative Cell Death, and Reperfusion Injury. *Journal of Biological Chemistry,* 279**,** 34682-34690.

ZHOU, L. L., ZHOU, L. Y., LUO, K. Q. & CHANG, D. C. 2005. Smac/DIABLO and cytochrome c are released from mitochondria through a similar mechanism during UV-induced apoptosis. *Apoptosis,* 10**,** 289-299.

ZHUANG, X., MASSON, J., GINGRICH, J. A., RAYPORT, S. & HEN, R. 2005. Targeted gene expression in dopamine and serotonin neurons of the mouse brain. *Journal of Neuroscience Methods,* 143**,** 27-32.

ZOU, H., LI, Y., LIU, X. & WANG, X. 1999. An APAF-1·Cytochrome c Multimeric Complex Is a Functional Apoptosome That Activates Procaspase-9. *Journal of Biological Chemistry,* 274**,** 11549-11556.

ZUCHNER, S., MERSIYANOVA, I. V., MUGLIA, M., BISSAR-TADMOURI, N., ROCHELLE, J., DADALI, E. L., ZAPPIA, M., NELIS, E., PATITUCCI, A., SENDEREK, J., PARMAN, Y., EVGRAFOV, O., JONGHE, P. D., TAKAHASHI, Y., TSUJI, S., PERICAK-VANCE, M. A., QUATTRONE, A., BATTOLOGLU, E., POLYAKOV, A. V., TIMMERMAN, V., SCHRODER, J. M. & VANCE, J. M. 2004. Mutations in the mitochondrial GTPase mitofusin 2 cause Charcot-Marie-Tooth neuropathy type 2A. *Nat Genet,* 36**,** 449-451.

Published work

1. Yixing Wu, Kay E. Davies and Peter L. Oliver (2016) “The antioxidant protein Oxr1 influences aspects of mitochondrial morphology.” Free Radical Biology and Medicine 95: 255-267.

2. Mattea J. Finelli, Kevin. X. Liu, Yixing. Wu, Peter. L. Oliver and Kay. E. Davies (2015) "Oxr1 improves pathogenic cellular features of ALS-associated FUS and TDP-43 mutations." Human Molecular Genetics 24(12): 3529-3544.